NTIA Report 14-506

Effects of Radar Interference on LTE (FDD) eNodeB and UE Receiver Performance in the 3.5 GHz Band

Geoffrey A. Sanders
John E. Carroll
Frank H. Sanders
Robert L. Sole

report series

U.S. DEPARTMENT OF COMMERCE • National Telecommunications and Information Administration

NTIA Report 14-506

Effects of Radar Interference on LTE (FDD) eNodeB and UE Receiver Performance in the 3.5 GHz Band

Geoffrey A. Sanders
John E. Carroll
Frank H. Sanders
Robert L. Sole

U.S. DEPARTMENT OF COMMERCE

July 2014

DISCLAIMER

Certain commercial equipment and materials are identified in this report to specify adequately the technical aspects of the reported results. In no case does such identification imply recommendation or endorsement by the National Telecommunications and Information Administration, nor does it imply that the material or equipment identified is the best available for this purpose.

This report only describes the impacts of interference on a prototype 3.5 GHz LTE network at the physical layer. In this report, the LTE network is treated as a “black box” and the response of a subset of LTE parameters, identified as most-critical by an industry participant working with NTIA, are presented. The LTE diagnostic parameters used in this report were recorded by the industry participant and were made available to the authors for post-analysis.

CONTENTS

FIGURES

TABLES

ABBREVIATIONS/ACRONYMS AND SYMBOLS

BLER	block error rate
CQI	Channel quality indicator
CSV	comma separated variable
DC	duty cycle
EIRP	effective isotropic radiated power
eNB	E-UTRAN Node B or Evolved Node B
FCC	Federal Communications Commission
FDD	frequency division duplexing
FDR	frequency dependent rejection
FNPRM	Further Notice of Proposed Rulemaking
GHz	Gigahertz
HARQ	hybrid automatic repeat request
I	interference power
ITS	Institute for Telecommunication Sciences (NTIA)
kHz	kilohertz
LNA	low noise amplifier
LTE	Long Term Evolution
MCS	modulation coding scheme
MHz	Megahertz
MIMO	multiple input multiple output
ms	milliseconds
N	noise power
nmi	nautical miles
NPRM	Notice of Proposed Rulemaking

NTIA	National Telecommunications and Information Administration
OOB	out of band
OSM	Office of Spectrum Management
P0N	fixed-frequency carrier wave pulse modulation
PW	pulse width
PRR	pulse repetition rate
Q3N	swept-frequency carrier wave pulse modulation
RB	resource block
RF	radio frequency
RLM	radio link monitoring
RSSI	received signal strength indicator
S	LTE received signal power
TDD	time division duplexing
TDWR	Terminal Doppler Weather Radar
UE	user equipment
VSG	vector signal generator

EXECUTIVE SUMMARY

In late 2012, the Federal Communications Commission (FCC) issued a Notice of Proposed Rulemaking (NPRM) in FCC Docket 12-354 [1], followed by a Further Notice of Proposed Rulemaking (FNPRM) [2] in April 2014, regarding possible future spectrum sharing between radar and non-radar systems in the band 3550–3650 MHz (3.5 GHz). These documents called for tests and measurements to investigate the compatibility of broadband communications systems and incumbent Federal radars operating in that band. In response, personnel from the National Telecommunications and Information Administration (NTIA)'s Office of Spectrum Management (OSM) and NTIA's Institute for Telecommunication Sciences (ITS) have performed interference-effects tests in which simulated radar signals were injected into a prototype 4G Long Term Evolution (LTE) Frequency Division Duplexing (FDD) network that operates in the 3.5 GHz band.

Prototype LTE units, provided by an industry participant, for the 3.5 GHz band were used during these tests as no commercially available hardware existed at the time of the testing. Being prototypes, the tested LTE units used prototype RF front-end hardware with a nominal 7 dB receiver noise figure. These tests did *not* investigate high-power effects such as LTE receiver saturation or front-end overload. Interference power levels as high as -25 dBm were injected into the radio RF front-ends.

The industry participant configured a laboratory LTE network for the tests and maintained it as an actual deployment during all phases of testing. The testing was done via hardline RF connections that were free of any external RF sources that could possibly affect the test results.

Twenty-four interference waveforms were injected into both the uplink and downlink paths of the prototype LTE network; the tests were performed in a closed-loop test bed under steady-state conditions and the interference was synthesized using up to two vector signal generators (VSGs) at a time. The interference injection was done separately on either the uplink or the downlink RF path. Diagnostic LTE system software, running in the background, collected performance data. The desired downlink signal power was held at a constant level throughout the tests, set to a nominal level by the LTE engineers who assisted the testing. The desired uplink signal power was set to a nominal starting level and verified before each new interference waveform data collection. The uplink signal level varied during the tests due to power control, which is part of normal LTE operation, and could increase power by as much as 25 dB from the nominal starting point.

For the downlink tests, data throughput, block error rate (BLER) of the first hybrid automatic repeat request (HARQ) transmission, and modulation coding scheme (MCS) were recorded for post-test analysis. For the uplink tests, UE transmit signal power, MCS, BLER of the first transmission of HARQ, and resource block (RB) usage were recorded as a function of interference power level. Nominal rates of data throughput were 48 Mbps and 12 Mbps for the downlink and uplink, respectively. Call initiation and hand-off performance were not tested.

Each interference waveform was specified by pulse modulation, pulse width, and pulse repetition rate. Pulse modulation for each waveform was either simple pulsing of a fixed-frequency carrier

wave (referred to as P0N) or else swept-frequency for the duration of each pulse (called chirping or Q3N). The radar waveforms were *not* exact replications of any existing or planned future operational 3.5 GHz radar emissions. By not exactly replicating any operational or possible future radar waveforms, the authors avoided issues with association, classification and identification of particular waveforms with individual radar systems. This approach also made the test results applicable to radar interference effects on LTE receivers on a general rather than system-specific basis. The radar interference waveform parameters were carefully tailored to span the entire range of all existing and anticipated future waveforms that do/may occur in the 3.5 GHz spectrum. A band-limited Gaussian noise waveform was included along with two waveforms from a test that was previously performed by the European CEPT Electronic Communications Committee (ECC). A waveform that replicated a widely deployed type of weather radar which operates in the band 5600–5650 MHz was also tested.

Two interference scenarios were tested: continuous and burst. Continuous pulse interference testing allowed prolonged collection of LTE system performance statistics. However, in real-world situations, radar beams do not often dwell on fixed points in space, producing continuous pulse streams at individual locations. Rather, radar beams ordinarily scan rapidly across points in space. This means that receivers ordinarily see radar interference as short, intermittent bursts of pulses. In this study, such short, intermittent bursts were injected into the LTE network to replicate the way that deployed LTE networks would typically encounter radar interference.

For continuous-interference tests, the waveforms were injected at steady-state power levels during nominal 60 second intervals of data collection. The injected power for each interference waveform started at a low level and was increased in discrete steps until reaching a point where the throughput decreased to 0 Mbps or until the VSG power maxed out at the limit of permissible power into the LTE network. The impacts of the waveforms on the respective receiver's performance parameters were processed to produce graphs showing the impact that each waveform had on the receiver's performance as a function of the received interference power level.

For burst interference tests, selected interference waveforms were injected in 20 pulse bursts spaced 5 seconds apart, thus replicating the behavior typical of radar beam scanning. Interference power levels as high as -25 dBm were injected while data throughput and MCS were monitored.

For the continuous-interference downlink case, all P0N interference waveforms produced appreciable effects on data throughput when interference, *I*, was greater than -65 dBm. Some Q3N waveforms degraded data throughput when interference, *I*, was -85 dBm. As the interference power level was increased, the interference impact increased.

For the continuous-interference uplink case, at least one of the four measured parameters (throughput, UE transmit power, BLER, and RB usage) were affected by increasing interference power. It is believed that since the UE was able to vary transmit power and RB usage, the uplink was more adaptable to interference than the downlink.

Concerning the results of burst testing, at the highest interference power levels (*I* between -50 dBm and -30 dBm), downlink data throughput rates were minimally affected for all tested burst interference waveforms. The effect is observed as momentary, evenly-spaced (every 5 seconds)

reductions in throughput. The Q3N-4 (10% duty cycle) waveform had the greatest impact, producing momentary reductions of up to 7 Mbps (from 48 Mbps to 41 Mbps). There were no discernable impacts on uplink data throughput rates.

The authors do not determine the acceptability of radar interference effects on LTE network performance. The data in this report can be used as a building block in the construction of band sharing criteria for radar transmitters and LTE receivers, supporting possible future spectrum sharing at 3.5 GHz.

More work is needed in this area to support sharing in the 3.5 GHz band. Topics for additional testing could include: these same types of tests with commercially available 3.5 GHz LTE receivers, an investigation of LTE receiver saturation and gain compressions due to pulsed signals, investigation of interference into an LTE network with multiple user equipment devices, and measuring the emissions of additional 3.5 GHz LTE transmitters. NTIA is prepared to work with other government agencies and industry to accomplish these goals.

EFFECTS OF RADAR INTERFERENCE ON LTE (FDD) ENODEB AND UE RECEIVER PERFORMANCE IN THE 3.5 GHZ BAND

Geoffrey A. Sanders,[1] John E. Carroll,[1] Frank H. Sanders,[1] Robert L. Sole[2]

In response to proposals to introduce new radio systems into 3.5 GHz radio spectrum in the United States, the authors have performed measurements and analysis on effects of interference, from a variety of radar waveforms, to the performance of a prototype 3.5 GHz Long Term Evolution (LTE) network, consisting of one base station (an eNodeB) and one client (referred to as user equipment or UE) utilizing frequency-division duplexing (FDD). This work has been prompted by the possibility that LTE receivers may eventually share spectrum with radar operations in this spectrum range. Radar pulse parameters used in this testing spanned the range of both existing and anticipated future radar systems in the 3.5 GHz spectrum range. Effects of radar interference on the LTE uplink and downlink throughput, block error rate (BLER), and modulation coding scheme (MCS) were measured. Additionally, for the uplink tests, resource block (RB) usage and UE transmit power were recorded. Effects on LTE performance are presented as a function of radar pulse parameters and the incident power level of radar pulses into the LTE receivers. The authors do not determine the interference protection criterion for LTE networks. Rather, the data presented can be used by spectrum managers and engineers as a building block in the construction of band sharing criteria for radar transmitters and LTE receivers, supporting possible future spectrum sharing at 3.5 GHz.

Key words: Block error rate (BLER); chirped pulses; Long Term Evolution (LTE); P0N pulses; radar; spectrum sharing; frequency-division duplexing (FDD); evolved-Node B (eNB); Q3N pulses

1 INTRODUCTION

In December of 2012, the Federal Communications Commission (FCC) issued a Notice of Proposed Rulemaking (NPRM) [1] followed by a Further Notice of Proposed Rulemaking (FNPRM) [2] in April of 2014, regarding possible future spectrum sharing between radar and non-radar systems in radio spectrum near 3.5 GHz. In response to this NPRM and FNPRM, personnel from NTIA's Office of Spectrum Management (OSM) and NTIA's Institute for Telecommunication Sciences (ITS) have performed interference-effects tests in which simulated radar signals were injected into a prototype Long Term Evolution (LTE) frequency-division duplexing (FDD) network, operating in

[1] The authors are with the Institute for Telecommunication Sciences, National Telecommunications and Information Administration (NTIA), U.S. Dept. of Commerce, Boulder, CO 80305.
[2] The author is with the Office of Spectrum Management, NTIA, U.S. Dept. of Commerce, Washington, DC 20230.

the 3.5 GHz frequency band. Interference was injected into both the base station, known as an eNodeB (eNB) in LTE networks, and a single client, called user equipment (UE) The interference was injected into the uplink (UE to eNB) and downlink (eNB to UE) RF paths separately.[3] The eNB transmitter operated with 9 MHz of bandwidth centered at 3600 MHz and the UE transmitter operated with up to 7.2 MHz of bandwidth centered at 3520.9 MHz.

A prototype micro-cell LTE system was used in the NTIA tests described in this report. Current plans for LTE operations at 3.5 GHz in the United States envision the use of micro-cell LTE systems, as described in [1]. The authors have performed similar testing on a macro-cell network as described in [3]. The differences between micro and macro-cell LTE systems are understood to be primarily in eNB antenna types, heights, and gains along with transmitter power levels. Error correction and other signal processing parameters inherent to the LTE protocol are understood to be identical between the two types of systems.

The tests described in this report were performed in March 2014 at an industry laboratory in Colorado. The effects of radar interference on data throughput, block error rate (BLER) of the first hybrid automatic repeat request (HARQ) transmission (hereafter referred to as just BLER), and modulation coding scheme (MCS) were observed and recorded for both uplink and downlink. Additionally, the effects of radar interference on UE transmit power and UE resource block (RB) usage were observed and recorded for the uplink tests. The test results, and the measurements that produced them, are described in this report.

The authors do not determine the interference protection criterion for nominal LTE network performance. Rather, the data presented in this report can be used by spectrum managers and engineers as a building block in the construction of band sharing criteria for radar transmitters and LTE receivers, supporting possible future spectrum sharing at 3.5 GHz.

1.1 Interference Coupling Scenario for Possible Future 3.5 GHz Spectrum Sharing

3.5 GHz spectrum is utilized by a variety of radar systems [4]. Many of these radars operate on ships in near-shore (littoral) waters around American coastlines. These radars are used for a variety of purposes and missions including air surveillance and air defense. Transmitted beams of these radars scan through 360 degrees of azimuth around their ship platforms, providing detection, surveillance and tracking of air-breathing aerial targets at distances of up to about 180–240 nautical miles (nmi) and of targets outside the Earth's atmosphere at larger distances. These radar beams transmit over both oceans and littoral shorelines. The air-search radar beam shapes often have cross sections in the shape of a 1/(squared cosecant) function. The lower edge of the radars' air-search and space-search beam is typically tilted above any given ship's local

[3] The interference was injected separately to isolate interference effects in the respective paths. In the real world, it is unlikely that uplinks and downlinks would experience interference simultaneously (i.e. it is unlikely that they would be co-linear with a radar beam).

horizon at an angle of about 0.5 to 1.0 angular degrees. Additional information about radar systems operating in the 3100–3650 MHz frequency band is presented in [4].

Traditional (legacy) long range air-search radar waveforms often use pulse widths (PWs) that are between 1 and 10 μs long, at pulse repetition rates (PRRs) of between 300 and 1,000 pulses/sec. The transmitted waveform duty cycle (DC, defined as time interval during which waveform power is transmitted divided by total time of the waveform's periodicity) of such radars is about 0.1 percent. Such radars use tube-type output devices (e.g., magnetrons, klystrons, crossed-field amplifiers) that generate effective isotropic radiated peak power levels (peak EIRP) of 1–10 GW. Newer radars often use solid-state output devices radiating peak EIRPs of 10–100 MW, but at the cost of longer PWs and higher DCs that can approach 10 percent.[4] The longer PWs of current and future solid state radars require, in turn, that transmitted pulses be frequency-modulated or phase coded to maintain adequate range resolution. The NTIA radar interference waveforms incorporate the characteristics of both legacy and newer radars.

Future LTE systems at 3.5 GHz are expected to operate with handheld user equipment (UE) units that will usually be at or near ground level. The UEs are expected to communicate with LTE eNBs that will typically be located at greater heights than the UEs, for example on the sides of buildings or on building rooftops. Because antenna beams for the radar systems of concern are tilted somewhat above local horizons, they should couple more strongly into LTE systems' eNB receivers than into the UE receivers. This coupling scenario is shown schematically in Figure 1. Although it is believed that radar interference would couple into LTE eNB receivers more strongly than into UE receivers, effects on both the uplink and downlink were examined in this study. To maximize coverage, LTE eNB antennas are typically situated at high locations such as at the tops of towers or building rooftops and, therefore, have a higher probability of receiving radar interference.

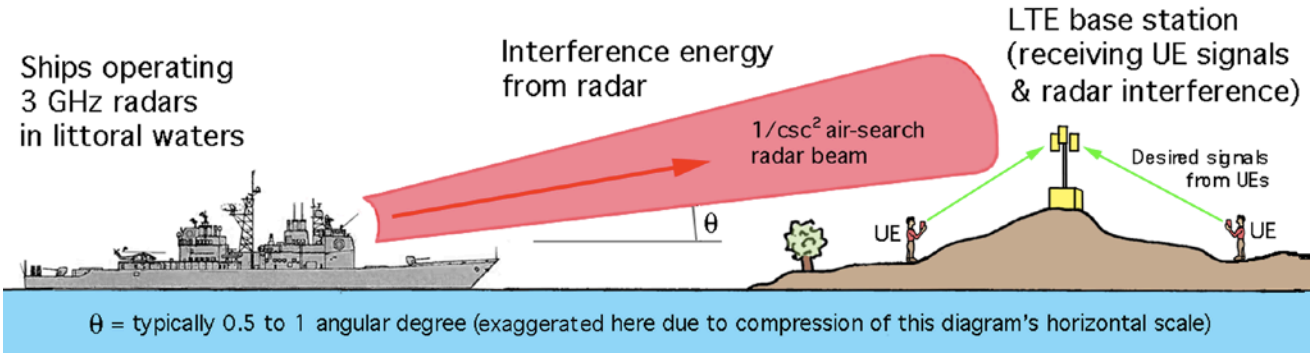

Figure 1. Schematic diagram showing coupling scenario between littoral radar transmitters and possible future 3.5 GHz LTE systems. By geometry, coupling from radar transmitters should occur more into LTE eNB receivers than into UEs.

[4] Solid-state radars can cause more interference than higher-power tube-transmitter radars because the peak EIRPs of the newer radars are still high enough to exceed interference thresholds for many systems, while their higher DCs of around 10 percent have more impact in the time domain than the 0.1 percent DCs of older radars.

1.2 Implementation of the Interference Scenario in an Interference-Effects Test Bed

The authors assembled a hardware implementation of the coupling scenarios of Figure 1 in a test bed with the assistance of an industry participant. This included an LTE UE, an LTE eNB, and a transmitter producing radar interference waveforms consisting of one or two vector signal generators (VSGs) for the uplink and downlink cases, respectively. This implementation is shown schematically in Figure 2 and as a more electronically-detailed diagram in Figure 3. A full description of the losses in the test bed LTE network is provided in Appendix A.

For the uplink tests, radar interference was injected into the receiver side of the LTE eNB along with desired LTE signals originating from an LTE UE. To do this, and to establish and maintain normal LTE communications during the testing, a link had to be established for regular, two-way communications between the eNB and UE.[5] In the LTE eNB receiver path, a radio frequency (RF) combiner was installed to couple radar signals into the eNB receiver along with the desired UE signals. This combiner requirement is shown in Figures 2 and 3.

For the downlink tests, radar interference was injected into the UE receiver on both transmit channels using two separate VSGs along with LTE traffic from the LTE eNB. Once again a regular two-way communication link between the eNB and UE was established while the interference was injected. This configuration is also shown in Figures 2 and 3.

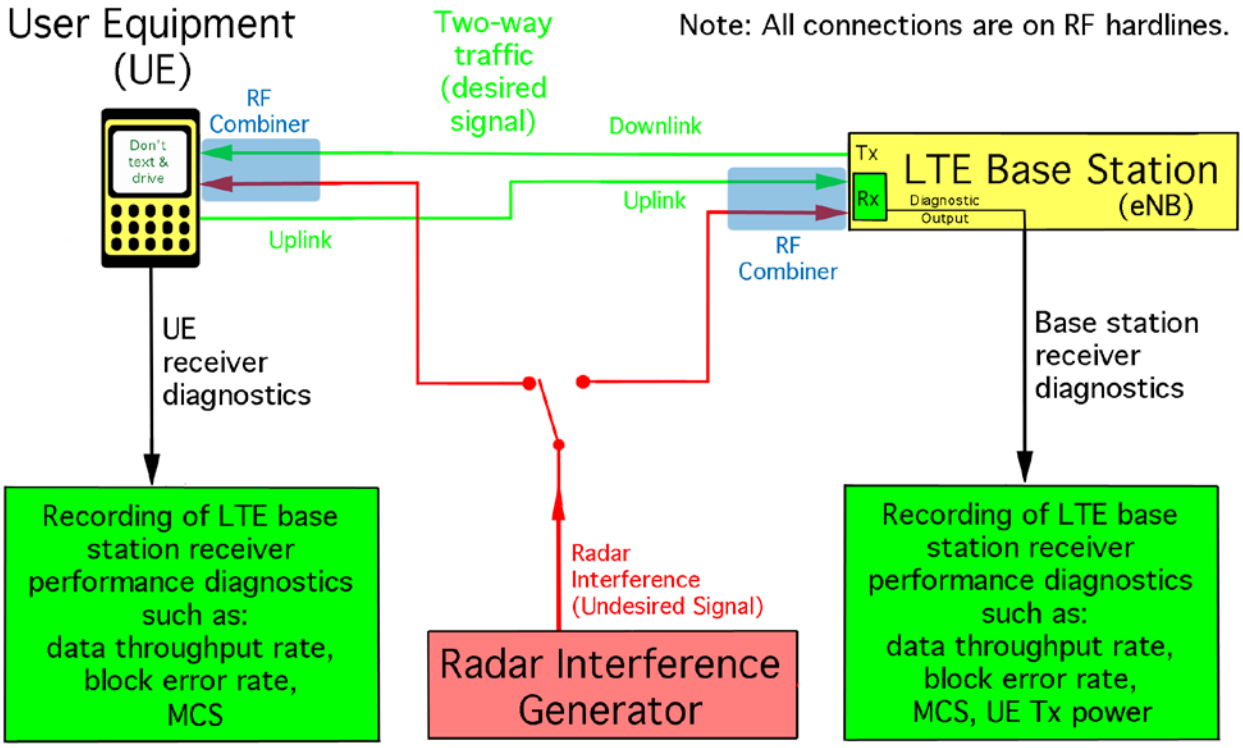

Figure 2. Simple diagram of the test bed for the radar-to-LTE interference scenario of Figure 1.

[5] It is noted that there could be utility in eventually testing an LTE eNB with multiple UE inputs.

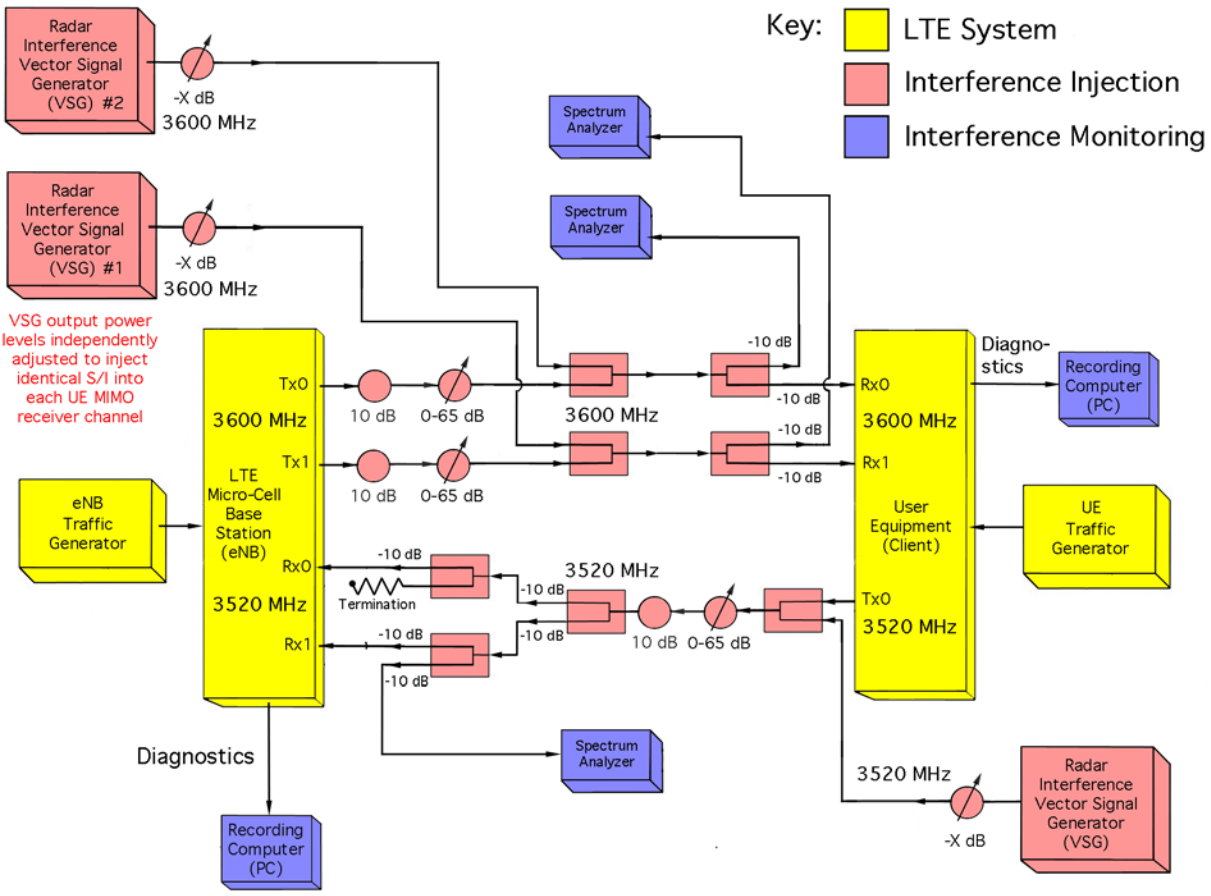

Figure 3. Detailed diagram of the interference-effects test bed of Figure 2.

The effects of interference were determined by observing and recording diagnostic outputs from either the LTE eNB receiver or the LTE UE receiver whilst radar interference was injected. The interference effects were measured as functions of the power levels and waveform modulations of the radar interference. The measured diagnostic parameters for the downlink case were data throughput, BLER, and MCS usage. For the uplink case, UE transmit power and RB usage were recorded in addition to the parameters recorded for the downlink case.

All RF connections within the test bed were via hardlines; the LTE communication signal and the radar interference were not radiated. Hardlines were used so that the effects of radar interference could be observed without any effects from radio propagation, antenna performance, environmental noise or extraneous signals from other radio systems. While such collateral factors might well affect actual 3.5 GHz spectrum sharing, the purpose of this study was to understand the effects of radar interference alone; a hardline test bed was deemed to be the best approach for observing radar interference effects with a high degree of isolation and acuity. Propagation studies and analysis will eventually be needed to determine the exact power levels that would be coupled from radar transmitters to LTE receivers at actual field locations under a variety of ambient conditions and circumstances, as discussed in [4]. LTE performance degradation that might arise from additional factors associated with radiated signal environments should likewise be studied separately.

The authors programmed two Agilent 8267 (C and D variants) VSGs to generate radar interference waveforms in addition to a 10 MHz wide Gaussian noise waveform. The interference waveforms are described in detail in Section 2.

For the downlink case, two VSGs were required for the Gaussian noise tests to remove any signal correlation. Each VSG was programmed with a unique 10 MHz wide Gaussian noise signal and each was combined with one of the eNB transmit channels as shown in Figure 3.[6]

While two VSGs were not required for the radar waveform interference injection, it was decided to continue using two for consistency. The radar waveforms transmitted by the two VSGs were synchronized using an Agilent 33250 arbitrary waveform generator outputting a trigger pulse to each of the two VSGs. Power levels from each VSG were calibrated at the beginning of each interference waveform test to be the same level on both receive channel paths and the VSGs' time sources were synchronized via a 10 MHz reference signal.

For the uplink case, only a single VSG was required as there was only one interference injection coupler. This is consistent with the understood operation of an LTE UE at the time these tests were conducted, where there is typically only one data stream transmitted from the UE. In future LTE implementations the UE will support multiple transmitters. It is believed this will make an LTE network more robust to interference.

[6] Originally a single VSG was used to inject the Gaussian noise signal into both channels via a splitter. The LTE network was able to use the correlated nature of the split Gaussian noise signal received at the UE to cancel it out to some extent, thereby significantly reducing the effects of the interference. The authors, along with engineers from the industry participant, decided that in a real world situation, a Gaussian noise signal received at the UE would be uncorrelated so it was decided to use two separate VSGs loaded with distinct Gaussian noise waveforms.

2 INTERFERENCE-EFFECTS TESTING PROCEDURES

2.1 LTE Operation During Testing

As shown in Figures 2 and 3, the UE and eNB units operated with traffic generators and communicated via hardline connection. The UE and eNB operated with frequency diversity and 80 MHz of separation between uplink and downlink channels. The eNB communicated with the UE using two MIMO channels across 9 MHz (50 RBs, each 180 kHz wide) of bandwidth, centered at 3600 MHz. The UE communicated with the eNB using a single channel centered at 3520.9 MHz, using a nominal 40 RBs. Path loss in both uplink and downlink directions was simulated via adjustable attenuators in the RF path to values recommended by the industry participant as being within nominal coverage. The attenuators in the uplink RF path were set such that the signal power level from the UE into the eNB receiver was -85 dBm without interference. Conversely, the attenuators in the downlink RF path were set such that the signal power level from the eNB into the UE receiver was -75 dBm without interference. LTE receiver performance for the eNB and the UE (data throughput, BLER,[7] MCS, UE transmit power,[8] and RBs) was monitored by diagnostic software throughout the testing. The nominal throughput was approximately 48 Mbps in the downlink and approximately 12 Mbps in the uplink as configured by the industry participant.

2.2 Radar and Gaussian Noise Interference Waveforms

The interference effects of twenty-three radar waveforms and a 10 MHz wide Gaussian noise signal were tested. Each radar waveform was pulsed and was specified by modulation, pulse width (PW), and pulse repetition rate (PRR). Radar pulses were modulated as either fixed-frequency carrier waves (designated P0N) or as linearly increasing swept-frequency carriers (called chirping, designated Q3N).[9] The radar waveforms were *not* exact replications of any existing or planned future operational 3.5 GHz radar emissions. By not exactly replicating any operational or possible future radar waveforms, the authors avoided issues of identification of waveforms with operational radar systems. This approach was also intended to make the test results applicable to radar interference effects on LTE receivers on a generic rather than a system-specific basis. The radar interference waveform parameter space was designed, however, to span the entire range of all existing and possible future radar waveforms that do/may occur in 3.5 GHz band. Emission spectra of the interference waveforms tested are provided in Appendix B of [3].

---

[7] BLER is defined as the number of erroneous transport data block transmissions divided by the total number of transport data block transmissions.

[8] The UE was configured by the industry participant to have a maximum possible transmit power of -10 dBm.

[9] P0N and Q3N designations are used to identify these modulations in the *NTIA Manual of Regulations and Procedures for Federal Radio Frequency Management* (the NTIA "Redbook"), Section 9.8.2. http://www.ntia.doc.gov/page/2011/manual-regulations-and-procedures-federal-radio-frequency-management-redbook

A Gaussian noise waveform, of 10 MHz bandwidth, was programmed and used in the testing. The Gaussian noise testing provided a baseline check on the results of the radar interference testing. The authors estimated, in advance of the testing, that Gaussian noise testing should verify that the LTE test bed system would yield interference effects even if some or none of radar waveforms were to produce identifiable interference effects.

The technical characteristics of the radar interference waveforms are shown for P0N and Q3N pulse modulations in Tables 1 and 2, respectively. Each entry includes a code printed in red by which each waveform was identified in the VSG's on-board memory; these codes were used in the field-data logs to identify each waveform as testing progressed. The programmed interference waveforms included a 10 MHz wide Gaussian noise waveform described above, plus a waveform similar to that of a terminal Doppler weather radar (TDWR) and two waveforms (designated ECC-1 and -2) that were used in similar previous interference testing in Europe [5].

Table 1. P0N (carrier wave) pulsed radar waveform parameters.

Duty Cycle (percent)	PRR = 1,000/sec	PRR = 3,000/sec	PRR = 10,000/sec
0.1	PW = 1 μs P0N-1	PW = 0.33 μs P0N-2	PW = 0.1 μs P0N-3
1	PW = 10 μs P0N-4	PW = 3.33 μs P0N-5	PW = 1 μs P0N-6
3	PW = 30 μs P0N-7	PW = 10 μs P0N-8	PW = 3 μs P0N-9
10	PW = 100 μs P0N-10	PW = 33.3 μs P0N-11	PW = 10 μs P0N-12

Table 2. Q3N (swept-frequency) pulsed radar waveform parameters, 1 MHz/μs chirp.

Duty Cycle (percent)	Chirped Pulse Group 1		Chirped Pulse Group 2		Chirped Pulse Group 3	
	PW (μs)	PRR (s^{-1})	PW (μs)	PRR (s^{-1})	PW (μs)	PRR (s^{-1})
1	10	1000 Q3N-1	1	10,000 Q3N-2	0.33	30,000 Q3N-3
10	100 → 10	1,000 → 10,000 Q3N-4	10	10,000 Q3N-5*	3.3	30,303 Q3N-6
20	200 → 10	1,000 → 20,000 Q3N-7	20 → 10	20,000 Q3N-8*	6.6	30,303 Q3N-9
30	300 → 10	1,000 → 30,000 Q3N-10	30 → 10	10,000 → 30,000 Q3N-11*	10	30,000 Q3N-12*

* These waveforms were not used for testing with this LTE network because they were redundant to other waveforms created when the pulse width was adjusted to maintain a maximum 10 MHz wide chirp.

Table 3. Additional special interference waveforms used in testing.

Duty Cycle (percent)	Waveform Names	PW (μs)	PRR (pulses/sec)
0.4	ECC-1 WFM-1	4	1,000
3	ECC-2 WFM-2	100	300
0.05	TDWR P0N-13	1	2,000

An overall goal of the interference waveform design was to vary interference duty cycle (DC) values in an approximately logarithmic progression: 1 percent, 3 percent 10 percent, and so forth. PW and PRR values were adjusted to achieve these DCs. For the P0N pulses, setting DC was straightforward: $DC = PW \cdot PRR$. The P0N pulses were centered at 3600 MHz for the downlink testing and 3520 MHz for the uplink testing. Two additional P0N-1 tests were performed on the downlink path at +2 MHz and +4 MHz offsets from 3600 MHz (3602 MHz and 3604 MHz, respectively).

For the Q3N (chirped) pulses, achieving the proper duty cycle can be more complicated. While the goal for a DC progression was the same for the chirped pulses as for the P0N pulses, the chirp bandwidth was an additional degree of freedom in the waveform design. The authors dealt with this by holding the chirp frequency-sweeping rate constant at 1 MHz per microsecond.[10] In order to maintain a 1 MHz/microsecond chirp rate within the 10 MHz LTE receiver bandwidth while also maintaining DC, pulse widths could not be allowed to exceed 10 μs. This adjustment to *PW* required adjustment of *PRR* to maintain duty cycle. The relationship is one of proportionality:

$$DC = \tau' \cdot PRR' = \tau_0 \cdot PRR_0$$

where τ_0 = full pulse width of a chirped radar pulse, PRR_0 = full pulse repetition rate for chirped radar pulses, τ' = reduced pulse width for testing, and PRR' = increased pulse repetition rate for testing. Since the reduced pulse widths chirped 10 MHz in 10 μs and were 10 μs long, the adjusted PRR values were computed as:

$$PRR' = \frac{\tau_0 \cdot PRR_0}{\tau'} = \frac{\tau_0 \cdot PRR_0}{10\ \mu s}$$

These adjustments are shown in Table 2. The chirp direction monotonically increased in frequency and the center frequencies of the Q3N signals were 3600 MHz and 3520 MHz for the downlink and uplink tests, respectively. Making these Q3N adjustments for PWs greater than 10 microseconds created redundant test waveforms with identical parameters. The authors decided to only use one of each of the redundant waveforms. The following waveforms were not used during this test effort: Q3N-5 (same as Q3N-4), Q3N-8 (same as Q3N-7), Q3N-11 (same as Q3N-10), and Q3N-12 (same as Q3N-10).

[10] A chirp rate of 1 MHz per microsecond represents a nominal chirp rate for modern radars.

2.3 Testing Methodology

The overall concept of the testing methodology was to measure and record the LTE diagnostics of data throughput, BLER, and MCS usage for both the downlink and uplink, and additionally UE transmit power and RB usage for the uplink. These diagnostics were recorded for a wide range of interference power levels, *I*, for every interference waveform listed in Tables 1–3 except for the redundant waveforms.

The ratio of S_{avg}/I was measured with monitoring spectrum analyzer(s) (Figure 3) in an 8 MHz resolution bandwidth, and recorded. Peak detection was used to measure radar interference power and average detection was used for the Gaussian noise interference measurements; S_{avg} was always measured using average detection, consistent with the LTE diagnostic software. The value of S_{avg}/I (in dB) was used to determine *I* in the receiver by subtracting it from the known value of S_{avg} = -75 dBm for the downlink and S_{avg} = -85 dBm for the uplink initial condition (with no interference).

Interference power, *I*, for the downlink case needed to be calculated as total power in the UE receiver downlink bandwidth of 9 MHz. For the uplink, *I* was calculated in the 7.2 MHz bandwidth of the eNB receiver (with no interference). It was assumed, for the purposes of this study, that the respective LTE receiver bandwidths were the same as the nominal emission bandwidths for the both the uplink and downlink. It is noted that for the uplink case, the UE was able to change the number of resource blocks in use, thereby changing the total bandwidth. The 7.2 MHz eNB receiver bandwidth represents the nominal 40 RBs in use by the UE when there was no interference. [11]

For each interference waveform, the testing proceeded by first establishing a communication link between the eNB and the UE in a non-interference state (that is, with the VSG RF output turned off). Interference from the VSG was then injected continuously at a power level that did not appear to affect throughput, shown on a real-time diagnostic display, while the diagnostic software recorded dedicated electronic (comma-separated variable, or CSV format) files containing several key diagnostics including: data throughput, BLER, MCS, UE transmit power, eNB received signal strength indicator (RSSI), and dedicated RBs for both the uplink and downlink. Diagnostics were recorded for approximately 60 seconds,[12] after which the recording was stopped. The interference power was then increased (usually in 5 or 10 dB increments) and the LTE diagnostic software was restarted. This process was repeated until throughput decreased to zero or until the VSG reached the maximum available output power level (while not exceeding an upper limit for reverse power into the LTE system). It should be noted that the closed loop rate control algorithm of the eNB scheduler was set to achieve a target BLER on first transmission to 10% for the downlink and 30% for the uplink.

In addition to the continuous interference tests described above, burst tests were also performed using selected radar interference waveforms. For these tests, a communication link was

[11] The average internal inherent noise level of the UE receiver was calculated based on a 7 dB noise figure (provided by the industry participant) to be -97.5 dBm in a 9 MHz bandwidth for the downlink and -98.4 dBm in a 7.2 MHz bandwidth for the uplink.

[12] 120–180 seconds for subsequent radar interference burst testing.

established and the diagnostic software was started. Radar interference was then injected by bursting 20 radar pulses,[13] with the PWs and PRRs described in Tables 1–3, every 5 seconds. This simulated a radar azimuthal scan with a 72 degree/sec rotation rate. For all burst tests performed on the downlink, the interference power level, *I*, was set such that it was equal to or greater than the value of *I* that caused significant throughput degradation during the respective continuous test. For the uplink case, the interference power level, *I*, was set to -25 dBm. For the downlink, *I* was between -50 dBm and -30 dBm. Diagnostics were recorded for approximately 120–180 seconds with the interference on. For the downlink case radar waveforms P0N-5, P0N-8, P0N-11, Q3N-1, Q3N-4, Q3N-7, and Q3N-10 were burst-tested. For the uplink case radar waveforms P0N-1, P0N-2, P0N-5, P0N-8, P0N-10, P0N-11, Q3N-1, Q3N-4, Q3N-6, Q3N-7, Q3N-9, and Q3N-10 were burst-tested. More cases were tested for the uplink because the authors believe this is the real-world scenario in which interference would be the most prominent.

[13] For volume air-search radars in general, a nominal 15 to 20 pulse echo returns must be integrated to declare a target.

3 INTERFERENCE-EFFECTS TEST RESULTS

3.1 Downlink Interference-Effects Results

3.1.1 Continuous Interference Testing

Figures 4–29 show the effects of radar waveform interference and Gaussian noise interference on LTE UE receiver (downlink) data throughput (blue, upper line) and BLER (green, lower line). For each data point on each graph, the circle indicates the mean throughput or BLER as calculated from all of the data samples recorded by the diagnostic software for each interference waveform power level. The number of samples used to calculate mean and standard deviation was approximately 100 for throughput and over 2,000 for BLER. The error bars associated with each point show the standard deviation from the mean. In the figures, a smoothing spline was used to demonstrate general trends for both throughput and BLER.

Each plot is followed by a table (Tables 5–30) indicating how the MCS was affected by the interference waveforms as the interference power level was varied. Downlink multi-antenna transmissions are reported with a “Rank 1” or “Rank 2” label in each table and are mutually exclusive. These rank values indicate the number of useful transmission layers as determined from UE reporting and, ultimately, indicate the transmission mode used by the test bed network at any given time [6]. In addition to showing which MCSs were used in each rank, the tables also indicate what percentage of the time each rank was used during the data recording for the given interference power level, *I*.

The interference power levels, *I*, shown in the MCS tables coincide with the points in the graph showing the effects of the same interference waveform on throughput and BLER. Table 4 provides a key indicating what each of the numbers in the MCS tables means in terms of MCS, channel quality indicator (CQI) and spectral efficiency [7].

The LTE network was configured to have a signal to noise ratio (*S/N)* of +22.5 dB for the baseline downlink condition (with no interference) and was set by the industry participant as standard practice.

Table 4. Relationship between MCS, CQI, modulation, and spectral efficiency.

MCS	CQI	Modulation	Spectral Efficiency	MCS	CQI	Modulation	Spectral Efficiency
0	2	QPSK	0.2344	16	9	16 QAM	2.5684
1			0.3057	17		64 QAM	2.5684
2	3		0.3770	18	10		2.7305
3			0.4893	19			3.0264
4	4		0.6016	20	11		3.3223
5			0.7393	21			3.6123
6	5		0.8770	22	12		3.9023
7			1.0264	23			4.2128
8	6		1.1758	24	13		4.5234
9			1.3262	25			4.8193
10		16 QAM	1.3262	26	14		5.1152
11	7		1.4766	27			5.3349
12			1.6953	28	15		5.5547
13	8		1.9141	29		QPSK	Reserved
14			2.1602	30		16 QAM	
15	9		2.4063	31		64 QAM	

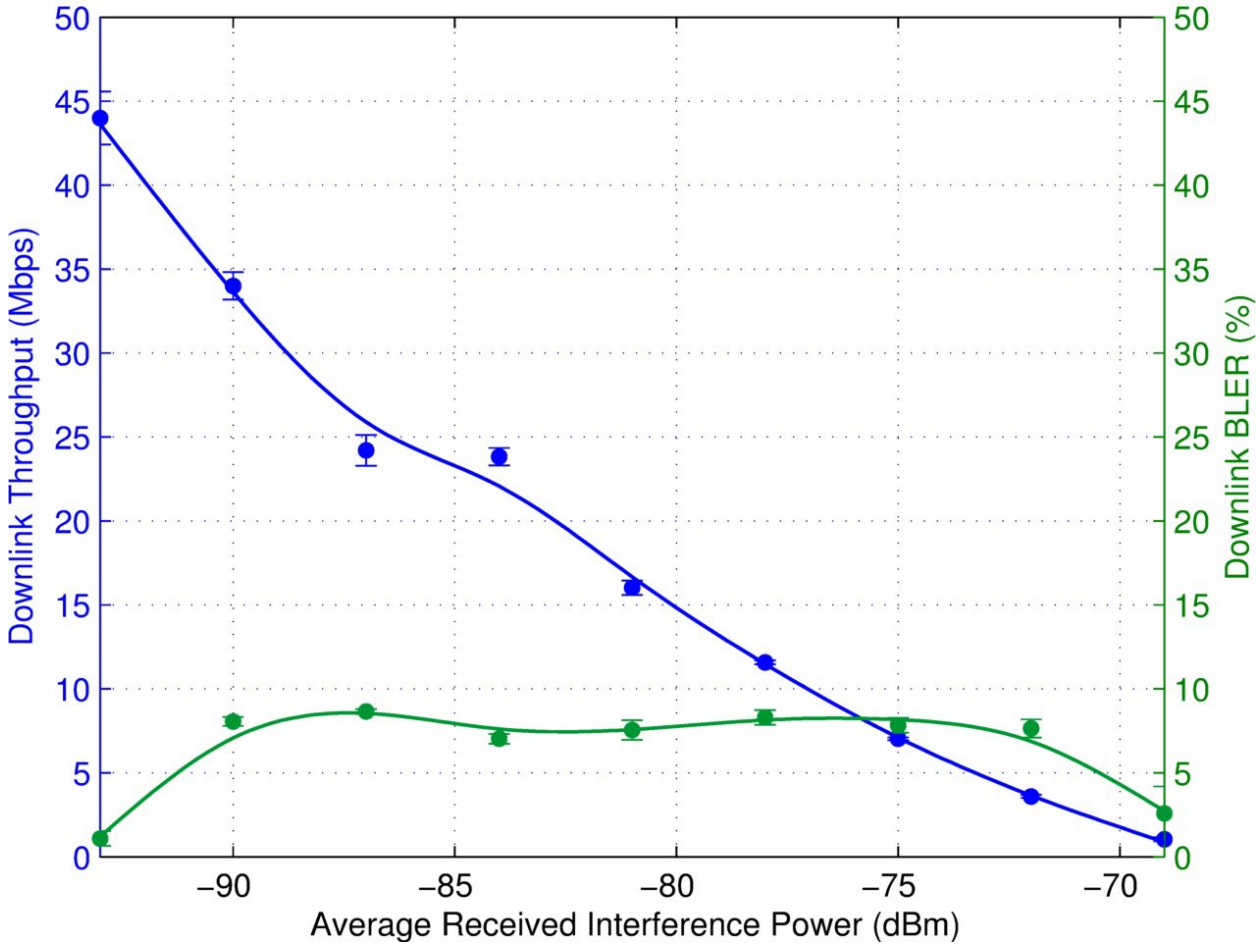

Figure 4. Data throughput and BLER for 10 MHz wide Gaussian noise interference.

Table 5. MCS state for 10 MHz wide Gaussian noise interference.

I dBm	Rank 1				Rank 2						
					Channel 0			Channel 1			% Time Used
	Min MCS	Most Frequent MCS	Max MCS	% Time Used	Min MCS	Most Frequent MCS	Max MCS	Min MCS	Most Frequent MCS	Max MCS	
-93	2	23	23	1.90	7	23	23	1	23	23	98.10
-90	6	22	22	1.80	9	22	23	9	22	23	98.20
-87	10	19	22	0.75	4	19	21	2	19	21	99.25
-84	15	16	16	3.70	13	15	23	13	15	23	96.30
-81	3	13	18	2.72	4	11	23	8	11	15	97.28
-78	0	9	10	1.49	6	8	13	4	8	23	98.51
-75	4	6	22	2.42	3	5	22	3	5	23	97.58
-72	1	2	3	2.11	0	2	23	0	2	14	97.89
-69	0	0	15	98.23	0	0	23	0	0	23	1.77

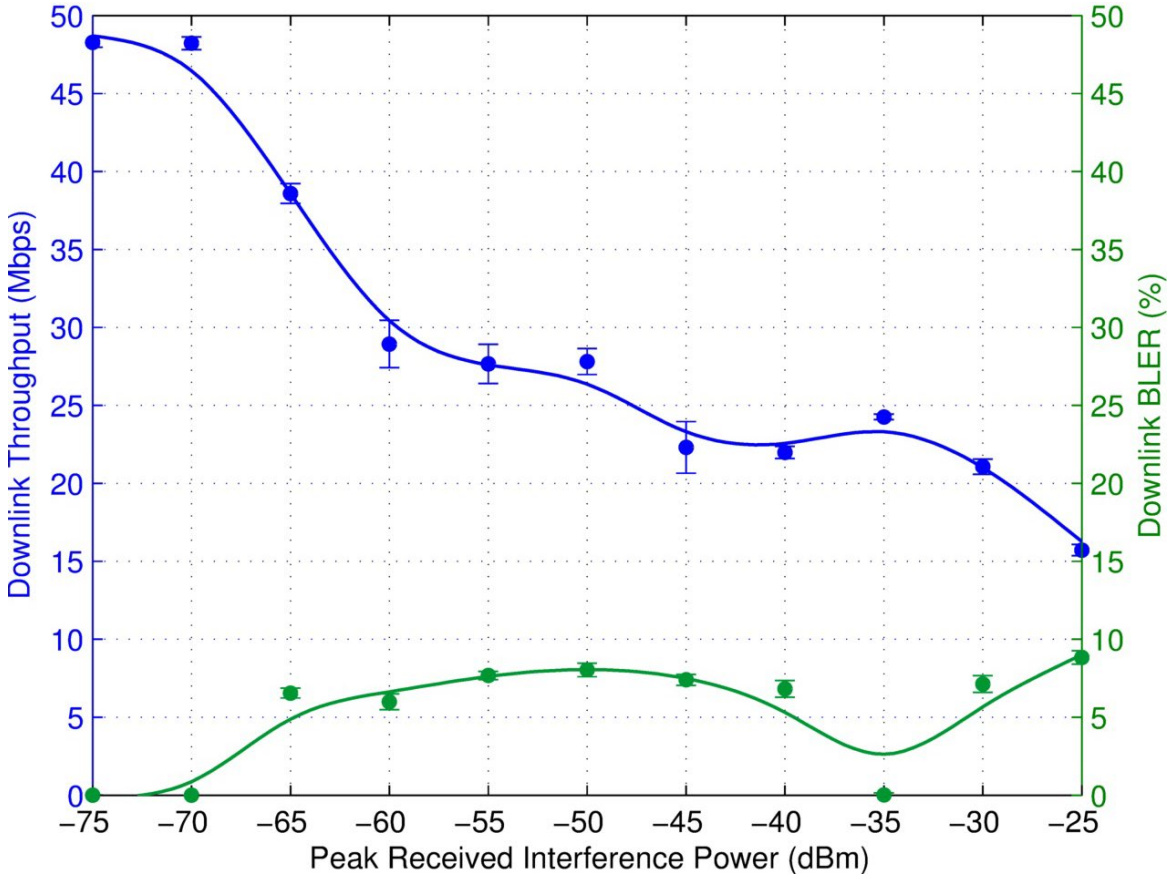

Figure 5. Data throughput and BLER for P0N-1 (PW = 1 µs, PRR = 1,000/sec, DC = 0.1%) interference.

Table 6. MCS state for P0N-1 (PW = 1 µs, PRR = 1000/sec, DC = 0.1%) interference.

I dBm	Rank 1				Rank 2						
					Channel 0			Channel 1			% Time Used
	Min MCS	Most Frequent MCS	Max MCS	% Time Used	Min MCS	Most Frequent MCS	Max MCS	Min MCS	Most Frequent MCS	Max MCS	
-75	N/A	N/A	N/A	0	2	23	23	14	23	23	100
-70	N/A	N/A	N/A	0	16	23	23	7	23	23	100
-65	N/A	N/A	N/A	0	1	22	23	6	22	23	100
-60	N/A	N/A	N/A	0	6	21	23	15	21	23	100
-55	N/A	N/A	N/A	0	6	20	23	5	20	23	100
-50	N/A	N/A	N/A	0	10	19	23	1	19	23	100
-45	N/A	N/A	N/A	0	11	15	23	11	15	23	100
-40	N/A	N/A	N/A	0	5	14	23	7	14	23	100
-35	N/A	N/A	N/A	0	3	21	23	0	21	23	100
-30	N/A	N/A	N/A	0	2	14	23	3	14	23	100
-25	N/A	N/A	N/A	0	7	12	17	3	12	16	100

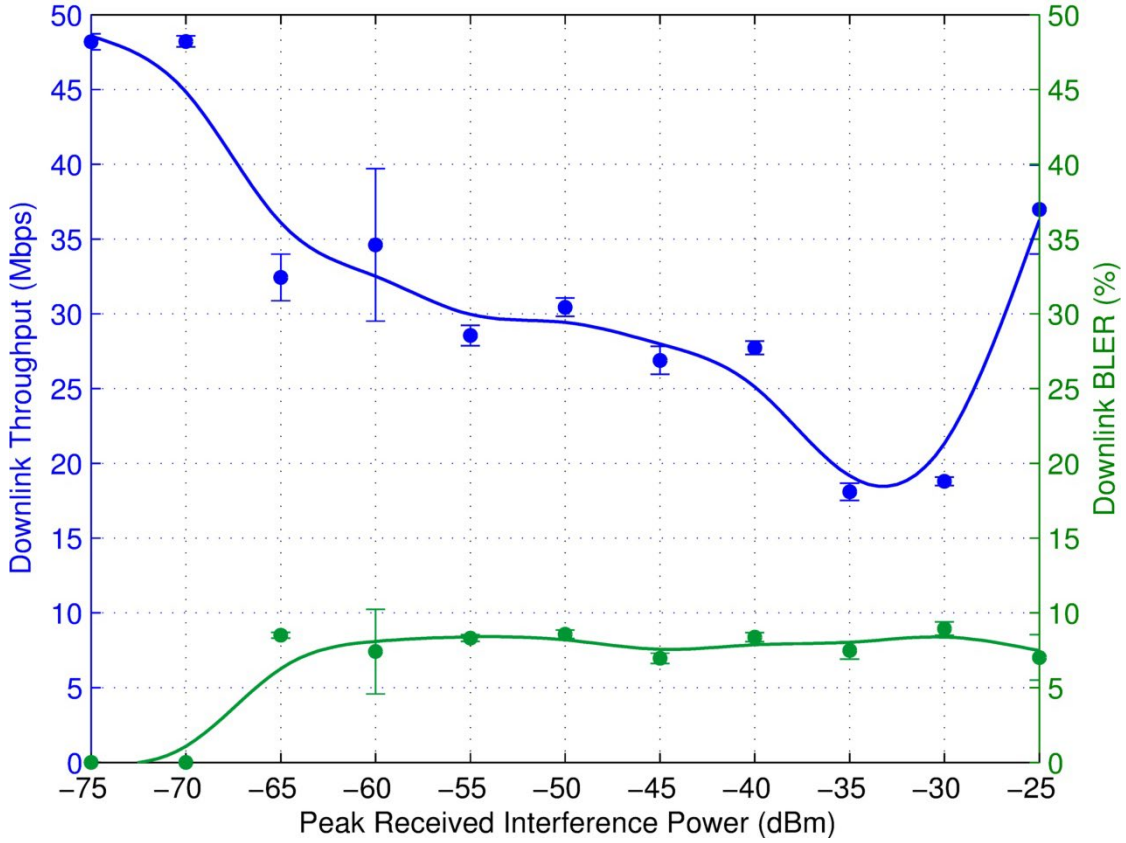

Figure 6. Data throughput and BLER for P0N-1 (PW = 1 µs, PRR = 1,000/sec, DC = 0.1%) interference off-tuned from the LTE eNB center transmit frequency by 2 MHz.

Table 7. MCS state for P0N-1 (PW = 1 µs, PRR = 1000/sec, DC = 0.1%) interference off-tuned from the LTE eNB center transmit frequency by 2 MHz.

I dBm	Rank 1				Rank 2						
					Channel 0			Channel 1			% Time Used
	Min MCS	Most Frequent MCS	Max MCS	% Time Used	Min MCS	Most Frequent MCS	Max MCS	Min MCS	Most Frequent MCS	Max MCS	
-75	6	6	10	0.01	4	23	23	1	23	23	99.99
-70	12	12	12	0.00	17	23	23	7	23	23	100.00
-65	23	23	23	0.80	1	23	23	4	23	23	99.20
-60	21	22	23	0.80	15	22	23	12	22	23	99.20
-55	4	20	23	1.06	3	20	23	7	20	23	98.94
-50	20	21	21	0.73	17	20	23	2	20	23	99.27
-45	16	19	21	3.27	3	19	23	8	19	23	96.73
-40	5	20	23	1.05	3	19	23	1	19	23	98.95
-35	9	14	23	2.44	8	13	23	8	13	23	97.56
-30	3	14	23	0.12	1	13	23	9	13	23	99.88
-25	5	23	23	2.81	7	22	23	9	22	23	97.19

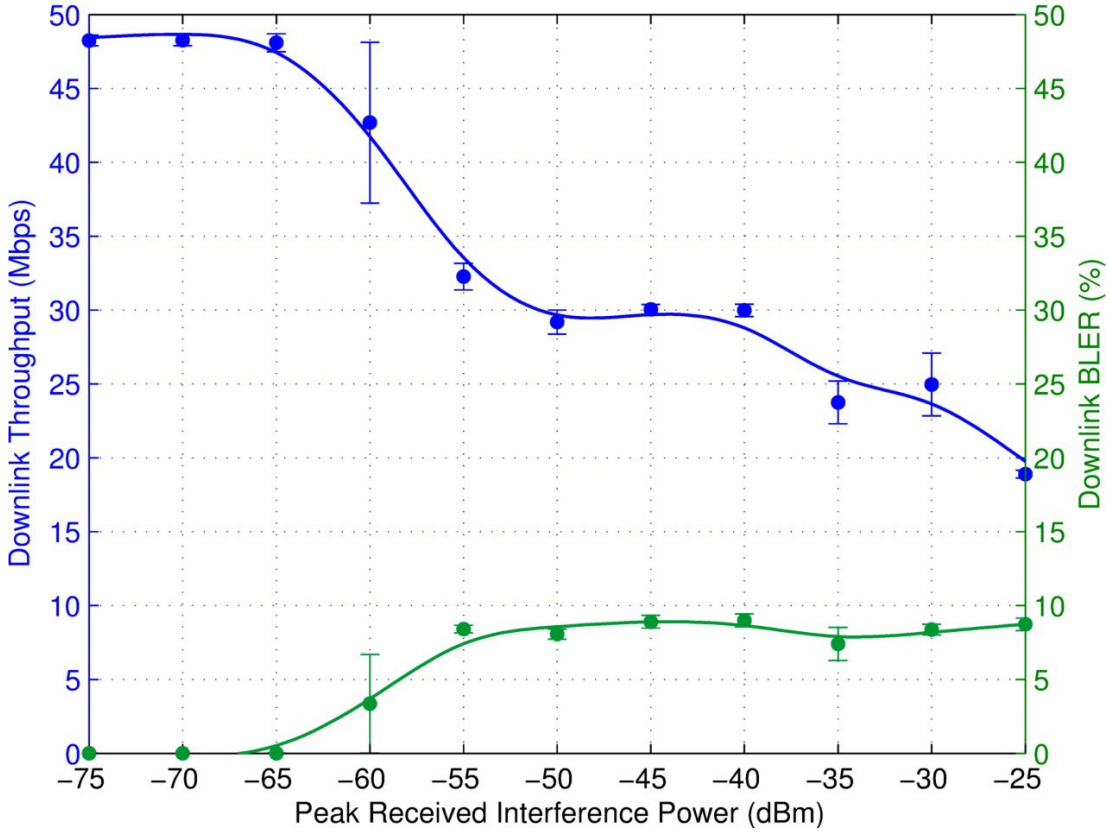

Figure 7. Data throughput and BLER for P0N-1 (PW = 1 µs, PRR = 1,000/sec, DC = 0.1%) interference off-tuned from the LTE eNB center transmit frequency by 4 MHz.

Table 8. MCS state for P0N-1 (PW = 1 µs, PRR = 1000/sec, DC = 0.1%) interference off-tuned from the LTE eNB center transmit frequency by 4 MHz.

I dBm	Rank 1				Rank 2						
					Channel 0			Channel 1			% Time Used
	Min MCS	Most Frequent MCS	Max MCS	% Time Used	Min MCS	Most Frequent MCS	Max MCS	Min MCS	Most Frequent MCS	Max MCS	
-75	N/A	N/A	N/A	0.00	0	23	23	7	23	23	100.00
-70	10	23	23	0.08	12	23	23	4	23	23	99.92
-65	21	23	23	0.37	1	23	23	4	23	23	99.63
-60	3	23	23	2.46	13	23	23	6	23	23	97.54
-55	9	21	23	1.21	3	22	23	8	22	23	98.79
-50	19	20	23	1.79	10	20	23	0	20	23	98.21
-45	18	20	21	0.29	14	19	22	13	19	22	99.71
-40	6	20	21	0.14	4	19	21	15	19	23	99.86
-35	7	16	23	2.71	4	18	23	0	18	23	97.29
-30	15	19	20	1.28	1	19	21	7	19	22	98.72
-25	13	14	22	0.57	9	13	19	9	13	18	99.43

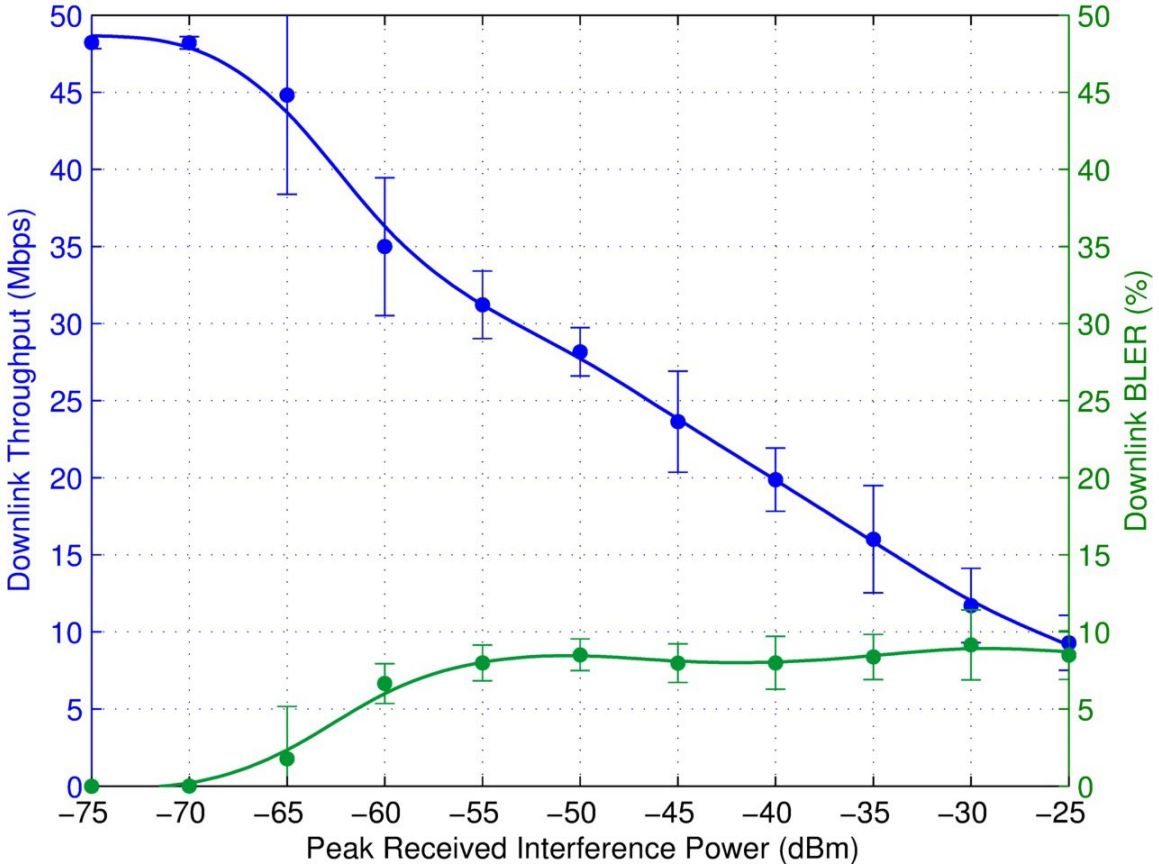

Figure 8. Data throughput and BLER for P0N-2 (PW = 0.33 µs, PRR = 3,000/sec, DC = 0.1%) interference.

Table 9. MCS state for P0N-2 (PW = 0.33 µs, PRR = 3000/sec, DC = 0.1%) interference.

I dBm	Rank 1				Rank 2						
					Channel 0			Channel 1			% Time Used
	Min MCS	Most Frequent MCS	Max MCS	% Time Used	Min MCS	Most Frequent MCS	Max MCS	Min MCS	Most Frequent MCS	Max MCS	
-75	N/A	N/A	N/A	0	14	23	23	13	23	23	100
-70	N/A	N/A	N/A	0	1	23	23	13	23	23	100
-65	N/A	N/A	N/A	0	0	23	23	0	23	23	100
-60	N/A	N/A	N/A	0	4	23	23	0	23	23	100
-55	N/A	N/A	N/A	0	11	21	23	8	21	23	100
-50	N/A	N/A	N/A	0	7	18	23	7	18	23	100
-45	N/A	N/A	N/A	0	0	18	23	3	18	23	100
-40	N/A	N/A	N/A	0	0	14	23	0	14	23	100
-35	N/A	N/A	N/A	0	0	13	23	0	13	23	100
-30	N/A	N/A	N/A	0	0	6	22	0	6	22	100
-25	N/A	N/A	N/A	0	0	6	23	0	6	23	100

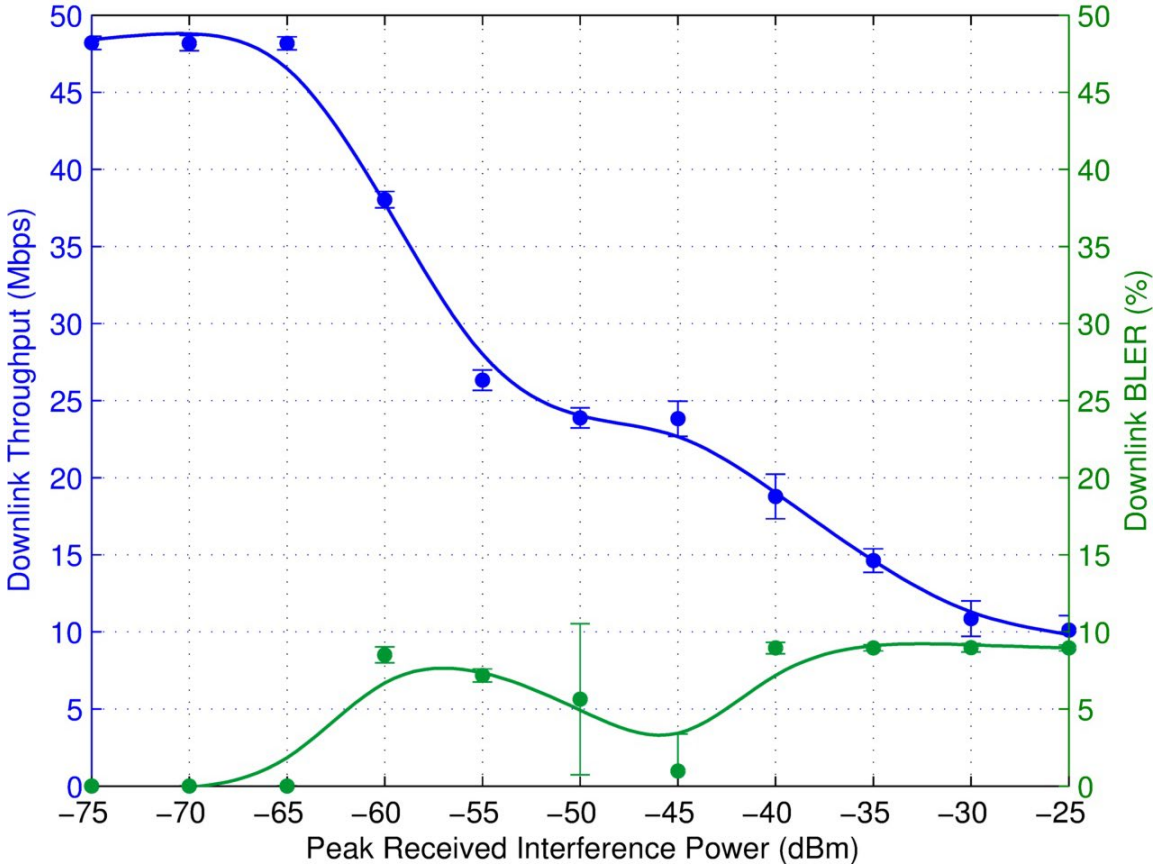

Figure 9. Data throughput and BLER for P0N-3 (PW = 0.1 µs, PRR = 10,000/sec, DC = 0.1%) interference.

Table 10. MCS state for P0N-3 (PW = 0.1 µs, PRR = 10,000/sec, DC = 0.1%) interference.

I dBm	Rank 1				Rank 2						
					Channel 0			Channel 1			% Time Used
	Min MCS	Most Frequent MCS	Max MCS	% Time Used	Min MCS	Most Frequent MCS	Max MCS	Min MCS	Most Frequent MCS	Max MCS	
-75	N/A	N/A	N/A	0.00	9	23	23	2	23	23	100.00
-70	N/A	N/A	N/A	0.00	10	23	23	12	23	23	100.00
-65	N/A	N/A	N/A	0.00	23	23	23	23	23	23	100.00
-60	N/A	N/A	N/A	0.00	2	21	23	1	21	23	100.00
-55	N/A	N/A	N/A	0.00	14	19	23	4	19	23	100.00
-50	N/A	N/A	N/A	0.00	5	23	23	4	23	23	100.00
-45	N/A	N/A	N/A	0.00	0	6	23	3	6	23	100.00
-40	1	22	23	99.76	0	0	11	0	0	20	0.24
-35	11	18	21	99.99	4	4	15	0	18	18	0.01
-30	N/A	N/A	N/A	0.00	10	10	19	8	8	13	100.00
-25	1	13	23	99.50	23	23	23	23	23	23	0.50

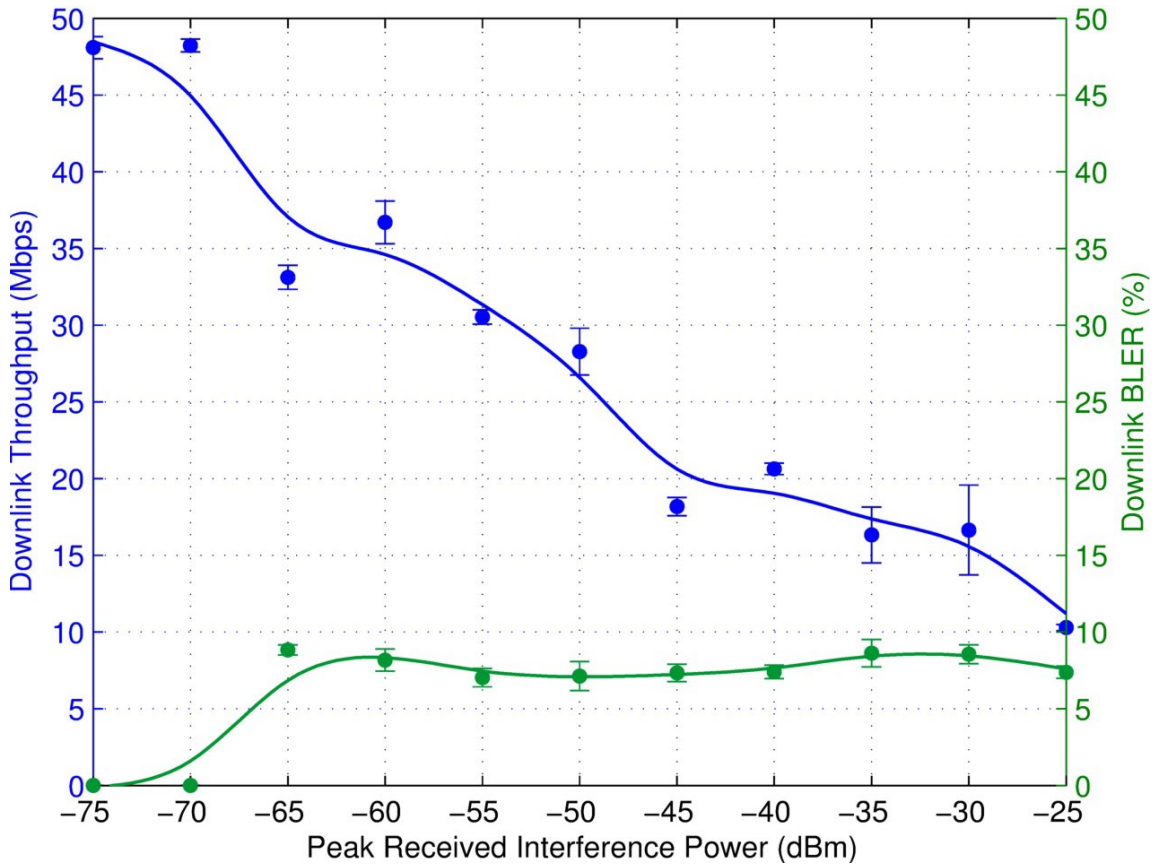

Figure 10. Data throughput and BLER for P0N-4 (PW = 10 µs, PRR = 1,000/sec, DC = 1.0%) interference.

Table 11. MCS state for P0N-4 (PW = 10 µs, PRR = 1000/sec, DC = 1.0%) interference.

I dBm	Rank 1				Rank 2						
					Channel 0			Channel 1			% Time Used
	Min MCS	Most Frequent MCS	Max MCS	% Time Used	Min MCS	Most Frequent MCS	Max MCS	Min MCS	Most Frequent MCS	Max MCS	
-75	N/A	N/A	N/A	0.00	17	23	23	6	23	23	100.00
-70	5	5	18	0.01	23	23	23	5	23	23	99.99
-65	0	0	23	0.27	6	22	23	19	22	23	99.73
-60	0	0	23	1.96	2	22	23	12	22	23	98.04
-55	0	20	20	3.27	8	19	23	2	19	23	96.73
-50	0	0	23	3.13	1	19	23	0	19	23	96.87
-45	0	14	23	2.98	0	13	23	5	13	23	97.02
-40	0	0	23	2.68	11	14	23	6	14	23	97.32
-35	0	0	22	0.79	4	12	23	4	12	23	99.21
-30	0	0	21	0.88	5	13	22	3	13	22	99.12
-25	0	8	22	2.82	4	7	20	4	7	21	97.18

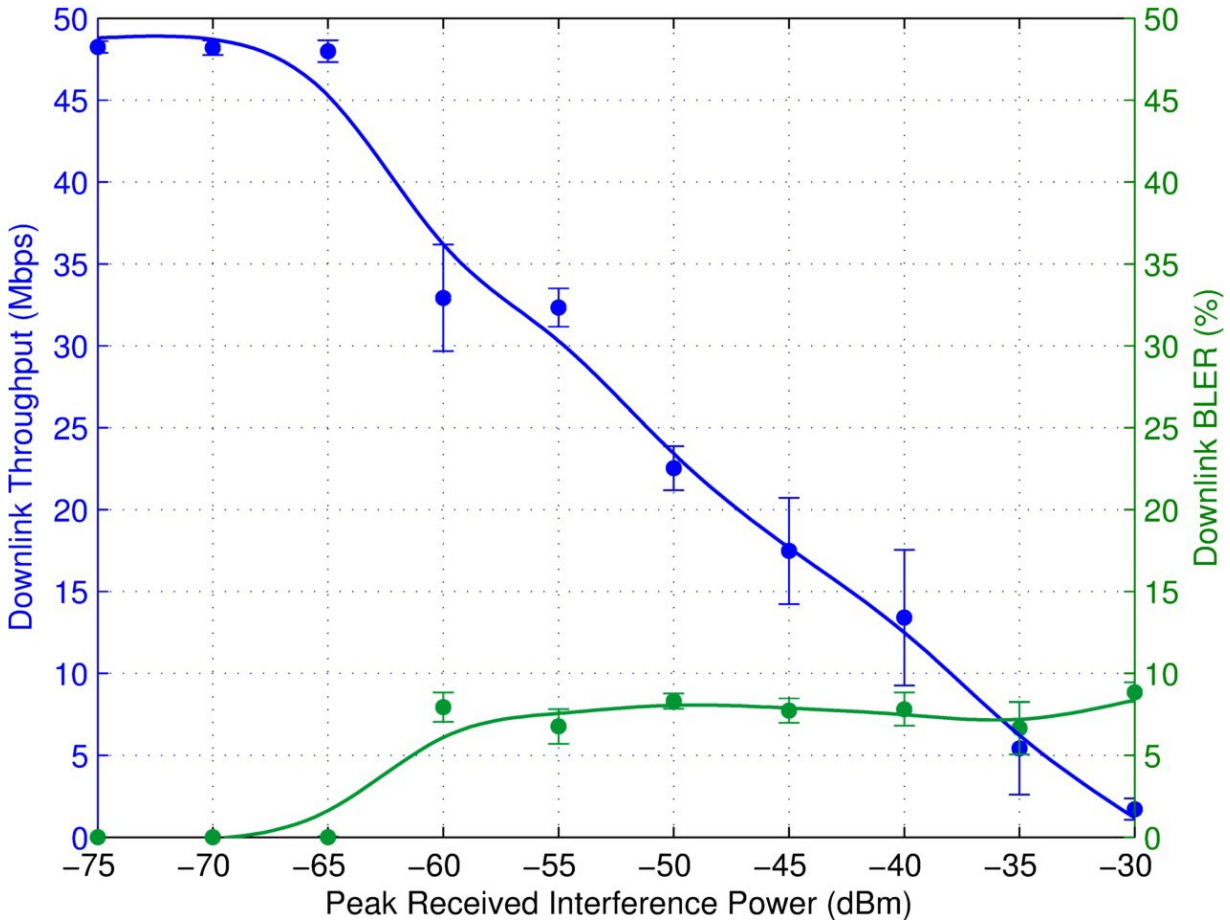

Figure 11. Data throughput and BLER for P0N-5 (PW = 3.33 µs, PRR = 3,000/sec, DC = 1%) interference.

Table 12. MCS state for P0N-5 (PW = 3.33 µs, PRR = 3,000/sec, DC = 1%) interference.

I dBm	Rank 1				Rank 2						
					Channel 0			Channel 1			% Time Used
	Min MCS	Most Frequent MCS	Max MCS	% Time Used	Min MCS	Most Frequent MCS	Max MCS	Min MCS	Most Frequent MCS	Max MCS	
-75	13	13	13	0.00	1	23	23	4	23	23	100.00
-70	3	11	23	0.01	5	23	23	23	23	23	99.99
-65	0	0	23	0.07	23	23	23	7	23	23	99.93
-60	0	21	23	2.13	8	21	23	1	21	23	97.87
-55	0	21	22	3.68	13	20	23	3	20	23	96.32
-50	0	0	23	1.32	7	15	23	1	15	23	98.68
-45	0	0	23	4.22	3	13	23	0	13	23	95.78
-40	0	11	17	4.49	2	7	23	2	7	23	95.51
-35	0	8	23	39.67	0	5	23	0	5	23	60.33
-30	0	2	23	94.69	0	23	23	0	23	23	5.31

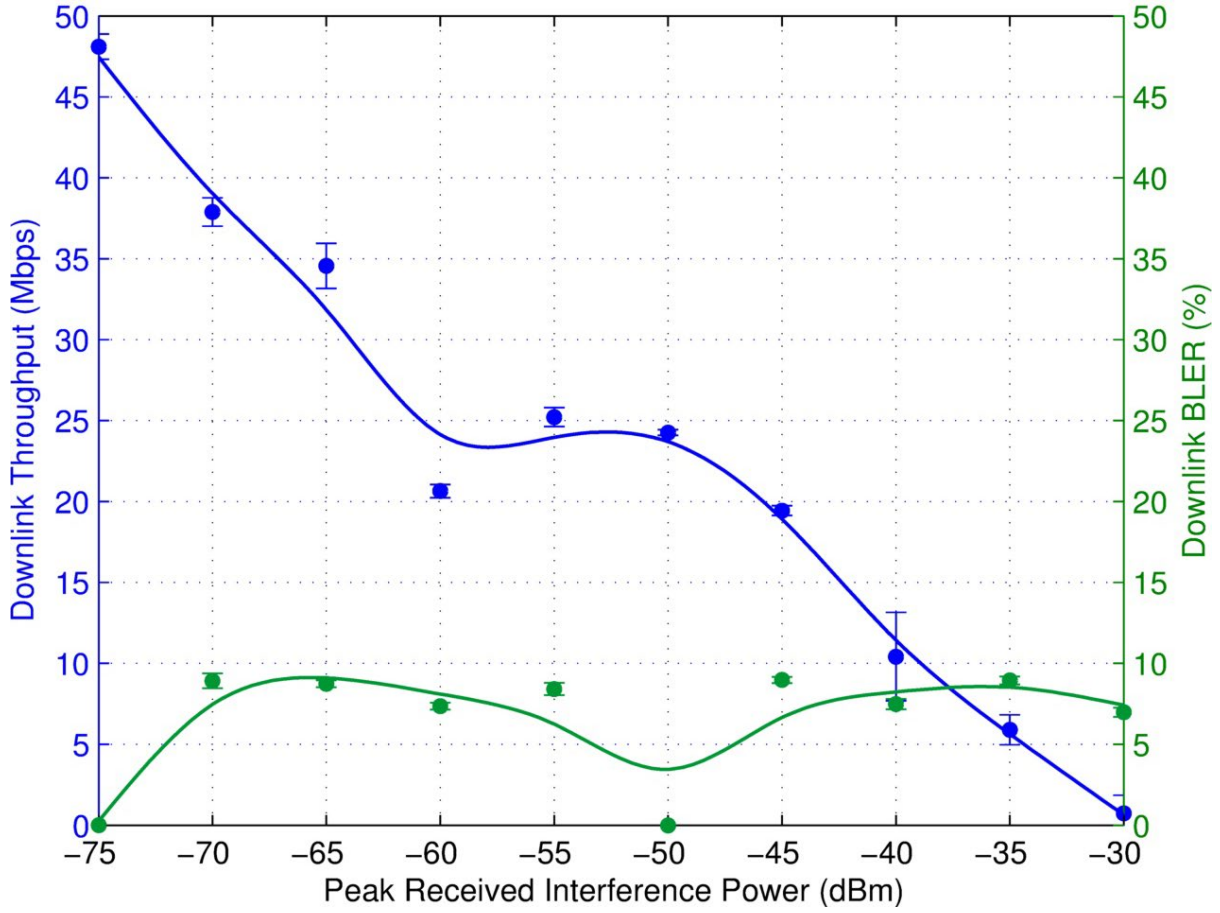

Figure 12. Data throughput and BLER for P0N-6 (PW = 1.0 µs, PRR = 10,000/sec, DC = 1%) interference.

Table 13. MCS state for P0N-6 (PW = 1.0 µs, PRR = 10,000/sec, DC = 1%) interference.

I dBm	Rank 1				Rank 2						
					Channel 0			Channel 1			% Time Used
	Min MCS	Most Frequent MCS	Max MCS	% Time Used	Min MCS	Most Frequent MCS	Max MCS	Min MCS	Most Frequent MCS	Max MCS	
-75	0	0	23	0.01	5	23	23	2	23	23	99.99
-70	0	22	23	0.19	19	21	23	5	21	23	99.81
-65	0	0	23	0.40	9	23	23	2	23	23	99.60
-60	0	0	23	2.91	11	14	23	4	14	23	97.09
-55	0	0	19	1.20	2	18	23	14	18	23	98.80
-50	20	23	23	99.99	13	14	23	2	20	20	0.01
-45	17	22	23	99.26	0	23	23	10	23	23	0.74
-40	0	17	23	99.21	3	23	23	9	23	23	0.79
-35	1	8	23	99.25	2	23	23	3	23	23	0.75
-30	0	4	23	46.31	9	23	23	9	23	23	53.69

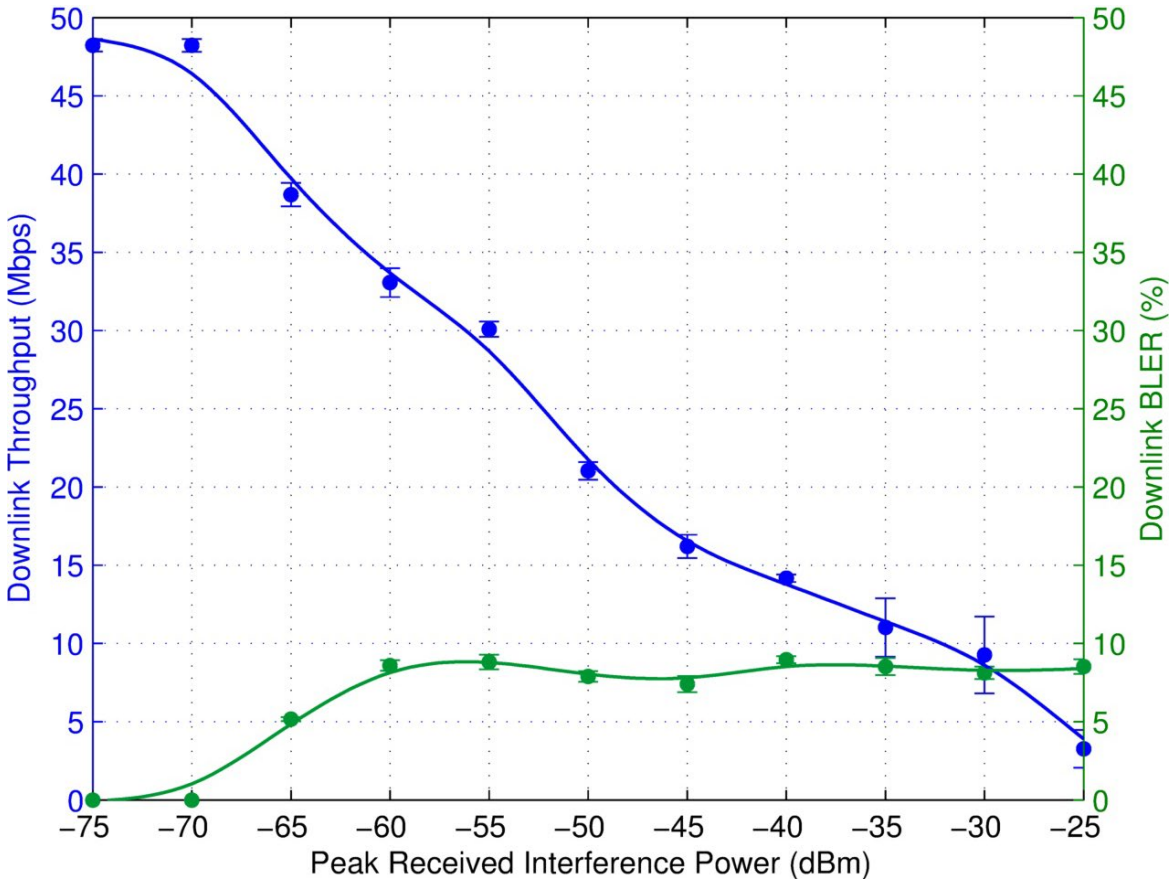

Figure 13. Data throughput and BLER for P0N-7 (PW = 30 µs, PRR = 1,000/sec, DC = 3%) interference.

Table 14. MCS state for P0N-7 (PW = 30 µs, PRR = 1,000/sec, DC = 3%) interference.

I dBm	Rank 1				Rank 2						
					Channel 0			Channel 1			% Time Used
	Min MCS	Most Frequent MCS	Max MCS	% Time Used	Min MCS	Most Frequent MCS	Max MCS	Min MCS	Most Frequent MCS	Max MCS	
-75	0	0	23	0.01	13	23	23	5	23	23	99.99
-70	N/A	N/A	N/A	0.00	5	23	23	10	23	23	100.00
-65	0	23	23	0.01	9	23	23	2	23	23	99.99
-60	0	22	23	0.72	4	22	23	2	22	23	99.28
-55	0	0	20	0.41	3	18	23	4	18	23	99.59
-50	0	0	22	1.93	5	15	22	12	15	22	98.07
-45	0	18	23	32.83	2	12	23	5	12	23	67.17
-40	0	18	23	96.38	2	11	23	2	11	23	3.62
-35	0	15	23	98.86	4	23	23	4	23	23	1.14
-30	1	15	23	98.88	4	23	23	4	23	23	1.12
-25	0	6	23	97.18	3	23	23	2	23	23	2.82

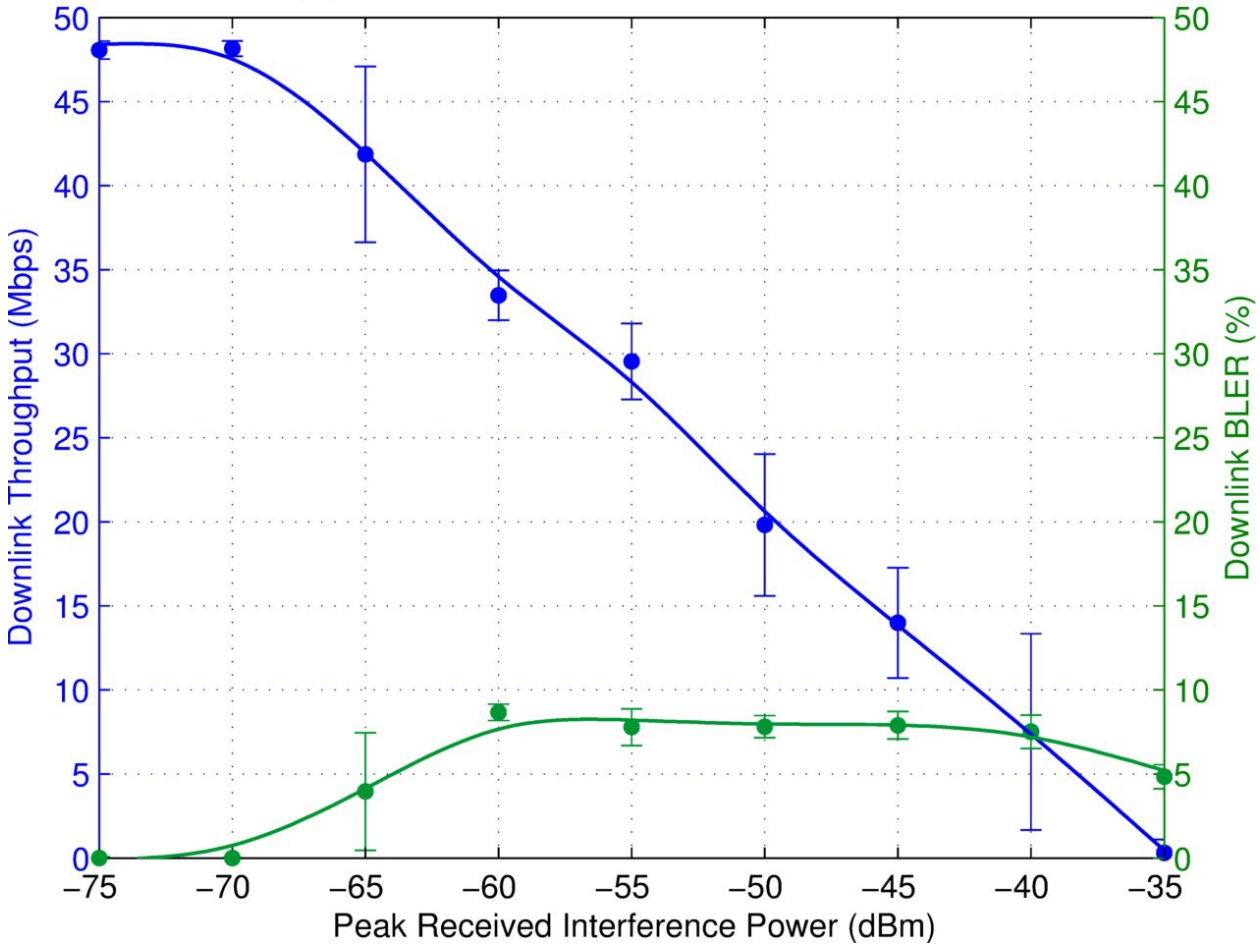

Figure 14. Data throughput and BLER for P0N-8 (PW = 10 µs, PRR = 3,000/sec, DC = 3%) interference.

Table 15. MCS state for P0N-8 (PW = 10 µs, PRR = 3,000/sec, DC = 3%) interference.

I dBm	Rank 1				Rank 2						
					Channel 0			Channel 1			% Time Used
	Min MCS	Most Frequent MCS	Max MCS	% Time Used	Min MCS	Most Frequent MCS	Max MCS	Min MCS	Most Frequent MCS	Max MCS	
-75	0	0	23	0.03	23	23	23	21	23	23	99.97
-70	9	9	9	0.00	4	23	23	2	23	23	100.00
-65	0	0	23	1.55	5	23	23	8	23	23	98.45
-60	0	0	23	0.62	2	22	23	11	22	23	99.38
-55	0	0	23	1.96	2	20	23	5	20	23	98.04
-50	0	0	23	3.72	3	15	23	3	15	23	96.28
-45	0	0	23	6.37	0	12	23	0	12	23	93.63
-40	0	8	23	9.63	0	6	23	0	6	23	90.37
-35	0	0	23	62.39	0	23	23	0	23	23	37.61

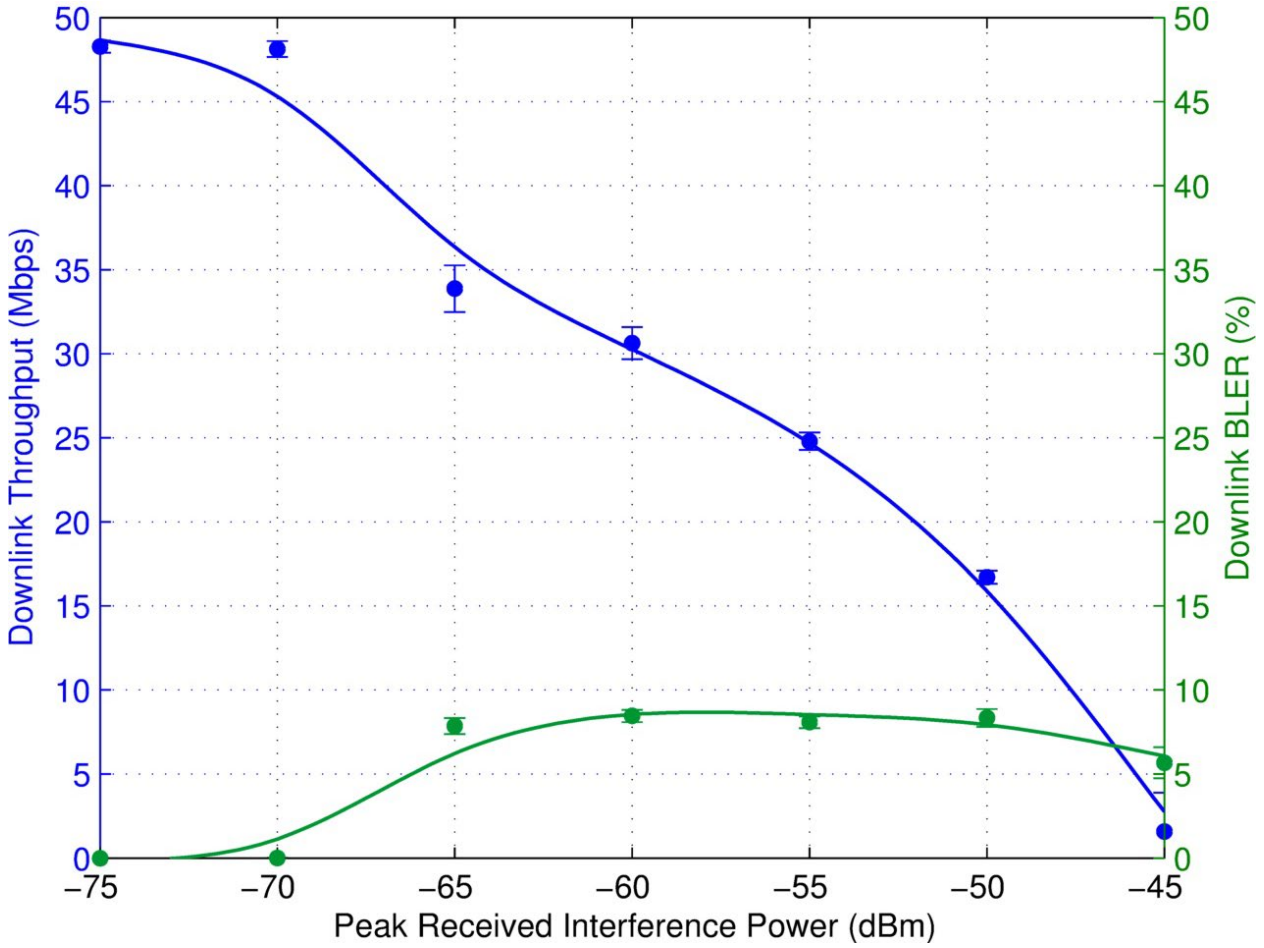

Figure 15. Data throughput and BLER for P0N-9 (PW = 3 µs, PRR = 10,000/sec, DC = 3%) interference.

Table 16. MCS state for P0N-9 (PW = 3 µs, PRR = 10,000/sec, DC = 3%) interference.

I dBm	Rank 1				Rank 2						
					Channel 0			Channel 1			% Time Used
	Min MCS	Most Frequent MCS	Max MCS	% Time Used	Min MCS	Most Frequent MCS	Max MCS	Min MCS	Most Frequent MCS	Max MCS	
-75	N/A	N/A	N/A	0.00	3	23	23	7	23	23	100.00
-70	0	23	23	0.02	11	23	23	0	23	23	99.98
-65	0	23	23	1.89	4	23	23	10	23	23	98.11
-60	0	0	22	1.00	3	21	23	7	21	23	99.00
-55	0	0	23	1.53	10	18	23	12	18	23	98.47
-50	0	0	19	1.14	8	12	19	5	12	19	98.86
-45	0	8	23	30.24	0	23	23	0	23	23	69.76

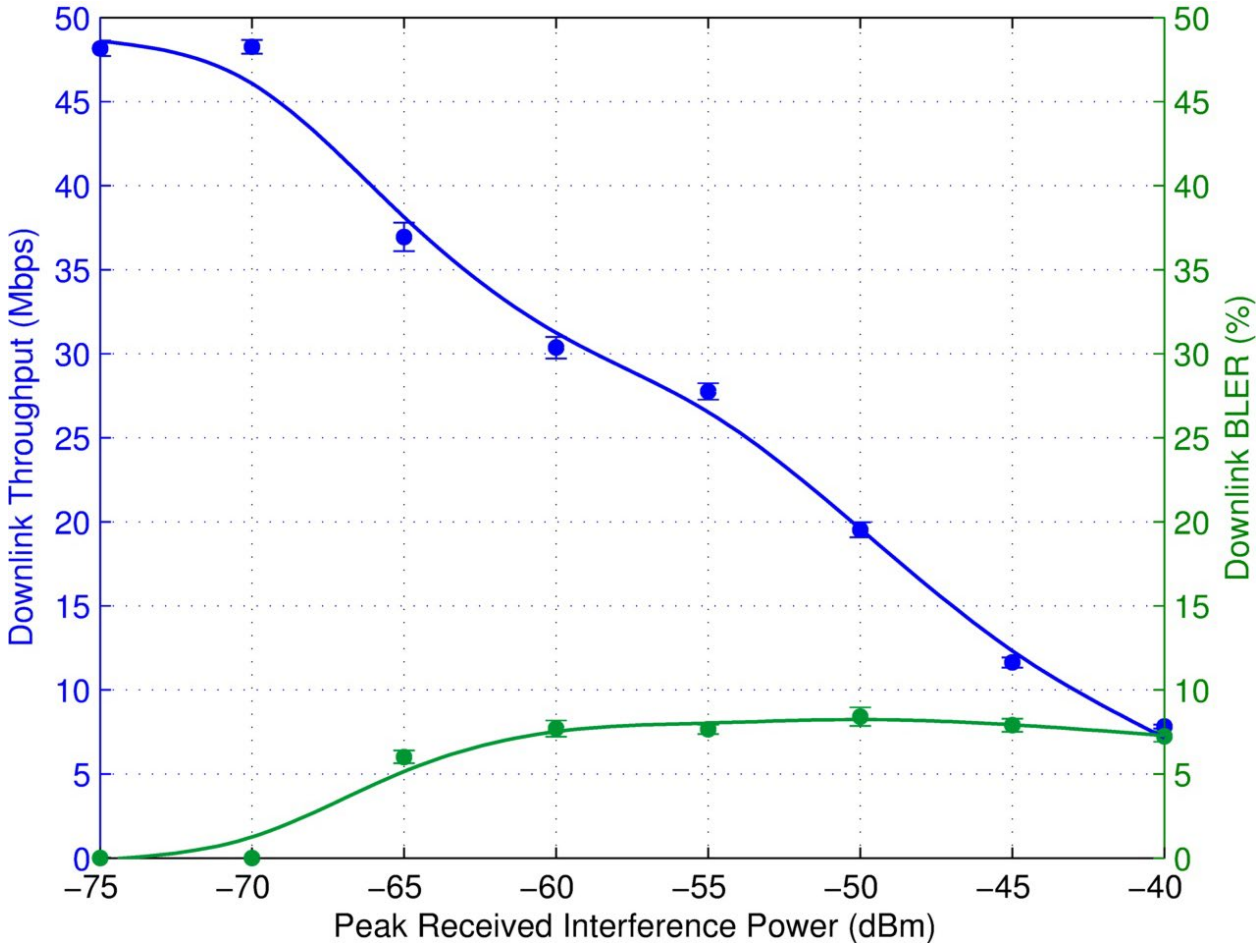

Figure 16. Data throughput and BLER for P0N-10 (PW = 100 µs, PRR = 1,000/sec, DC = 10%) interference.

Table 17. MCS state for P0N-10 (PW = 100 µs, PRR = 1,000/sec, DC = 10%) interference.

I dBm	Rank 1				Rank 2						
					Channel 0			Channel 1			% Time Used
	Min MCS	Most Frequent MCS	Max MCS	% Time Used	Min MCS	Most Frequent MCS	Max MCS	Min MCS	Most Frequent MCS	Max MCS	
-75	18	18	18	0.00	16	23	23	2	23	23	100.00
-70	N/A	N/A	N/A	0.00	1	23	23	5	23	23	100.00
-65	0	23	23	5.35	9	22	23	10	22	23	94.65
-60	0	21	21	2.29	2	20	23	5	20	23	97.71
-55	0	0	19	2.29	10	18	23	1	18	23	97.71
-50	0	15	20	1.26	11	12	23	1	12	20	98.74
-45	0	8	15	2.04	5	8	17	3	8	17	97.96
-40	0	0	23	3.21	0	5	23	2	5	23	96.79

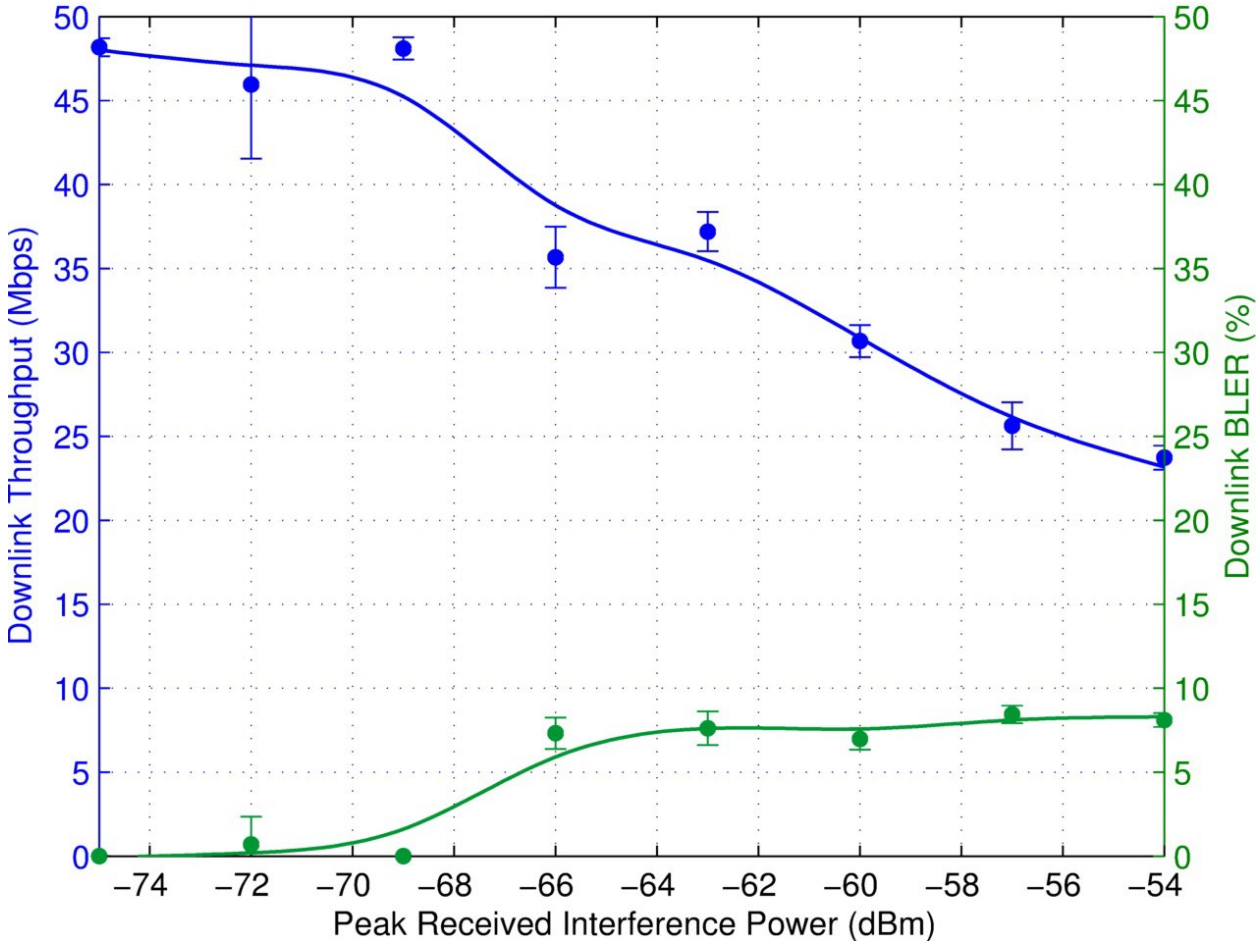

Figure 17. Data throughput and BLER for P0N-11 (PW = 33.3 µs, PRR = 3,000/sec, DC = 10%) interference.

Table 18. MCS state for P0N-11 (PW = 33.3 µs, PRR = 3,000/sec, DC = 10%) interference.

I dBm	Rank 1				Rank 2						
					Channel 0			Channel 1			% Time Used
	Min MCS	Most Frequent MCS	Max MCS	% Time Used	Min MCS	Most Frequent MCS	Max MCS	Min MCS	Most Frequent MCS	Max MCS	
-75	N/A	N/A	N/A	0.00	1	23	23	1	23	23	100.00
-72	0	23	23	1.65	9	23	23	2	23	23	98.35
-69	0	0	23	0.02	1	23	23	4	23	23	99.98
-66	0	0	23	1.60	20	23	23	19	23	23	98.40
-63	0	0	23	2.06	4	22	23	17	22	23	97.94
-60	0	0	22	3.25	12	20	23	7	20	23	96.75
-57	0	0	23	1.16	0	18	23	9	18	23	98.84
-54	0	0	23	1.67	11	17	23	0	17	23	98.33

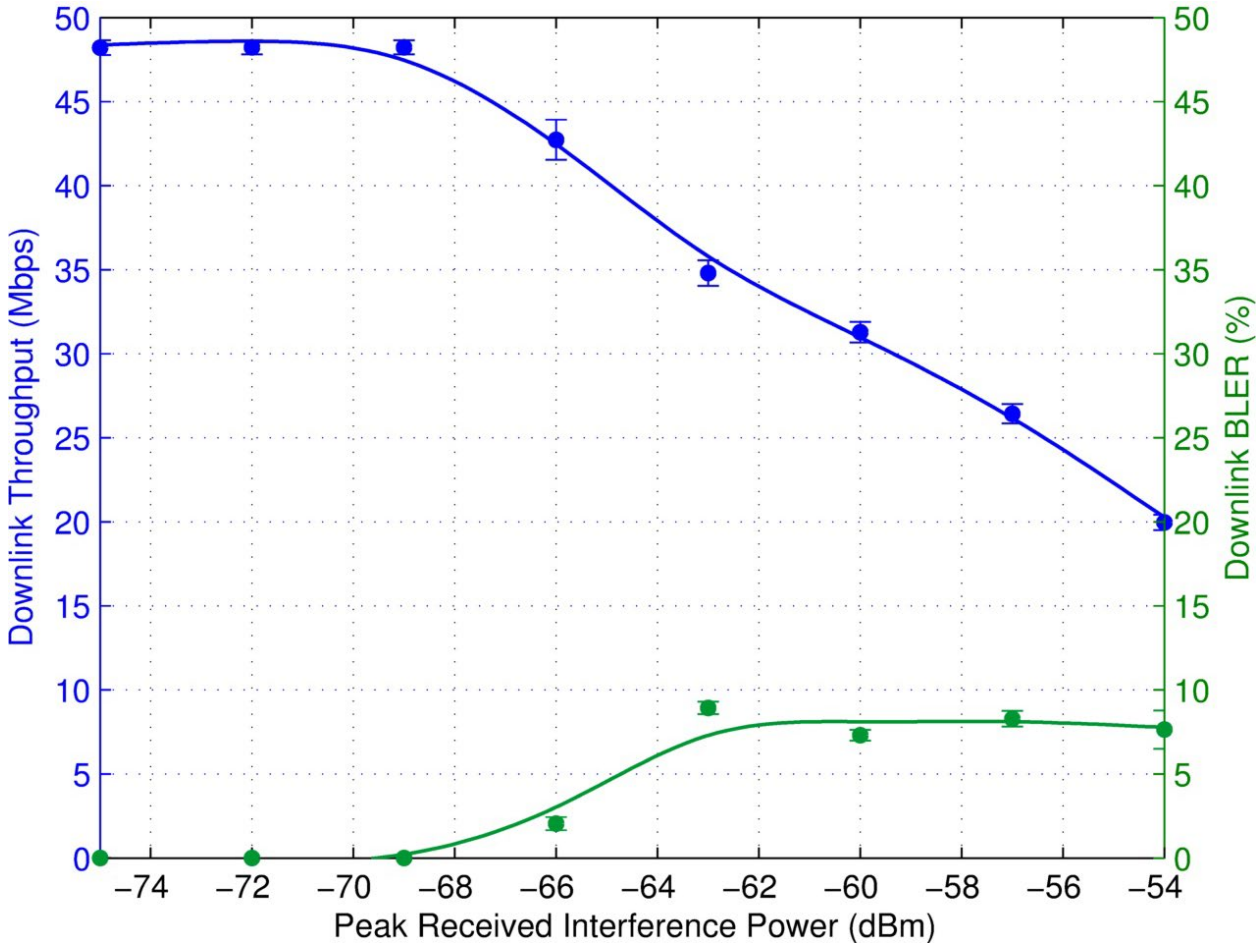

Figure 18. Data throughput and BLER for P0N-12 (PW = 10 µs, PRR = 10,000/sec, DC = 10%) interference.

Table 19. MCS state for P0N-12 (PW = 10 µs, PRR = 10,000/sec, DC = 10%) interference.

I dBm	Rank 1				Rank 2						
					Channel 0			Channel 1			% Time Used
	Min MCS	Most Frequent MCS	Max MCS	% Time Used	Min MCS	Most Frequent MCS	Max MCS	Min MCS	Most Frequent MCS	Max MCS	
-75	9	9	9	0.01	1	23	23	2	23	23	99.99
-72	2	23	23	0.02	2	23	23	10	23	23	99.98
-69	4	4	21	0.01	0	23	23	13	23	23	99.99
-66	0	23	23	1.74	23	23	23	7	23	23	98.26
-63	0	0	23	0.09	20	22	23	18	22	23	99.91
-60	0	0	23	2.86	0	20	23	14	20	23	97.14
-57	0	0	23	1.37	7	18	23	13	18	23	98.63
-54	0	0	21	2.54	0	14	23	0	14	23	97.46

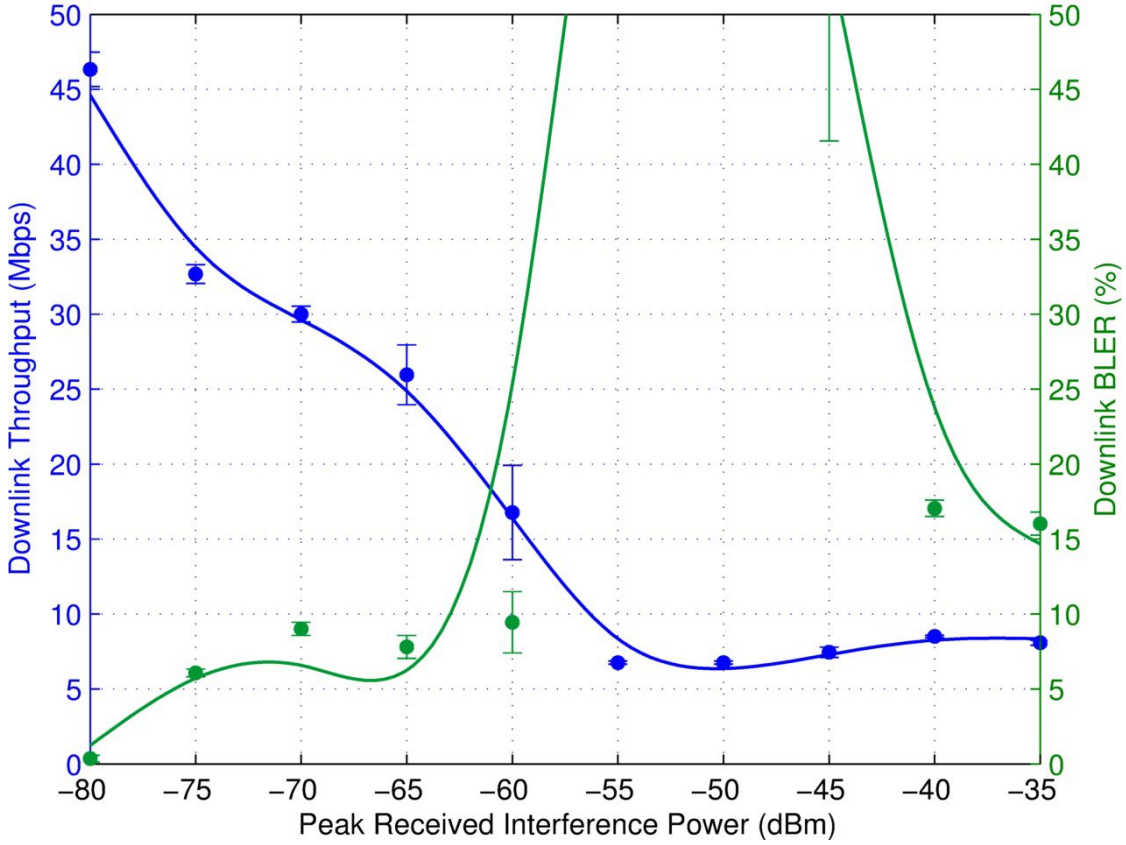

Figure 19. Data throughput and BLER for Q3N-1 (PW = 10 µs, PRR = 1,000/sec, DC = 1%) interference.[14]

Table 20. MCS State for Q3N-1 (PW = 10 µs, PRR = 1,000/sec, DC = 1%) interference.

I dBm	Rank 1				Rank 2						
					Channel 0			Channel 1			% Time Used
	Min MCS	Most Frequent MCS	Max MCS	% Time Used	Min MCS	Most Frequent MCS	Max MCS	Min MCS	Most Frequent MCS	Max MCS	
-80	0	0	23	0.74	8	23	23	5	23	23	99.26
-75	0	0	21	5.15	18	20	23	18	20	23	94.85
-70	0	0	23	0.47	15	19	23	0	19	23	99.53
-65	0	0	23	2.35	0	19	23	1	19	23	97.65
-60	0	0	22	1.58	1	13	23	0	13	23	98.42
-55	0	0	22	0.21	2	8	23	4	8	23	99.79
-50	0	0	21	0.12	4	8	23	1	8	23	99.88
-45	0	0	21	0.15	4	8	23	4	8	23	99.85
-40	0	0	21	0.15	0	6	23	4	6	23	99.85
-35	0	19	19	0.15	0	6	23	4	6	23	99.85

[14] The BLER points that are off the graph are believed to be the result of erroneous diagnostic software behavior.

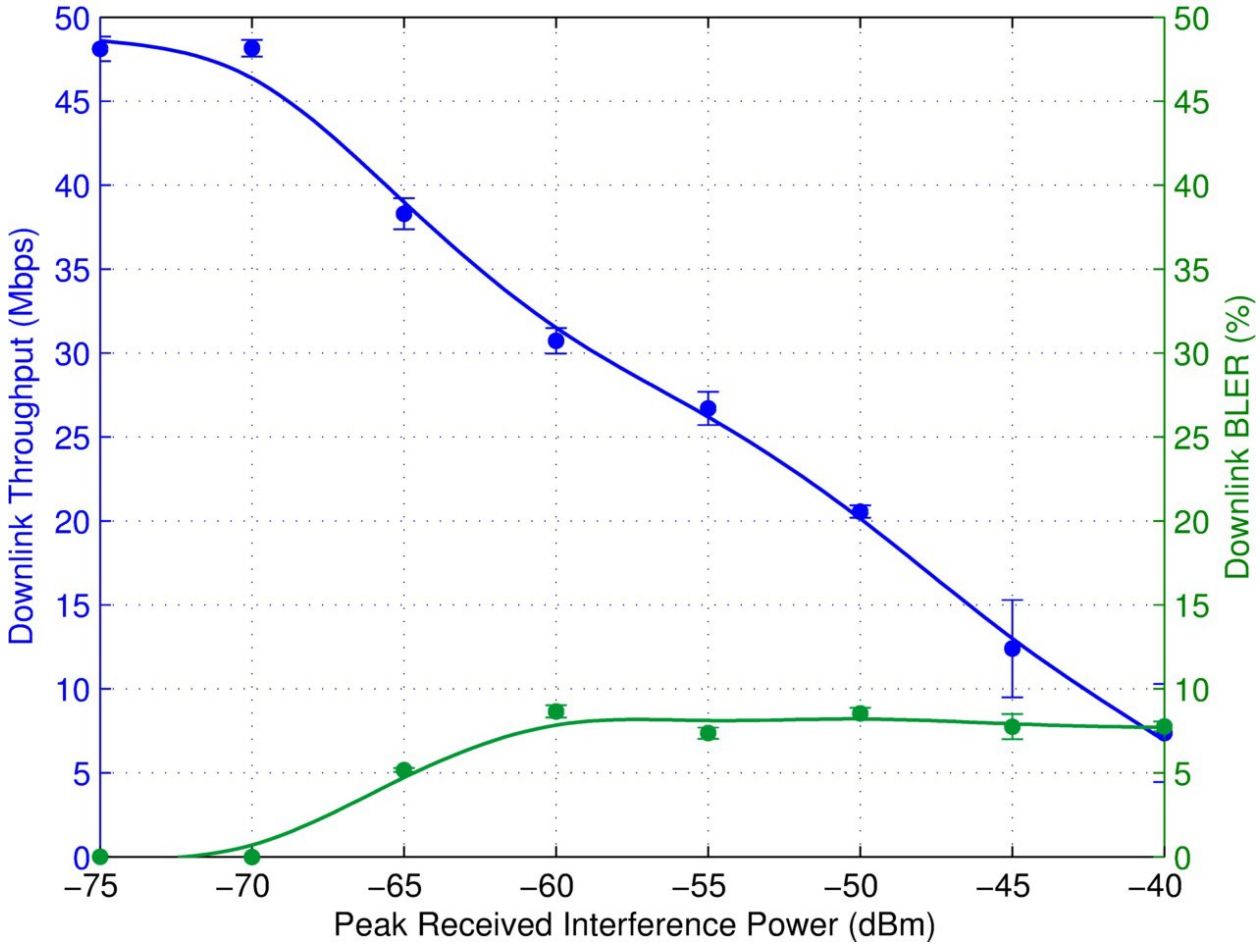

Figure 20. Data throughput and BLER for Q3N-2 (PW = 1 µs, PRR = 10,000/sec, DC = 1.0%) interference.

Table 21. MCS state for Q3N-2 (PW = 1 µs, PRR = 10,000/sec, DC = 1.0%) interference.

I dBm	Rank 1				Rank 2						
					Channel 0			Channel 1			% Time Used
	Min MCS	Most Frequent MCS	Max MCS	% Time Used	Min MCS	Most Frequent MCS	Max MCS	Min MCS	Most Frequent MCS	Max MCS	
-75	0	0	15	0.01	3	23	23	12	23	23	99.99
-70	0	0	5	0.01	8	23	23	3	23	23	99.99
-65	0	0	23	0.03	15	23	23	23	23	23	99.97
-60	0	21	22	0.58	0	21	23	0	21	23	99.42
-55	0	0	21	2.82	4	18	23	4	18	23	97.18
-50	0	0	21	0.81	11	14	21	11	14	21	99.19
-45	0	18	19	9.40	0	12	23	1	12	23	90.60
-40	0	14	23	99.30	1	23	23	10	23	23	0.70

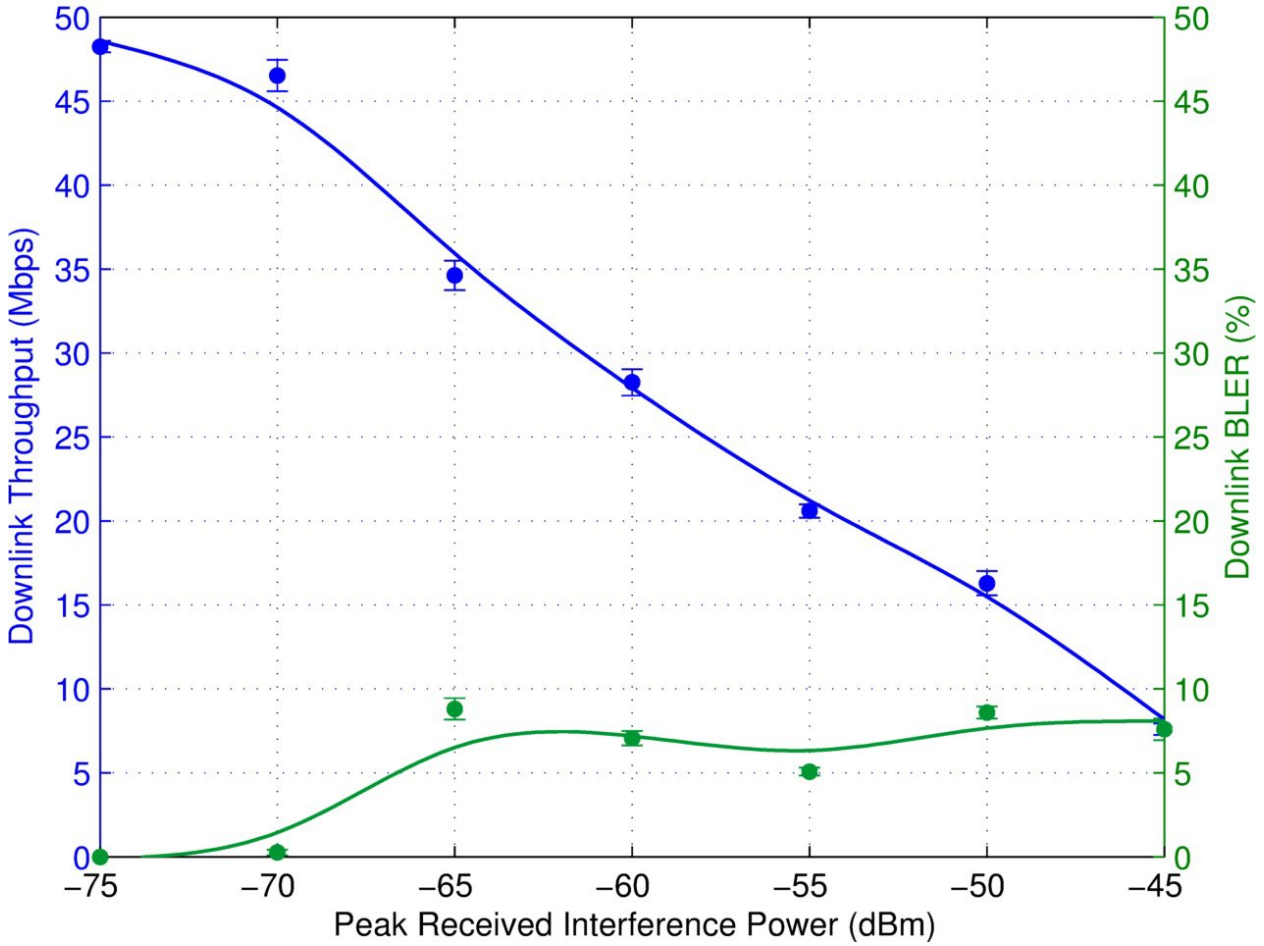

Figure 21. Data throughput and BLER for Q3N-3 (PW = 0.33 µs, PRR = 30,000/sec, DC = 1%) interference.

Table 22. MCS state for Q3N-3 (PW = 0.33 µs, PRR = 30,000/sec, DC = 1%) interference.

I dBm	Rank 1				Rank 2						
					Channel 0			Channel 1			% Time Used
	Min MCS	Most Frequent MCS	Max MCS	% Time Used	Min MCS	Most Frequent MCS	Max MCS	Min MCS	Most Frequent MCS	Max MCS	
-75	2	23	23	0.02	12	23	23	4	23	23	99.98
-70	0	0	23	0.77	20	23	23	23	23	23	99.23
-65	0	0	23	0.42	7	22	23	1	22	23	99.58
-60	0	20	23	3.28	9	20	23	6	20	23	96.72
-55	0	15	23	6.87	3	14	23	7	14	23	93.13
-50	0	13	13	0.50	1	12	17	8	12	19	99.50
-45	0	0	8	2.78	2	5	14	2	5	9	97.22

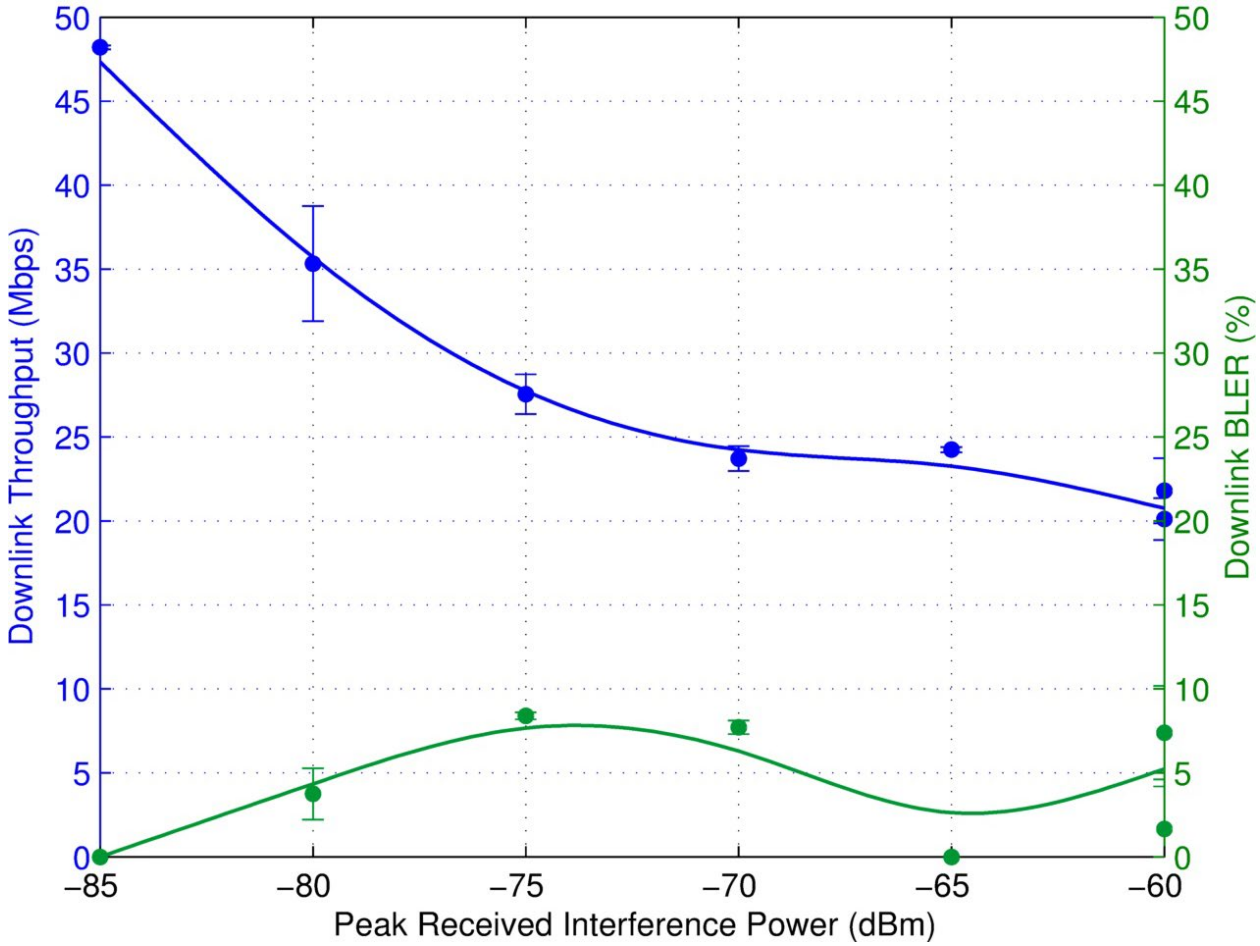

Figure 22. Data throughput and BLER for Q3N-4 (PW = 10 µs, PRR = 10,000/sec, equivalent to PW = 100 µs, PRR = 1,000/sec), DC = 10%) interference.

Table 23. MCS state for Q3N-4 (PW = 10 µs, PRR = 10,000/sec, equivalent to PW = 100 µs, PRR = 1,000/sec), DC = 10%) interference.

I dBm	Rank 1				Rank 2						
					Channel 0			Channel 1			% Time Used
	Min MCS	Most Frequent MCS	Max MCS	% Time Used	Min MCS	Most Frequent MCS	Max MCS	Min MCS	Most Frequent MCS	Max MCS	
-85	0	0	23	0.02	15	23	23	6	23	23	99.98
-80	0	0	23	3.71	5	23	23	10	23	23	96.29
-75	0	21	22	1.10	4	21	22	15	21	22	98.90
-70	0	0	23	2.51	13	16	22	10	16	19	97.49
-65	1	23	23	100.0	N/A	N/A	N/A	N/A	N/A	N/A	0.00
-60	6	23	23	100.0	15	15	15	8	8	8	0.00
-60	12	23	23	100.0	1	1	1	7	7	12	0.00

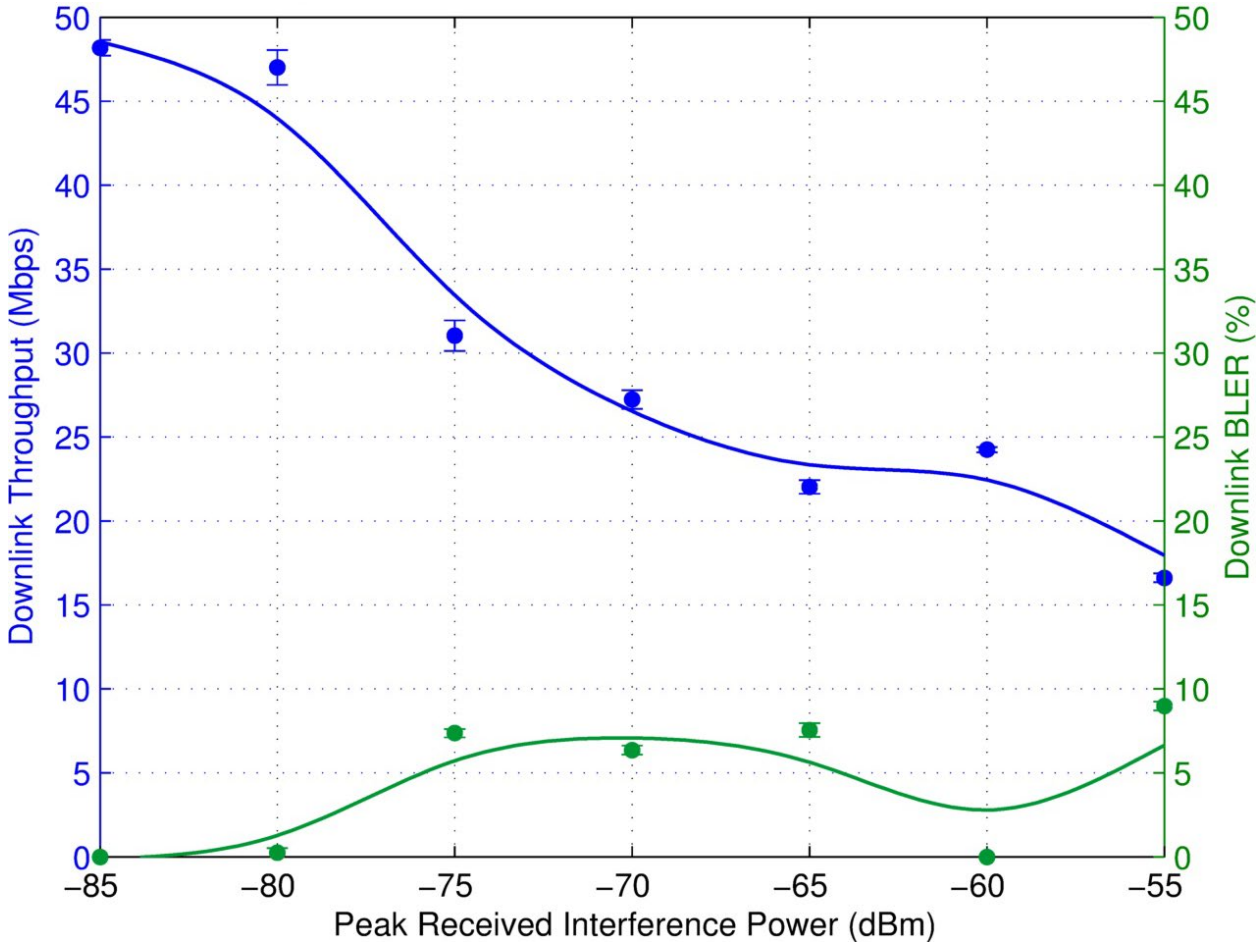

Figure 23. Data throughput and BLER for Q3N-6 (PW = 3.3 µs, PRR = 30,303/sec, DC = 10%) interference.

Table 24. MCS state for Q3N-6 (PW = 3.3 µs, PRR = 30,303/sec, DC = 10%) interference.

I dBm	Rank 1				Rank 2						
					Channel 0			Channel 1			% Time Used
	Min MCS	Most Frequent MCS	Max MCS	% Time Used	Min MCS	Most Frequent MCS	Max MCS	Min MCS	Most Frequent MCS	Max MCS	
-85	N/A	N/A	N/A	0.00	4	23	23	10	23	23	100.00
-80	0	23	23	0.83	9	23	23	23	23	23	99.17
-75	0	22	22	2.82	1	21	23	4	21	23	97.18
-70	0	19	20	4.27	2	19	23	17	19	23	95.73
-65	0	15	23	2.57	0	15	23	1	15	23	97.43
-60	18	23	23	99.99	11	23	23	10	23	23	0.01
-55	15	20	23	99.99	11	11	21	1	1	20	0.01

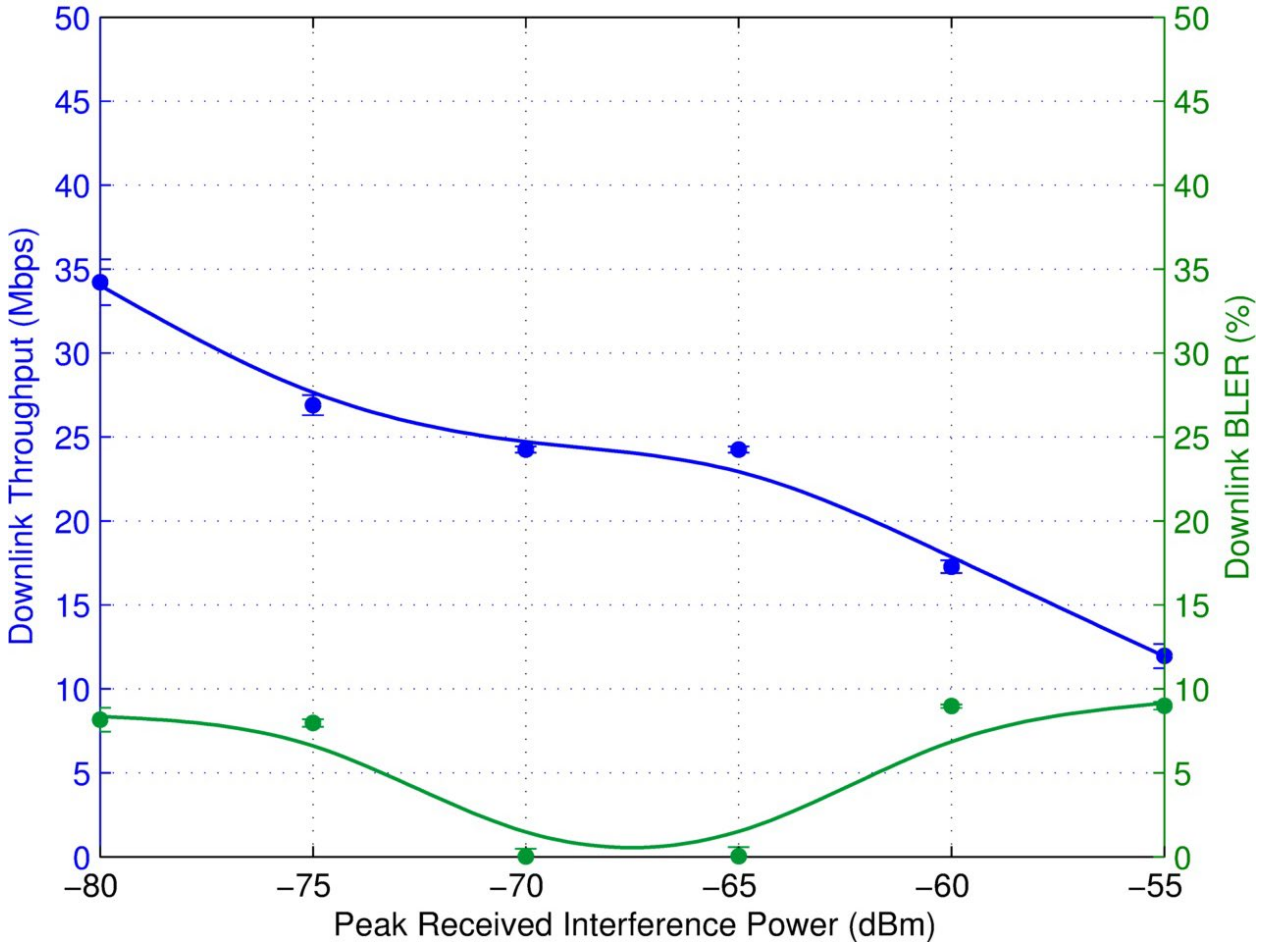

Figure 24. Data throughput and BLER for Q3N-7 (PW = 10 µs, PRR = 20,000/sec, equivalent to PW = 200 µs, PRR = 1,000/sec), DC = 20%) interference.

Table 25. MCS state for Q3N-7 (PW = 10 µs, PRR = 20,000/sec, equivalent to PW = 200 µs, PRR = 1,000/sec), DC = 20%) interference.

I dBm	Rank 1				Rank 2						
					Channel 0			Channel 1			% Time Used
	Min MCS	Most Frequent MCS	Max MCS	% Time Used	Min MCS	Most Frequent MCS	Max MCS	Min MCS	Most Frequent MCS	Max MCS	
-80	0	22	23	1.54	18	22	23	11	22	23	98.46
-75	0	0	19	2.10	14	19	22	14	19	22	97.90
-70	6	23	23	100.0	15	17	17	13	13	17	0.00
-65	12	23	23	100.0	0	0	0	6	6	6	0.00
-60	13	21	23	99.99	12	12	22	10	18	23	0.01
-55	10	16	23	99.54	6	23	23	3	23	23	0.46

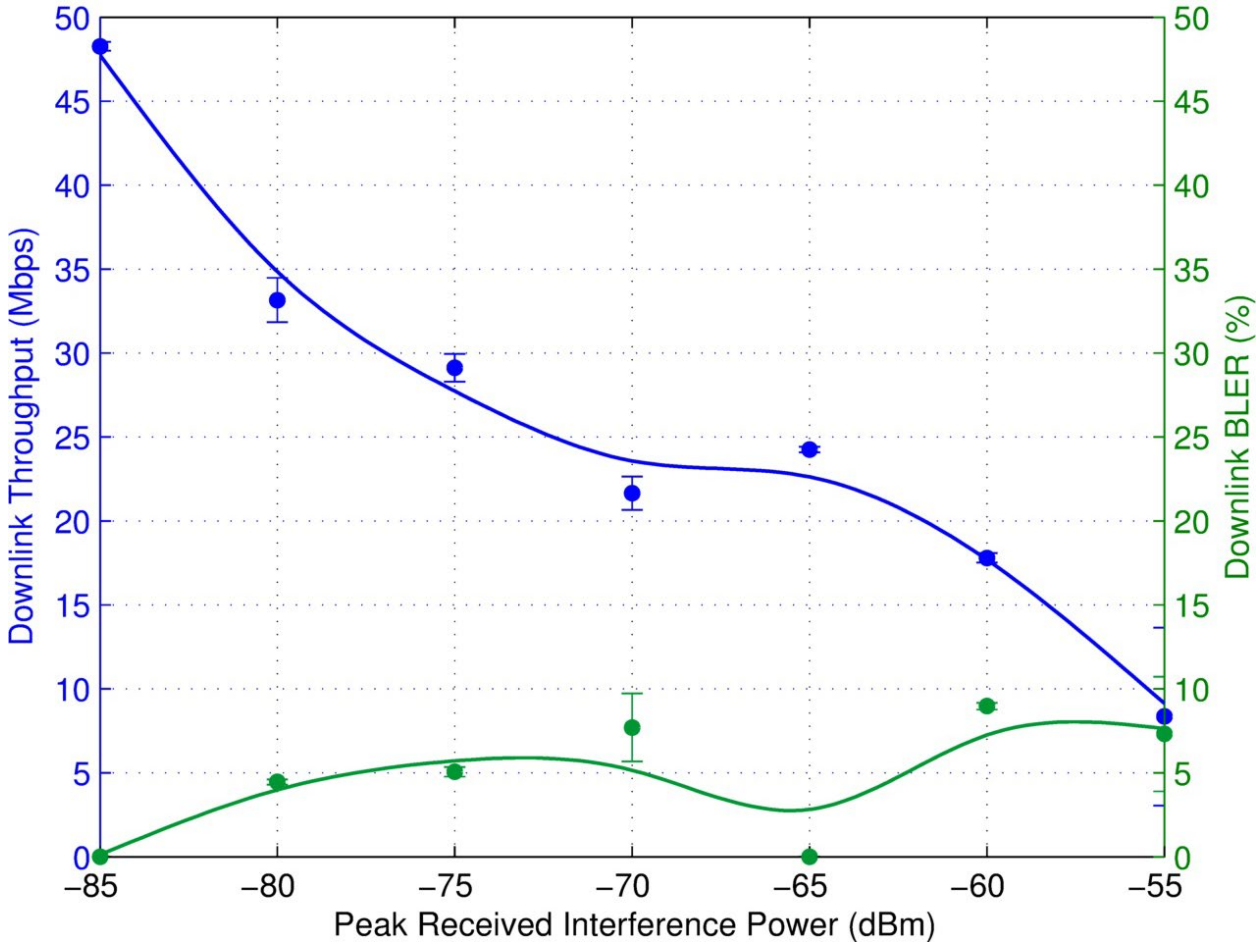

Figure 25. Data throughput and BLER for Q3N-9 (PW = 6.6 µs, PRR = 30,303/sec, DC = 20%) interference.

Table 26. MCS state for Q3N-9 (PW = 6.6 µs, PRR = 30,303/sec, DC = 20%) interference.

I dBm	Rank 1				Rank 2						
					Channel 0			Channel 1			% Time Used
	Min MCS	Most Frequent MCS	Max MCS	% Time Used	Min MCS	Most Frequent MCS	Max MCS	Min MCS	Most Frequent MCS	Max MCS	
-85	0	0	23	0.01	1	23	23	3	23	23	99.99
-80	0	22	23	8.13	1	22	23	3	22	23	91.87
-75	0	20	20	6.92	5	19	23	3	19	23	93.08
-70	0	23	23	46.65	11	14	23	11	14	23	53.35
-65	4	23	23	100.0	18	18	18	7	7	19	0.00
-60	14	21	23	99.99	14	14	14	7	7	13	0.01
-55	1	15	23	88.22	2	23	23	10	23	23	11.78

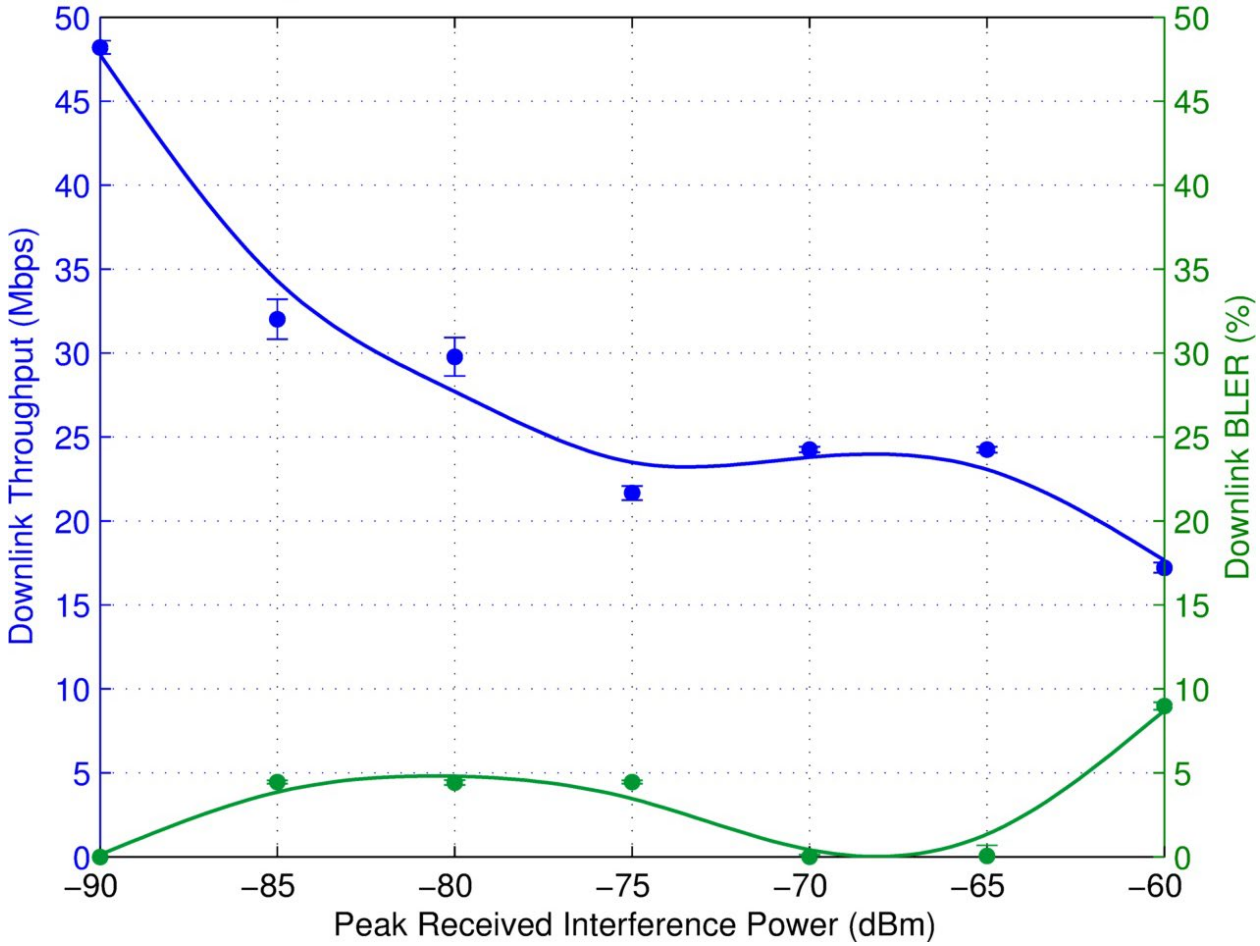

Figure 26. Data throughput and BLER for Q3N-10 (PW = 10 µs, PRR = 30,000/sec, equivalent to PW = 300 µs, PRR = 1,000/sec), DC = 30%) interference.

Table 27. MCS state for Q3N-10 (PW = 10 µs, PRR = 30,000/sec, equivalent to PW = 300 µs, PRR = 1,000/sec), DC = 30%) interference.

I dBm	Rank 1				Rank 2						
					Channel 0			Channel 1			% Time Used
	Min MCS	Most Frequent MCS	Max MCS	% Time Used	Min MCS	Most Frequent MCS	Max MCS	Min MCS	Most Frequent MCS	Max MCS	
-90	11	11	23	0.00	2	23	23	23	23	23	100.00
-85	3	23	23	8.23	2	23	23	18	23	23	91.77
-80	0	0	21	8.33	1	20	21	5	20	21	91.67
-75	0	0	16	8.33	2	15	19	3	15	21	91.67
-70	0	23	23	99.13	0	13	18	8	13	18	0.87
-65	12	23	23	100.0	6	6	12	1	1	20	0.00
-60	7	21	23	100.0	11	11	23	5	5	13	0.00

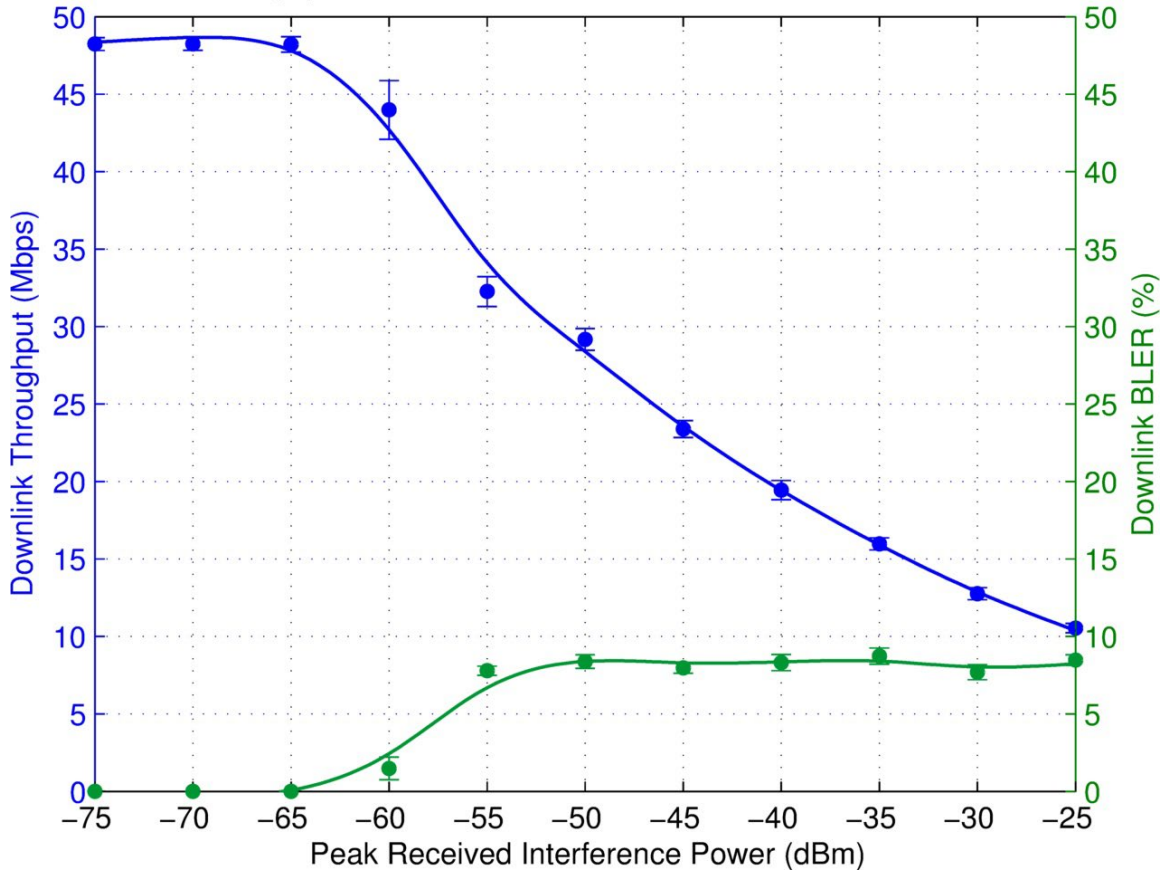

Figure 27. Data throughput and BLER for ECC-1/WFM-1 (PW = 4 µs, PRR = 1,000/sec, DC = 0.4%) interference.

Table 28. MCS state for ECC-1/WFM-1 (PW = 4 µs, PRR = 1,000/sec, DC = 0.4%) interference.

I dBm	Rank 1				Rank 2						
					Channel 0			Channel 1			% Time Used
	Min MCS	Most Frequent MCS	Max MCS	% Time Used	Min MCS	Most Frequent MCS	Max MCS	Min MCS	Most Frequent MCS	Max MCS	
-75	0	0	23	0.01	20	23	23	1	23	23	99.99
-70	14	14	14	0.00	13	23	23	4	23	23	100.00
-65	3	3	23	0.01	1	23	23	13	23	23	99.99
-60	0	0	23	1.44	6	23	23	5	23	23	98.56
-55	0	22	23	2.19	4	21	23	2	21	23	97.81
-50	0	0	20	1.10	2	19	23	5	19	23	98.90
-45	0	0	23	1.78	12	17	23	12	17	23	98.22
-40	0	0	23	1.25	11	12	23	11	12	23	98.75
-35	0	0	20	0.48	0	11	23	0	11	23	99.52
-30	0	0	23	2.89	0	8	23	0	8	23	97.11
-25	0	14	23	67.65	0	7	23	0	7	23	32.35

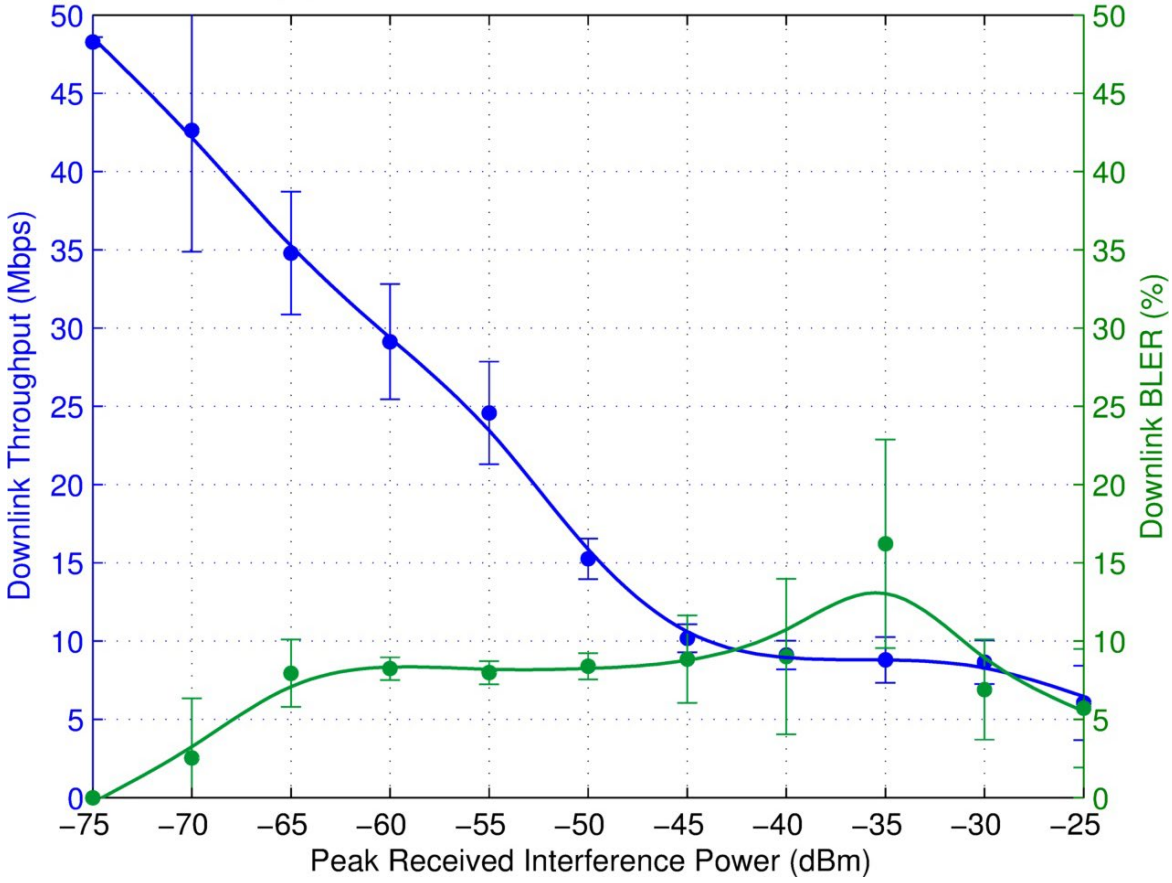

Figure 28. Data throughput and BLER for ECC-2/WFM-2 (PW = 100 µs, PRR = 300/sec, DC = 3%) interference.

Table 29. MCS state for ECC-2/WFM-2 (PW = 100 µs, PRR = 300/sec, DC = 3%) interference.

I dBm	Rank 1				Rank 2						
					Channel 0			Channel 1			% Time Used
	Min MCS	Most Frequent MCS	Max MCS	% Time Used	Min MCS	Most Frequent MCS	Max MCS	Min MCS	Most Frequent MCS	Max MCS	
-75	23	23	23	0.01	2	23	23	5	23	23	99.99
-70	0	23	23	0.39	13	23	23	20	23	23	99.61
-65	0	0	23	1.41	4	23	23	19	23	23	98.59
-60	0	0	23	1.33	0	20	23	7	20	23	98.67
-55	0	0	20	1.82	1	19	23	2	19	23	98.18
-50	0	0	21	1.17	4	12	23	4	12	23	98.83
-45	0	0	23	1.13	0	7	23	0	7	23	98.87
-40	0	0	23	0.95	0	6	23	0	6	23	99.05
-35	0	0	21	0.62	4	8	19	4	8	19	99.38
-30	0	2	20	1.66	0	6	23	0	6	23	98.34
-25	0	0	23	4.55	0	6	23	0	6	23	95.45

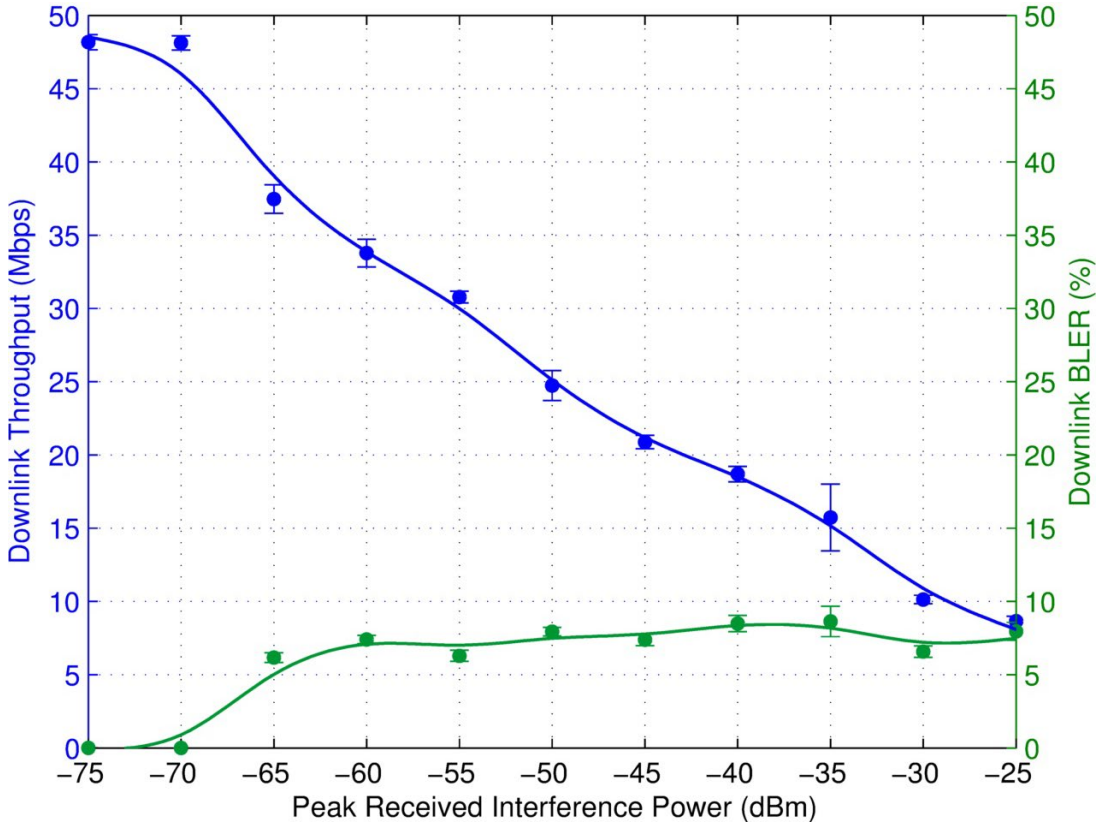

Figure 29. Data throughput and BLER for P0N-13/TDWR (PW = 1 µs, PRR = 2,000/sec, DC = 0.05%) interference.

Table 30. MCS state for P0N-13/TDWR (PW = 1 µs, PRR = 2,000/sec, DC = 0.05%) interference.

I dBm	Rank 1				Rank 2						
					Channel 0			Channel 1			% Time Used
	Min MCS	Most Frequent MCS	Max MCS	% Time Used	Min MCS	Most Frequent MCS	Max MCS	Min MCS	Most Frequent MCS	Max MCS	
-75	0	23	23	0.02	14	23	23	2	23	23	99.98
-70	0	23	23	0.06	1	23	23	6	23	23	99.94
-65	0	0	23	5.17	0	22	23	2	22	23	94.83
-60	0	0	22	2.97	8	21	23	11	21	23	97.03
-55	0	20	20	4.83	5	19	23	8	19	23	95.17
-50	0	0	23	1.89	9	19	23	5	19	23	98.11
-45	0	0	22	3.08	2	14	23	5	14	23	96.92
-40	0	14	20	0.94	3	13	23	2	13	23	99.06
-35	0	0	20	0.76	4	12	23	4	12	23	99.24
-30	0	0	23	4.11	4	7	23	0	7	23	95.89
-25	0	7	22	1.95	3	6	23	2	6	23	98.05

3.1.2 Burst Interference Testing

As noted previously, radar beams normally scan intermittently across fixed points in space. Burst interference testing replicated realistic radar-beam interference scenarios by injecting 20 pulses of radar interference every 5 seconds throughout the collection of diagnostic data. Figures 30–36 provide the results of the burst tests for the downlink. These graphs show how data throughput (top graph) and MCS (bottom graph) varied over time during the total duration of the data recording. MCS Rank 1 is presented as discrete points in these graphs because the LTE network infrequently used the rank 1 transmission strategy during these tests. Data points were collected every 0.627–100 ms. Keyed from timestamps contained in the diagnostic software data, the two graphs in each figure are time synchronized. Data recordings were manually initiated and, consequently, the data collection for each parameter began at offset times. For example, in Figure 30, one can see that the MCS recording both began before and stopped after the data throughput recording. The first timestamp in either the throughput data or the MCS data (whichever was started first) was used to determine the starting time of each graph.

For all burst tests performed on the downlink, the interference power level, *I*, was set such that it was equal to or greater than the value of *I* that caused significant throughput degradation during the respective continuous test.

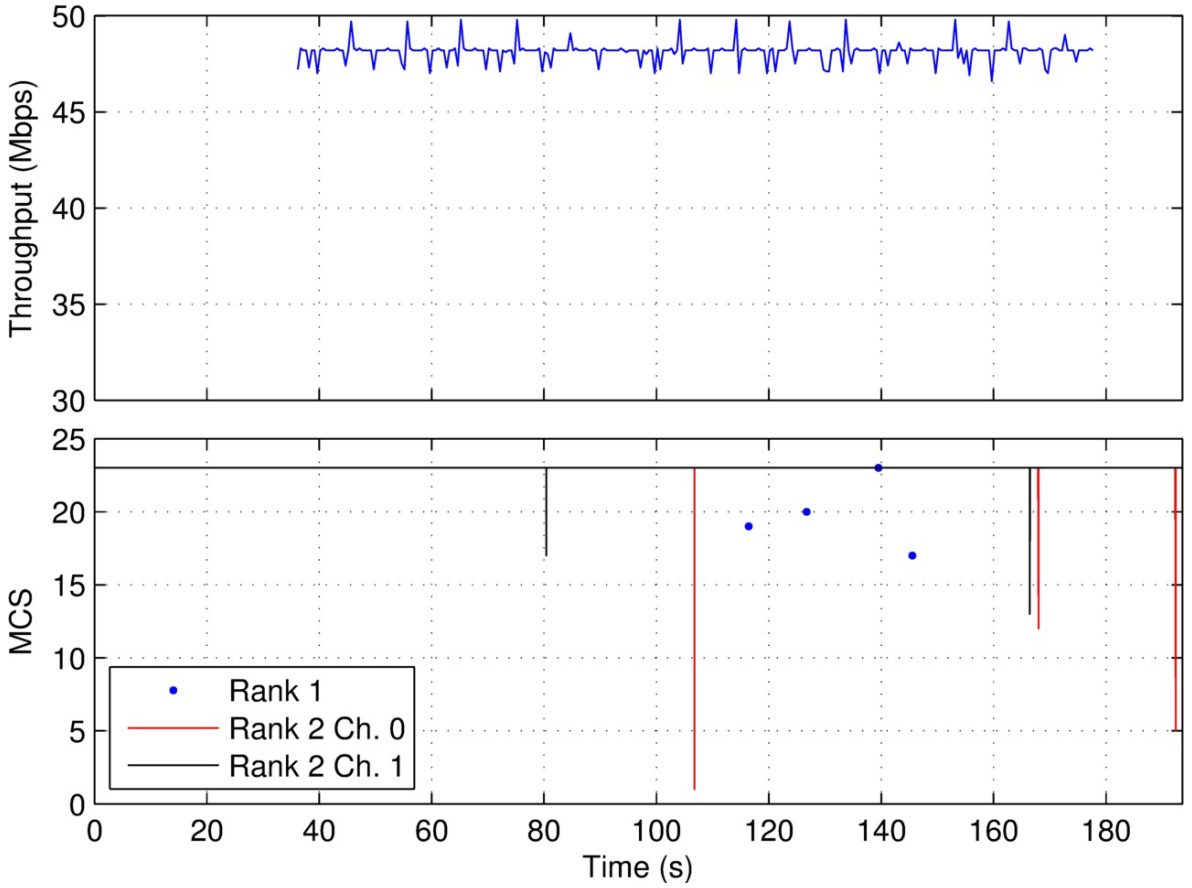

Figure 30. Data throughput and MCS state for P0N-5 interference (I_{peak} = -35 dBm).

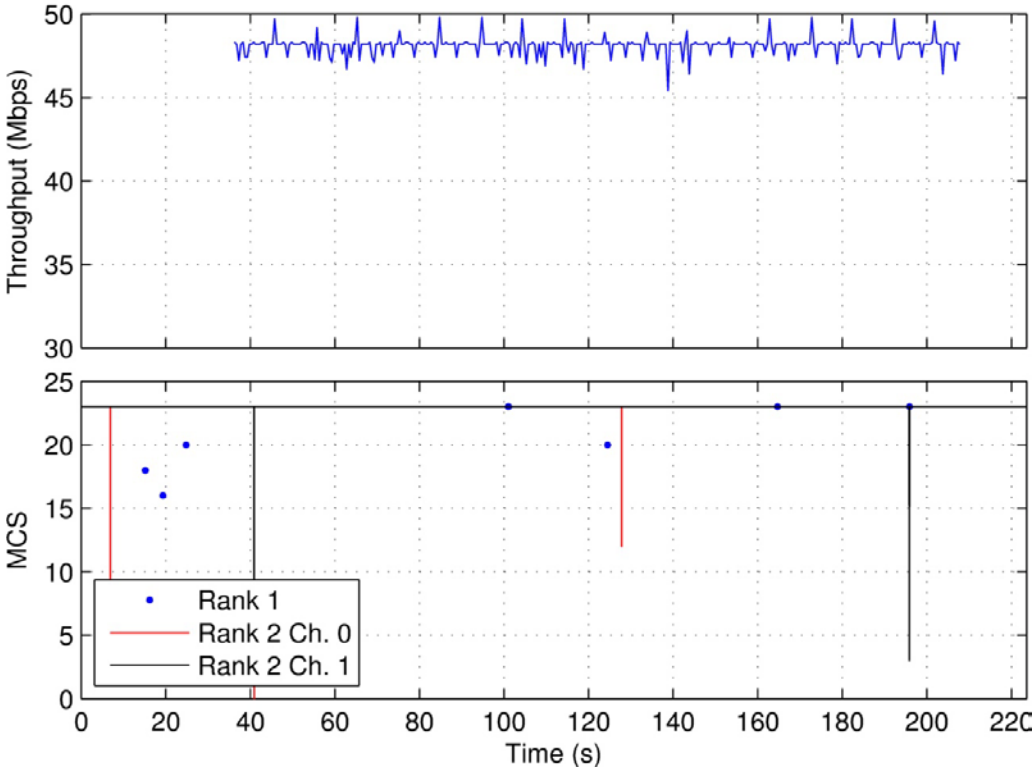

Figure 31. Data throughput and MCS state for P0N-8 interference (I_{peak} = -35 dBm).

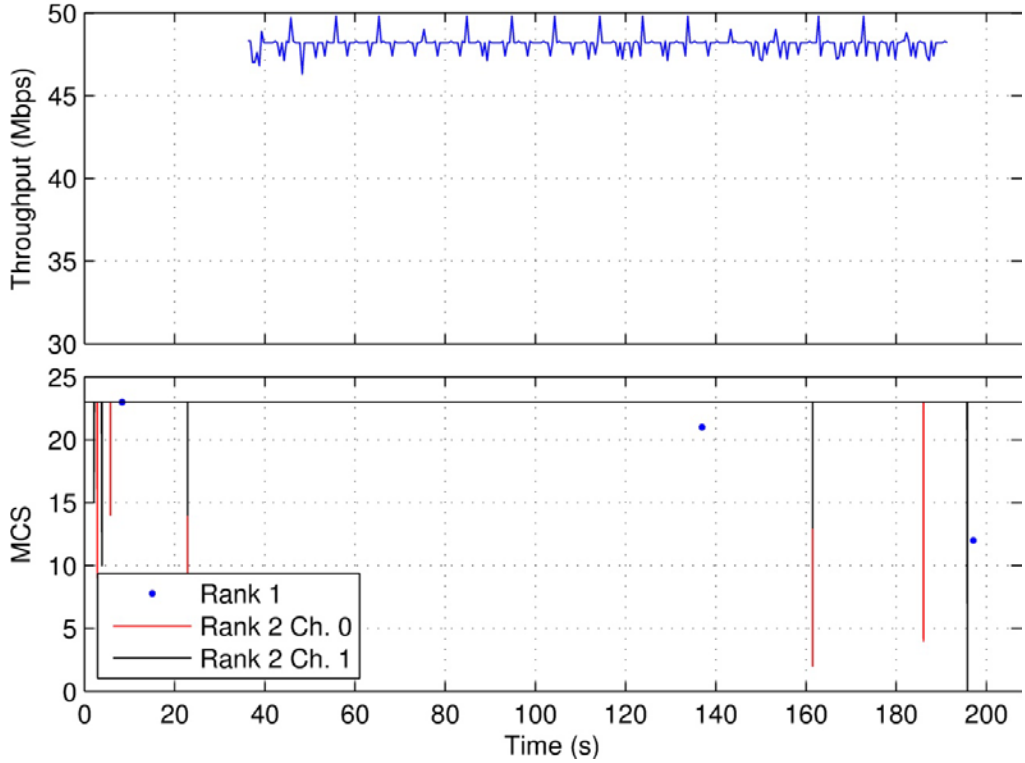

Figure 32. Data throughput and MCS state for P0N-11 interference (I_{peak} = -35 dBm).

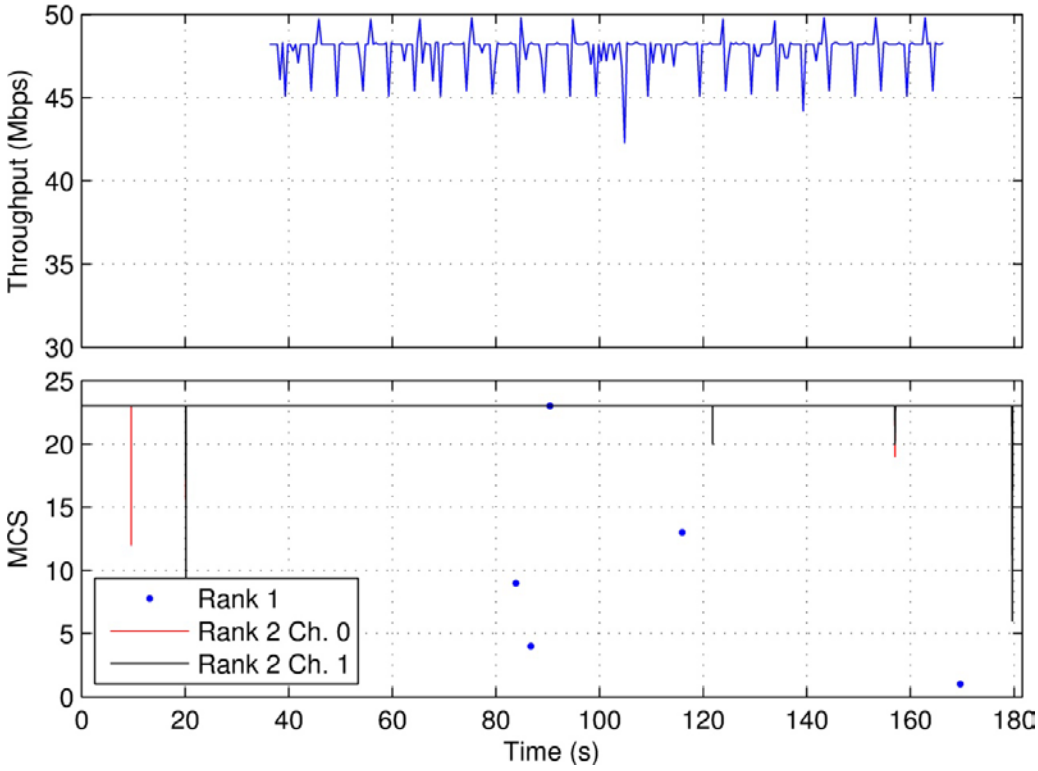

Figure 33. Data throughput and MCS state for Q3N-1 interference (I_{peak} = -30 dBm).

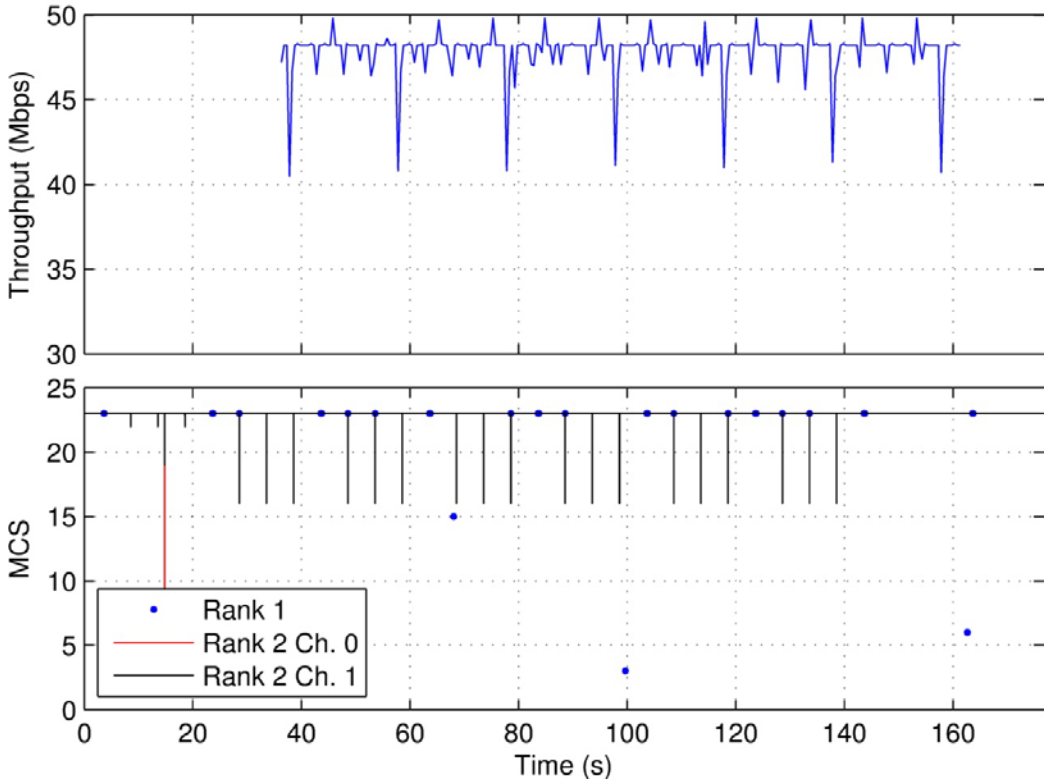

Figure 34. Data throughput and MCS state for Q3N-4 interference (I_{peak} = -45 dBm).

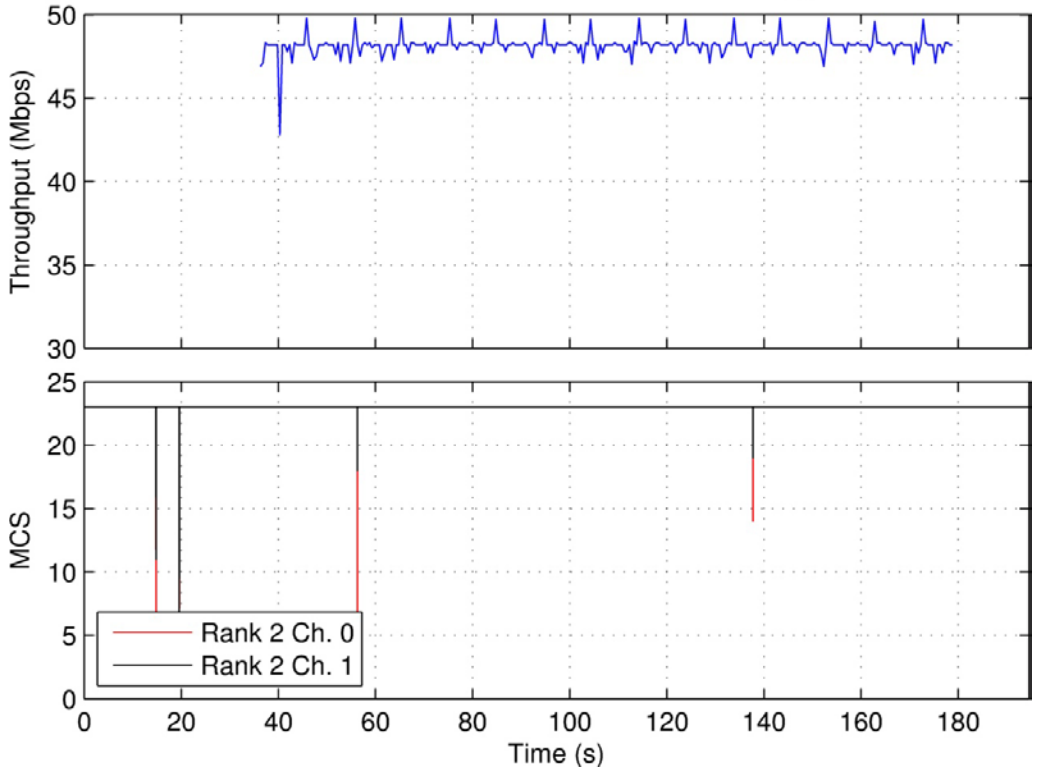

Figure 35. Data throughput and MCS state for Q3N-7 interference (I_{peak} = -50 dBm).

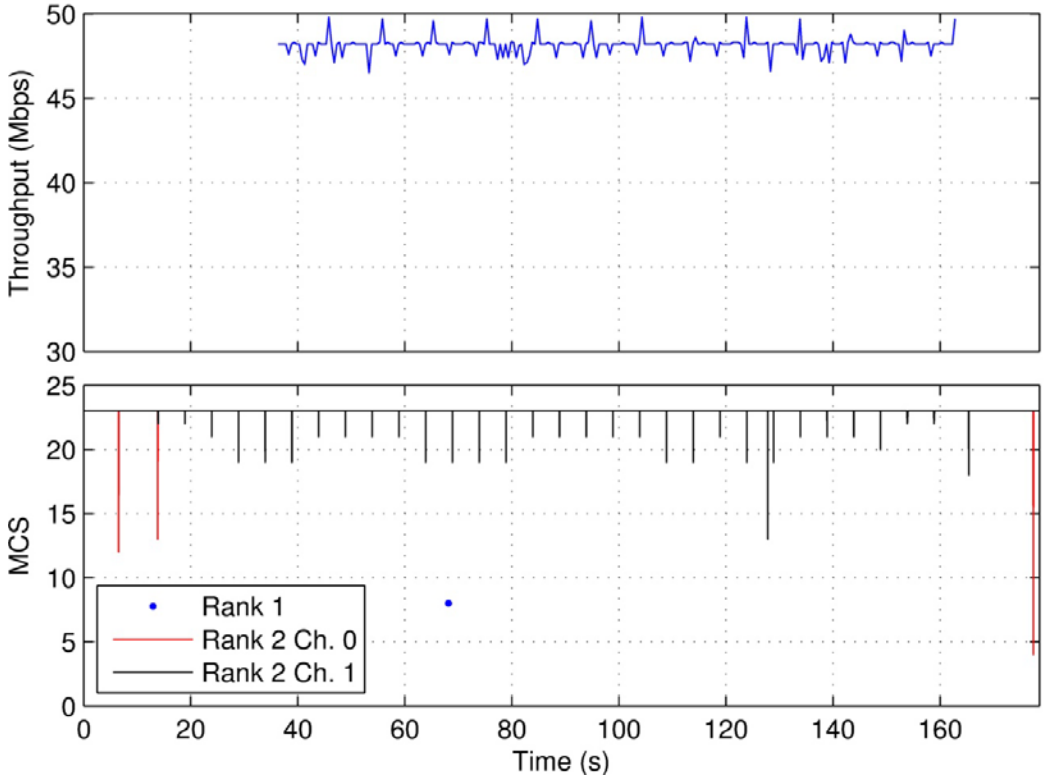

Figure 36. Data throughput and MCS state for Q3N-10 interference (I_{peak} = -50 dBm).

3.2 Uplink Interference-Effects Results

3.2.1 Continuous Interference Testing

Figures 37–60 show the effects of radar waveform interference and Gaussian noise interference on LTE eNB receiver (uplink) data throughput, BLER, RB usage, and UE transmit power level. Each figure is divided into three graphs. The top graph displays mean data throughput as blue points with error bars showing the standard deviation from the mean. The green line on the top graph depicts the mean UE transmit power level. The middle graph shows the mean BLER, again with standard-deviation error bars. The bottom graph shows how the mean number of RBs varied as *I* increased. In the figures, a smoothing spline was applied to demonstrate general trends for both data throughput and BLER as a function of interference power, *I*.

As with the downlink case, the number of samples used to calculate mean and standard deviation was approximately 100 for throughput and over 2,000 for BLER. The mean RB usage and mean UE transmit power were calculated from tens of thousands of samples provided by the diagnostic software.

Each plot is followed by a table (Tables 31–53) indicating how the MCS was affected by the interference waveforms as the interference level was increased. For the uplink, only a single transmission channel was used. The interference power levels, *I*, shown in the MCS tables coincide with the points in each graph showing the effects of the same interference waveform on throughput, UE transmit power, BLER, and RBs. Table 4 in Section 3.1.1 provides a key indicating what each of the numbers in the MCS tables means in terms of MCS.

The LTE network was configured to have a signal to noise ratio (*S/N)* of approximately +13 dB for the baseline uplink condition (with no interference) and was set by the industry participant as standard practice.

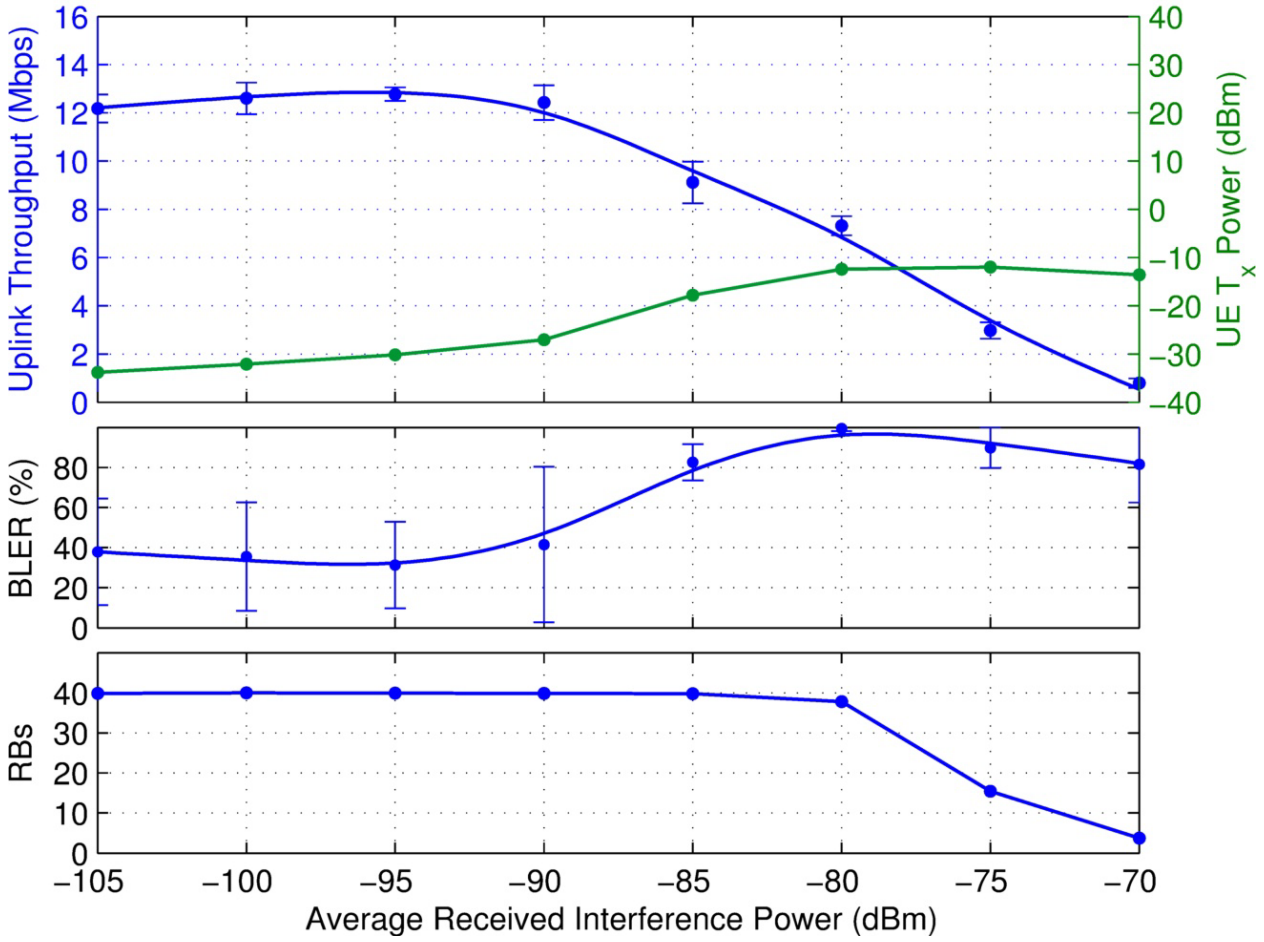

Figure 37. Data throughput, UE transmit (T_x) power, BLER, and RB usage for 10 MHz wide Gaussian noise interference.

Table 31. MCS state for 10 MHz wide Gaussian noise interference.

I dBm	Transmit Channel 0		
	Min MCS	Most Frequent MCS	Max MCS
-105	20	20	20
-100	20	20	20
-95	7	20	20
-90	7	20	20
-85	7	20	20
-80	18	19	20
-75	18	18	20
-70	9	20	20

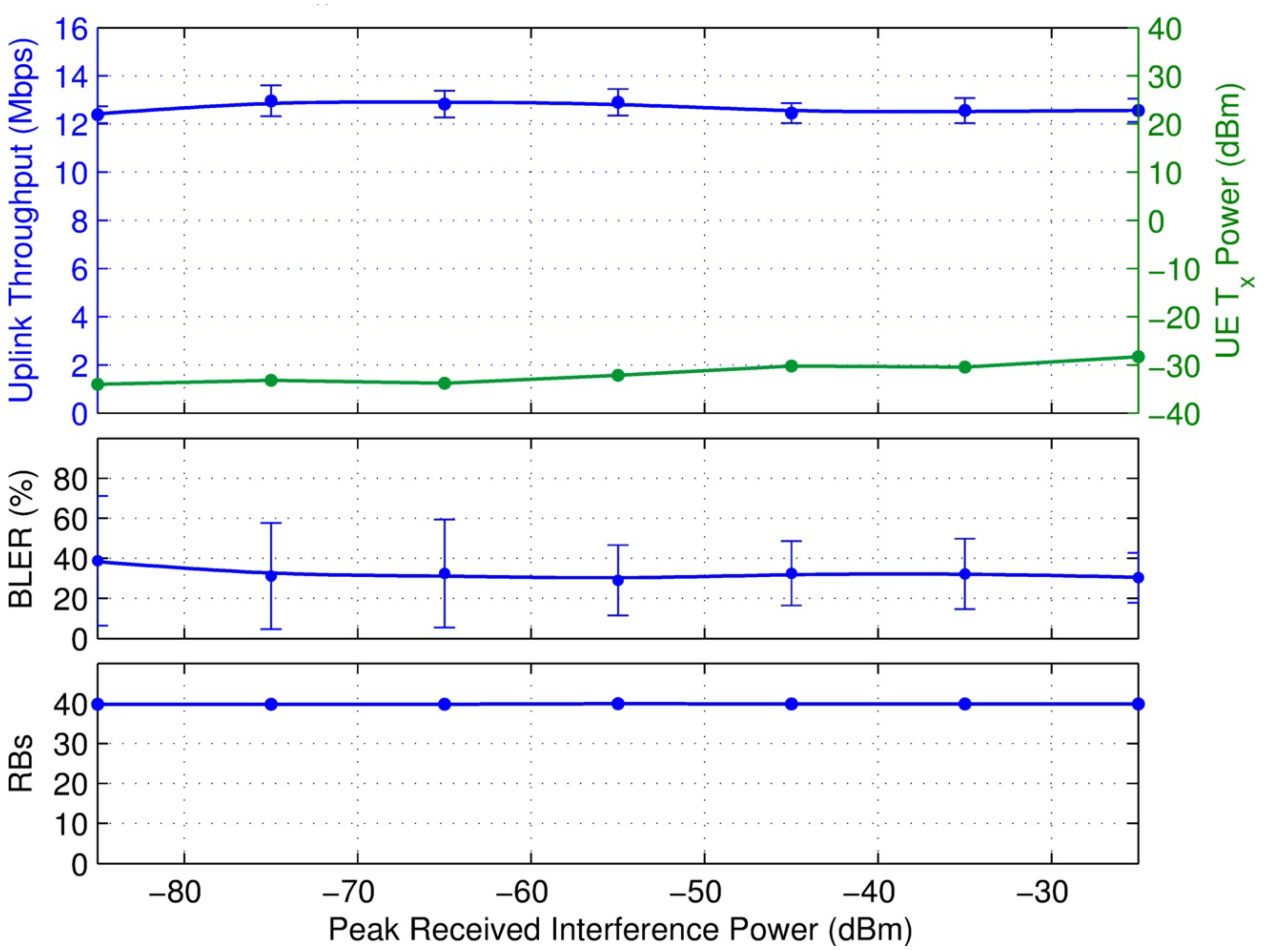

Figure 38. Data throughput, UE transmit (T_x) power, BLER, and RB usage for P0N-1 (PW = 1 µs, PRR = 1,000/sec, DC = 0.1%) interference.

Table 32. MCS state for P0N-1 (PW = 1 µs, PRR = 1,000/sec, DC = 0.1%) interference.

I dBm	Transmit Channel 0		
	Min MCS	Most Frequent MCS	Max MCS
-85	20	20	20
-75	20	20	20
-65	20	20	20
-55	20	20	20
-45	20	20	20
-35	20	20	20
-25	20	20	20

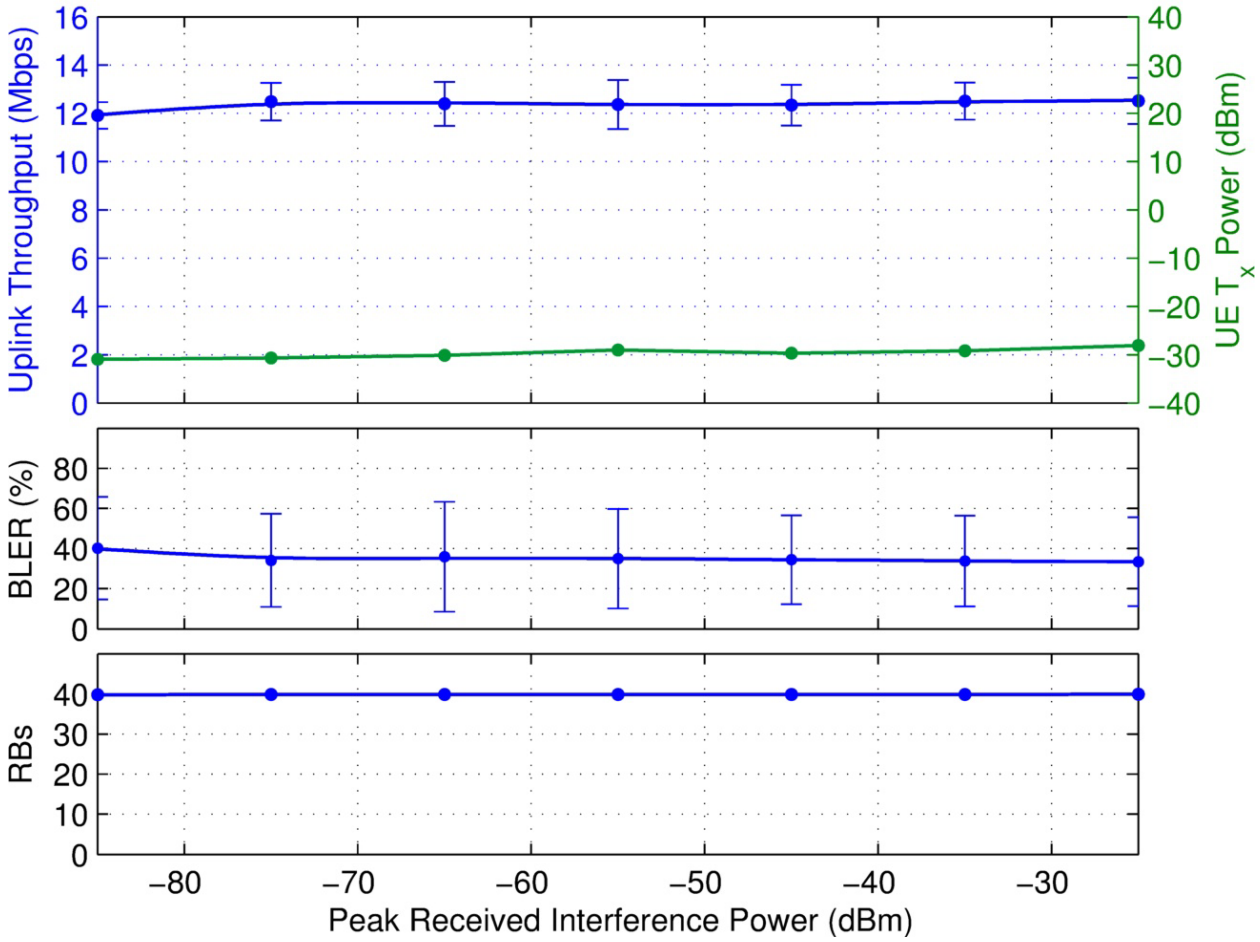

Figure 39. Data throughput, UE transmit (T_x) power, BLER, and RB usage for P0N-2 (PW = 0.33 µs, PRR = 3,000/sec, DC = 0.1%) interference.

Table 33. MCS state for P0N-2 (PW = 0.33 µs, PRR = 3,000/sec, DC = 0.1%) interference.

I dBm	Transmit Channel 0		
	Min MCS	Most Frequent MCS	Max MCS
-85	20	20	20
-75	20	20	20
-65	20	20	20
-55	20	20	20
-45	20	20	20
-35	20	20	20
-25	20	20	20

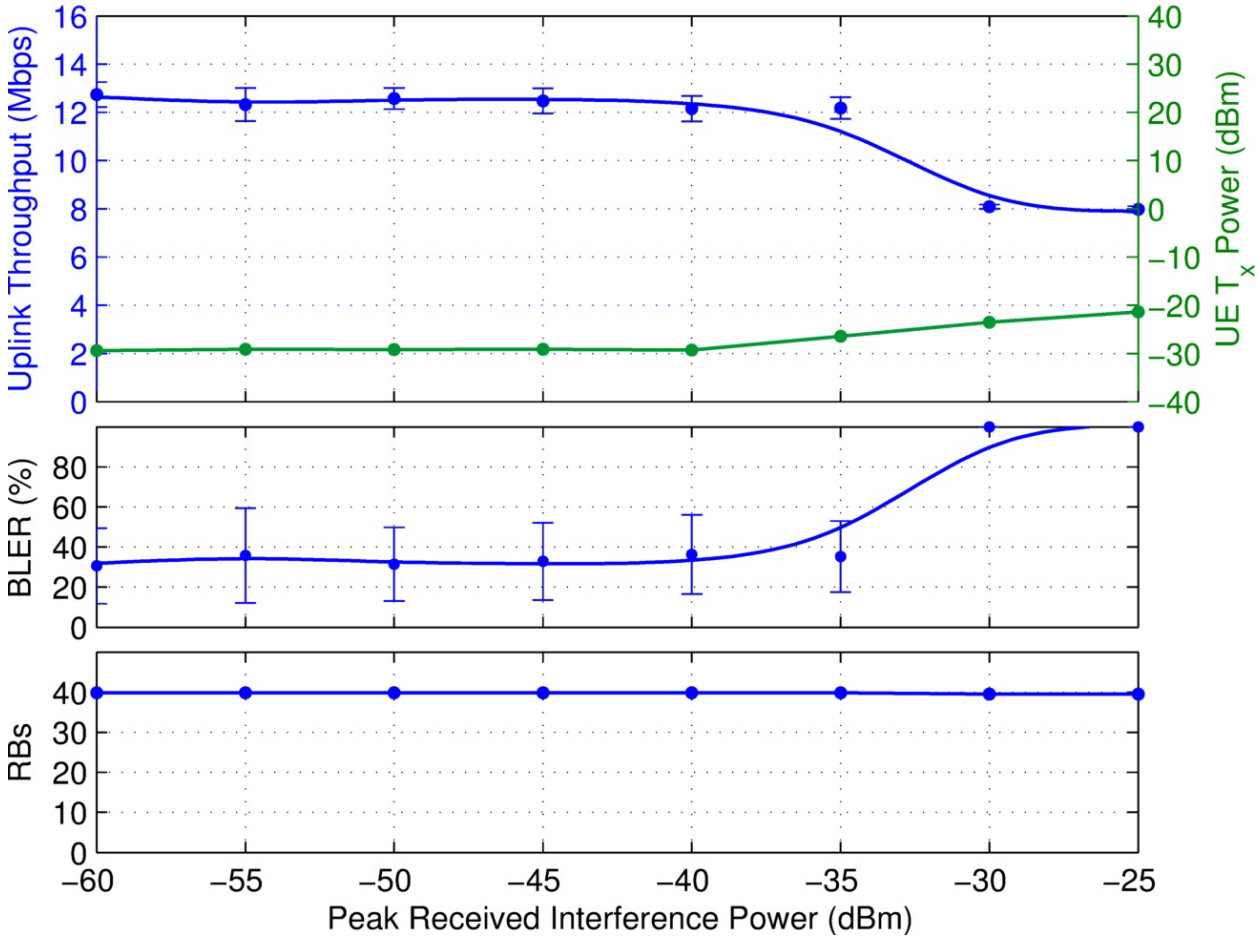

Figure 40. Data throughput, UE transmit (T_x) power, BLER, and RB usage for P0N-3 (PW = 0.1 µs, PRR = 10,000/sec, DC = 0.1%) interference.

Table 34. MCS state for P0N-3 (PW = 0.1 µs, PRR = 10,000/sec, DC = 0.1%) interference.

I dBm	Transmit Channel 0		
	Min MCS	Most Frequent MCS	Max MCS
-60	20	20	20
-55	20	20	20
-50	20	20	20
-45	20	20	20
-40	20	20	20
-35	20	20	20
-30	18	20	20
-25	19	20	20

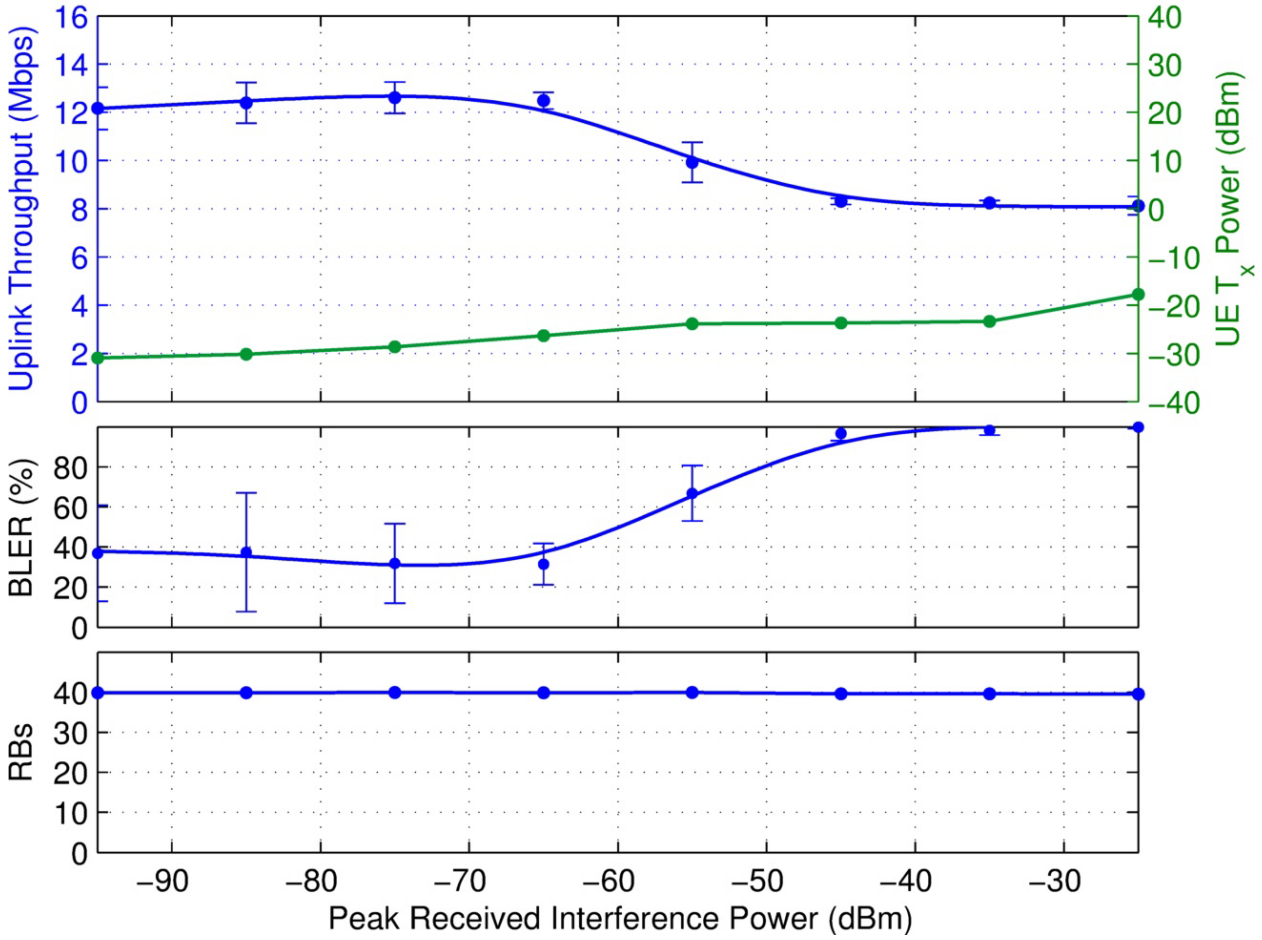

Figure 41. Data throughput, UE transmit (T_x) power, BLER, and RB usage for P0N-4 (PW = 10 µs, PRR = 1,000/sec, DC = 1%) interference.

Table 35. MCS state for P0N-4 (PW = 10 µs, PRR = 1,000/sec, DC = 1%) interference.

I dBm	Transmit Channel 0		
	Min MCS	Most Frequent MCS	Max MCS
-95	20	20	20
-85	20	20	20
-75	20	20	20
-65	20	20	20
-55	20	20	20
-45	20	20	20
-35	20	20	20
-25	20	20	20

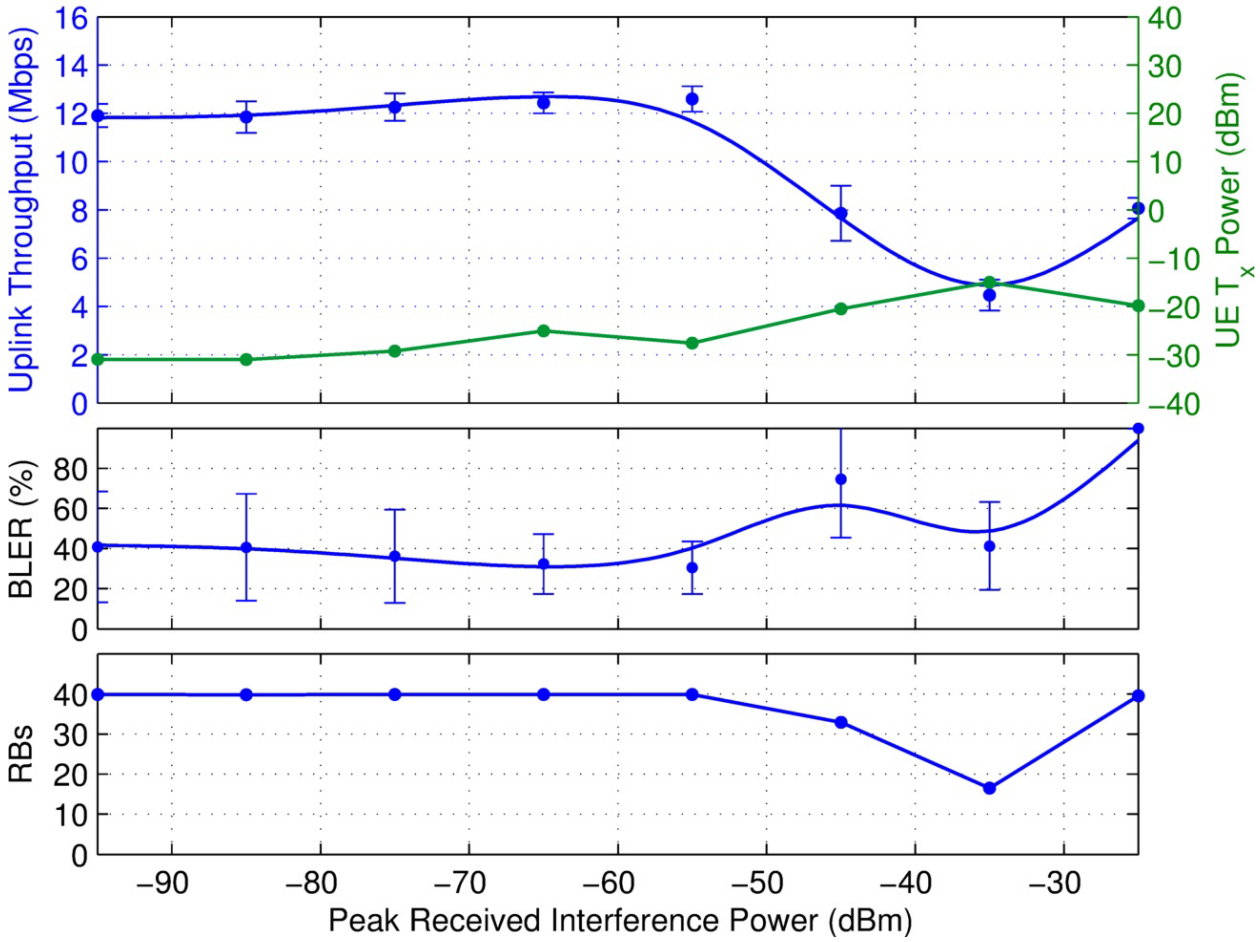

Figure 42. Data throughput, UE transmit (T_x) power, BLER, and RB usage for P0N-5 (PW = 3.33 µs, PRR = 3,000/sec, DC = 1%) interference.

Table 36. MCS state for P0N-5 (PW = 3.33 µs, PRR = 3,000/sec, DC = 1%) interference.

I dBm	Transmit Channel 0		
	Min MCS	Most Frequent MCS	Max MCS
-95	20	20	20
-85	20	20	20
-75	20	20	20
-65	20	20	20
-55	20	20	20
-45	18	20	20
-35	18	18	20
-25	20	20	20

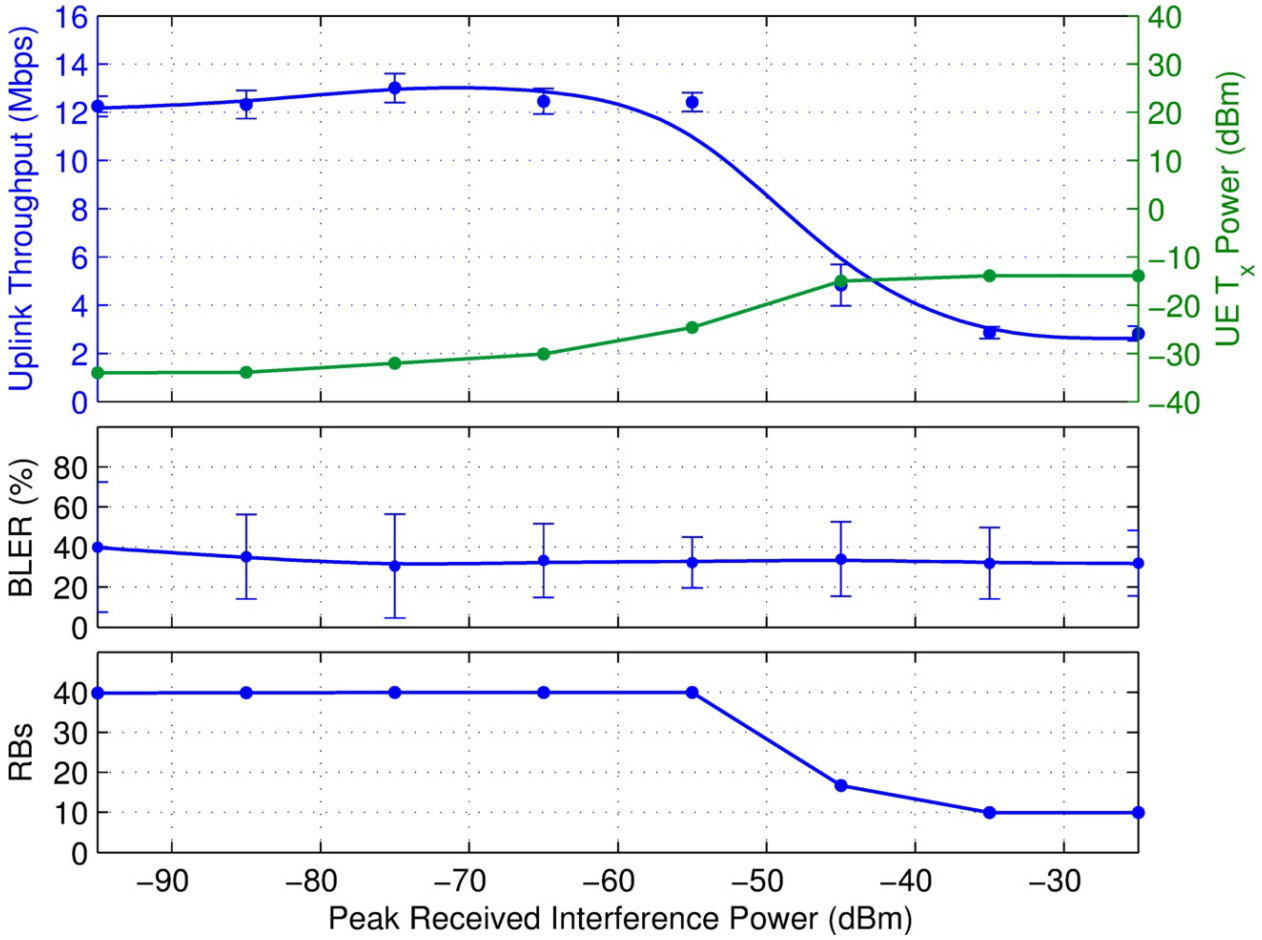

Figure 43. Data throughput, UE transmit (T_x) power, BLER, and RB usage for P0N-6 (PW = 1 µs, PRR = 10,000/sec, DC = 1%) interference.

Table 37. MCS state for P0N-6 (PW = 1 µs, PRR = 10,000/sec, DC = 1%) interference.

I dBm	Transmit Channel 0		
	Min MCS	Most Frequent MCS	Max MCS
-95	20	20	20
-85	20	20	20
-75	20	20	20
-65	20	20	20
-55	20	20	20
-45	18	20	20
-35	18	20	20
-25	17	20	20

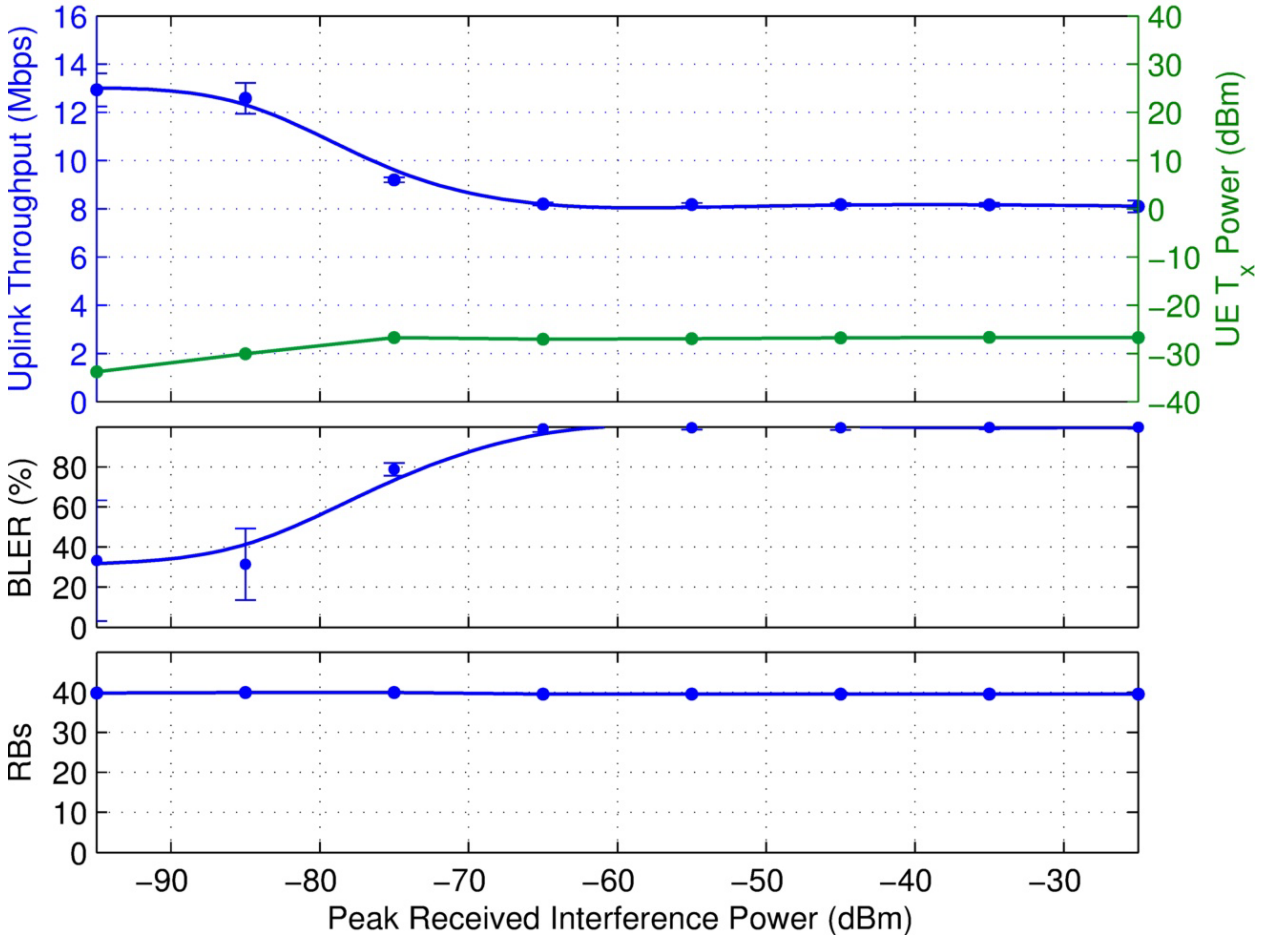

Figure 44. Data throughput, UE transmit (T_x) power, BLER, and RB usage for P0N-7 (PW = 30 µs, PRR = 1,000/sec, DC = 3%) interference.

Table 38. MCS state for P0N-7 (PW = 30 µs, PRR = 1,000/sec, DC = 3%) interference.

I dBm	Transmit Channel 0		
	Min MCS	Most Frequent MCS	Max MCS
-95	20	20	20
-85	20	20	20
-75	20	20	20
-65	20	20	20
-55	20	20	20
-45	20	20	20
-35	20	20	20
-25	20	20	20

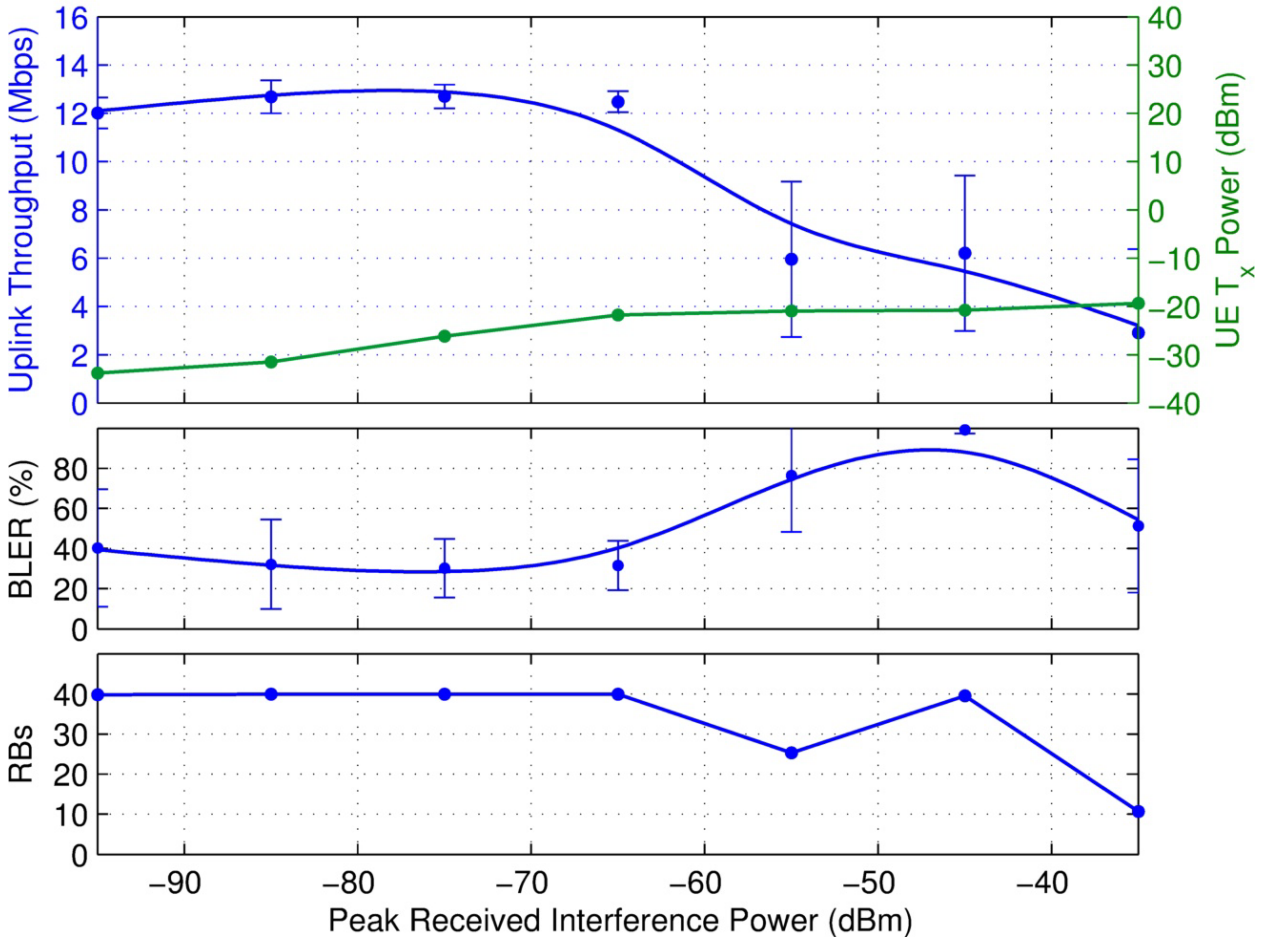

Figure 45. Data throughput, UE transmit (T_x) power, BLER, and RB usage for P0N-8 (PW = 10 µs, PRR = 3,000/sec, DC = 3%) interference.

Table 39. MCS state for P0N-8 (PW = 10 µs, PRR = 3,000/sec, DC = 3%) interference.

I dBm	Transmit Channel 0		
	Min MCS	Most Frequent MCS	Max MCS
-95	20	20	20
-85	20	20	20
-75	7	20	20
-65	20	20	20
-55	15	20	20
-45	20	20	20
-35	10	20	20

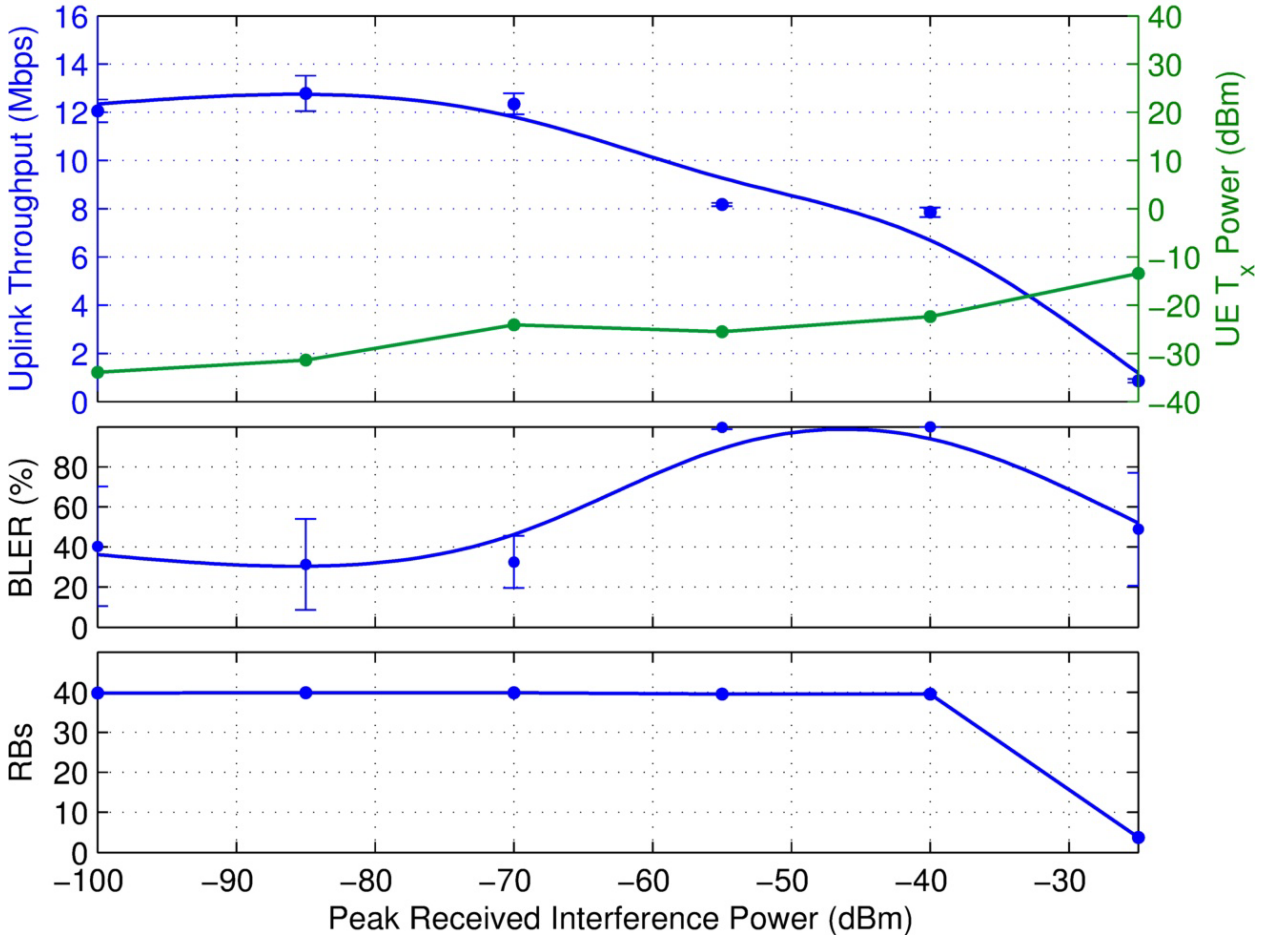

Figure 46. Data throughput, UE transmit (T_x) power, BLER, and RB usage for P0N-9 (PW = 3 µs, PRR = 10,000/sec, DC = 3%) interference.

Table 40. MCS state for P0N-9 (PW = 3 µs, PRR = 10,000/sec, DC = 3%) interference.

I dBm	Transmit Channel 0		
	Min MCS	Most Frequent MCS	Max MCS
-100	20	20	20
-85	20	20	20
-70	20	20	20
-55	20	20	20
-40	20	20	20
-25	13	20	20

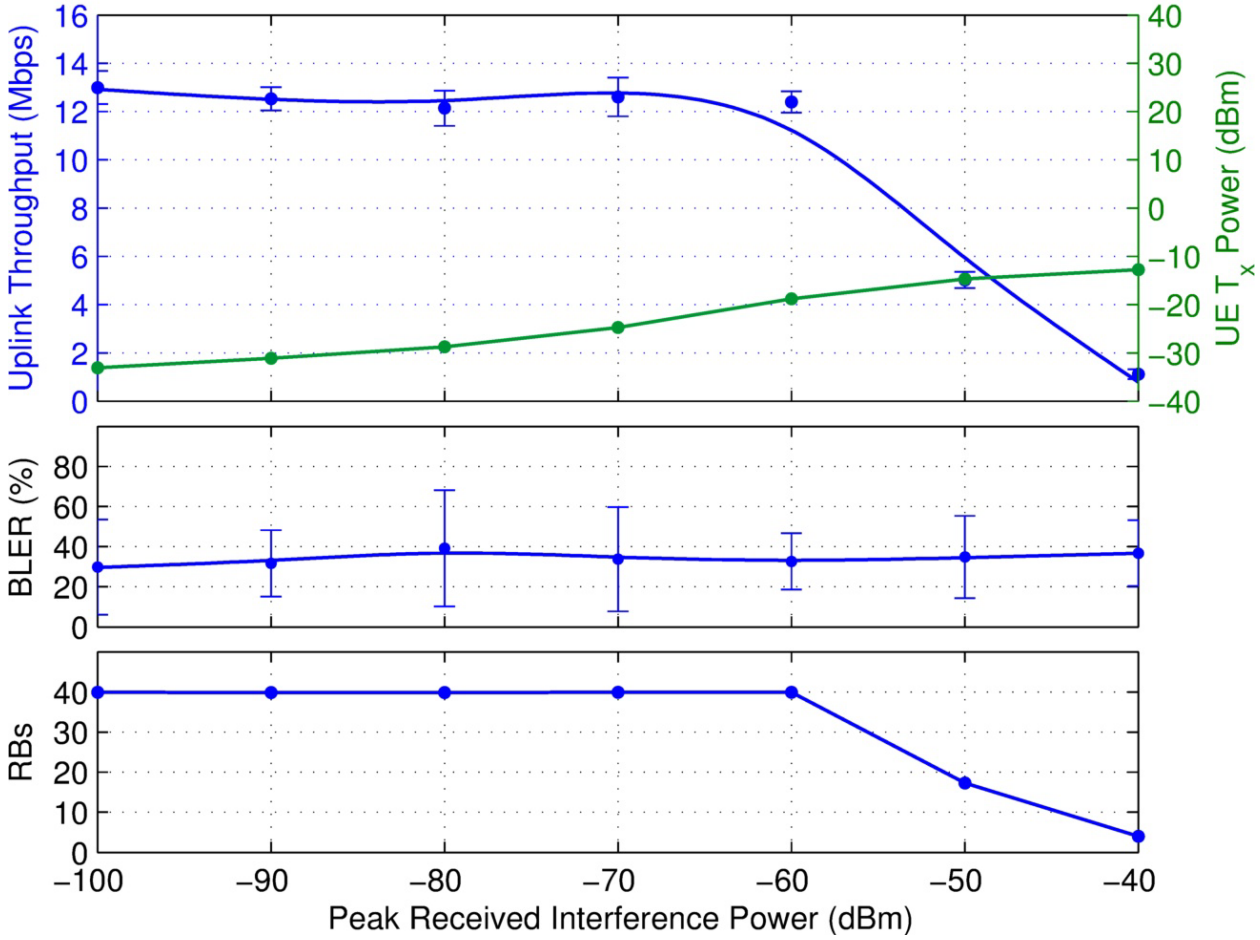

Figure 47. Data throughput, UE transmit (T_x) power, BLER, and RB usage for P0N-10 (PW = 100 µs, PRR = 1,000/sec, DC = 10%) interference.

Table 41. MCS state for P0N-10 (PW = 100 µs, PRR = 1,000/sec, DC = 10%) interference.

I dBm	Transmit Channel 0		
	Min MCS	Most Frequent MCS	Max MCS
-100	20	20	20
-90	20	20	20
-80	7	20	20
-70	20	20	20
-60	20	20	20
-50	18	20	20
-40	13	20	20

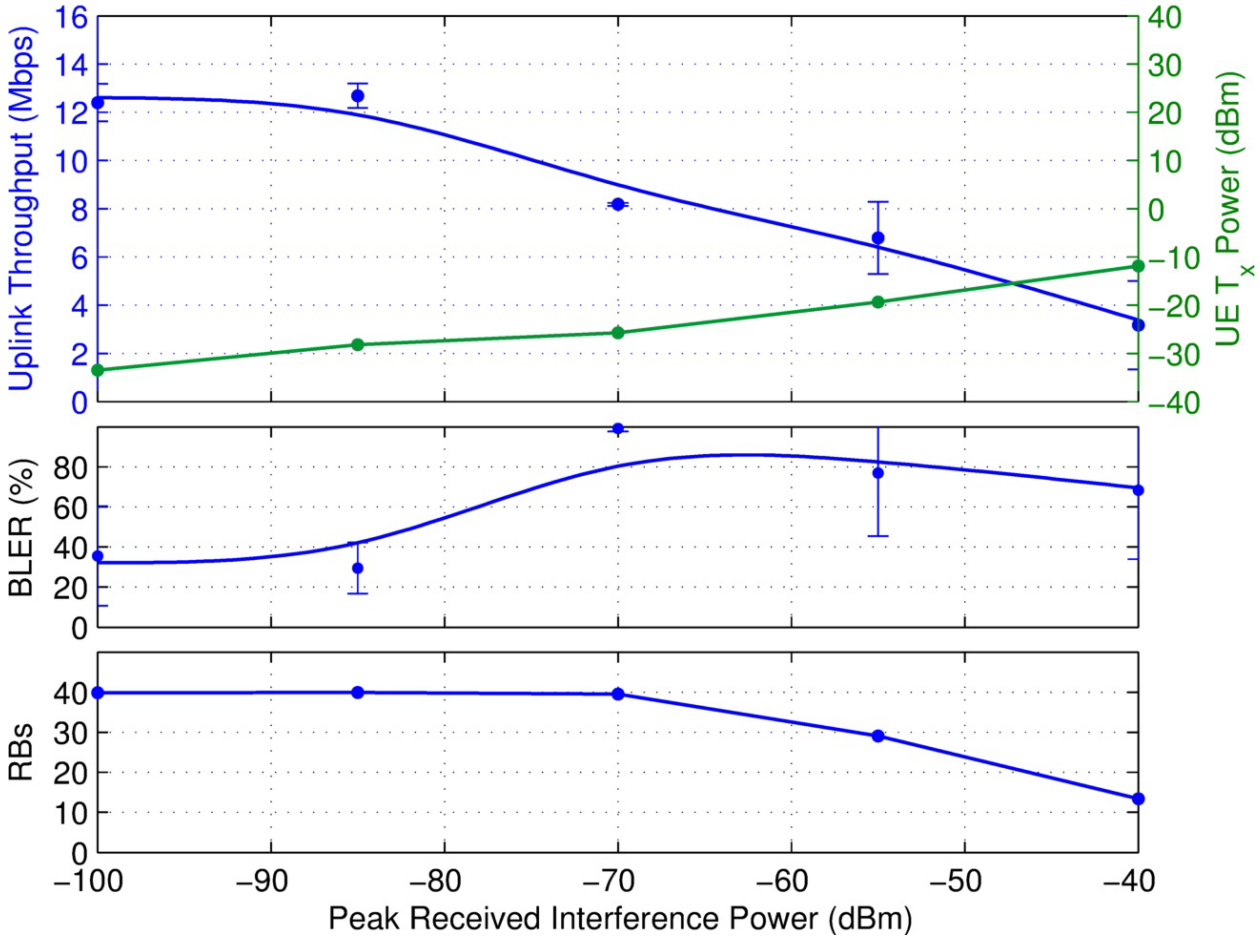

Figure 48. Data throughput, UE transmit (T_x) power, BLER, and RB usage for P0N-11 (PW = 33.3 µs, PRR = 3,000/sec, DC = 10%) interference.

Table 42. MCS state for P0N-11 (PW = 33.3 µs, PRR = 3,000/sec, DC = 10%) interference.

I dBm	Transmit Channel 0		
	Min MCS	Most Frequent MCS	Max MCS
-100	20	20	20
-85	20	20	20
-70	20	20	20
-55	18	20	20
-40	15	20	20

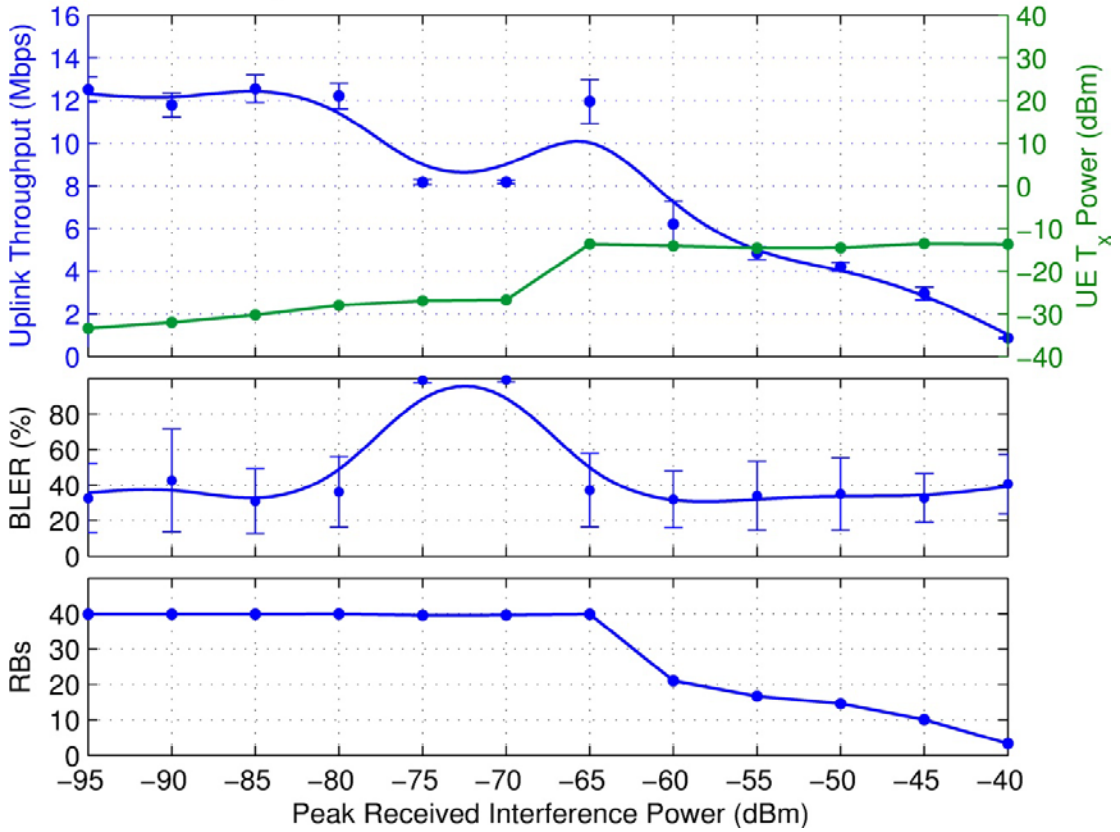

Figure 49. Data throughput, UE transmit (T_x) power, BLER, and RB usage for P0N-12 (PW = 10 µs, PRR = 10,000/sec, DC = 10%) interference.

Table 43. MCS state for P0N-12 (PW = 10 µs, PRR = 10,000/sec, DC = 10%) interference.

I dBm	Transmit Channel 0		
	Min MCS	Most Frequent MCS	Max MCS
-95	20	20	20
-90	20	20	20
-85	20	20	20
-80	20	20	20
-75	20	20	20
-70	20	20	20
-65	19	20	20
-60	18	20	20
-55	18	20	20
-50	17	20	20
-45	17	20	20
-40	15	20	20

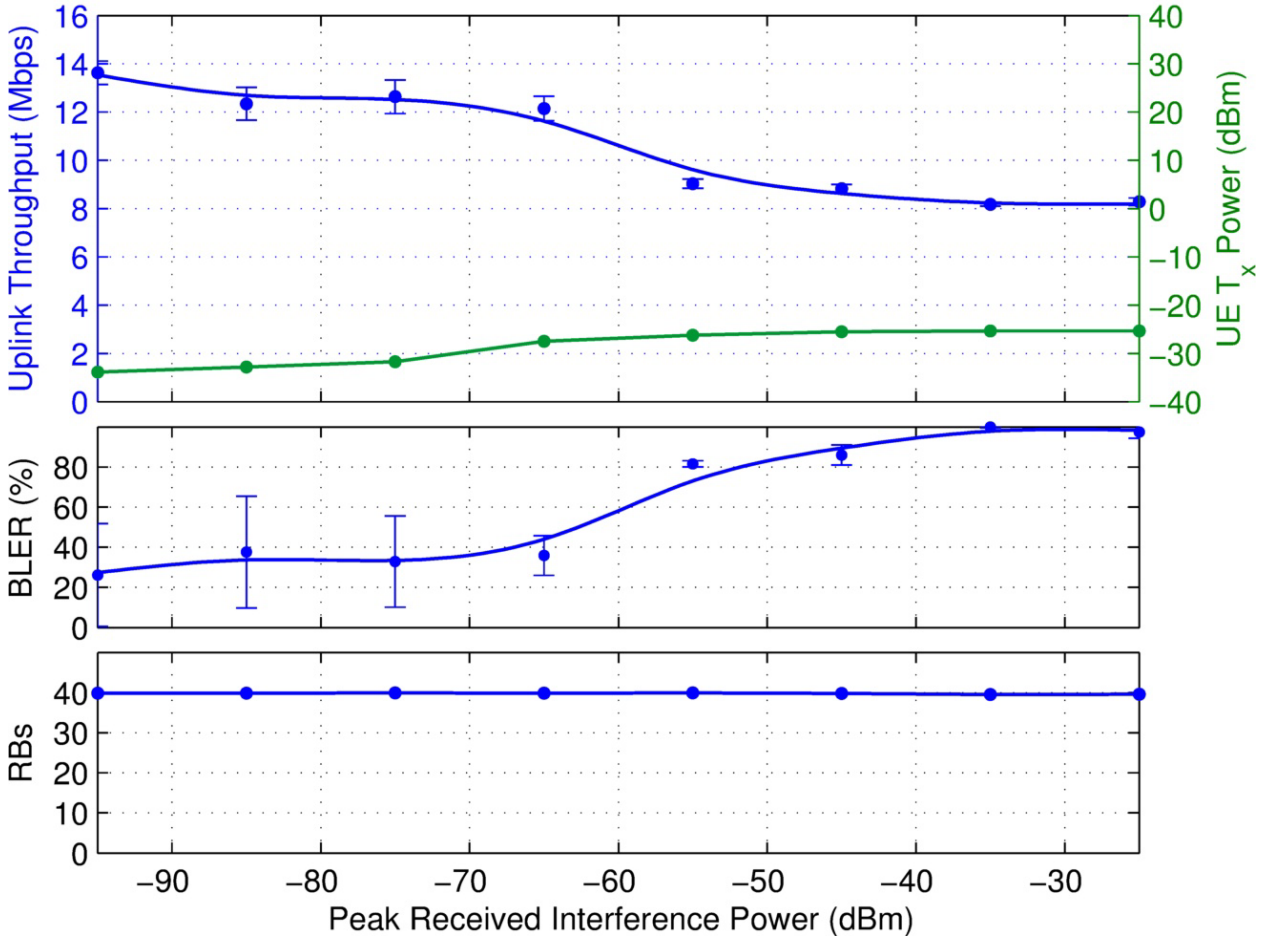

Figure 50. Data throughput, UE transmit (T_x) power, BLER, and RB usage for Q3N-1 (PW = 10 µs, PRR = 1,000/sec, DC = 1%) interference.

Table 44. MCS state for Q3N-1 (PW = 10 µs, PRR = 1,000/sec, DC = 1%) interference.

I dBm	Transmit Channel 0		
	Min MCS	Most Frequent MCS	Max MCS
-95	20	20	20
-85	20	20	20
-75	20	20	20
-65	20	20	20
-55	20	20	20
-45	20	20	20
-35	19	20	20
-25	20	20	20

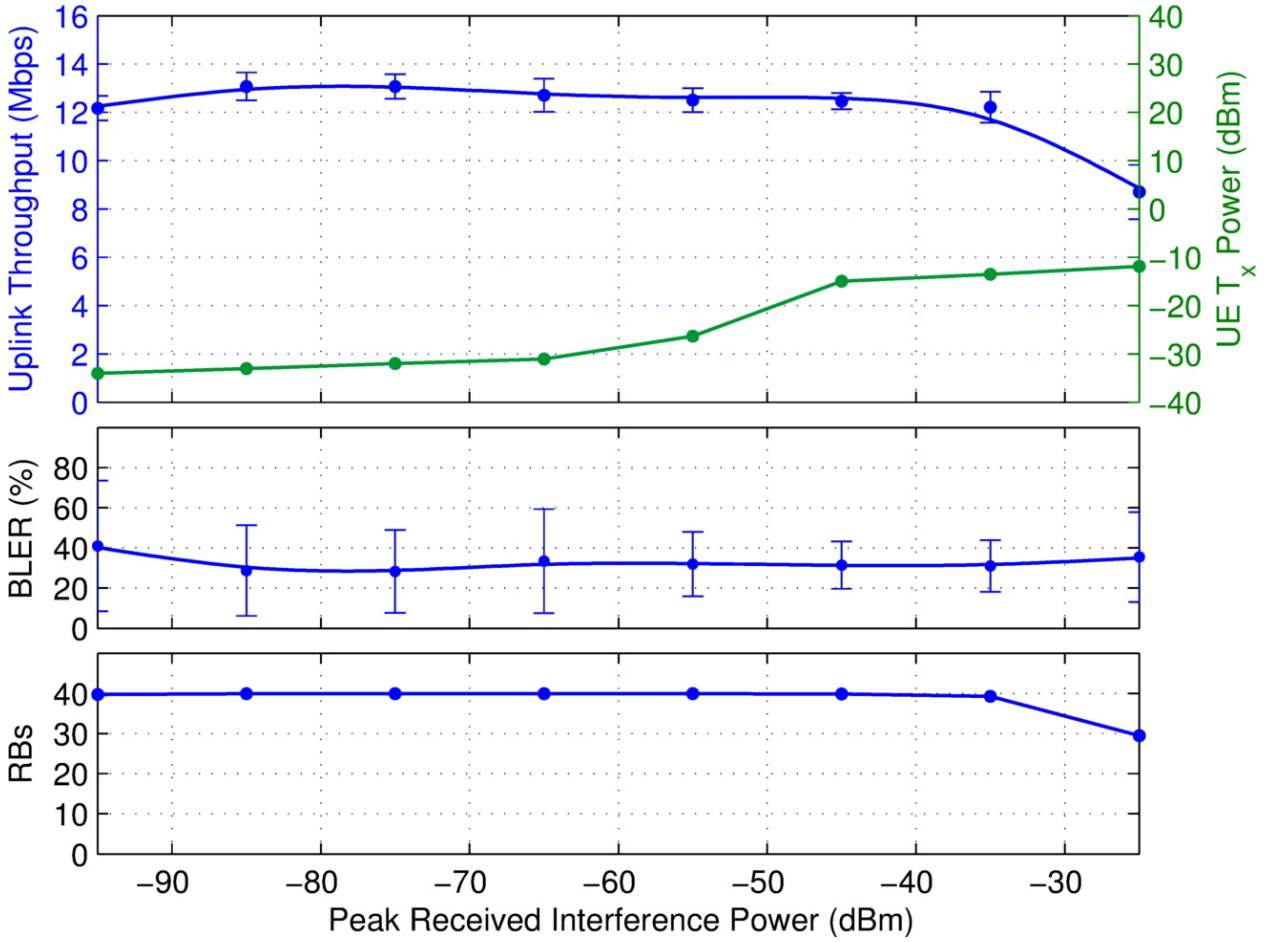

Figure 51. Data throughput, UE transmit (T_x) power, BLER, and RB usage for Q3N-2 (PW = 0.33 µs, PRR = 10,000/sec, DC = 1%) interference.

Table 45. MCS state for Q3N-2 (PW = 0.33 µs, PRR = 10,000/sec, DC = 1%) interference.

I dBm	Transmit Channel 0		
	Min MCS	Most Frequent MCS	Max MCS
-95	20	20	20
-85	20	20	20
-75	20	20	20
-65	20	20	20
-55	20	20	20
-45	18	20	20
-35	19	20	20
-25	18	19	20

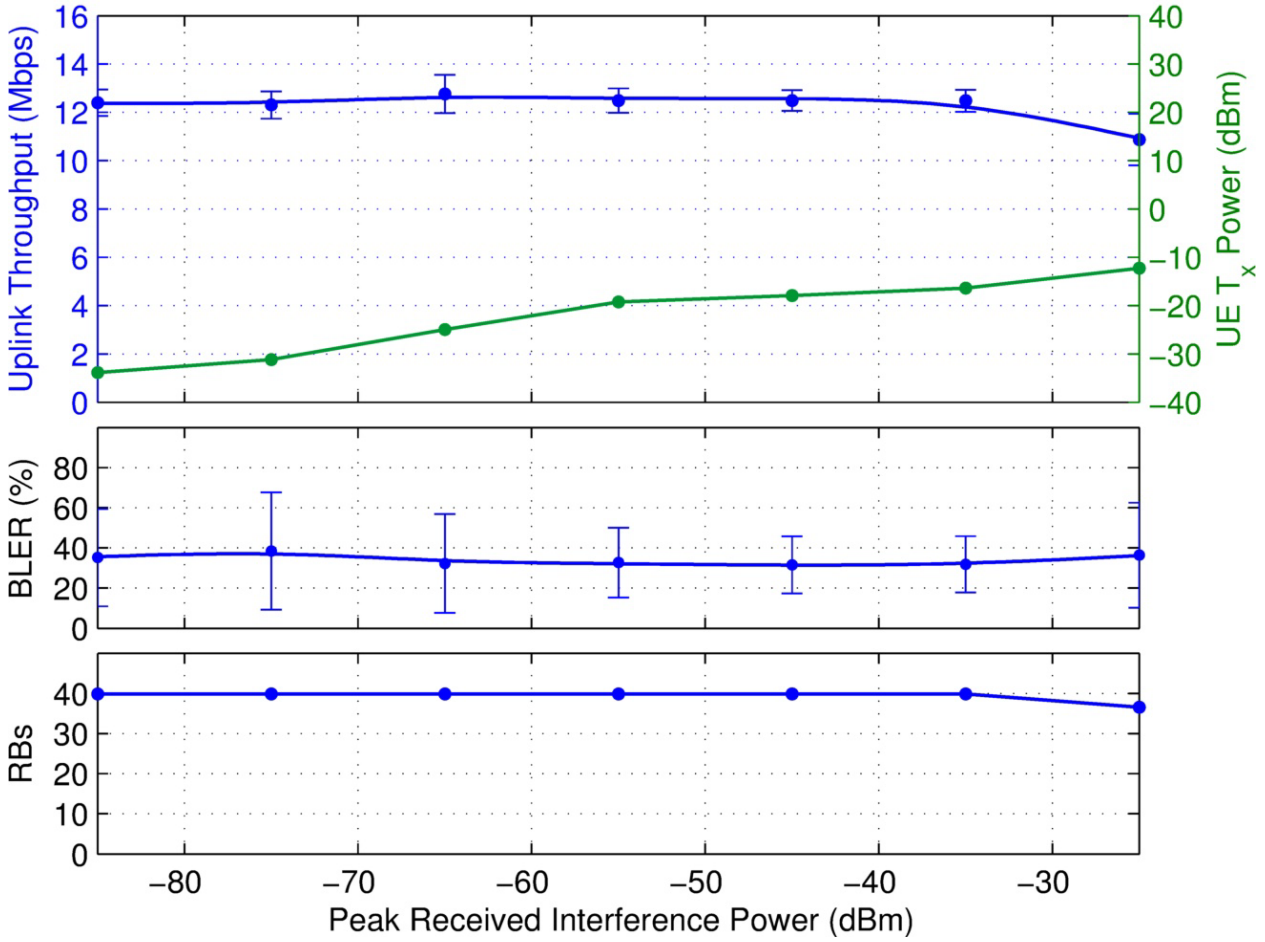

Figure 52. Data throughput, UE transmit (T_x) power, BLER, and RB usage for Q3N-3 (PW = 0.33 µs, PRR = 30,000/sec, DC = 1%) interference.

Table 46. MCS state for Q3N-3 (PW = 0.33 µs, PRR = 30,000/sec, DC = 1%) interference.

I dBm	Transmit Channel 0		
	Min MCS	Most Frequent MCS	Max MCS
-85	20	20	20
-75	20	20	20
-65	20	20	20
-55	20	20	20
-45	20	20	20
-35	20	20	20
-25	18	19	20

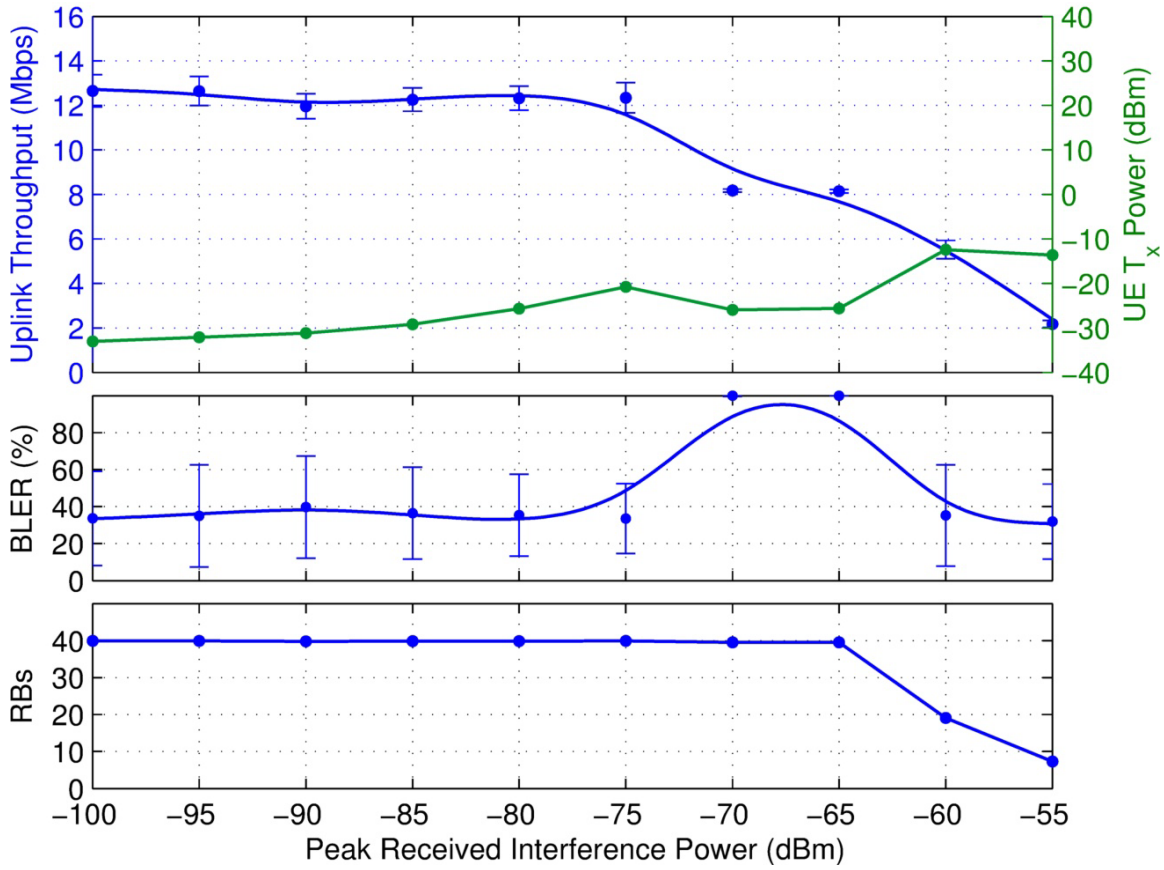

Figure 53. Data throughput, UE transmit (T_x) power, BLER, and RB usage for Q3N-4 (PW = 10 µs, PRR = 10,000/sec, equivalent to PW = 100 µs, PRR = 1,000/sec, DC = 10%) interference.

Table 47. MCS state for Q3N-4 (PW = 10 µs, PRR = 10,000/sec, equivalent to PW = 100 µs, PRR = 1,000/sec), DC = 10%) interference.

I dBm	Transmit Channel 0		
	Min MCS	Most Frequent MCS	Max MCS
-100	20	20	20
-95	20	20	20
-90	20	20	20
-85	20	20	20
-80	20	20	20
-75	20	20	20
-70	20	20	20
-65	17	20	20
-60	18	18	20
-55	17	20	20

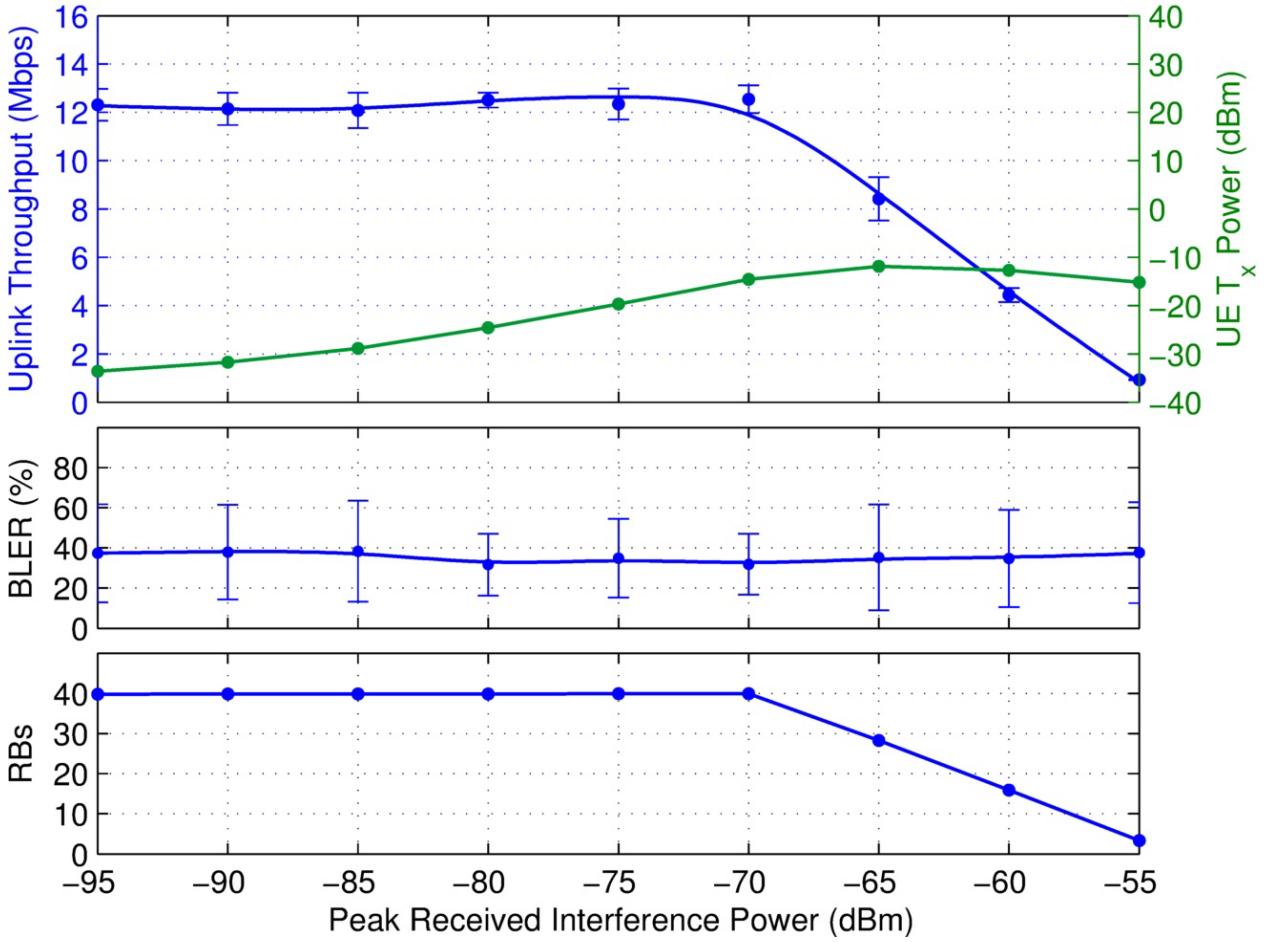

Figure 54. Data throughput, UE transmit (T_x) power, BLER, and RB usage for Q3N-6 (PW = 3.3 µs, PRR = 30,303/sec, DC = 10%) interference.

Table 48. MCS state for Q3N-6 (PW = 3.3 µs, PRR = 30,303/sec, DC = 10%) interference.

I dBm	Transmit Channel 0		
	Min MCS	Most Frequent MCS	Max MCS
-95	20	20	20
-90	20	20	20
-85	20	20	20
-80	20	20	20
-75	20	20	20
-70	20	20	20
-65	18	19	20
-60	18	18	20
-55	14	20	20

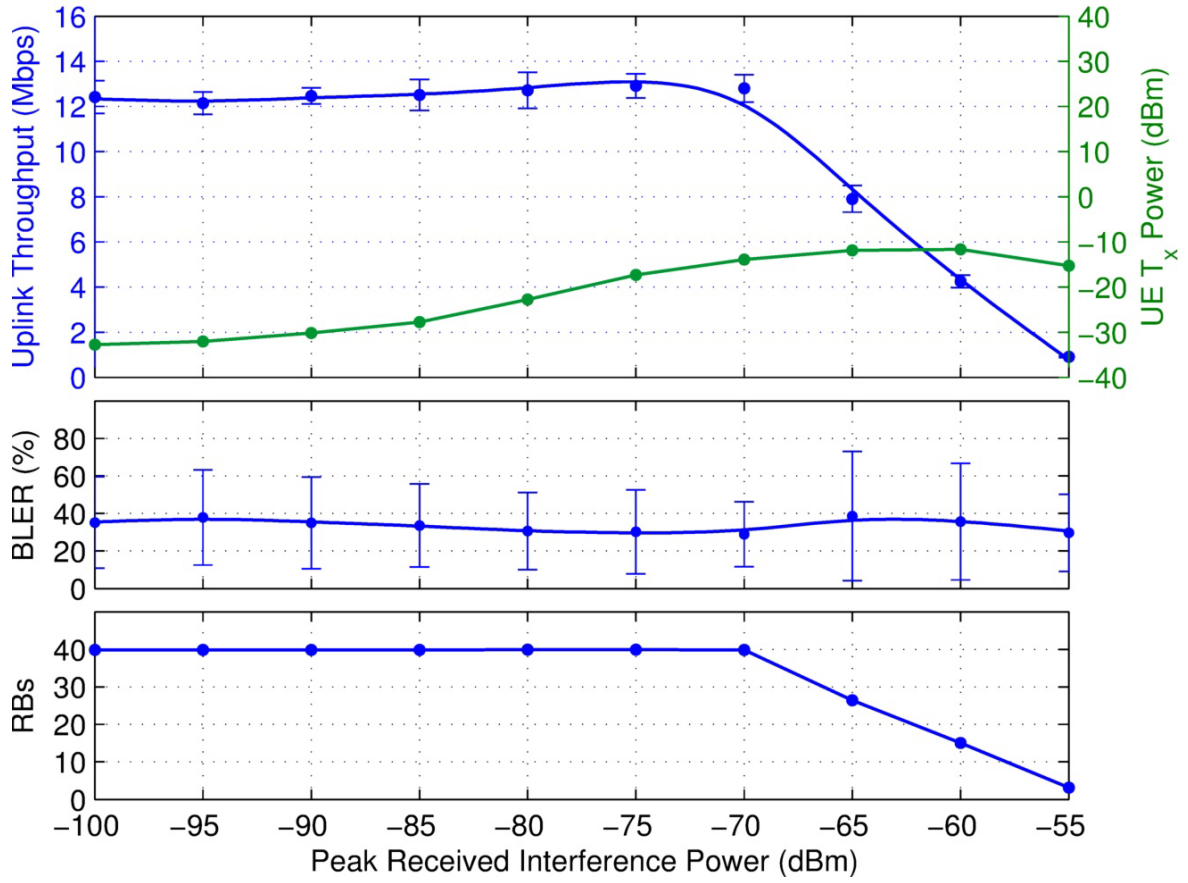

Figure 55. Data throughput, UE transmit (T_x) power, BLER, and RB usage for Q3N-7 (PW = 10 µs, PRR = 20,000/sec, equivalent to PW = 200 µs, PRR = 1,000/sec, DC = 20%) interference.

Table 49. MCS state for Q3N-7 (PW = 10 µs, PRR = 20,000/sec, equivalent to PW = 200 µs, PRR = 1,000/sec, DC = 20%) interference.

I dBm	Transmit Channel 0		
	Min MCS	Most Frequent MCS	Max MCS
-100	20	20	20
-95	20	20	20
-90	20	20	20
-85	20	20	20
-80	20	20	20
-75	20	20	20
-70	20	20	20
-65	18	19	20
-60	18	18	20
-55	14	20	20

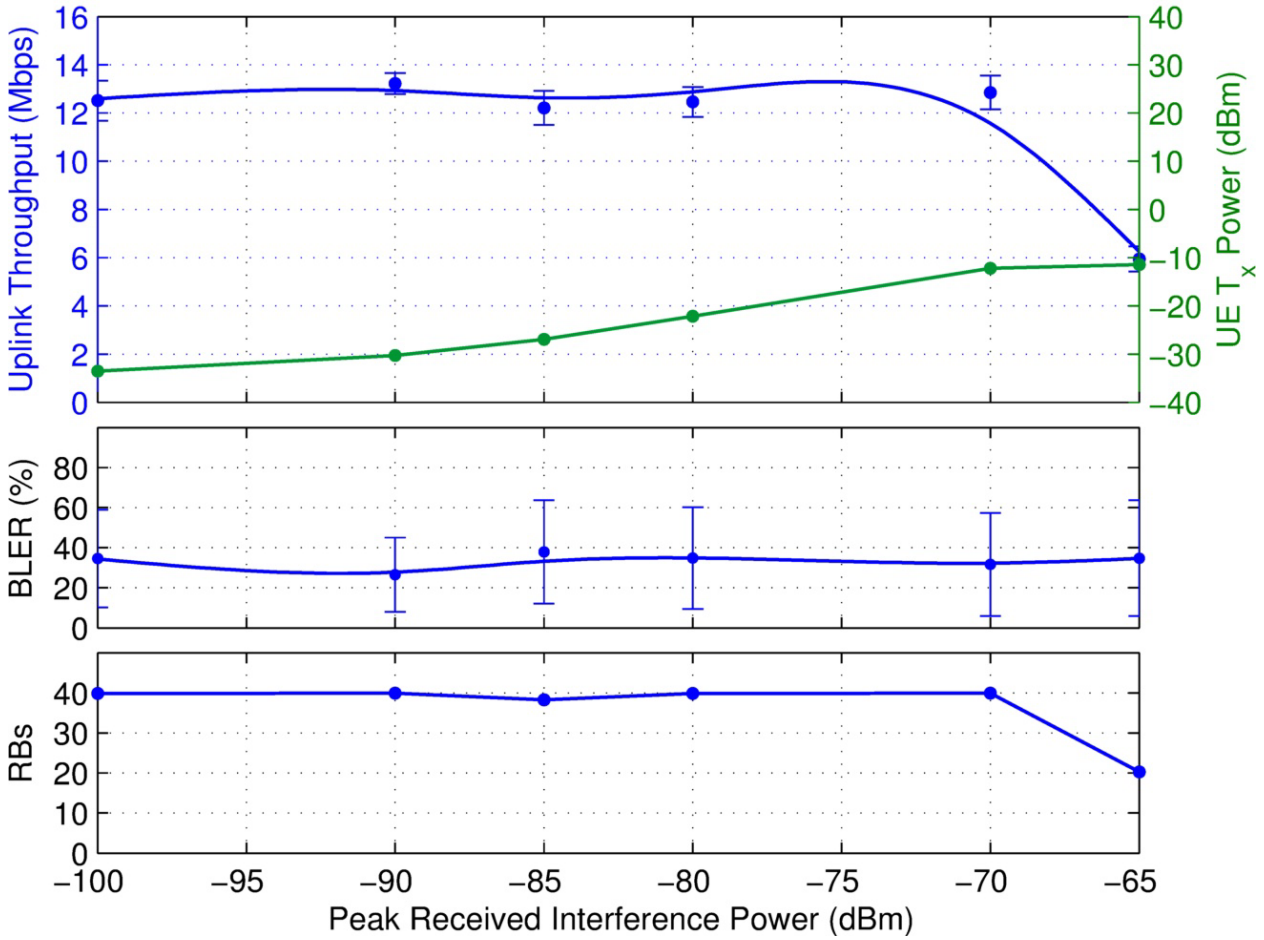

Figure 56. Data throughput, UE transmit (T_x) power, BLER, and RB usage for Q3N-9 (PW = 6.6 µs, PRR = 30,303/sec, DC = 20%) interference.

Table 50. MCS state for Q3N-9 (PW = 6.6 µs, PRR = 30,303/sec, DC = 20%) interference.

I dBm	Transmit Channel 0		
	Min MCS	Most Frequent MCS	Max MCS
-100	20	20	20
-90	20	20	20
-85	20	20	20
-80	20	20	20
-70	19	20	20
-65	18	18	20

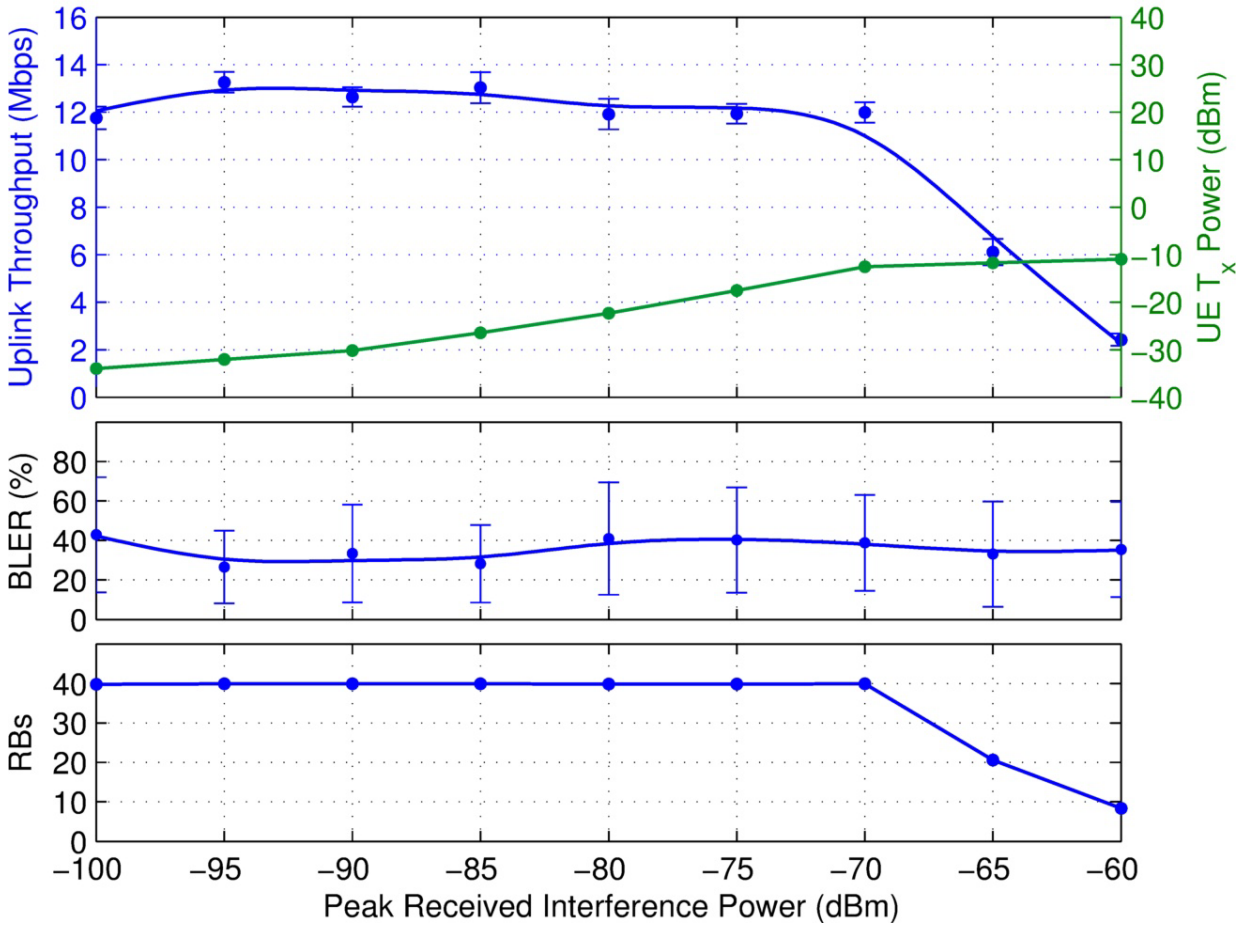

Figure 57. Data throughput, UE transmit (T_x) power, BLER, and RB usage for Q3N-10 (PW = 10 µs, PRR = 30,000/sec, equivalent to PW = 300 µs, PRR = 1,000/sec, DC = 30%) interference.

Table 51. MCS state for Q3N-10 (PW = 10 µs, PRR = 30,000/sec, equivalent to PW = 300 µs, PRR = 1,000/sec, DC = 30%) interference.

I dBm	Transmit Channel 0		
	Min MCS	Most Frequent MCS	Max MCS
-100	20	20	20
-95	20	20	20
-90	20	20	20
-85	20	20	20
-80	20	20	20
-75	20	20	20
-70	18	20	20
-65	18	18	20
-60	13	20	20

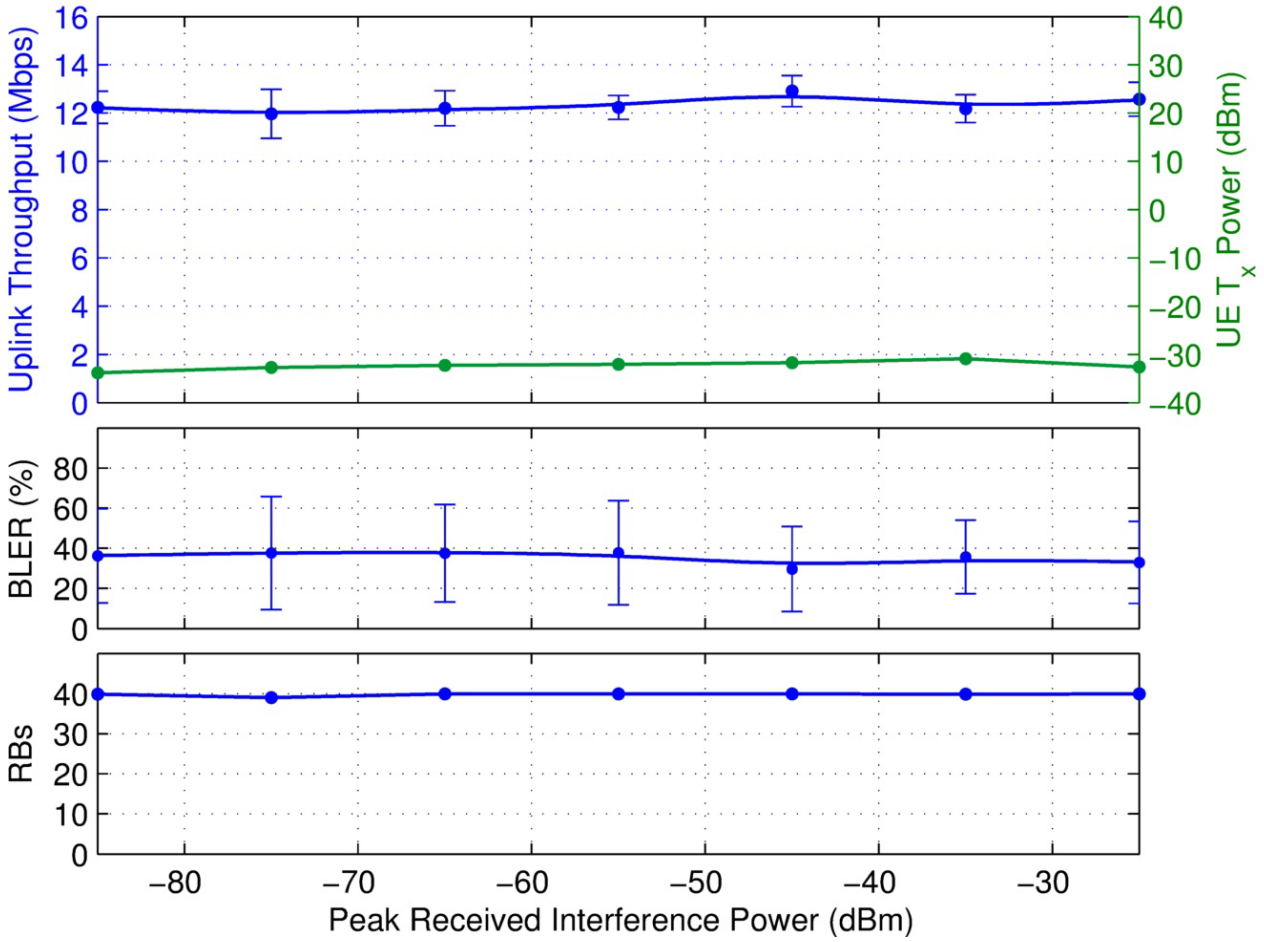

Figure 58. Data throughput, UE transmit (T_x) power, BLER, and RB usage for ECC-1/WFM-1 (PW = 4 µs, PRR = 1,000/sec, DC = 0.4%) interference.

Table 52. MCS state for ECC-1/WFM-1 (PW = 4 µs, PRR = 1,000/sec, DC = 0.4%) interference.

I dBm	Transmit Channel 0		
	Min MCS	Most Frequent MCS	Max MCS
-85	20	20	20
-75	20	20	20
-65	20	20	20
-55	20	20	20
-45	20	20	20
-35	20	20	20
-25	20	20	20

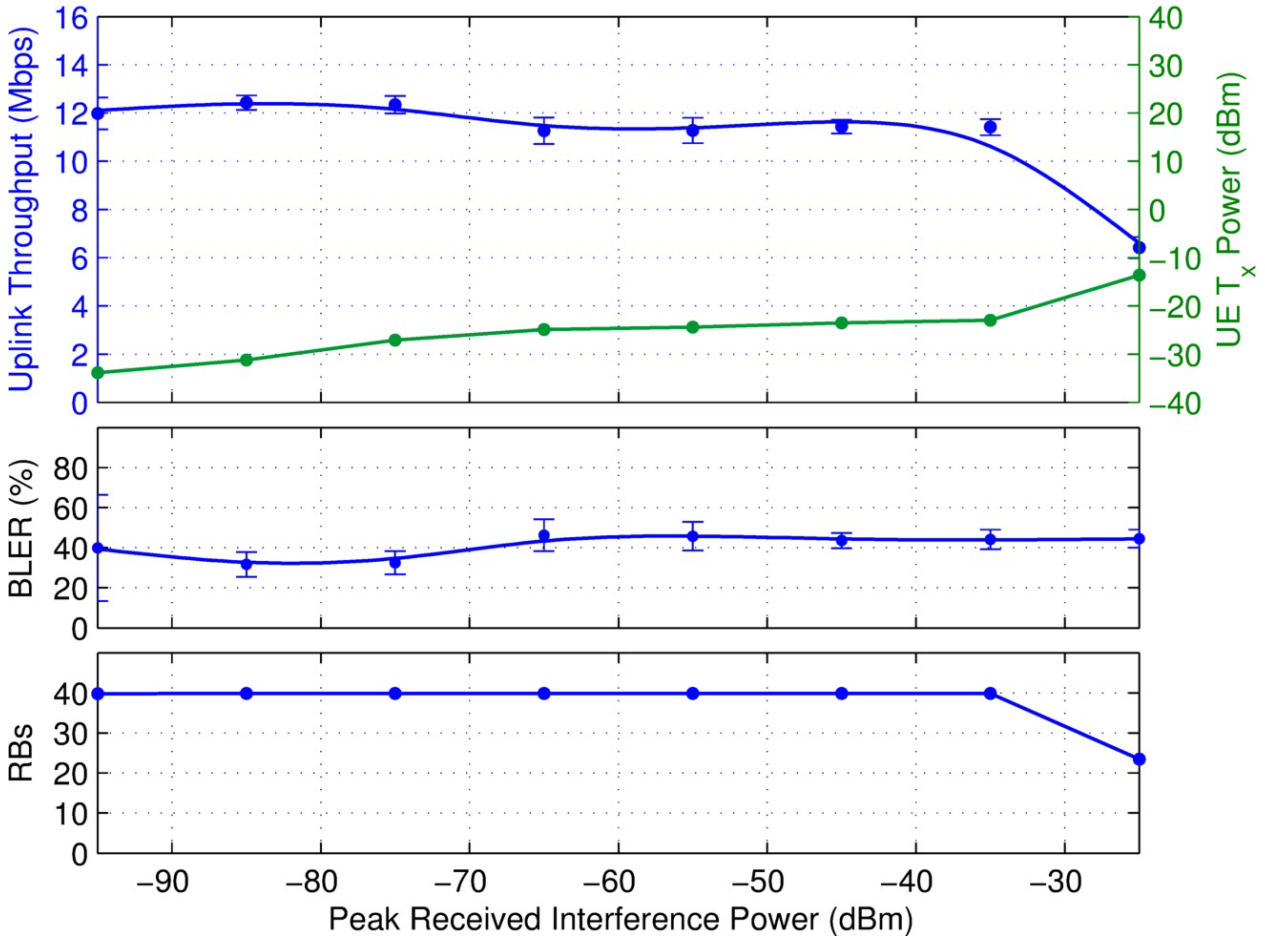

Figure 59. Data throughput, UE transmit (T_x) power, BLER, and RB usage for ECC-2/WFM-2 (PW = 100 µs, PRR = 300/sec, DC = 3%) interference.

Table 53. MCS state for ECC-2/WFM-2 (PW = 100 µs, PRR = 300/sec, DC = 3%) interference.

I dBm	Transmit Channel 0		
	Min MCS	Most Frequent MCS	Max MCS
-95	20	20	20
-85	20	20	20
-75	20	20	20
-65	20	20	20
-55	20	20	20
-45	20	20	20
-35	20	20	20
-25	17	20	20

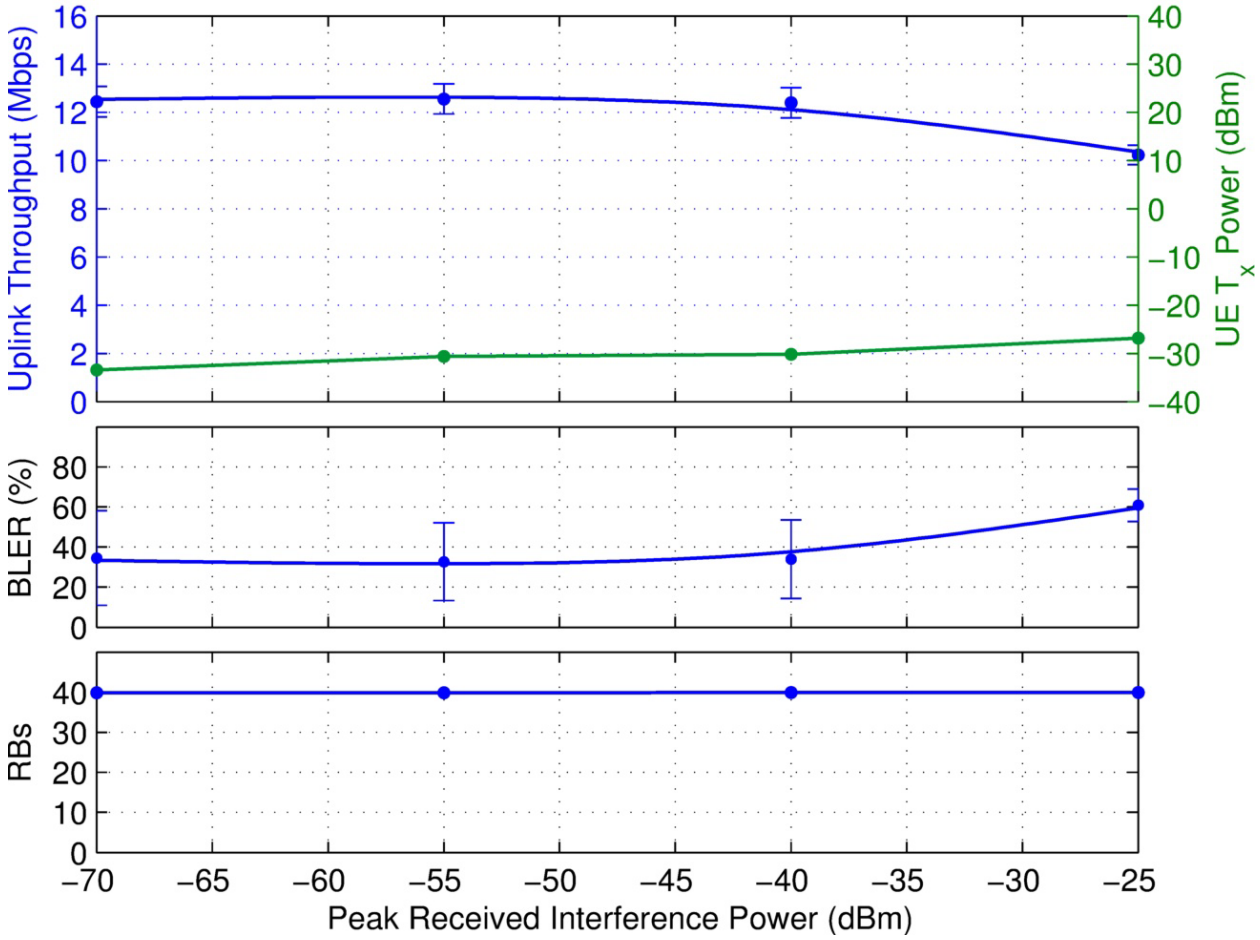

Figure 60. Data throughput, UE transmit (T_x) power, BLER, and RB usage for TDWR/P0N-13 (PW = 1 µs, PRR = 2,000/sec, DC = 3%) interference.

Table 54. MCS state for TDWR/P0N-13 (PW = 1 µs, PRR = 2,000/sec, DC = 3%) interference.

I dBm	Transmit Channel 0		
	Min MCS	Most Frequent MCS	Max MCS
-70	20	20	20
-55	20	20	20
-40	20	20	20
-25	20	20	20

3.2.2 Burst Interference Testing

As noted previously, radar beams normally scan intermittently across fixed points in space. Burst interference testing replicated realistic radar-beam interference scenarios by injecting 20 pulses of radar interference every 5 seconds throughout the collection of diagnostic data. Figures 61–72 provide the results of the burst tests for the uplink. These graphs show how data throughput (top graph) and MCS (bottom graph) varied over time during the total duration of the data recording. For the uplink, only a single transmission channel was used. The two graphs in each figure are time synchronized based on timestamps contained in the diagnostic software data, the same way the burst data was synchronized for the downlink. The first timestamp in either the throughput data or the MCS data (whichever was started first) was used to determine the starting time of each graph. For all burst tests performed on the uplink, I_{peak} = -25 dBm.

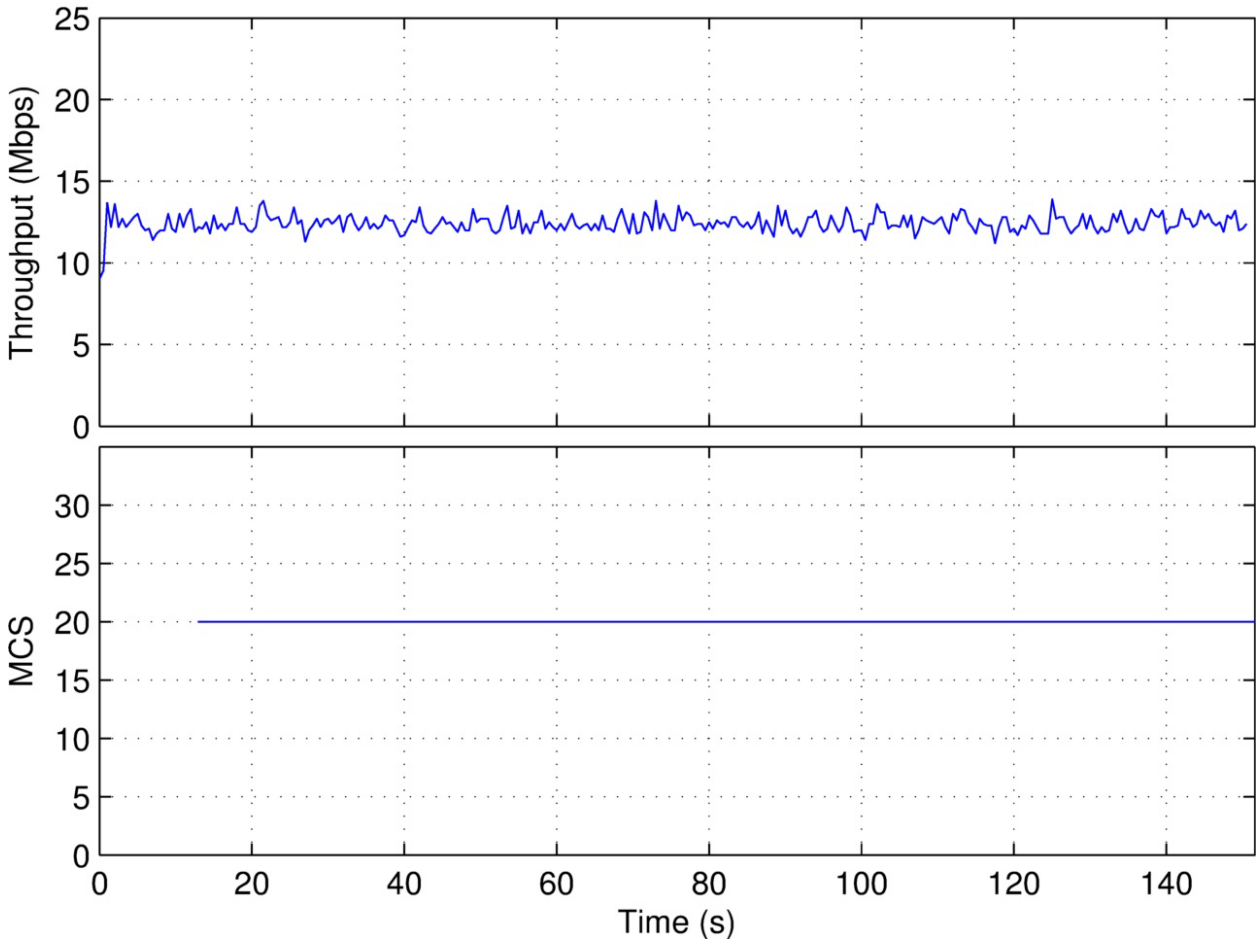

Figure 61. Data throughput and MCS state for P0N-1 interference.

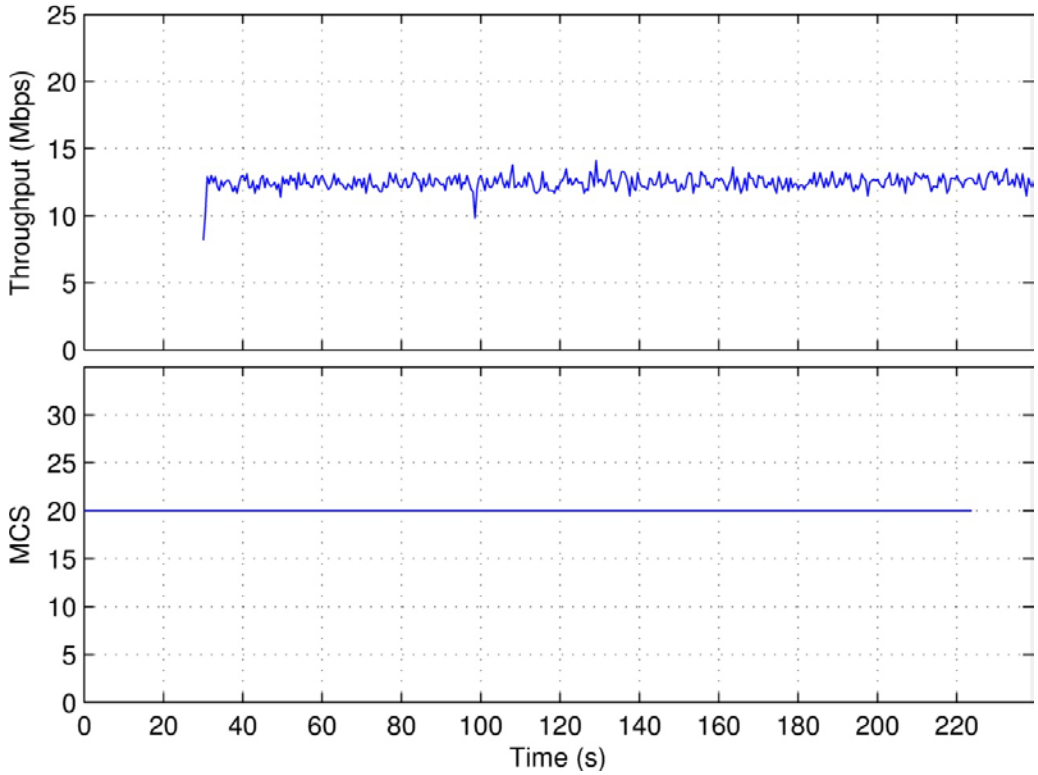

Figure 62. Data throughput and MCS state for P0N-2 interference.

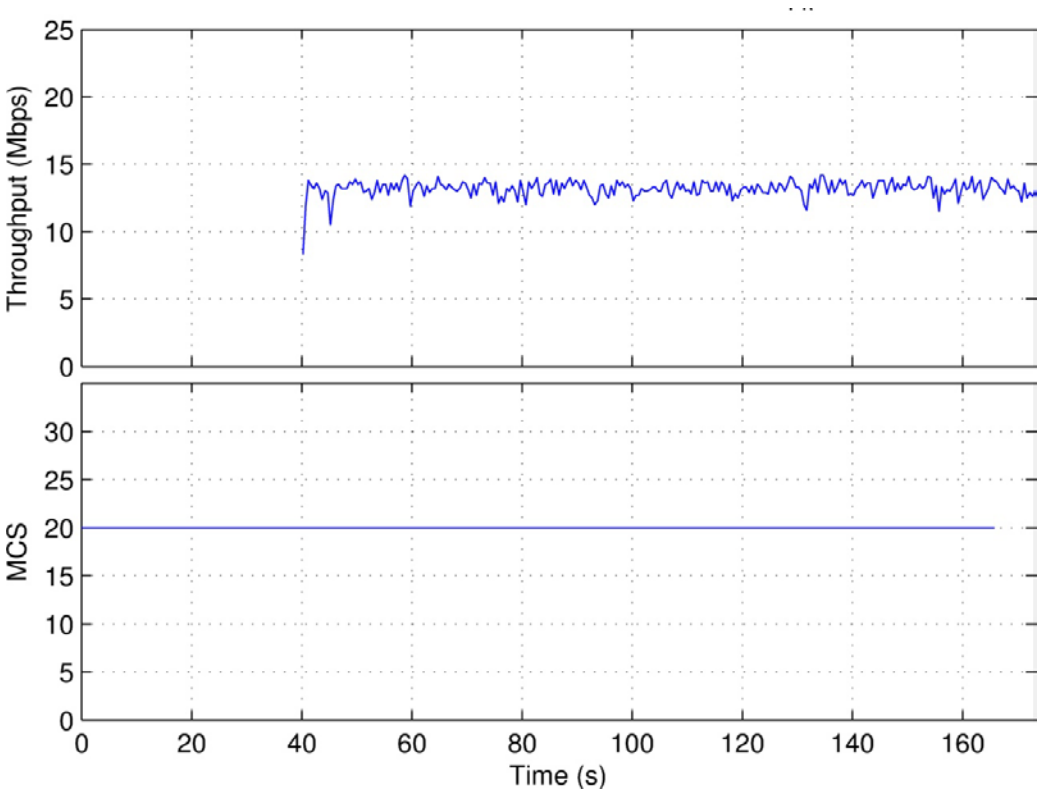

Figure 63. Data throughput and MCS state for P0N-5 interference.

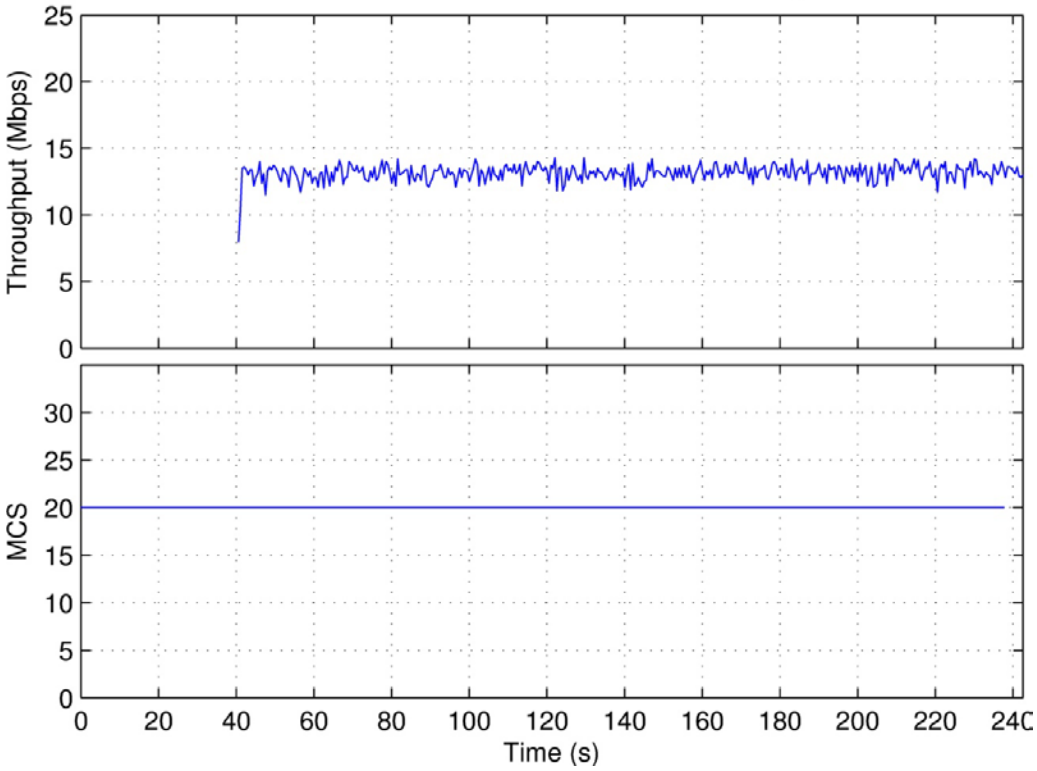

Figure 64. Data throughput and MCS state for P0N-8 interference.

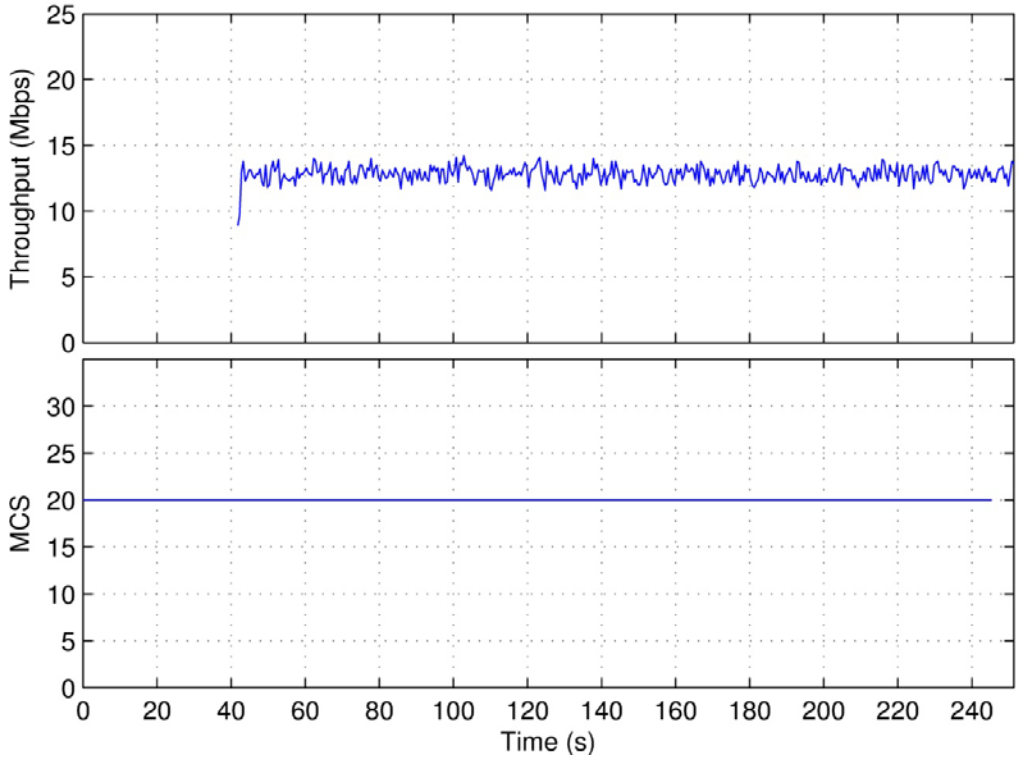

Figure 65. Data throughput and MCS state for P0N-10 interference.

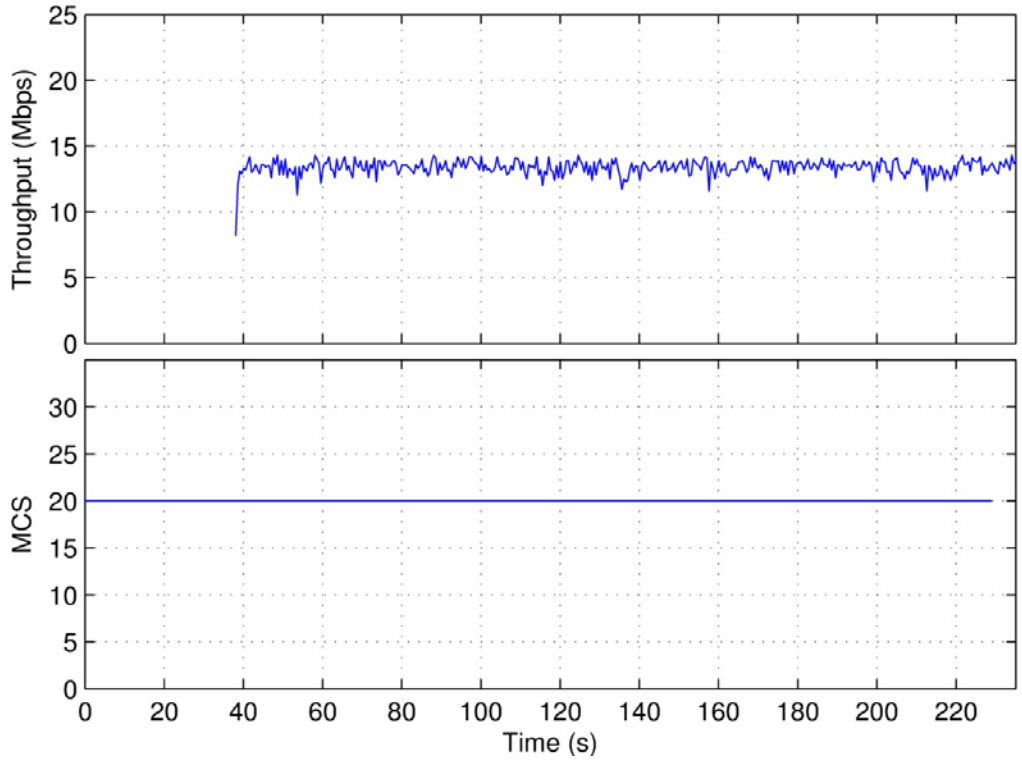

Figure 66. Data throughput and MCS state for P0N-11 interference.

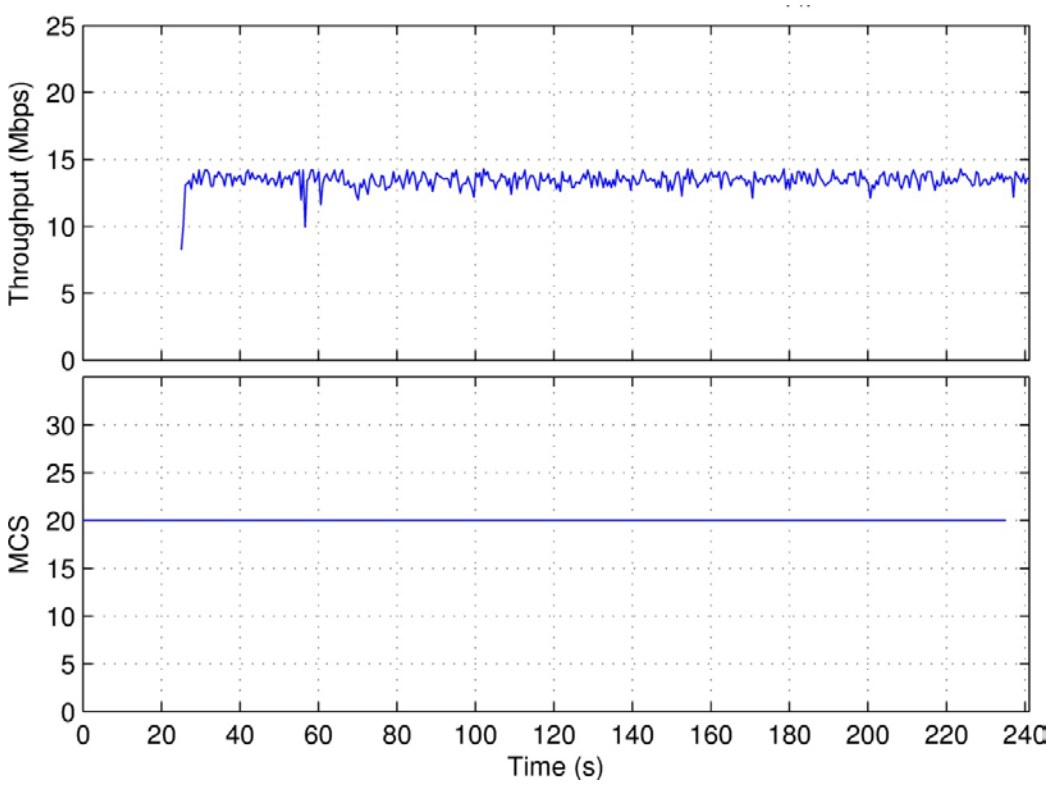

Figure 67. Data throughput and MCS state for Q3N-1 interference.

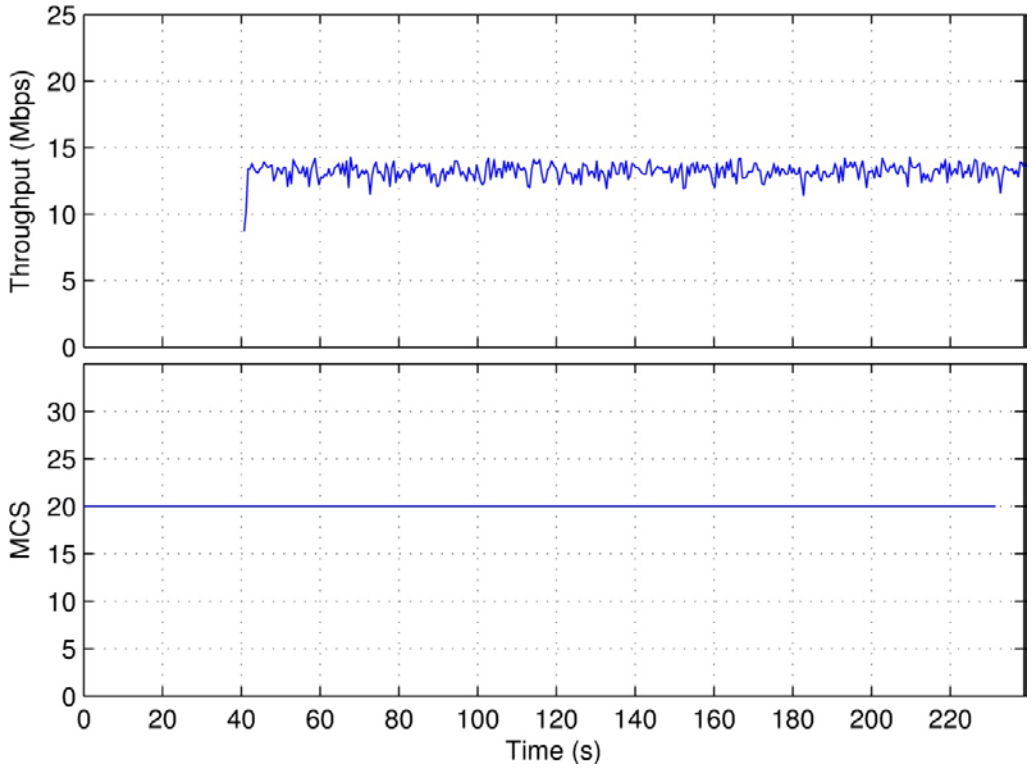

Figure 68. Data throughput and MCS state for Q3N-4 interference.

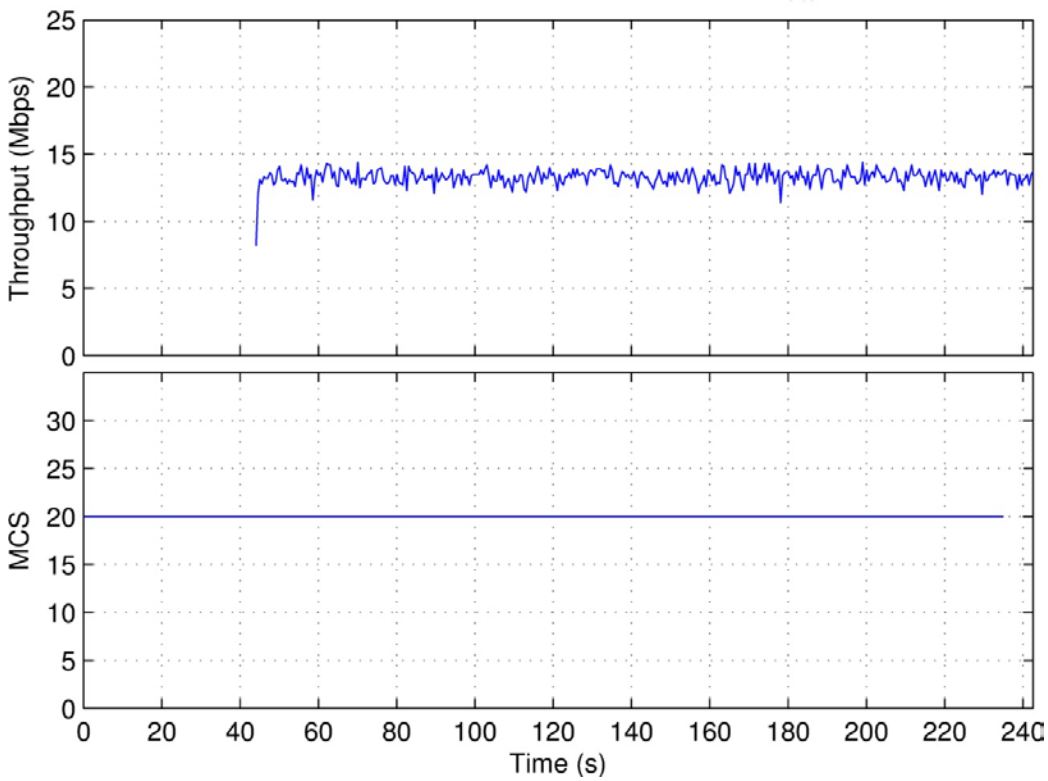

Figure 69. Data throughput and MCS state for Q3N-6 interference.

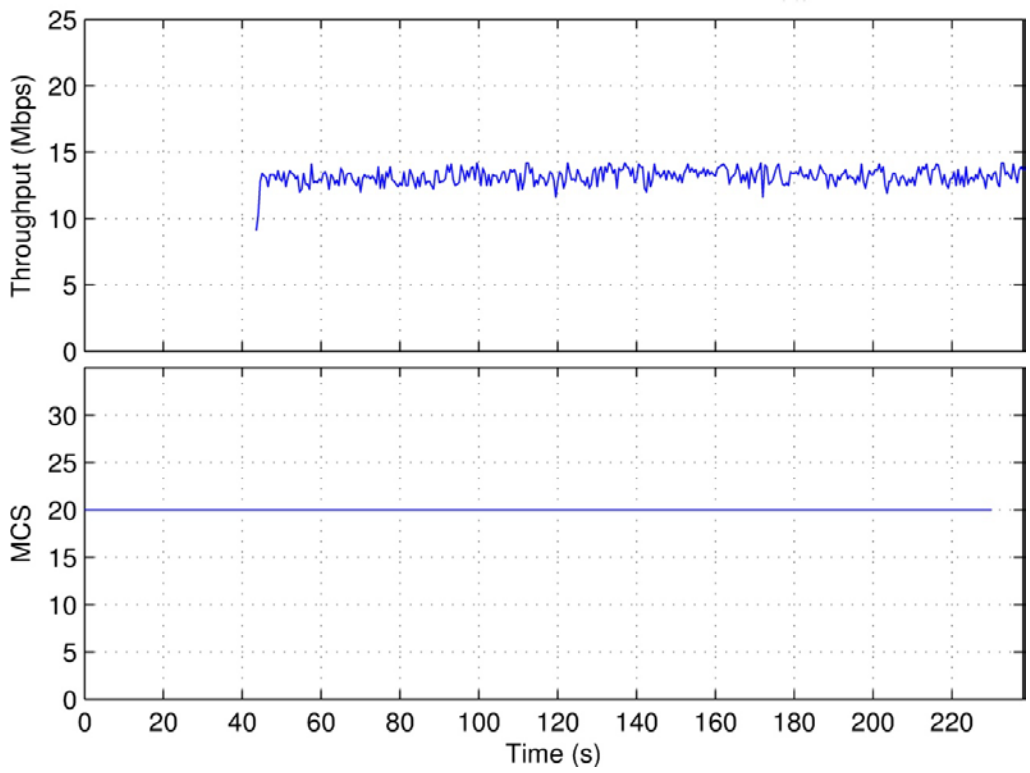

Figure 70. Data throughput and MCS state for Q3N-7 interference.

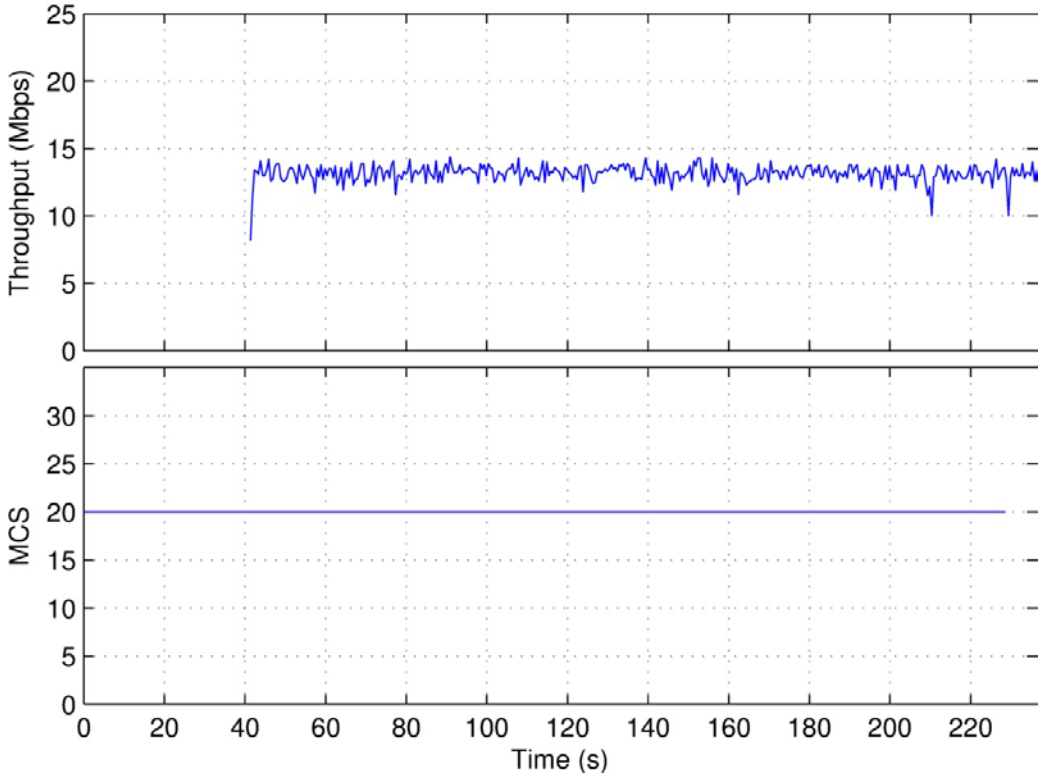

Figure 71. Data throughput and MCS state for Q3N-9 interference.

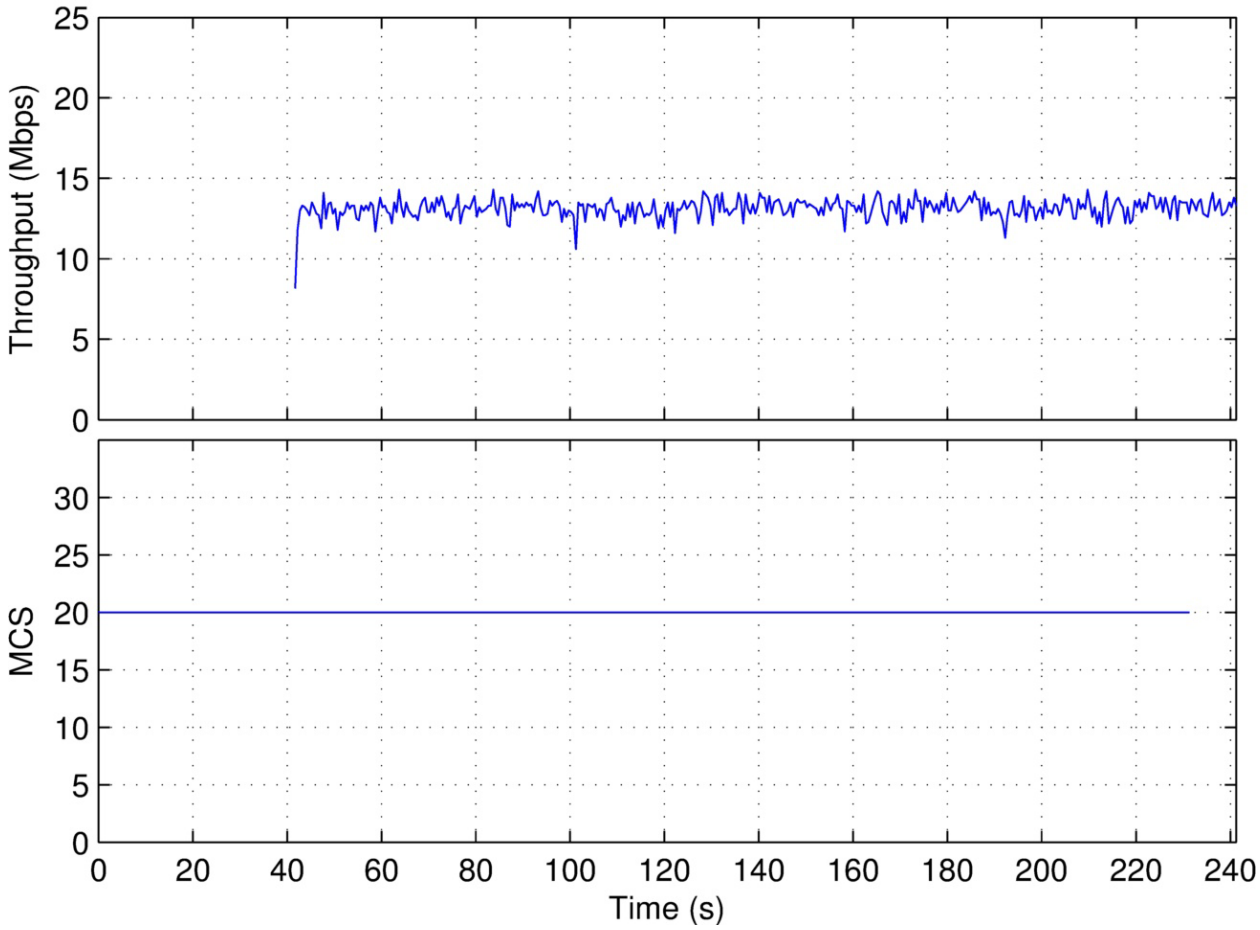

Figure 72. Data throughput and MCS state for Q3N-10 interference.

4 LTE EMISSION SPECTRUM MEASUREMENTS

4.1 LTE Emission Spectrum Measurement Procedure

While the authors had access to the LTE (FDD) prototype network during the course of the interference-effects measurements, they measured the emission spectrum of unfiltered LTE eNB and UE transmitters. The measurements were performed, with a slight variation, in accord with the procedures of [8], by measuring using both peak and average detection. The measurement set-up is shown in Figure 73. The spectra were measured with approximately 60 dB of dynamic range for the eNB and 65 dB for the UE. Dynamic range was limited for these measurements due to configuration of the downlink and uplink RF paths between the eNB and UE which could not be altered. The RF path loss from the eNB output to the preselector input was approximately 50 dB, and the RF path loss from the UE output to the preselector input was approximately 53 dB.

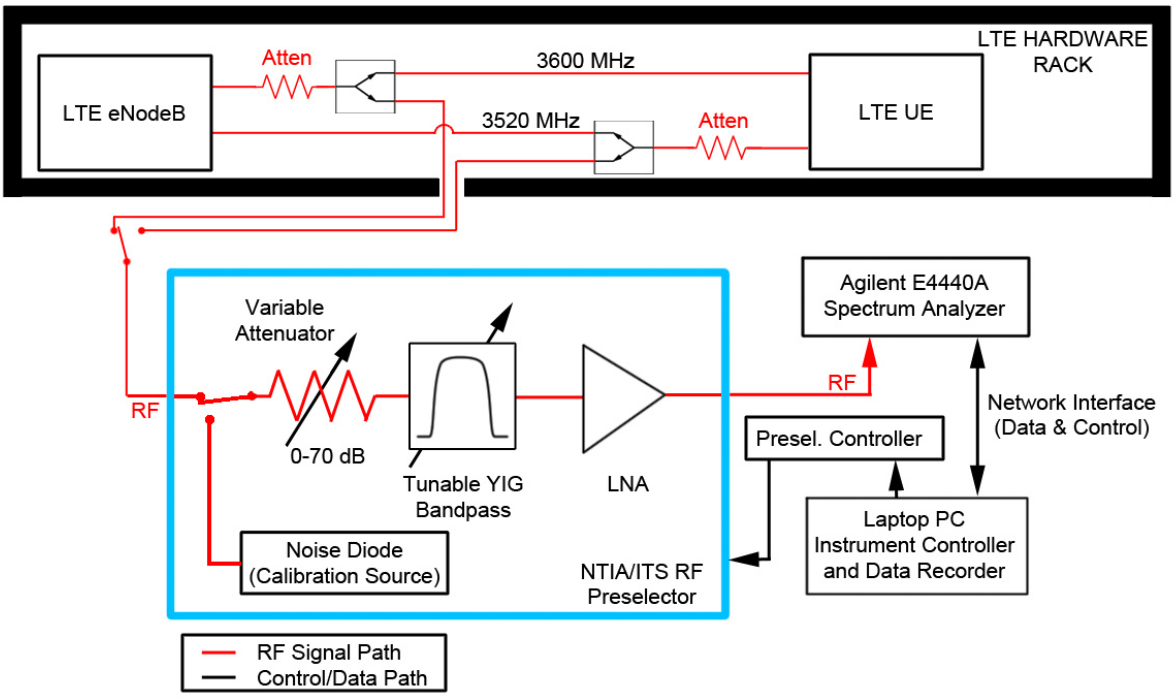

Figure 73. System set-up for the LTE emission spectra measurements.

The standard wide-dynamic range measurement procedure of [8] was followed exactly for the peak-detected spectrum measurements, the key aspect of this procedure being that the measurement progressed as a stepped-frequency rather than a swept-frequency process, allowing for control of dynamic range during the measurement. For the average spectra, however, the procedure was varied slightly. To obtain the average spectra data points, the spectrum analyzer collected 1,001 sample-detected points at each measured frequency in the spectrum. Then the linear-power root-mean-square (RMS) average of those 1,001 points was computed as the *average* emission spectrum power level at each frequency. Both the peak and average spectra

were measured with a dwell interval of 300 ms per frequency data point. The measurement bandwidth of 30 kHz was selected in accordance with [9] for both eNB and UE spectra.

4.2 LTE eNB Emission Spectra

The emission spectrum structure of the LTE eNB transmitter, as measured with both peak and average detection, is shown in Figure 74. The spectrum is similar to WiMAX emission spectra presented in a recent NTIA Report [10], and another LTE eNB emission spectrum presented in [3], around the fundamental. Due to the limited dynamic range of these measurements, it is not possible to determine whether or not the eNB emission spectrum examined in this study exhibits the same flat "porch" seen in the previous LTE and WiMAX emission measurements. The "porch" observed in the previous measurements began leveling off at about -60 dB relative to the fundamental. It is also noted that the spectrum is from a prototype 3.5 GHz LTE eNB.

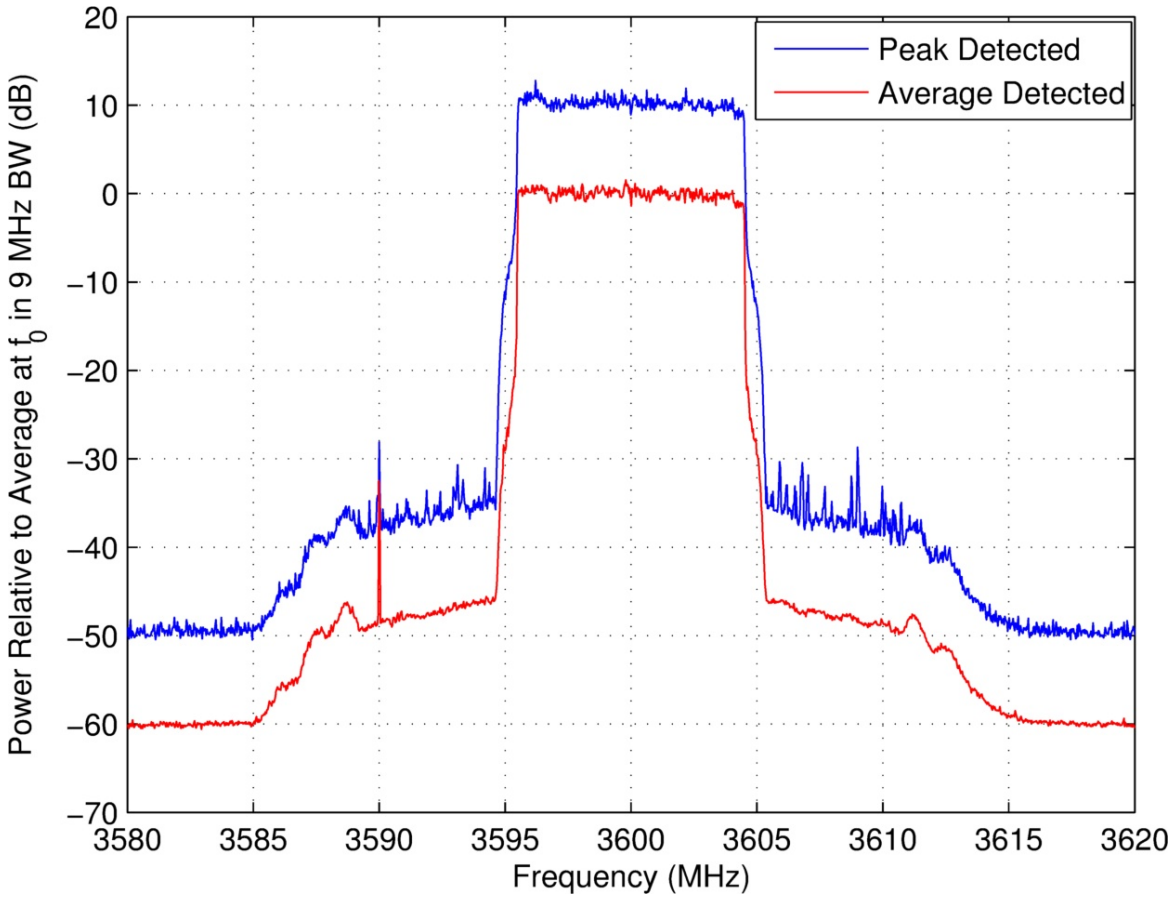

Figure 74. Peak-detected and average-detected LTE eNB emission spectra.

The spectra of other LTE eNBs, manufactured by other companies, may be assumed to generally look similar to Figure 74 around the fundamental. This is due to the fact that various existing manufacturers use similar transmitter designs and they obtain their transmitter power amplifiers from a limited number of suppliers who are all working from the same current technology base. There may, however, be differences in occupied bandwidth. For this FDD LTE network with

10 MHz channel bandwidth, the emission bandwidth of the eNB transmission was 9 MHz. For the TDD LTE network previously examined [3], the occupied bandwidth was closer to 18 MHz. Comparable TDD and FDD LTE systems might both use 20 MHz of total spectrum. The TDD LTE network would allocate that 20 MHz in a single spectrum channel carrying both eNB and UE data. The FDD LTE network would achieve the same performance by splitting the eNB and UE data across two spectrum channels of about 10 MHz each.

The roll-off of the LTE eNB emission spectrum is shown in Figure 75. This spectrum was recorded with all the same parameters as the full eNB emission spectrum using average detection, except that a measurement bandwidth of 1 kHz was used. The number of samples over which the average power was computed (1,001) and the dwell time (300 ms) for each frequency point remained the same as in the full spectrum measurement.

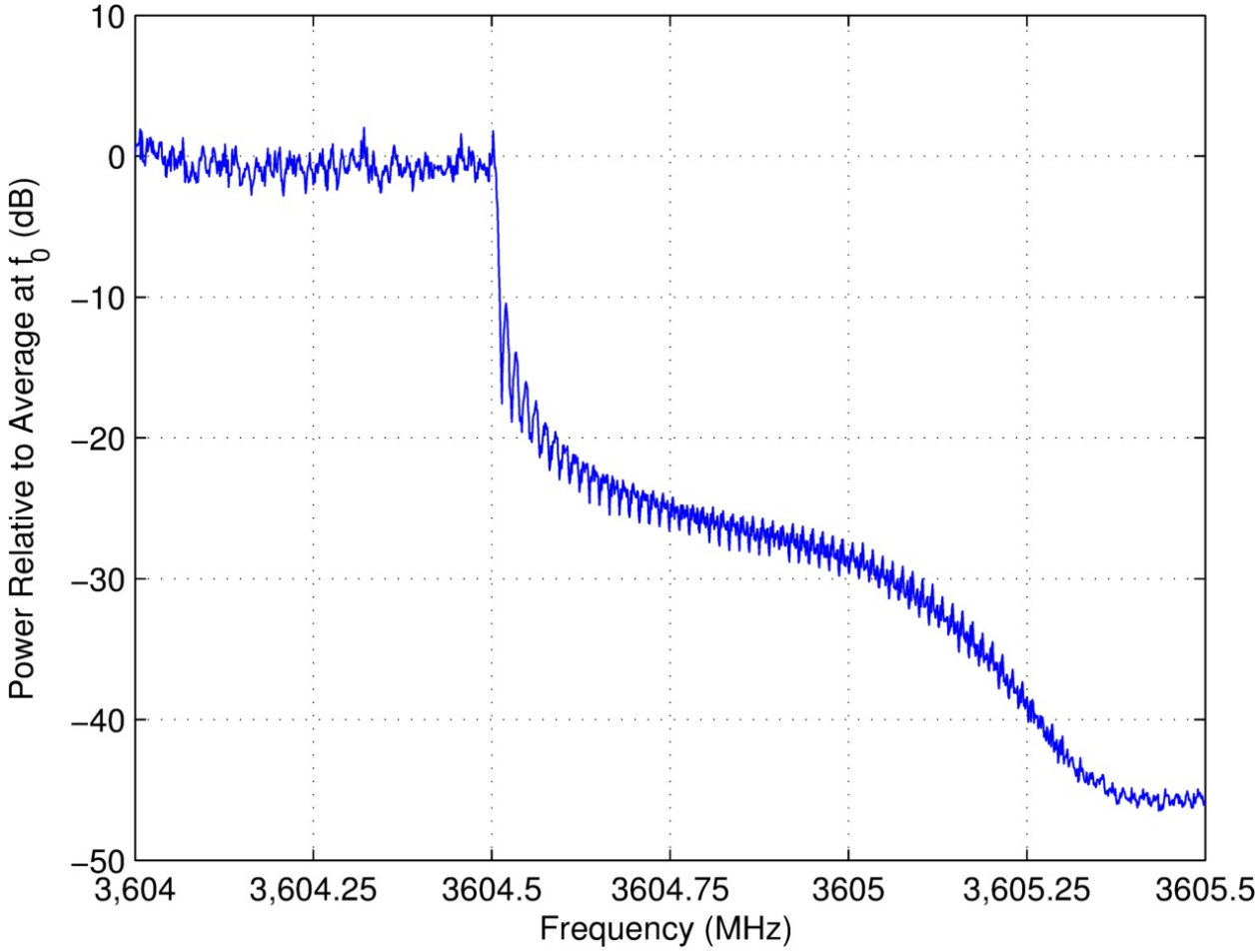

Figure 75. Roll-off of LTE eNB emission spectrum.

4.3 LTE UE Emission Spectra

The emission spectrum structure of the LTE UE transmitter, as measured with both peak and average detection, is shown in Figure 76. While the UE transmission is centered at f_0 = 3520 MHz, the lowest (in frequency) 10 RBs were unused, leaving only the upper 40 RBs

active. Each RB is 180 kHz wide so the total occupied bandwidth of the emission spectrum of the UE is 7.2 MHz, causing the center of the intentional emissions to appear to be at 3520.9 MHz. It should be noted that in the presence of interference, this spectrum can change dramatically as the UE changes the number of RBs in use. A change in RBs will change the total occupied bandwidth of the UE emission spectrum as:

$$BW = RB \cdot BW_{RB}$$

where, *BW* is the total emission bandwidth, *RB* is the number of resource blocks in use, and BW_{RB} is the bandwidth of a single resource block (180 kHz). The authors do not know how RBs are allocated in the presence of interference.

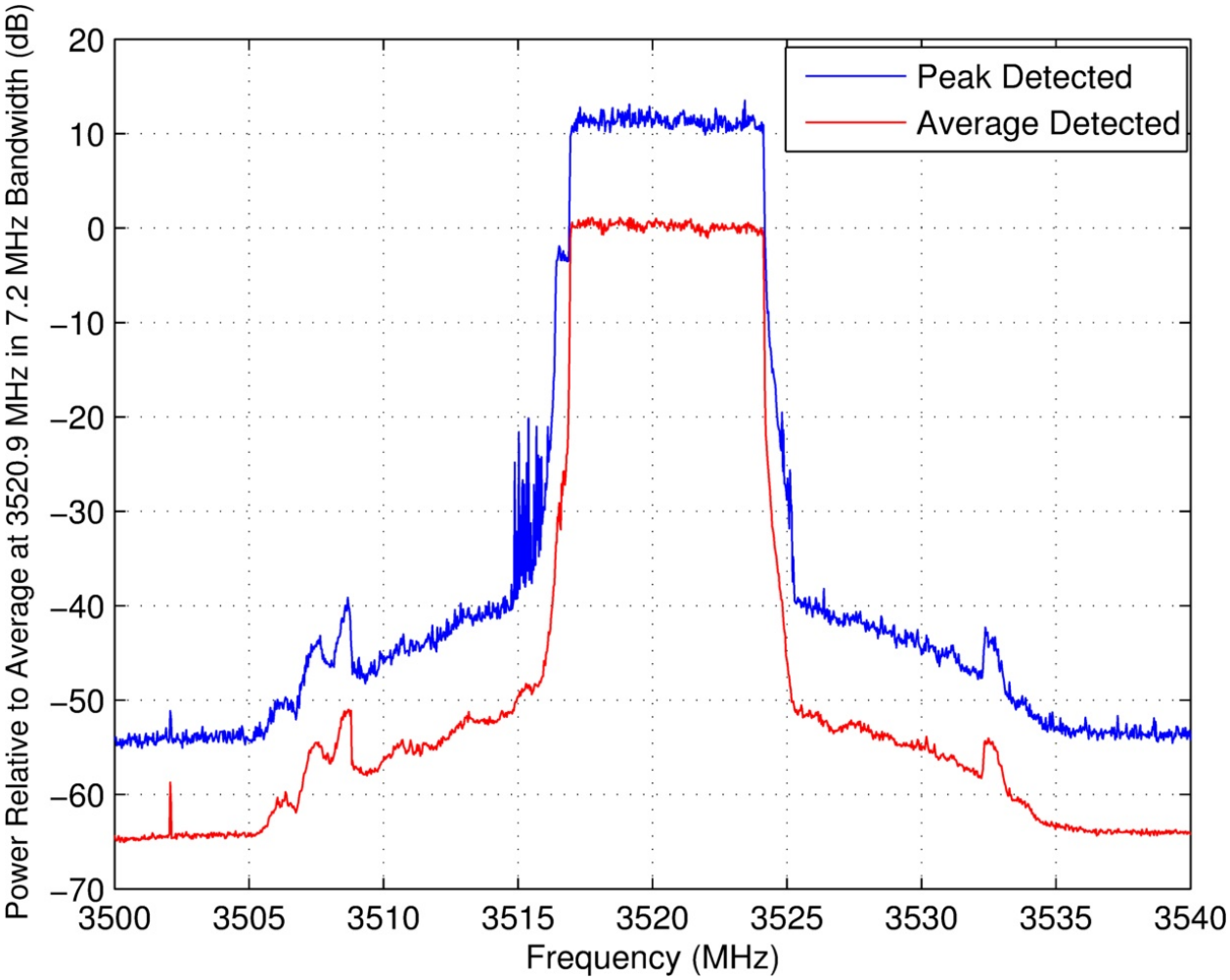

Figure 76. Peak-detected and average-detected LTE UE emission spectra.

5 SUMMARY AND CONCLUSIONS

5.1 Summary of Work and Results

The effects of radar interference on the performance of a prototype LTE (FDD) network have been assessed with a hardware test bed for a wide variety of radar waveforms. The parameters of the waveforms tested span the range of existing and likely future radar systems at 3.5 GHz. The LTE network that was tested is designed to be used as a micro-cell, but the test results are believed to likely be valid for other LTE systems. As a baseline, well-understood check on the radar interference results, a 10 MHz wide Gaussian noise signal was also injected into the LTE receivers.

5.2 Radar Interference Impacts on LTE UE Receiver Performance (Downlink)

5.2.1 Continuous Interference Impacts

The impacts of continuous interference waveforms on data throughput and BLER for the downlink direction are shown in Figures 4–29. Tables 5–30 show how the MCS was affected by the coinciding interference waveforms.

All P0N interference waveforms produced appreciable effects when interference, *I*, was greater than -65 dBm. Some Q3N waveforms degraded LTE performance when interference, *I*, was -85 dBm. The figures show that as the interference power level was increased, the interference impact increased.

Regarding results for specific waveforms and trends, the simple pulsed waveforms (P0N and ECC) that caused the most loss of data throughput were ECC-2, P0N-2, P0N-5 through P0N-10, and P0N-13, all resulting in throughput being reduced to 10 Mbps or less from a nominal 48 Mbps. This level of degradation did not occur until interference power levels, *I*, were greater than -45 dBm. All of the P0N waveforms eventually caused some reduction in data throughput in the downlink.

With respect to the chirped-pulsed (Q3N) waveforms, Q3N-1 through Q3N-3 and Q3N-9 caused the most reduction in data throughput, causing reductions to 10 Mbps or less from a nominal 48 Mbps. For these interference waveforms, this level of degradation of throughput occurred when interference power levels, *I*, were greater than -55 dBm. It is noted that Q3N waveform impacts began at lower interference levels than for the P0N waveforms. Among the Q3N waveforms, Q3N-4 caused the least data throughput loss, but still reduced the throughput to approximately 21 Mbps at I = -60 dBm.

It is beyond the scope of this report to determine *why* particular waveforms had the most or least effects. NTIA welcomes LTE operators and other technical readers to review these data and share their views on these test results.

5.2.2 Off-Tuned Continuous Interference Impacts

One radar interference waveform, P0N-1, was tested with the center frequency of the radar interference offset from the eNB center frequency by 2 and 4 MHz. In both cases, the radar interference remained co-channel with the LTE system since it was still within the occupied bandwidth of the LTE eNB emission. Figures 6 and 7 show the effects of the 2 and 4 MHz off-tune P0N-1 radar interference, respectively, on data throughput and BLER of the LTE downlink. Tables 7 and 8 show how MCS was impacted by the coinciding off-tune interference. For the most part, the impact of the off-tune interference was very similar to that of the center-tuned interference (Figure 5, Table 6).

5.2.3 Burst Interference Impacts

Figures 30–36 show the impact of radar burst interference on data throughput and MCS for the downlink. All tested burst interference waveforms demonstrate some effect on the downlink throughput. The effect is observed as momentary, evenly-spaced (every 5 seconds) reductions in throughput. The Q3N-1 and Q3N-4 interference waveforms had the most instantaneous impact on data throughput. The Q3N-1 waveform resulted in brief throughput reductions of 2.5 Mbps typically, with one reduction of approximately 5 Mbps. For the Q3N-4 interference case, there was a momentary 6 to 7 Mbps reduction in throughput occurring every 20 seconds, or every 4th radar burst, whilst other bursts resulted in momentary reductions of typically 1 Mbps.

Examining MCS, Q3N-4 and Q3N-10 were the only waveforms to exhibit an effect. This is observed as adjustments of the eNB MCS in 5 second intervals for both of these waveforms. No MCS changes were observed with other burst interference waveforms.

5.3 Radar Interference Impacts on LTE eNB Receiver Performance (Uplink)

5.3.1 Continuous Interference Impacts

For the uplink case, Figures 37–60 show how the interference waveforms impacted data throughput, UE transmit power, BLER, and RBs, and Tables 31–53 show how MCS was affected by the coinciding interference waveforms.

The figures show that at least one of the four measured parameters (throughput, UE transmit power, BLER, and RB usage) were effected by increasing interference power. It is believed that since the UE was able to vary transmit power and RB usage, the uplink was more adaptable to interference than the downlink.

Regarding results for specific waveforms and trends, the simple pulsed waveforms (P0N and ECC) that caused the most loss of data throughput were P0N-6, P0N-8 through P0N-10, and P0N-12, all resulting in throughput being reduced to less than 3 Mbps from a nominal 12.5 Mbps. This level of degradation was not achieved until interference, *I*, was greater than -40 dBm. Some waveforms exhibited little to no impact on data throughput at any tested

interference levels. The figures also show that, at times, the LTE system mitigated the interference and maintained data throughput by adjusting UE transmit power and/or RBs.

With respect to the chirped-pulsed waveforms, Q3N-4, Q3N-6, Q3N-7 and Q3N-10 caused the most data throughput loss, degrading to 2.5 Mbps or less. Q3N-3 caused the least data throughput reduction, only reducing throughput to about 11 Mbps when the interference power level was -25 dBm.

As already noted, it is beyond the scope of this report to determine *why* particular waveforms had the most or least effects. NTIA welcomes LTE operators and other technical readers to review these data and share their views on these test results.

5.3.2 Burst Interference Impacts

Figures 61–72 show the effects of radar burst interference on data throughput and MCS for the uplink case. For all interference waveforms tested, MCS never changed. Furthermore, radar burst interference had no discernable effect on throughput at an interference level of -25 dBm.

5.4 Recommendations for Future Work

1. Theoretical analysis is recommended to better understand *why* various radar interference waveforms have the particular effects that have been published in this report. LTE signal detection needs to be understood to perform such analyses.

2. When commercial 3.5 GHz LTE equipment becomes available, LTE receivers should be tested to determine the non-linear effects of saturation and front-end overload from radar signals.

3. More emission spectra of LTE transmitters should be measured.

4. The impact of radar interference on an LTE network with multiple UEs should be investigated.

5. Using data from this report and from the tasking described above, band sharing criteria need to be developed for spectrum sharing between 3.5 GHz radars and LTE systems.

6 REFERENCES

[1] Federal Communications Commission, “Proposal to Create a Citizen’s Broadband Service in the 3550-3650 MHz Band,” FCC Docket No. 12-354. http://www.fcc.gov/document/enabling-innovative-small-cell-use-35-ghz-band-nprm-order

[2] Federal Communications Commission, “Amendment of the Commission’s Rules with Regard to Commercial operations in the 3550-3650 MHz Band,” FCC GN Docket No. 12-354. http://apps.fcc.gov/ecfs/document/view?id=7521099242

[3] Sanders, F. H., J. E. Carroll, G. A. Sanders, and R. L. Sole, “Effects of Radar Interference on LTE Base Station Receiver Performance,” NTIA Technical Report TR-14-499, U.S. Dept. of Commerce, Dec. 2013. http://www.its.bldrdoc.gov/publications/2742.aspx

[4] U.S. Dept. of Commerce, National Telecommunications and Information Administration, “An Assessment of the Near-Term Viability of Accommodating Wireless Broadband Systems in the 1675-1710 MHz, 1755-1780 MHz, 3500-3650 MHz, 4200-4220 MHz and 4380-4400 MHz Bands (President's Spectrum Plan Report),” NTIA, U.S. Dept. of Commerce, Nov. 2010. http://www.ntia.doc.gov/report/2010/assessment-near-term-viability-accommodating-wireless-broadband-systems-1675-1710 MHz 17

[5] CEPT ECC Report 174, “Compatibility Between the Mobile Service in the Band 2500-2690 MHz and the radiodetermination service in the band 2700-2900 MHz,” CEPT Electronic Communications Committee, Mar. 2012. http://www.erodocdb.dk/docs/doc98/official/Pdf/ECCRep174.pdf

[6] “LTE; Evolved Universal Terrestrial Radio Access (E-UTRA); Physical layer procedures (3GPP TS 36.213 version 8.8.0 Release 8),” 3GPP, Section 7.2, October 2009. http://www.etsi.org/deliver/etsi_ts/136200_136299/136213/08.08.00_60/ts_136213v080800p.pdf

[7] “TBS and MCS Signaling and Tables,” Motorola Submission to 3GPP, March 31, 2008. http://www.3gpp.org/ftp/tsg_ran/WG1_RL1/TSGR1_52b/Docs/R1-081638.zip

[8] Sanders, F. H., R. L. Hinkle and B. J. Ramsey, “Measurement Procedures for the Radar Spectrum Engineering Criteria (RSEC),” NTIA Technical Report TR-05-420, U.S. Dept. of Commerce, Mar. 2005. http://www.its.bldrdoc.gov/publications/2450.aspx

[9] ETSI TS 137 104 V11.2.1 Release 11, “Digital cellular telecommunications system (Phase 2+); Universal Mobile Telecommunications System (UMTS); LTE; E-UTRA, UTRA and GSM/EDGE; Multi-Standard Radio (MSR) Base Station (BS) radio transmission and reception (3GPP TS 37.104 version 11.2.1 Release 11),” Oct. 2012. http://www.etsi.org/deliver/etsi_ts/137100_137199/137104/11.02.01_60/ts_137104v110201p.pdf

[10] Sanders, F. H., R. L. Sole, J. E. Carroll, G. S. Secrest and T. Lynn Allmon, "Analysis and Resolution of RF Interference to Radars Operating in the Band 2700-2900 MHz from

Broadband Communication Transmitters," NTIA Technical Report TR-13-490, U.S. Dept. of Commerce, Oct. 2012. http://www.its.bldrdoc.gov/publications/2684.aspx

7 ACKNOWLEDGEMENTS

The authors would like to thank Durga Malladi, Yongbin Wei, Dean Brenner, Peter Gaal, Matthew Kwon, John Kuzin, and Rajeev Krishnamurthi for making this measurement possible. The authors would also like to thank Sam Liu and Awaiz Khan for traveling to Colorado and working with ITS engineers to perform this study. A final thank-you goes to Vishwanth Kamala Govindaraju and Awaiz Khan, again, for providing help to ITS during post-processing and analysis.

APPENDIX A: LTE TEST BED SYSTEM LOSSES

All losses in the LTE network for both the uplink and downlink were measured by ITS engineers, as shown in Figure A–1. The losses in the uplink and downlink RF paths as well as the cable losses to monitoring and injection equipment were measured as follows:

- Uplink
  - Channel 0
    - Interference injection port to analyzer monitoring port = 49.9 dB
    - UE Tx port to analyzer monitoring port = 50.2 dB
    - Interference injection port to eNB Rx port = 51.5 dB
    - UE Tx port to eNB Rx port = 51.0 dB
  - Channel 1
    - Interference injection port to analyzer monitoring port = 50.0 dB
    - UE Tx-0 port to analyzer monitoring port = 50.6 dB
    - Interference injection port to eNB Rx port = 51.5 dB
    - UE Tx port to eNB Rx port = 51.4 dB
- Downlink
  - Channel 0
    - Interference injection port to analyzer monitoring port = 20.3 dB
    - eNB Tx port to analyzer monitoring port = 46.8 dB
    - Interference injection port to UE Rx port = 21.7 dB
    - eNB Tx port to UE Rx port = 48 dB
  - Channel 1
    - Interference injection port to analyzer monitoring port = 20.5 dB
    - eNB Tx port to analyzer monitoring port = 42.0 dB
    - Interference injection port to UE Rx port = 21.7 dB
    - eNB Tx port to UE Rx port = 42.5 dB
- Cables
  - From VSG to channel 0 interference injection port = 2.8 dB
  - From VSG to channel 1 interference injection port = 3.5 dB
  - Channels 0 and 1 analyzer monitoring port to spectrum analyzer = 0.7 dB

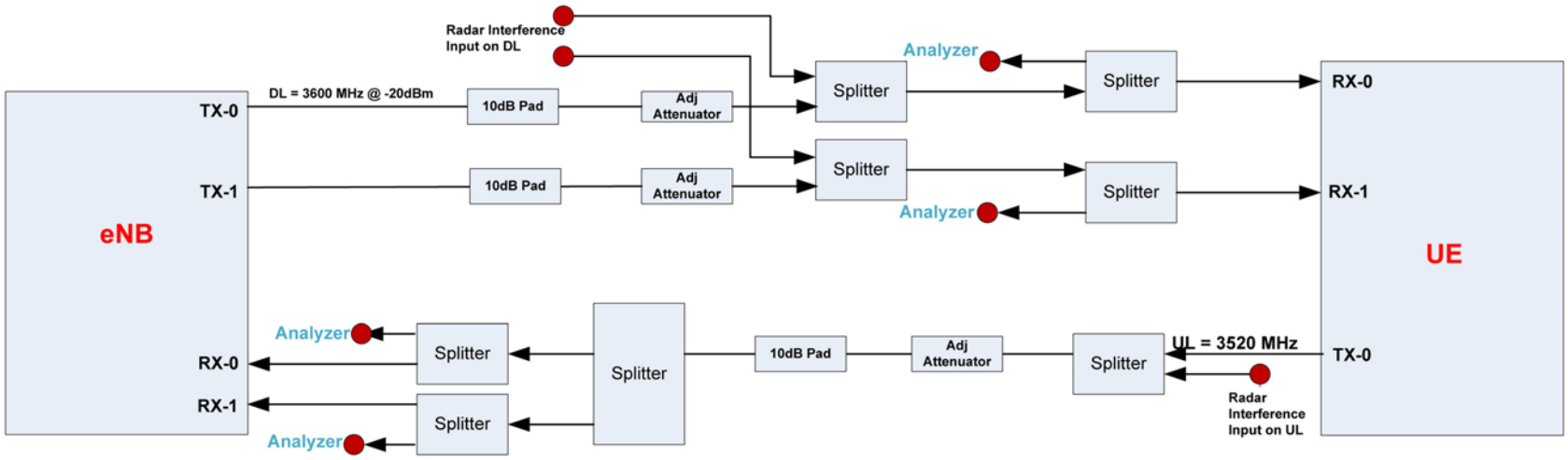

Figure A–1. Block diagram of the LTE network showing all the components in the RF path, interference injection points, and spectrum analyzer monitoring points.

APPENDIX B: COMPARISON FIGURES OF INTERFERENCE EFFECTS ON LTE (TDD) AND (FDD) UPLINKS

B.1 Notes on Comparison Figures of Interference Effects on LTE (TDD) and LTE (FDD) Uplinks

Figures from [3] showing the effects of interference into a TDD LTE uplink are reproduced here along with FDD LTE uplink throughput data (from this study) plotted as a function of *S/(I+N)* for comparison. Some interference waveforms from this study were not used in [3] and vice versa. Only figures using the same interference waveform parameters are compared.

In order to facilitate comparison, the data throughput results presented in the figures of Section 3.2.1 are now shown as a function of *S/(I+N)* (as opposed to only *I*); where *S* is the baseline received signal power (with no interference), *I* is the interference power level, and *N* is the internal noise level of the receiver. The values of *S*, *I*, and *N* used to compute *S/(I+N)* to represent the data from this study are as follows:

- *S* = -85 dBm,
- *N* = -98.4 dBm,
- *I* = displayed interference power levels in the figures from Section 3.2.1.

The baseline received desired signal of *S* = -85 dBm represents the nominal received signal power without interference from both studies. The internal inherent noise in the receiver is calculated to be -98.4 dBm in the 7.2 MHz bandwidth of the eNB receiver witha 7 dB noise figure. The value of *S/I* (in dB) was measured (as described in Section 2.3) and *I*, in the receiver, was calculated by subtracting *S/I* from the known value of *S* = -85 dBm for the uplink baseline condition (with no interference).

It is noted that these are distinctly different tests. The system in the [3] was a 20 MHz wide TDD macro-cell uplink without any UE transmit power or RB control. The system described in this report was a roughly 10 MHz wide FDD micro-cell uplink that was able to employ UE transmit power (thereby changing the value of *S*) and RB control. In [3], the allowable uplink BLER was set to 10% and for this study it was set to 30%. The TDD system in [3] used a channel emulator (frequency-selective multipath) between the UE and eNB whereas the system examined in this study did not. Finally, the noise figure of the TDD system in [3] was measured to be 3 dB whereas in the FDD system it was reported by the industry participant as 7 dB.

When comparing the throughput results for the TDD and FDD uplinks, the general trend of decreasing throughput as *S/(I+N)* decreases is observed for both systems for the majority of the interference waveforms. However, significant differences in degradation behavior are observed. Compared to the TDD uplink, the FDD LTE uplink examined in this study had substantially more flexibility in mitigating interference effects through the use of UE power control and the ability to reduce RB usage, thereby providing more power to the remaining available RBs. The relatively robust behavior of the FDD LTE uplink compared to the TDD uplink is likely explained by these dynamic capabilities. There were only two interference waveforms, P0N-7 and P0N-11, where the TDD system appears to be more capable of handling the respective interference waveforms.

B.2 Comparison Figures from the Two LTE Uplinks

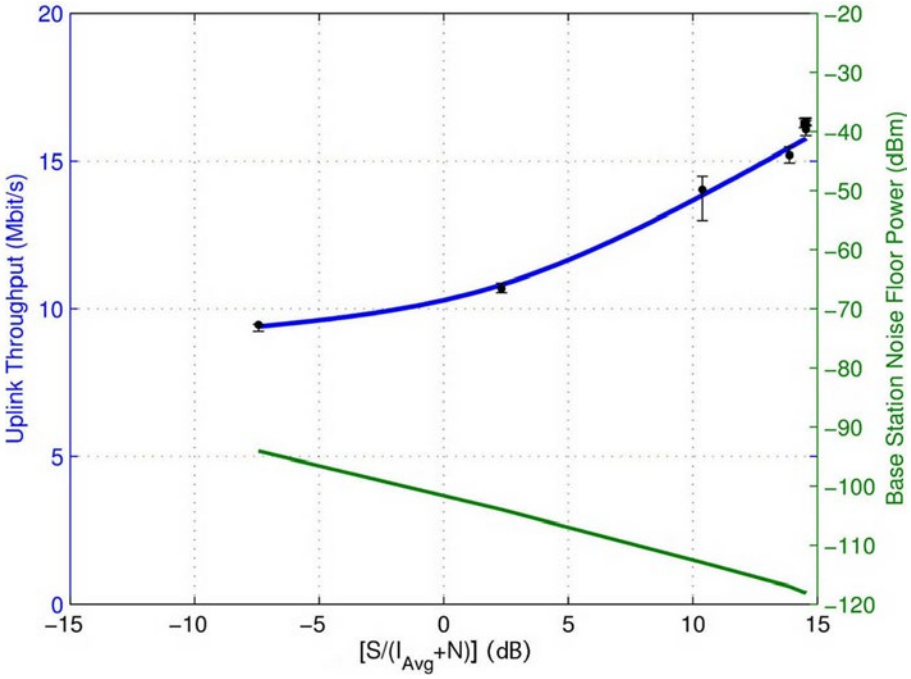

Figure B–1. Throughput and eNB Noise Floor for LTE (TDD) network for 20 MHz wide Gaussian noise interference (covering full LTE bandwidth).

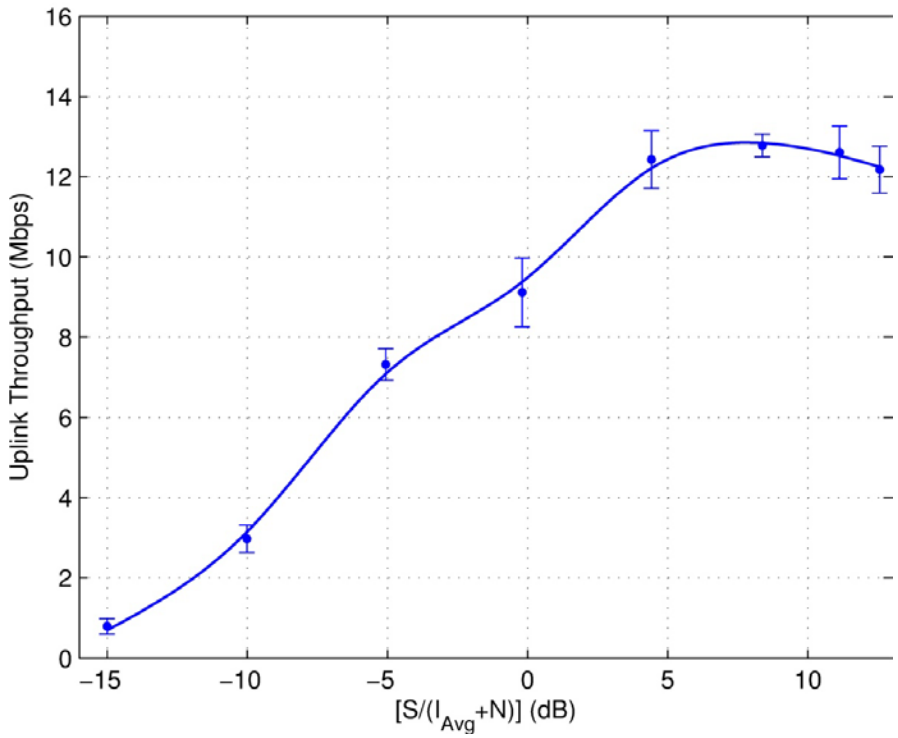

Figure B–2. Throughput, UE Tx power, BLER, and RBs for LTE (FDD) network for 10 MHz wide Gaussian noise interference (covering full LTE bandwidth).

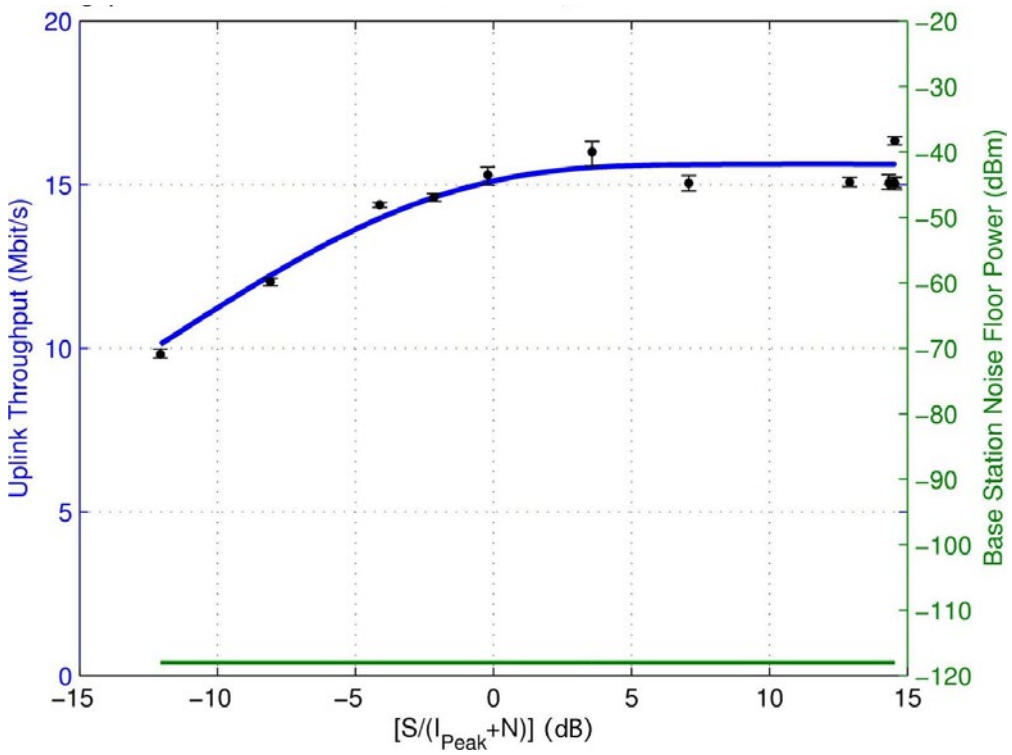

Figure B–3. Throughput and eNB Noise Floor for LTE (TDD) network for P0N-1 interference.

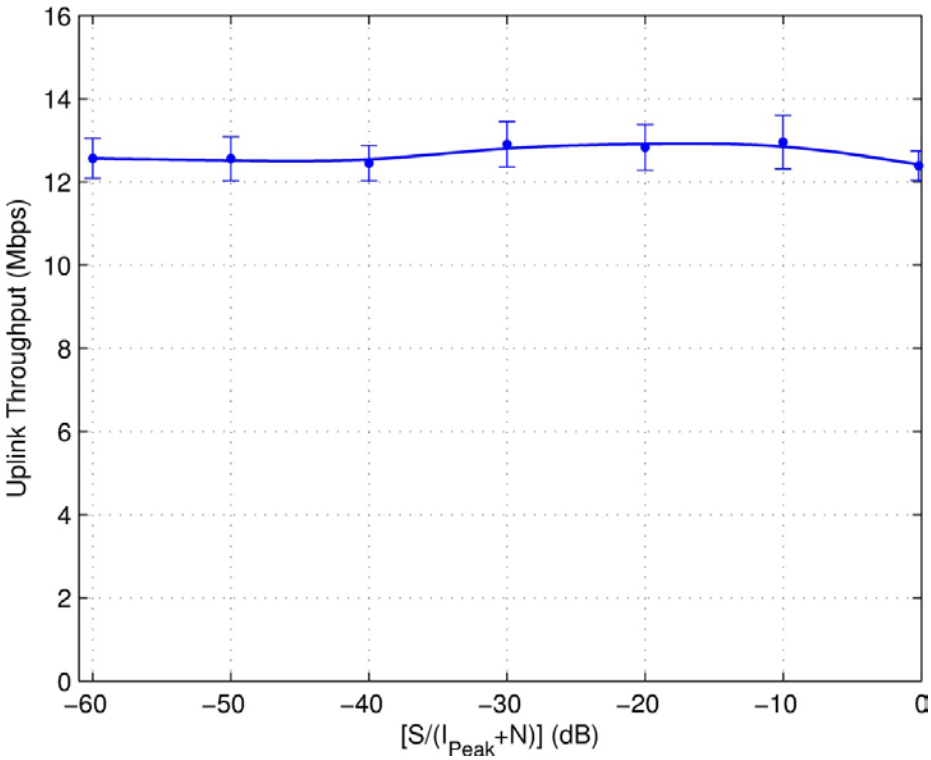

Figure B–4. Throughput, UE Tx power, BLER, and RBs for LTE (FDD) network for P0N-1 interference.

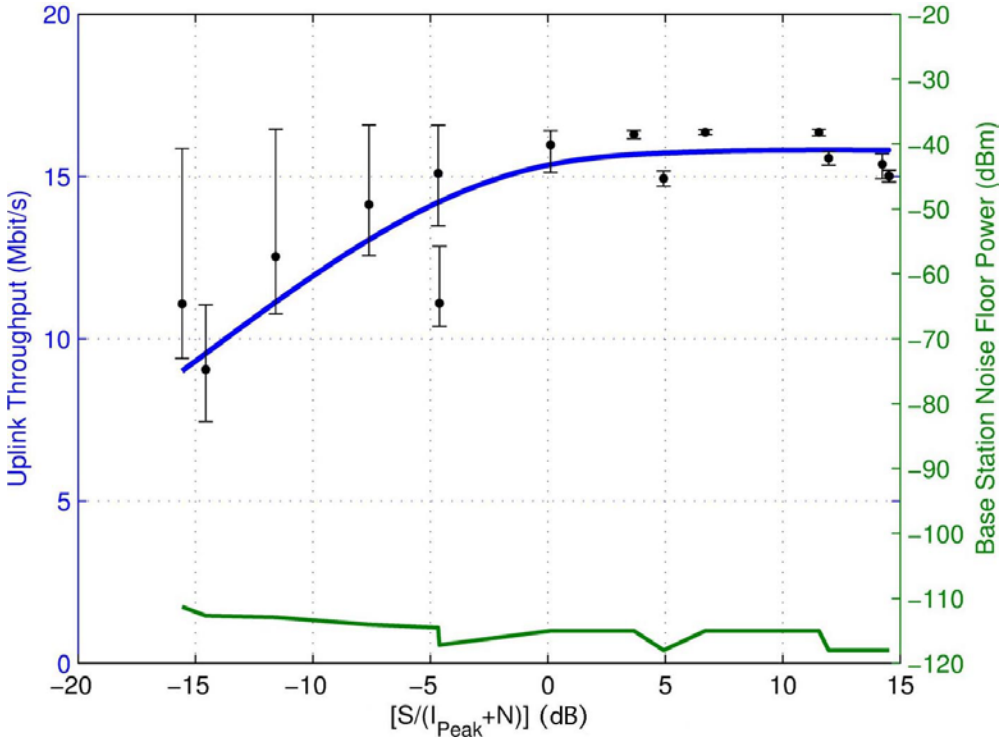

Figure B–5. Throughput and eNB Noise Floor for LTE (TDD) network for P0N-2 interference.

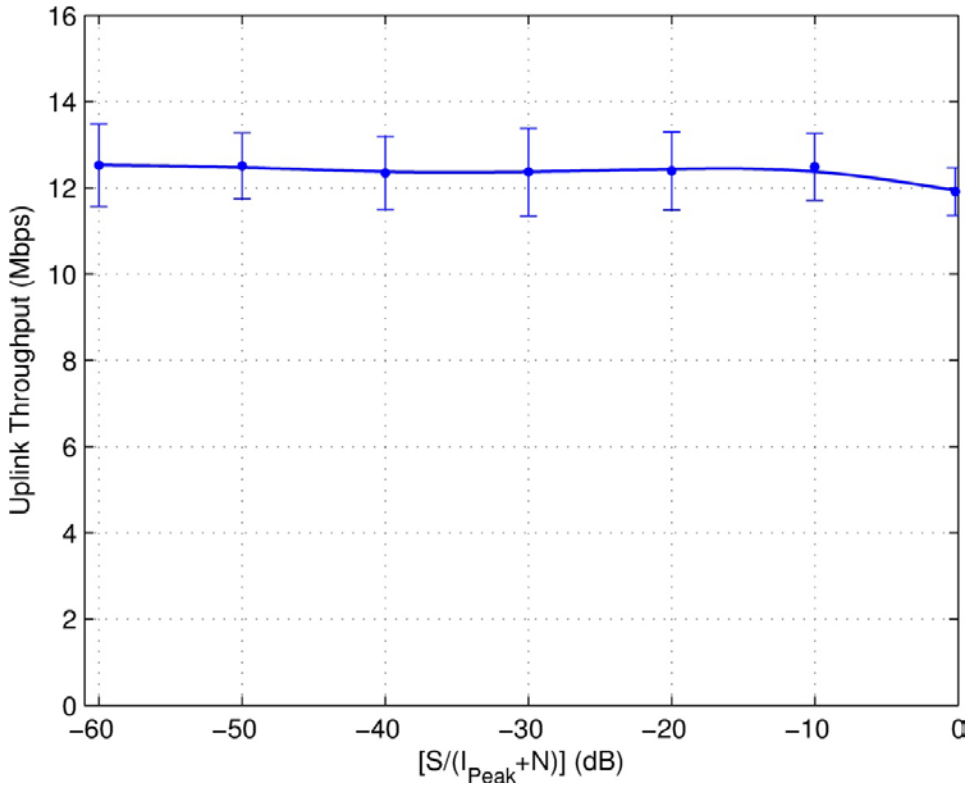

Figure B–6. Throughput, UE Tx power, BLER, and RBs for LTE (FDD) network for P0N-2 interference.

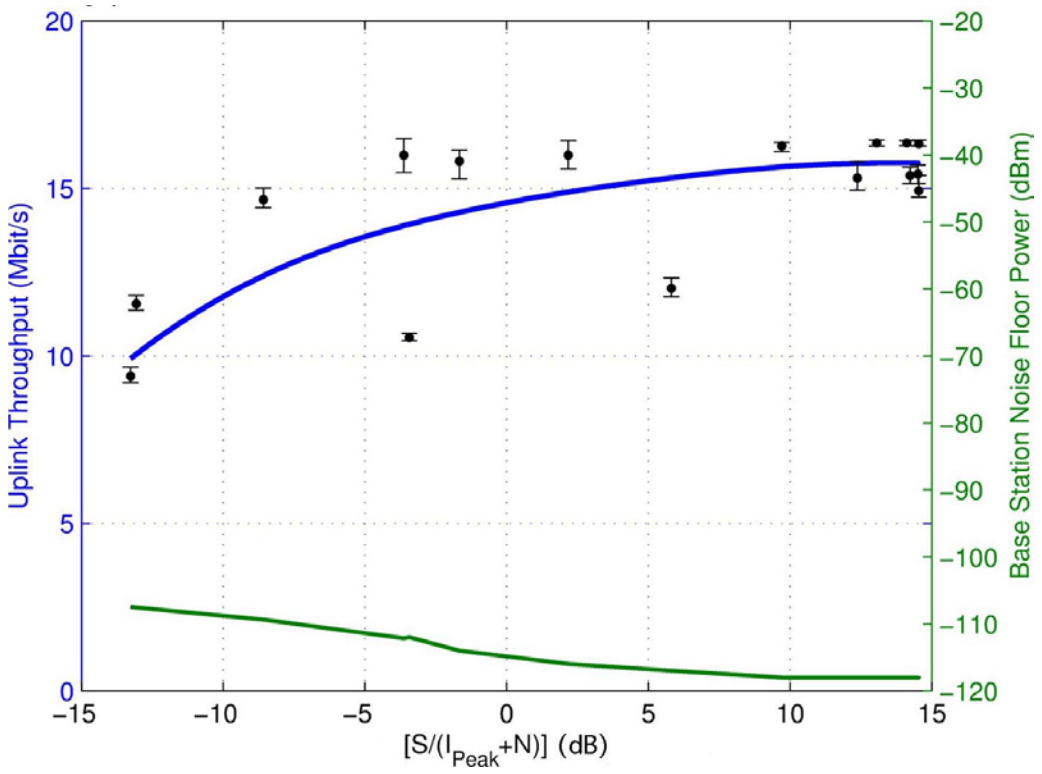

Figure B–7. Throughput and eNB Noise Floor for LTE (TDD) network for P0N-3 interference.

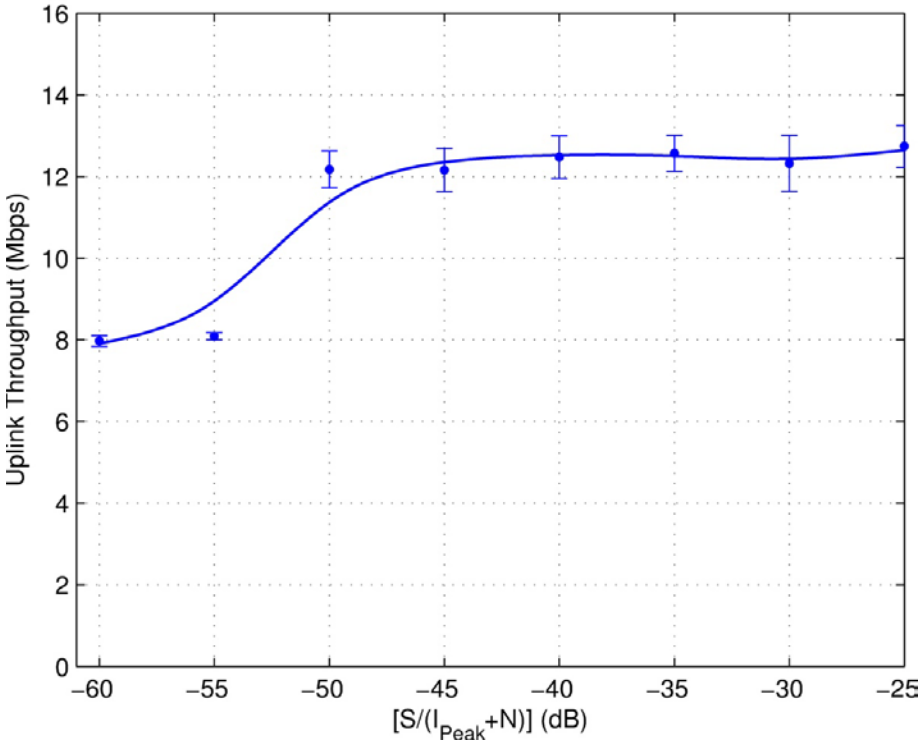

Figure B–8. Throughput, UE Tx power, BLER, and RBs for LTE (FDD) network for P0N-3 interference.

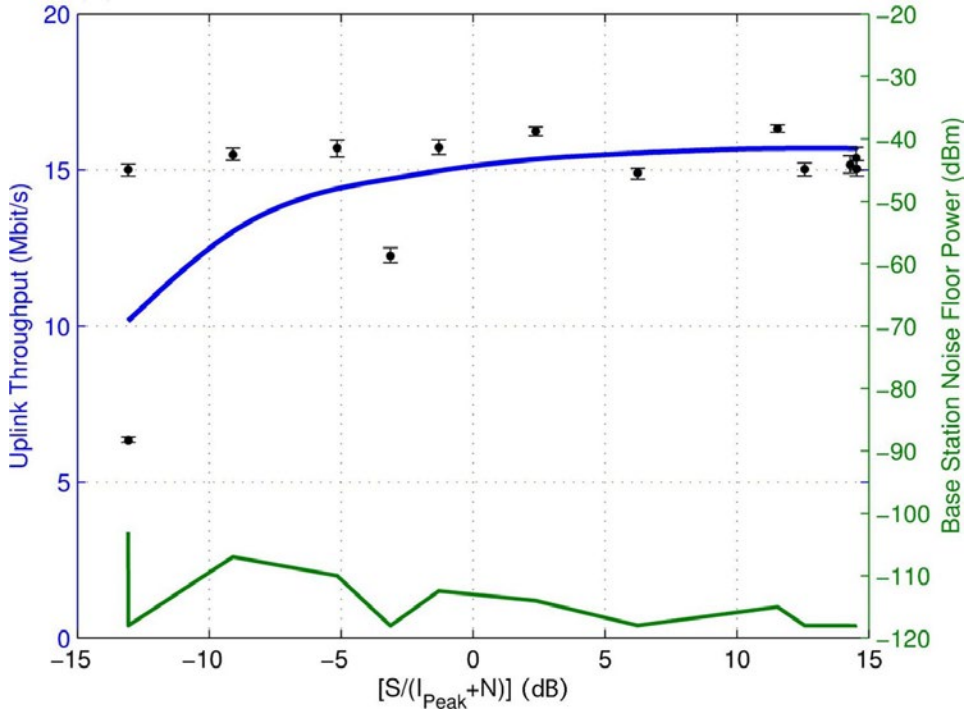

Figure B–9. Throughput and eNB Noise Floor for LTE (TDD) network for P0N-4 interference.

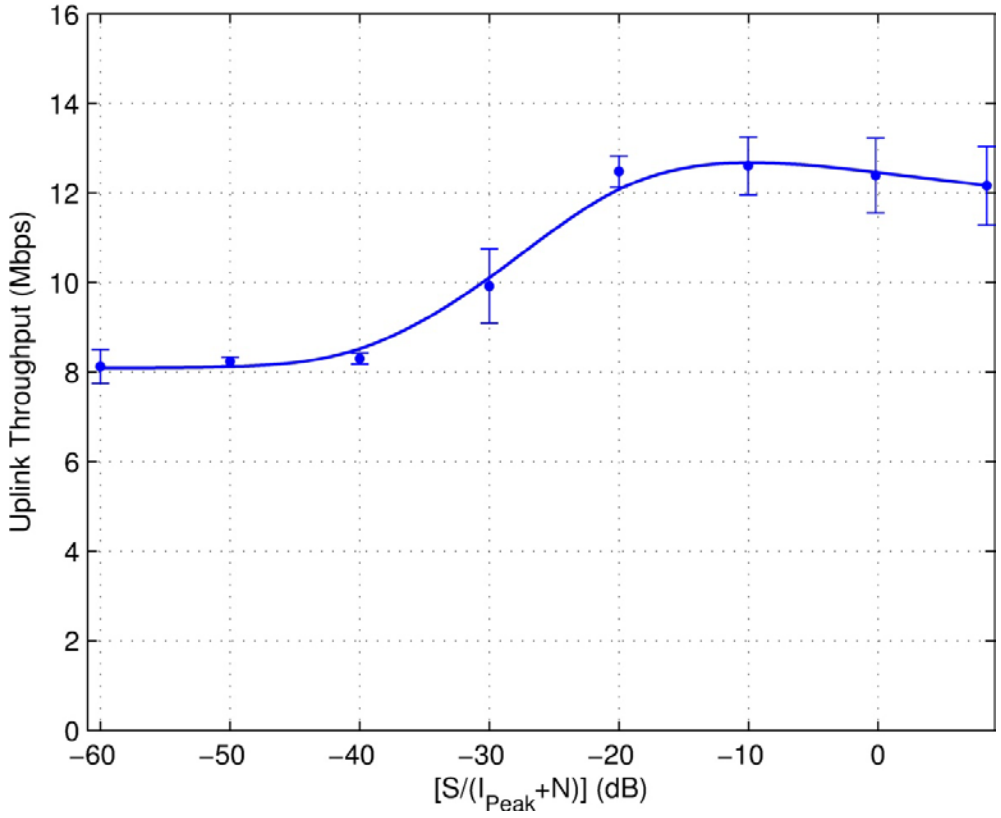

Figure B–10. Throughput, UE Tx power, BLER, and RBs for LTE (FDD) network for P0N-4 interference.

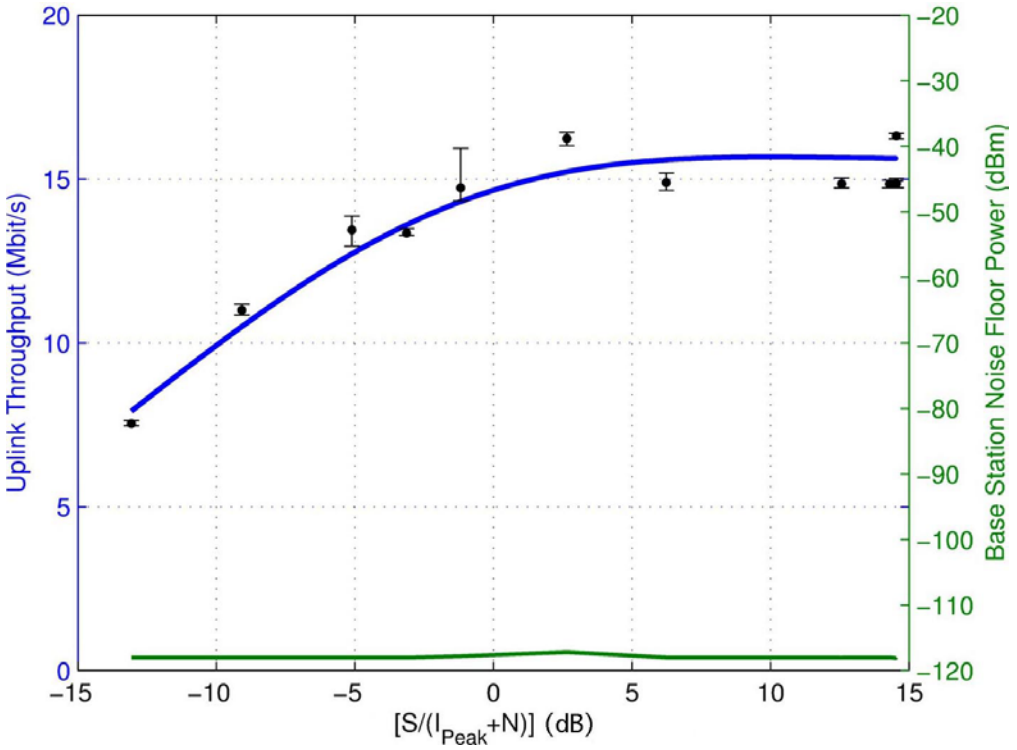

Figure B–11. Throughput and eNB Noise Floor for LTE (TDD) network for P0N-5 interference.

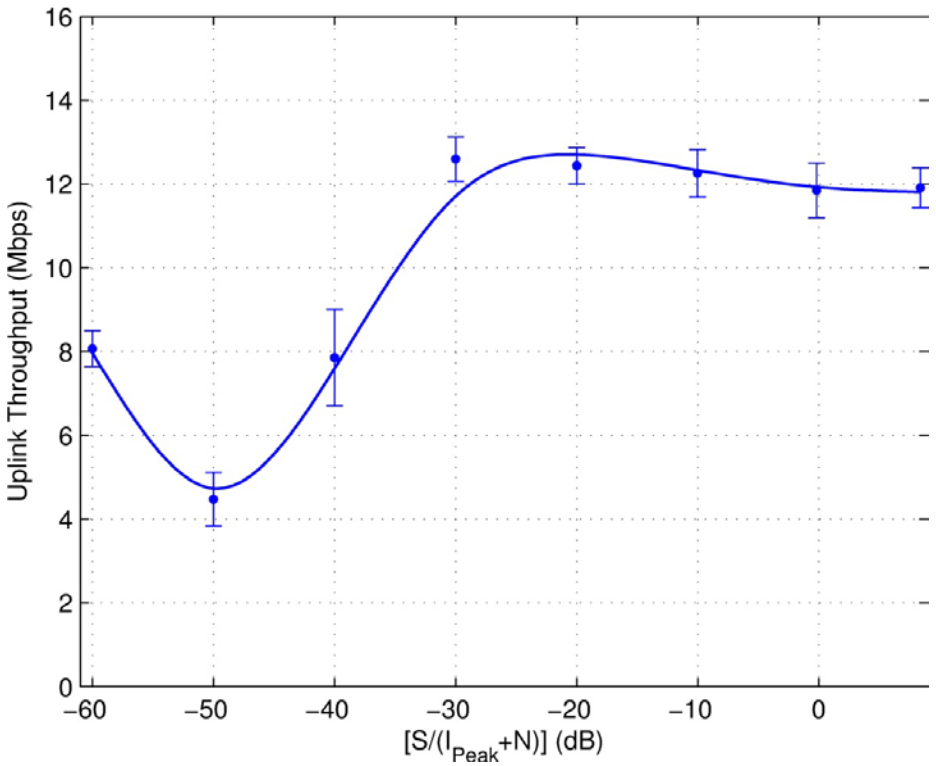

Figure B–12. Throughput, UE Tx power, BLER, and RBs for LTE (FDD) network for P0N-5 interference.

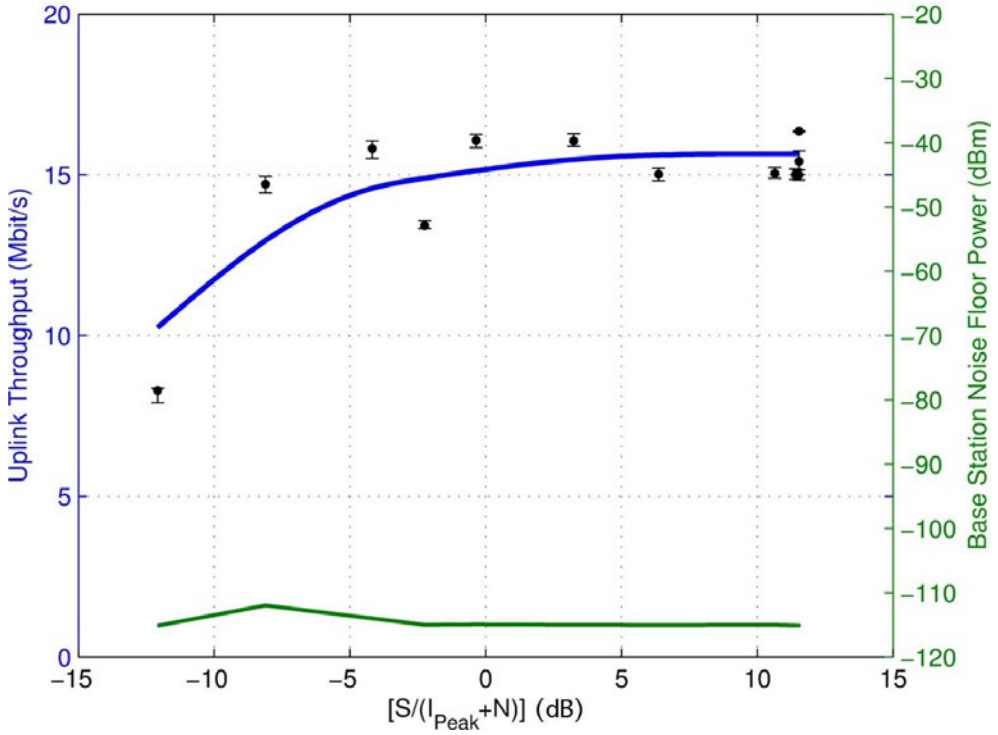

Figure B–13. Throughput and eNB Noise Floor for LTE (TDD) network for P0N-6 interference.

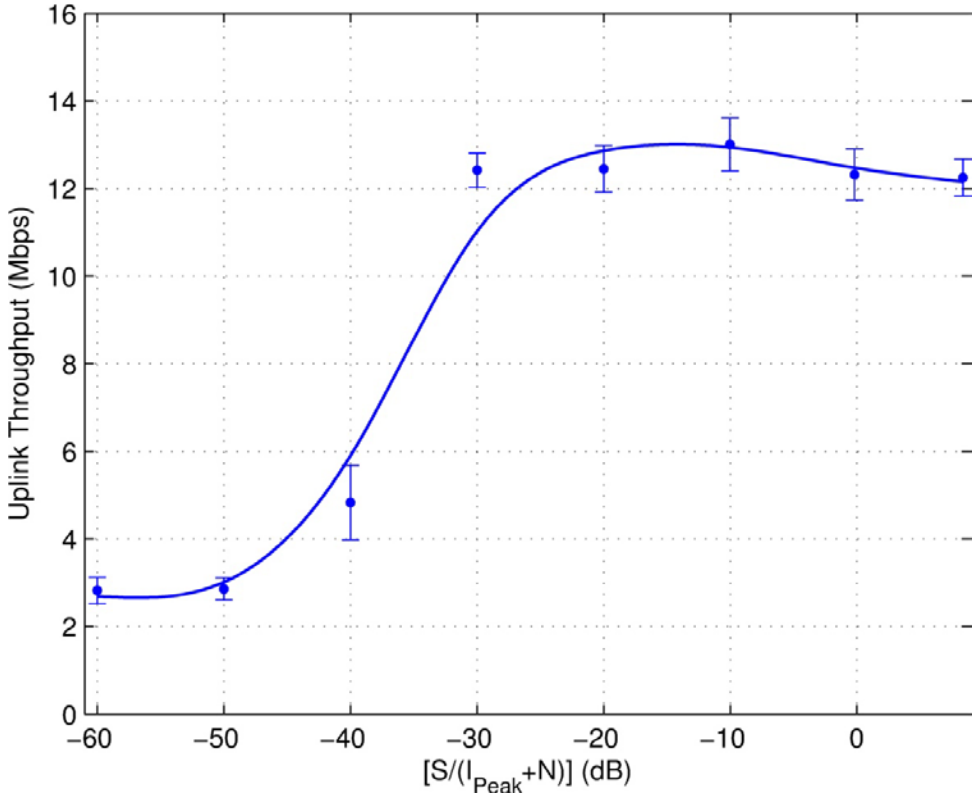

Figure B–14. Throughput, UE Tx power, BLER, and RBs for LTE (FDD) network for P0N-6 interference.

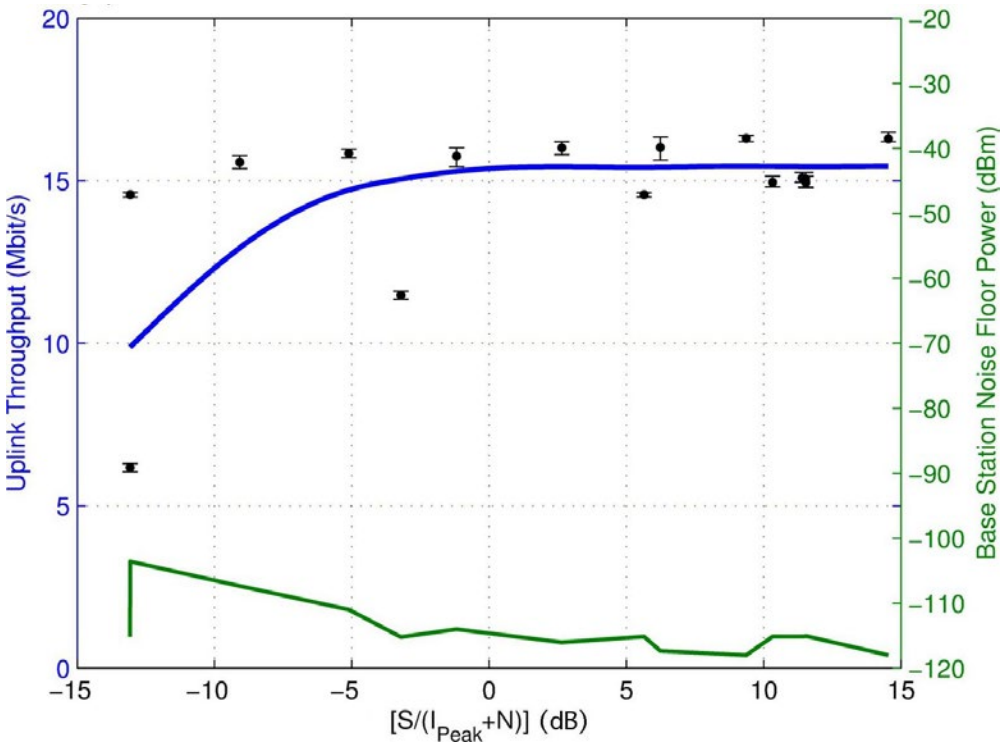

Figure B–15. Throughput and eNB Noise Floor for LTE (TDD) network for P0N-7 interference.

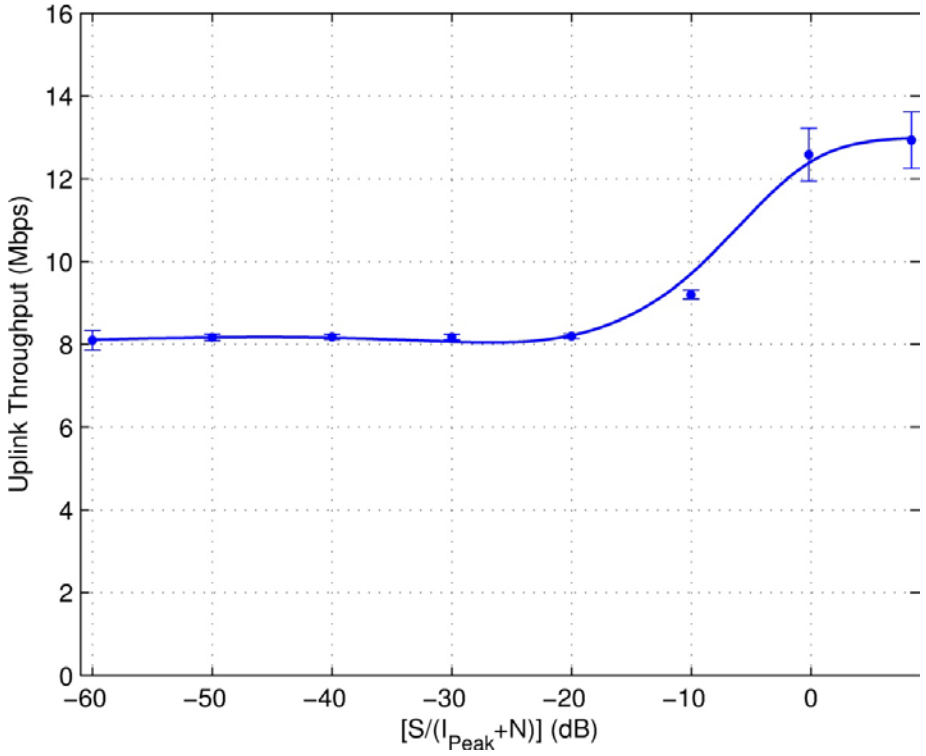

Figure B–16. Throughput, UE Tx power, BLER, and RBs for LTE (FDD) network for P0N-7 interference.

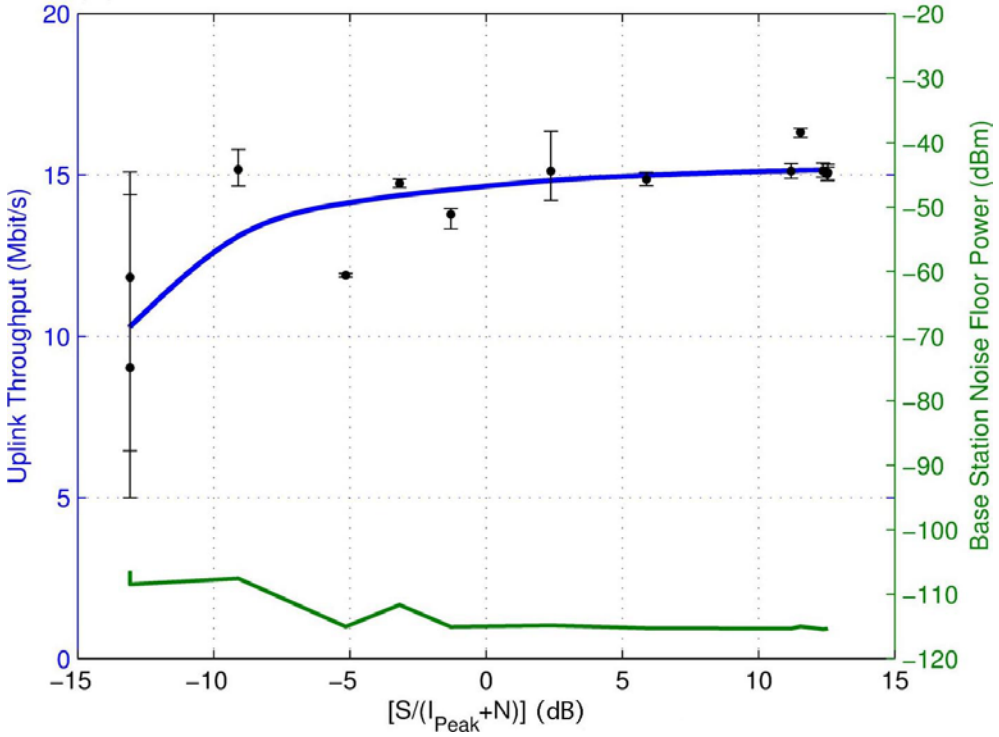

Figure B–17. Throughput and eNB Noise Floor for LTE (TDD) network for P0N-8 interference.

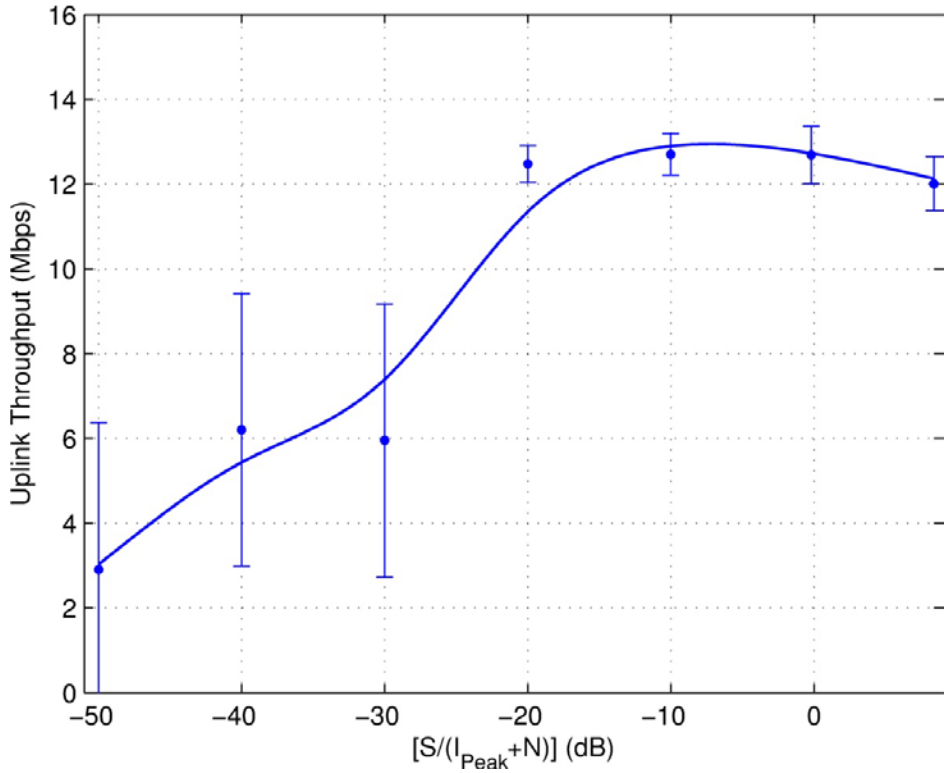

Figure B–18. Throughput, UE Tx power, BLER, and RBs for LTE (FDD) network for P0N-8 interference.

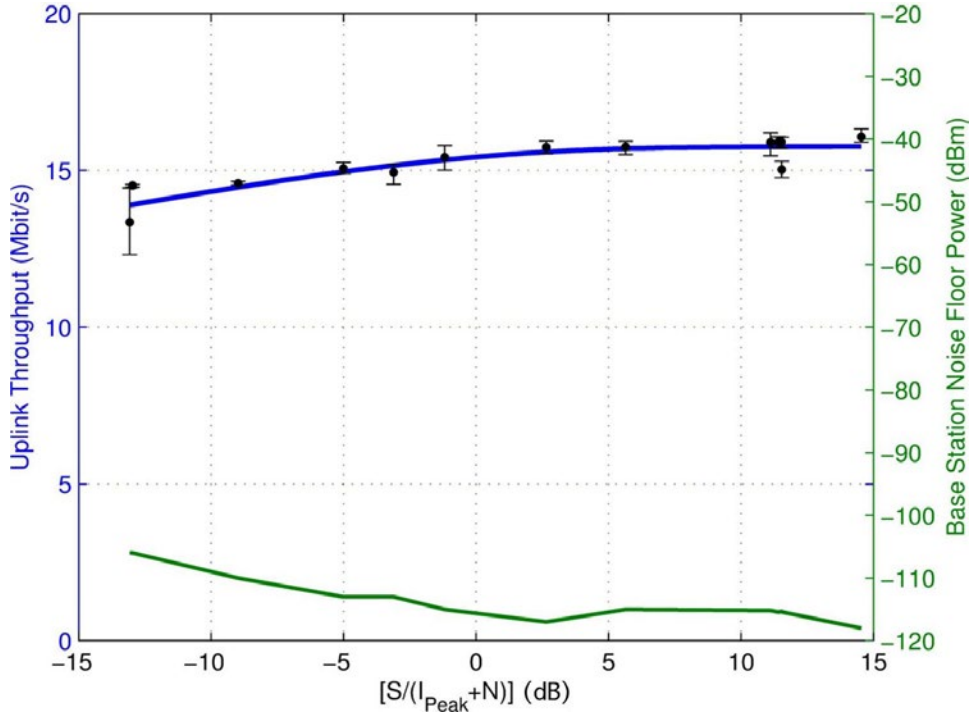

Figure B–19. Throughput and eNB Noise Floor for LTE (TDD) network for P0N-9 interference.

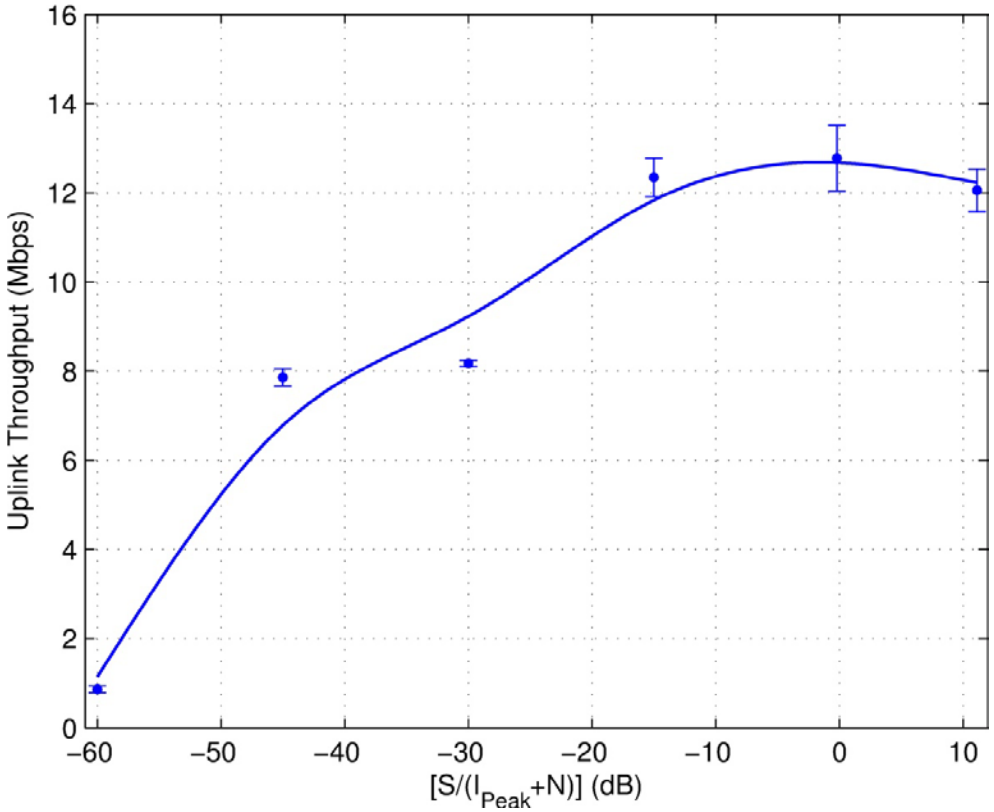

Figure B–20. Throughput, UE Tx power, BLER, and RBs for LTE (FDD) network for P0N-9 interference.

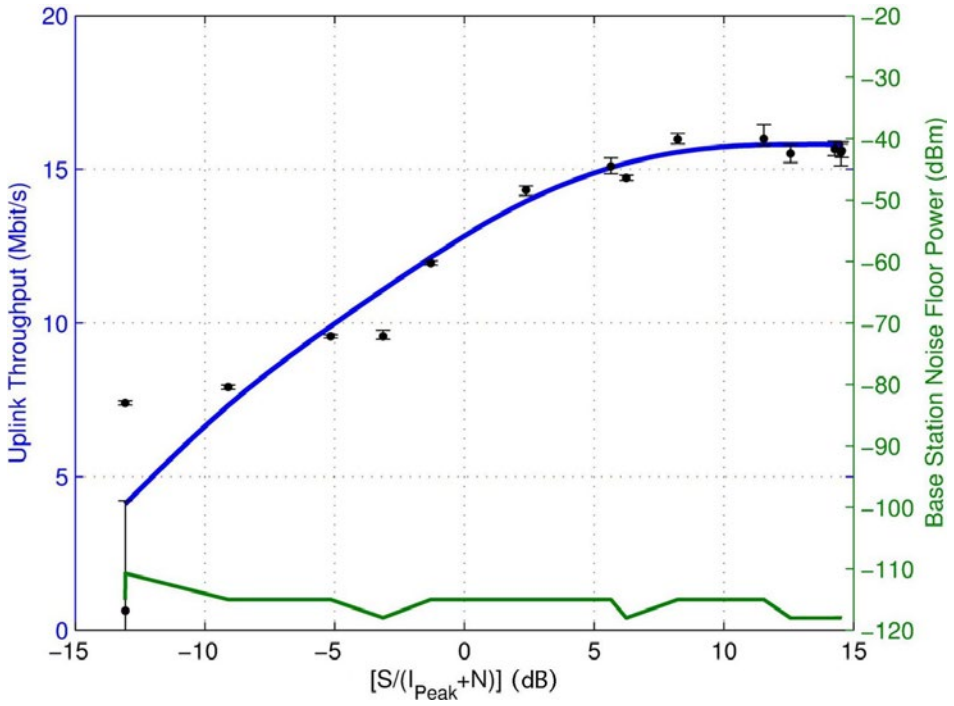

Figure B–21. Throughput and eNB Noise Floor for LTE (TDD) network for P0N-10 interference.

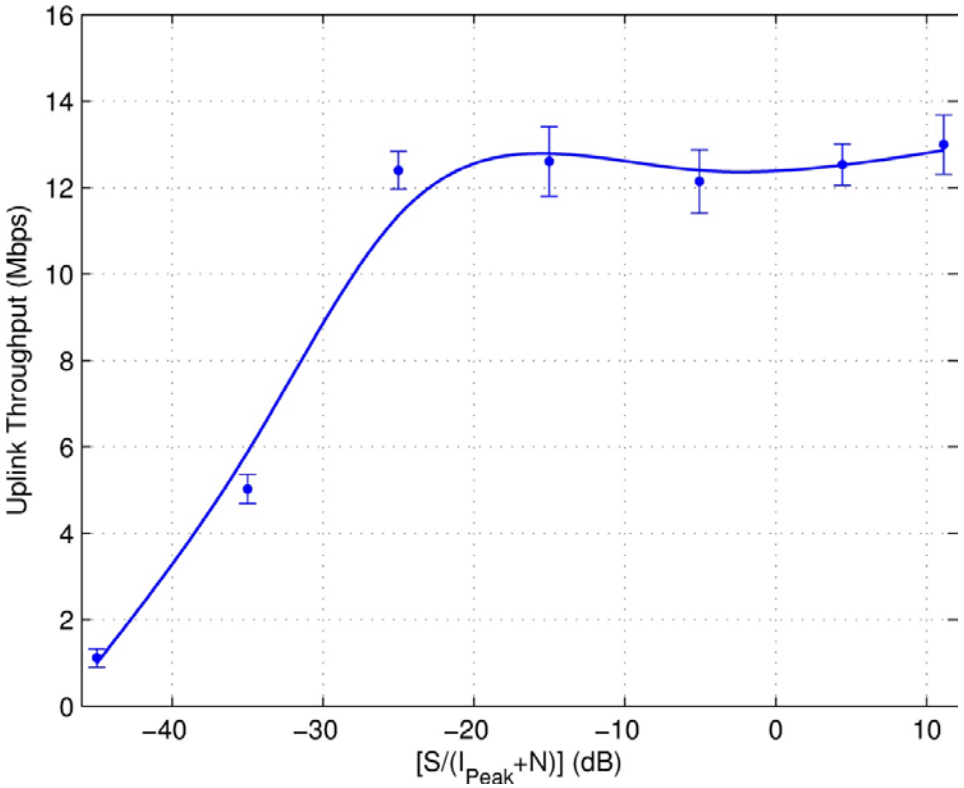

Figure B–22. Throughput, UE Tx power, BLER, and RBs for LTE (FDD) network for P0N-10 interference.

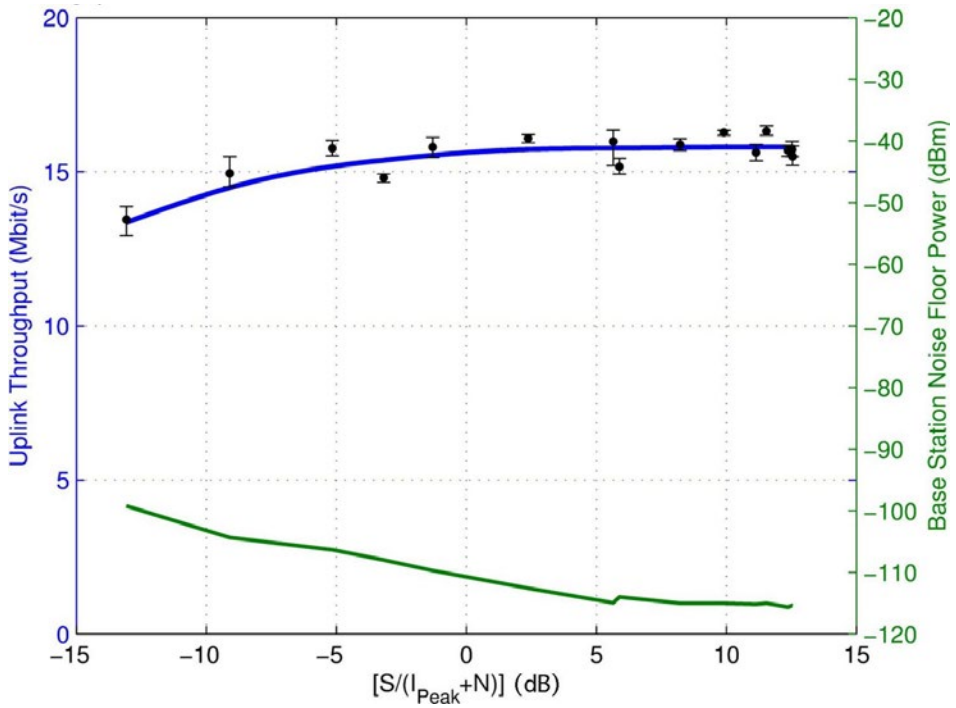

Figure B–23. Throughput and eNB Noise Floor for LTE (TDD) network for P0N-11 interference.

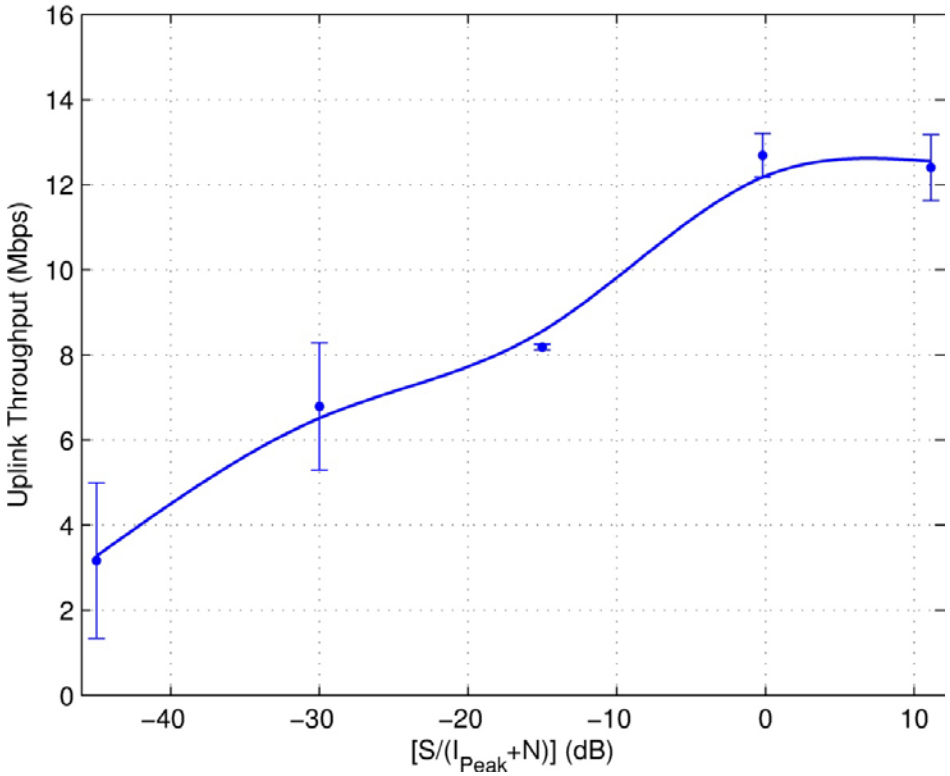

Figure B–24. Throughput, UE Tx power, BLER, and RBs for LTE (FDD) network for P0N-11 interference.

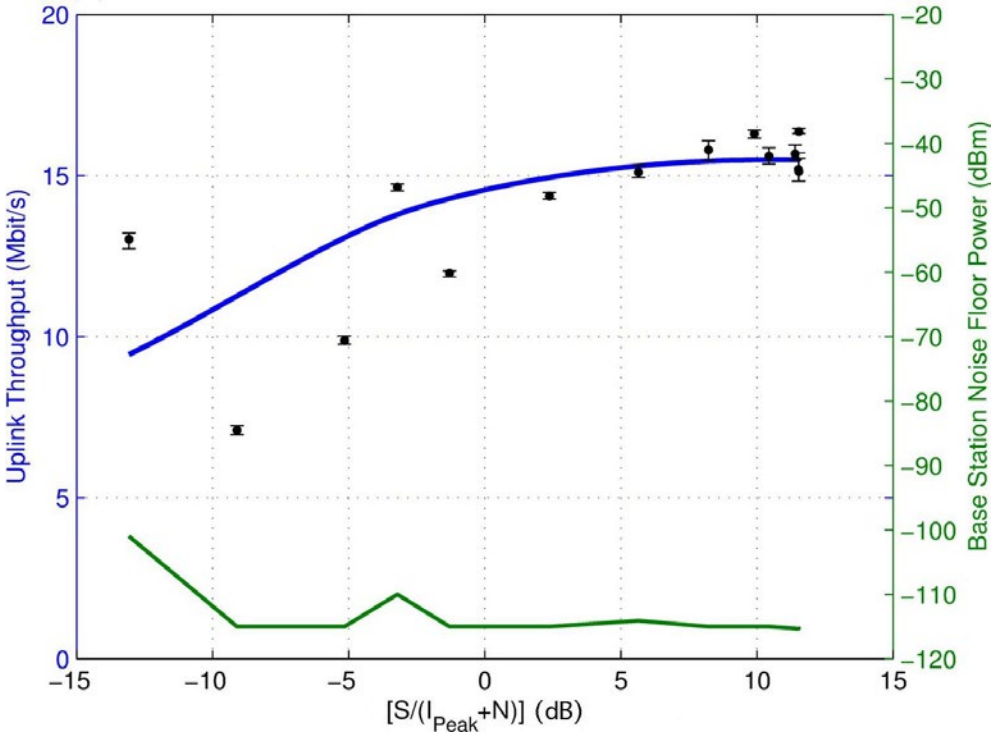

Figure B–25. Throughput and eNB Noise Floor for LTE (TDD) network for P0N-12 interference.

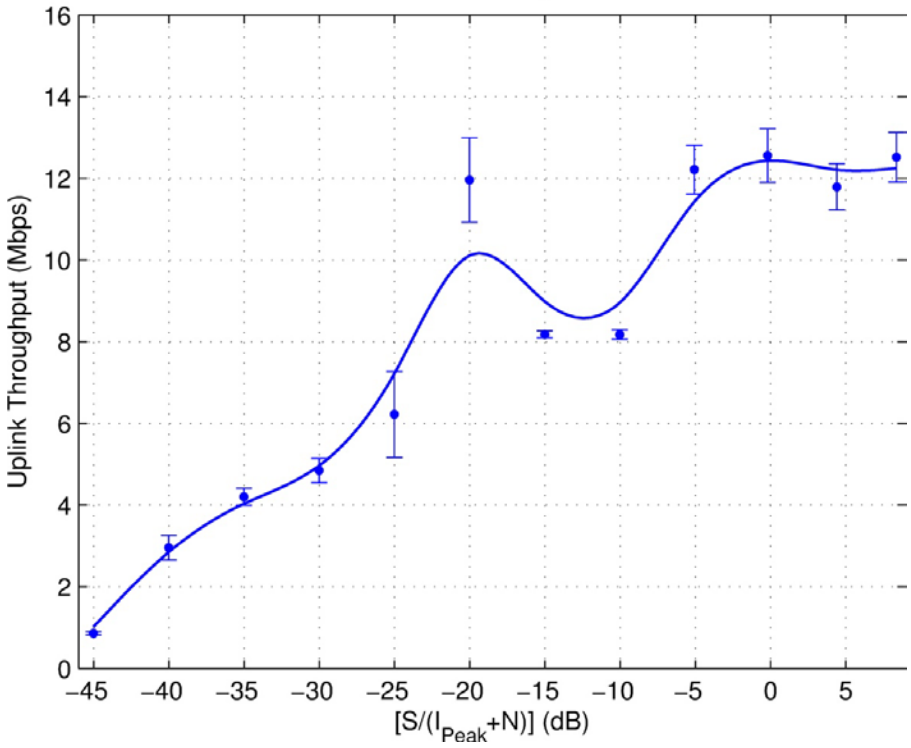

Figure B–26. Throughput, UE Tx power, BLER, and RBs for LTE (FDD) network for P0N-12 interference.

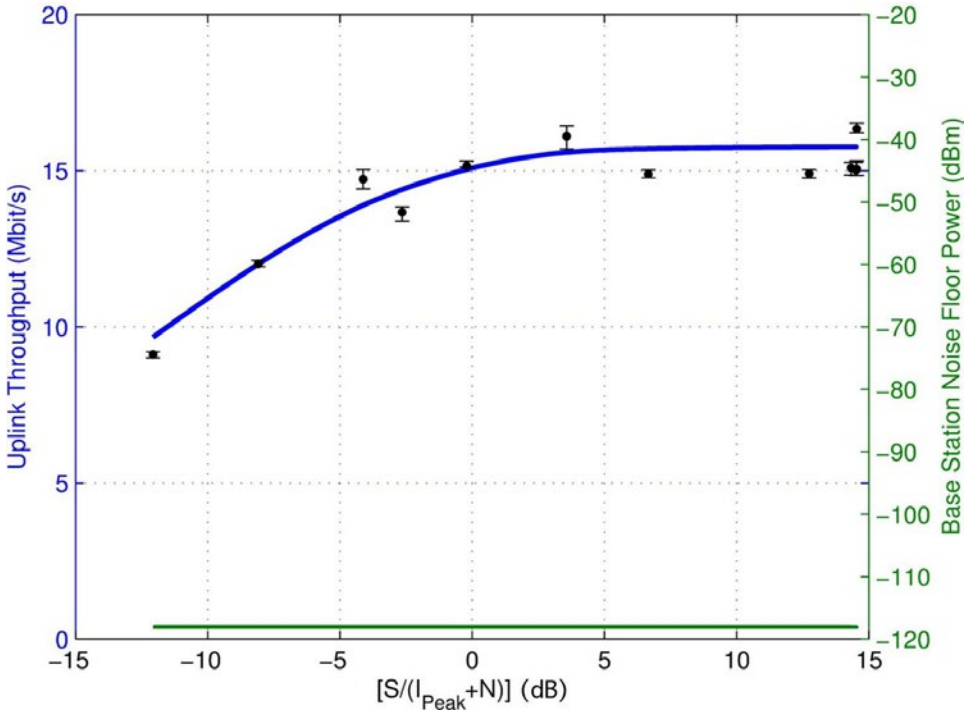

Figure B–27. Throughput and eNB Noise Floor for LTE (TDD) network for P0N-13/TDWR interference.

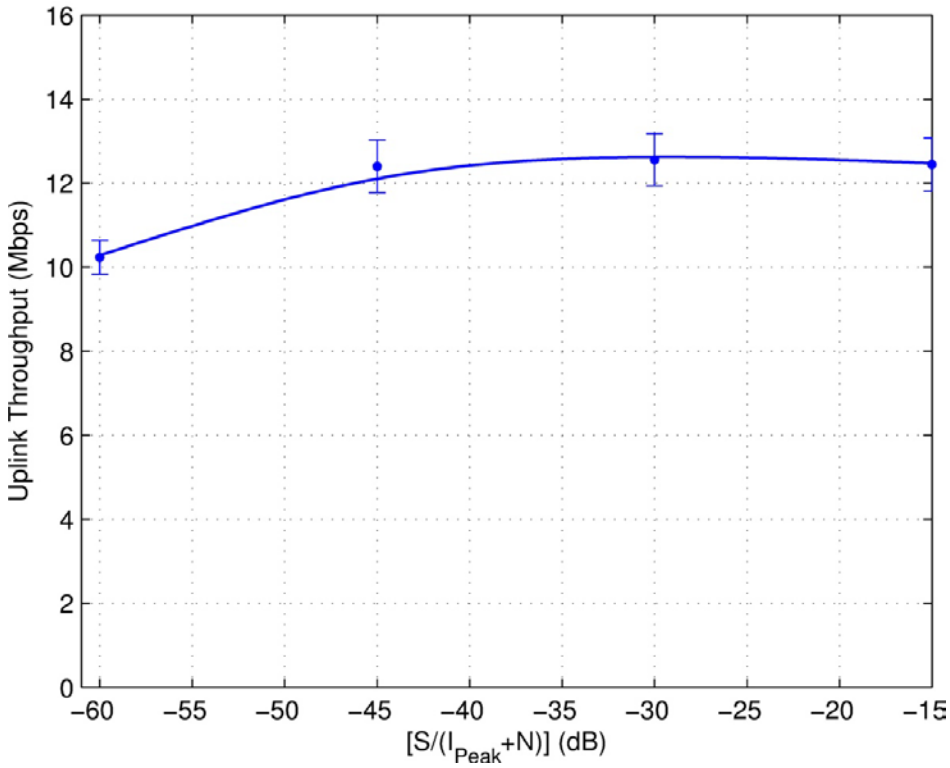

Figure B–28. Throughput, UE Tx power, BLER, and RBs for LTE (FDD) network for P0N-13/TDWR interference.

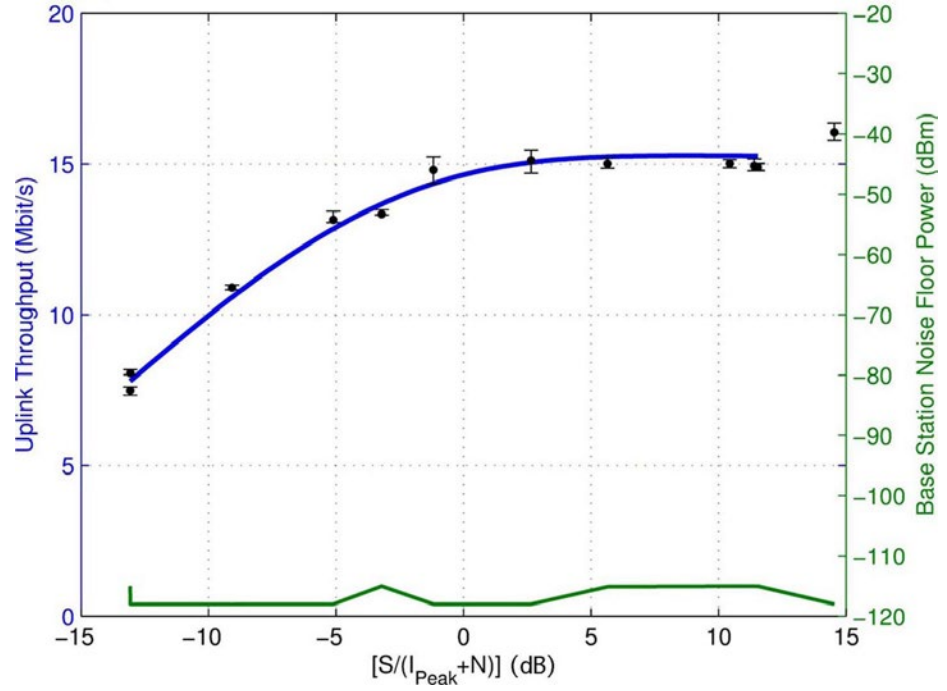

Figure B–29. Throughput and eNB Noise Floor for LTE (TDD) network for ECC-1/WFM-1 interference.

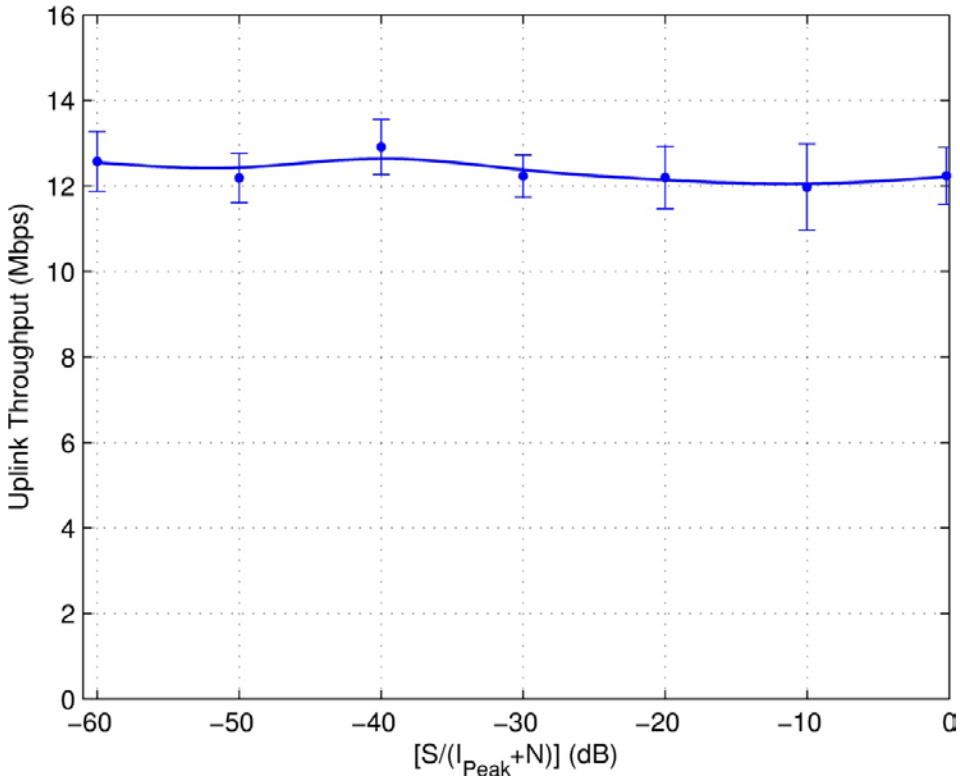

Figure B–30. Throughput, UE Tx power, BLER, and RBs for LTE (FDD) network for ECC-1/WFM-1 interference.

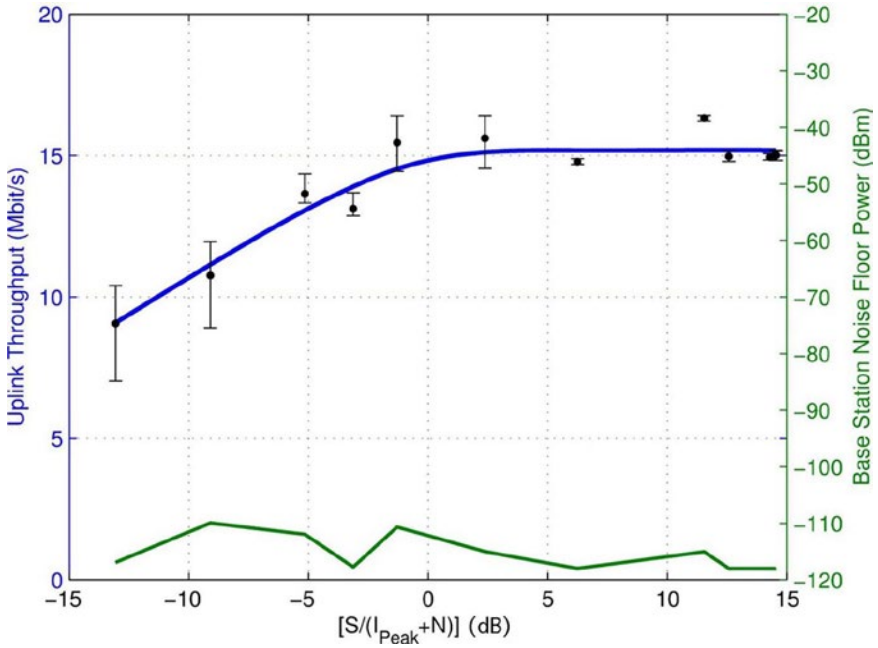

Figure B–31. Throughput and eNB Noise Floor for LTE (TDD) network for ECC-2/WFM-2 interference.

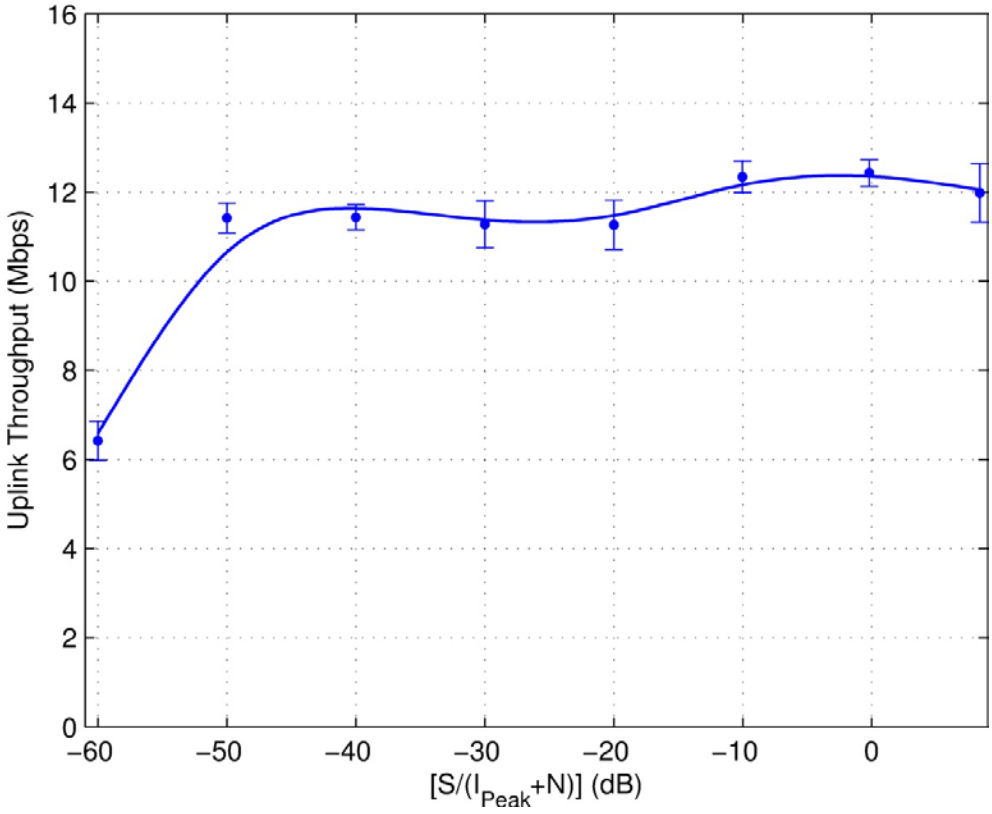

Figure B–32. Throughput, UE Tx power, BLER, and RBs for LTE (FDD) network for ECC-2/WFM-2 interference.

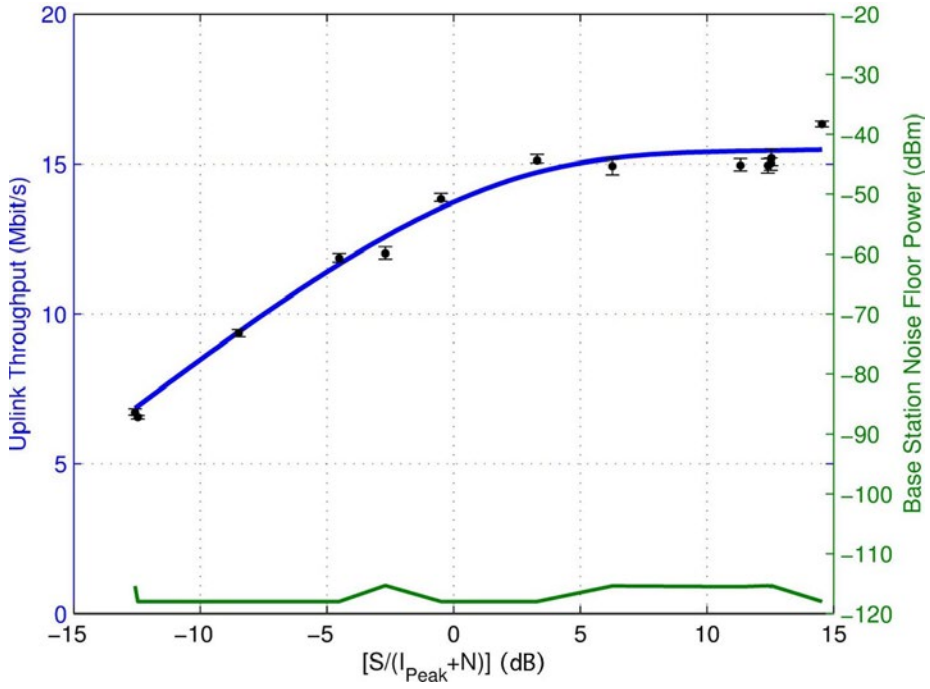

Figure B–33. Throughput and eNB Noise Floor for LTE (TDD) network for Q3N-1 interference.

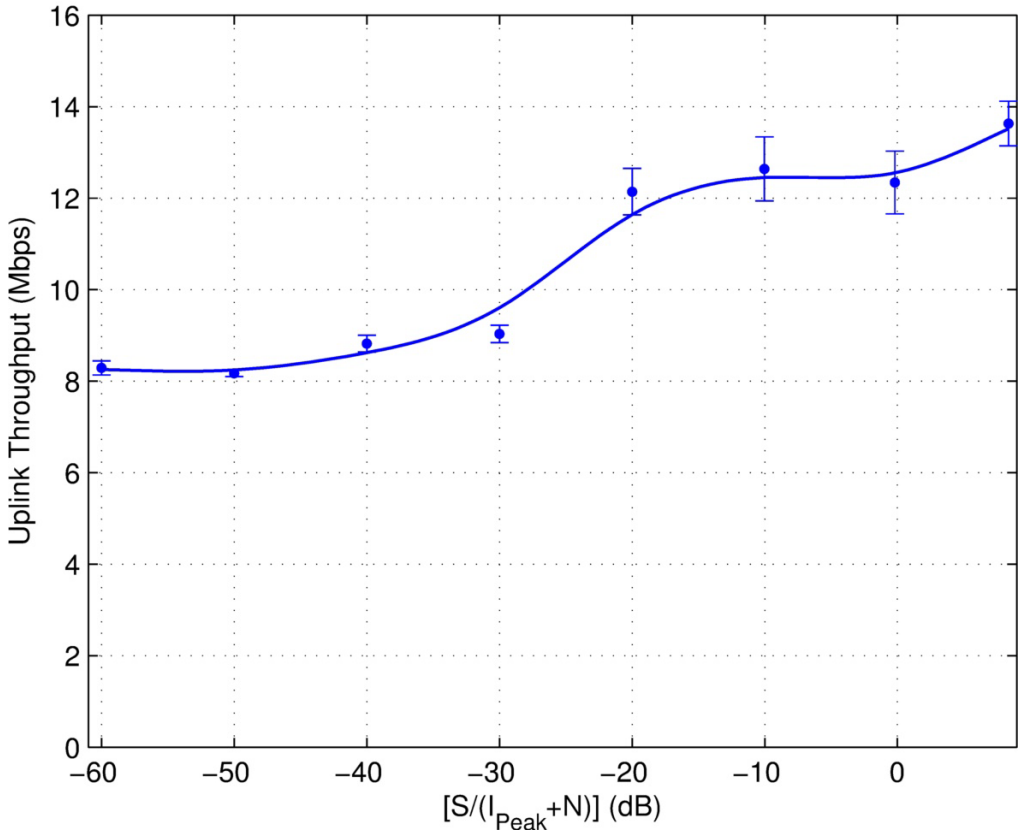

Figure B–34. Throughput, UE Tx power, BLER, and RBs for LTE (FDD) network for Q3N-1 interference.

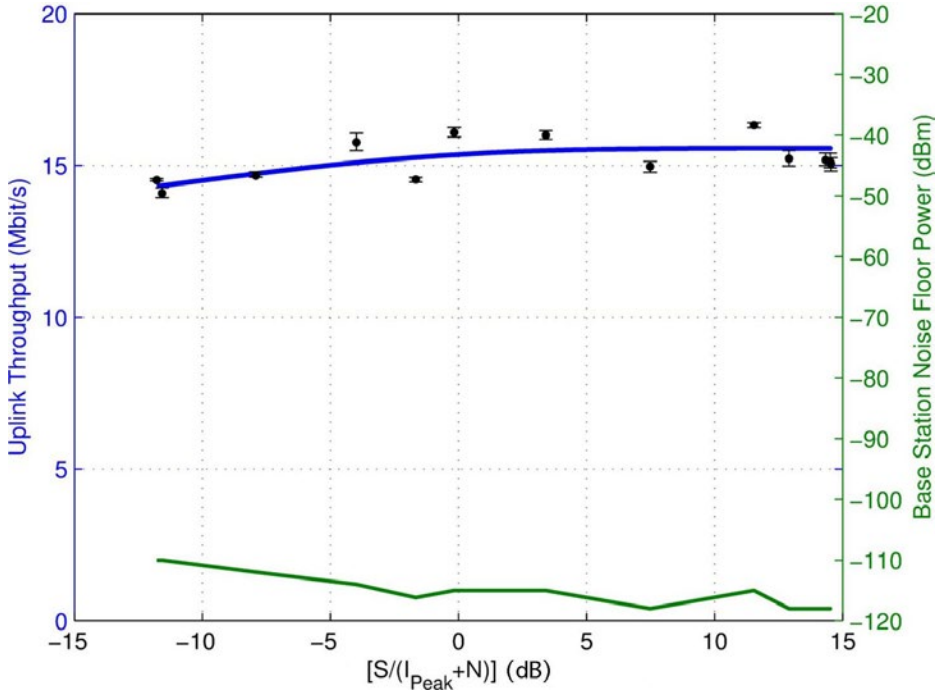

Figure B–35. Throughput and eNB Noise Floor for LTE (TDD) network for Q3N-2 interference.

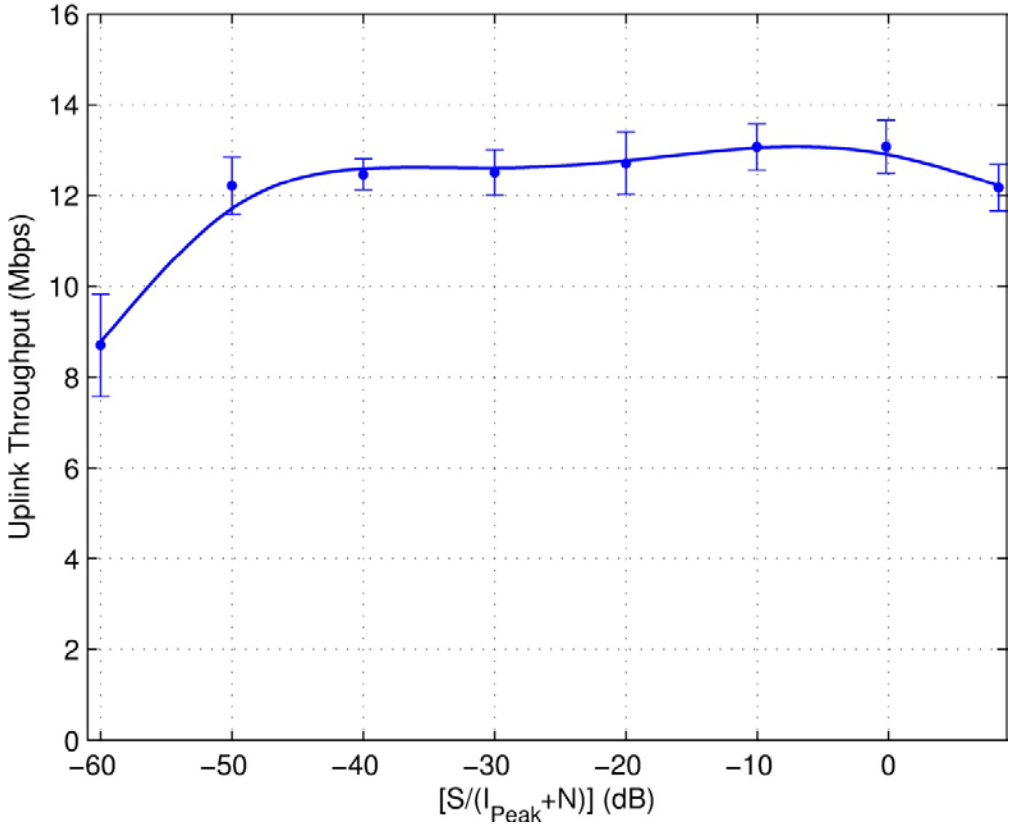

Figure B–36. Throughput, UE Tx power, BLER, and RBs for LTE (FDD) network for Q3N-2 interference.

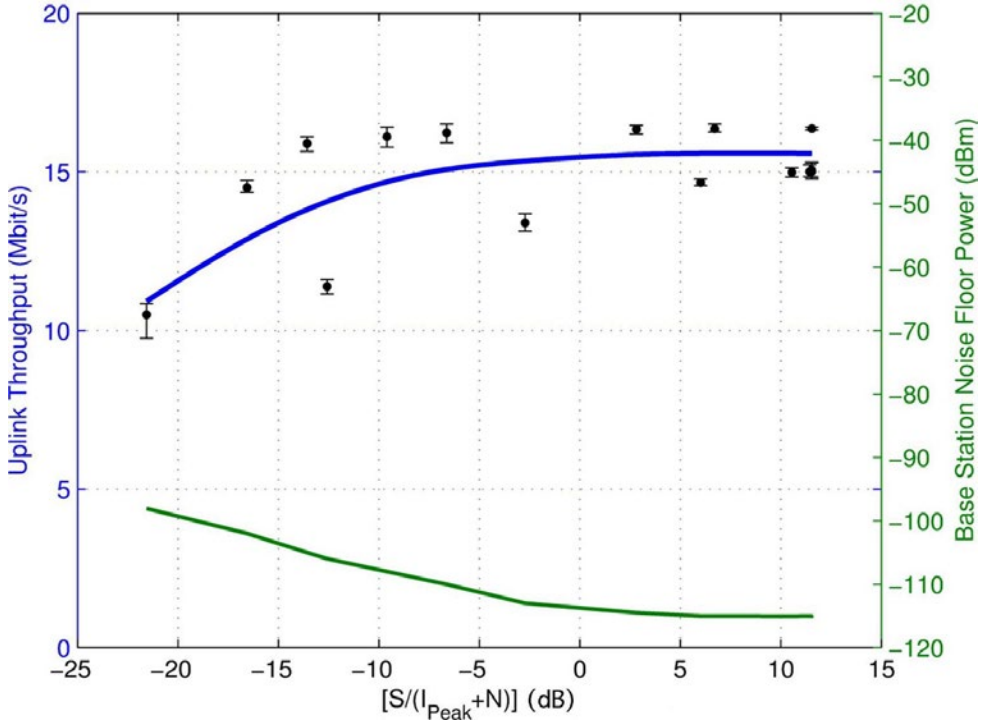

Figure B–37. Throughput and eNB Noise Floor for LTE (TDD) network for Q3N-3 interference.

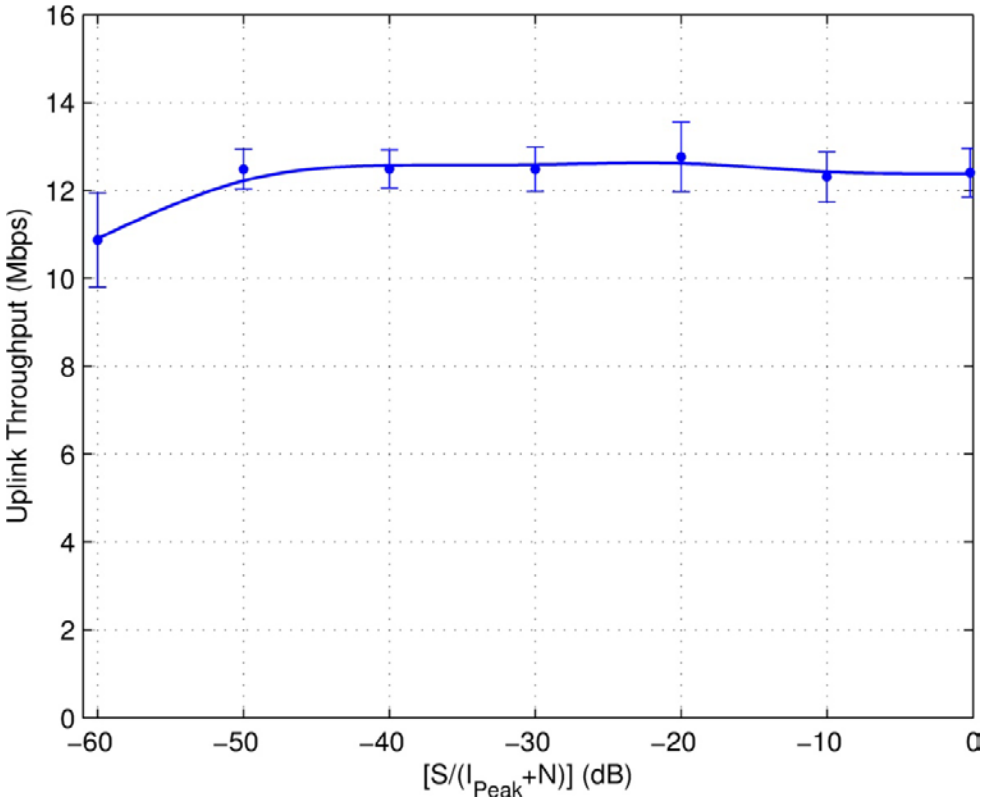

Figure B–38. Throughput, UE Tx power, BLER, and RBs for LTE (FDD) network for Q3N-3 interference.

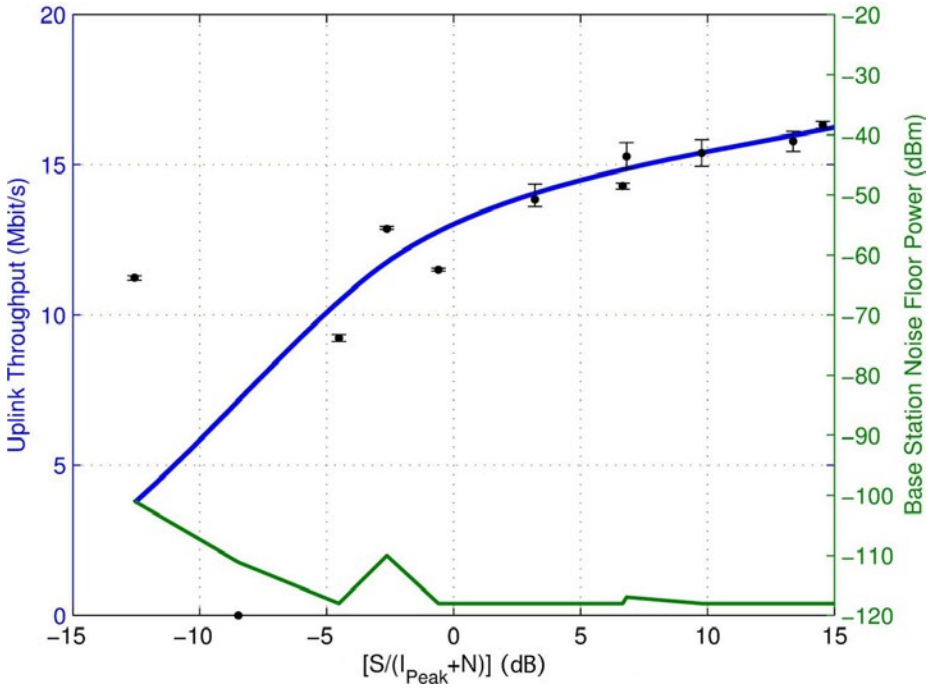

Figure B–39. Throughput and eNB Noise Floor for LTE (TDD) network for Q3N-5 interference.

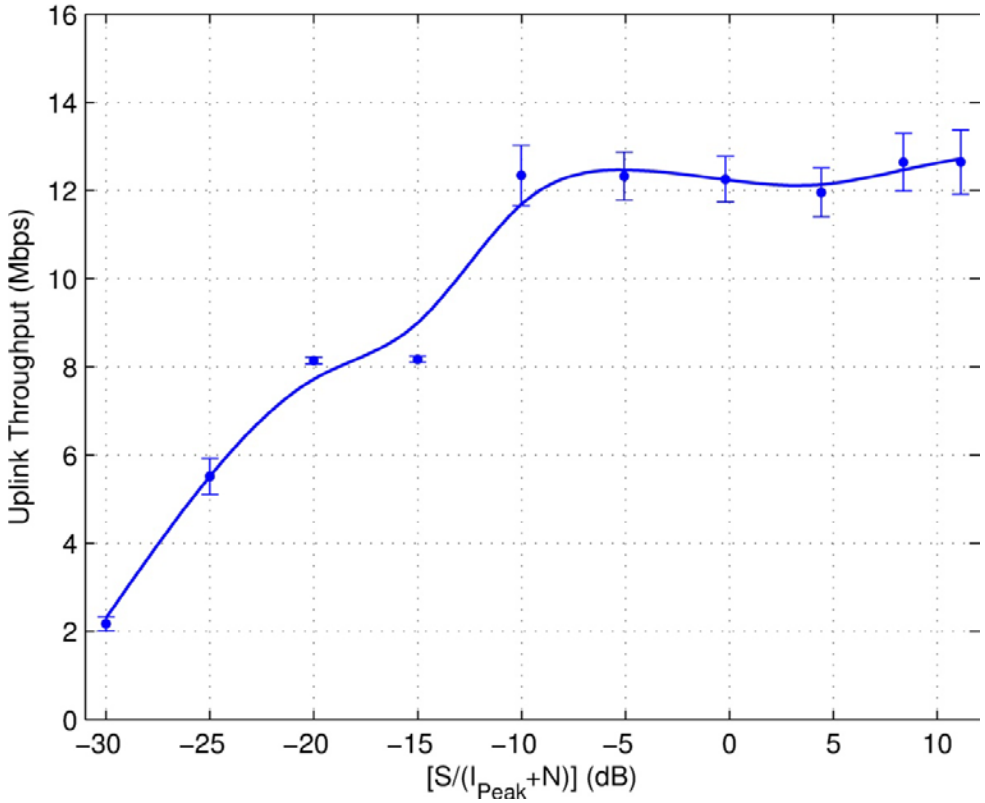

Figure B–40. Throughput, UE Tx power, BLER, and RBs for LTE (FDD) network for Q3N-4 interference (Q3N-4 waveform parameters are the same as Q3N-5 in previous study).

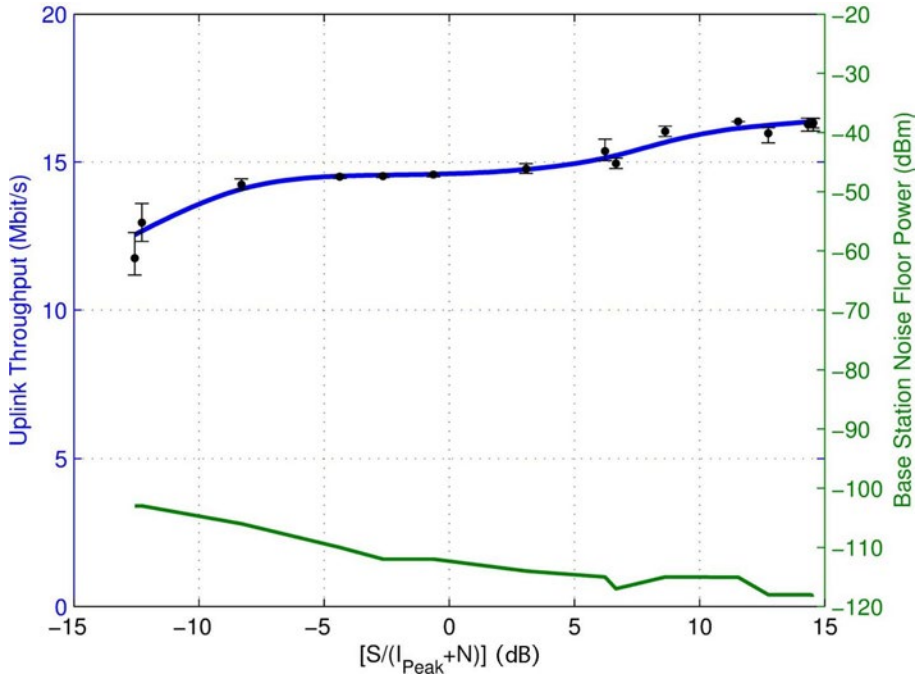

Figure B–41. Throughput and eNB Noise Floor for LTE (TDD) network for Q3N-6 interference.

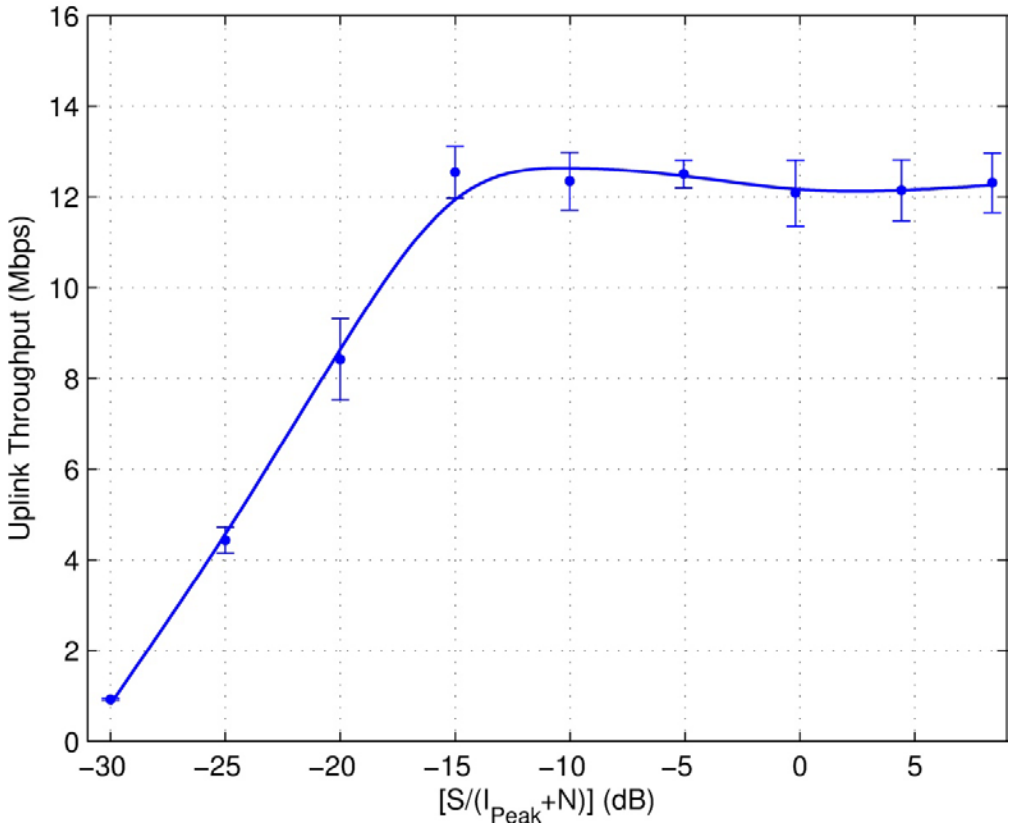

Figure B–42. Throughput, UE Tx power, BLER, and RBs for LTE (FDD) network for Q3N-6 interference.

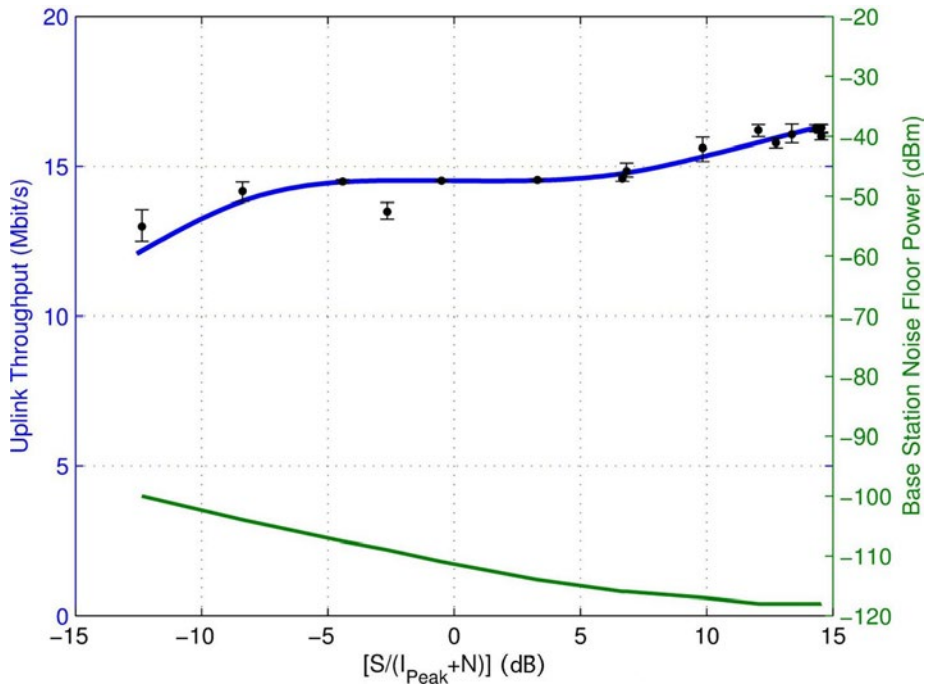

Figure B–43. Throughput and eNB Noise Floor for LTE (TDD) network for Q3N-9 interference.

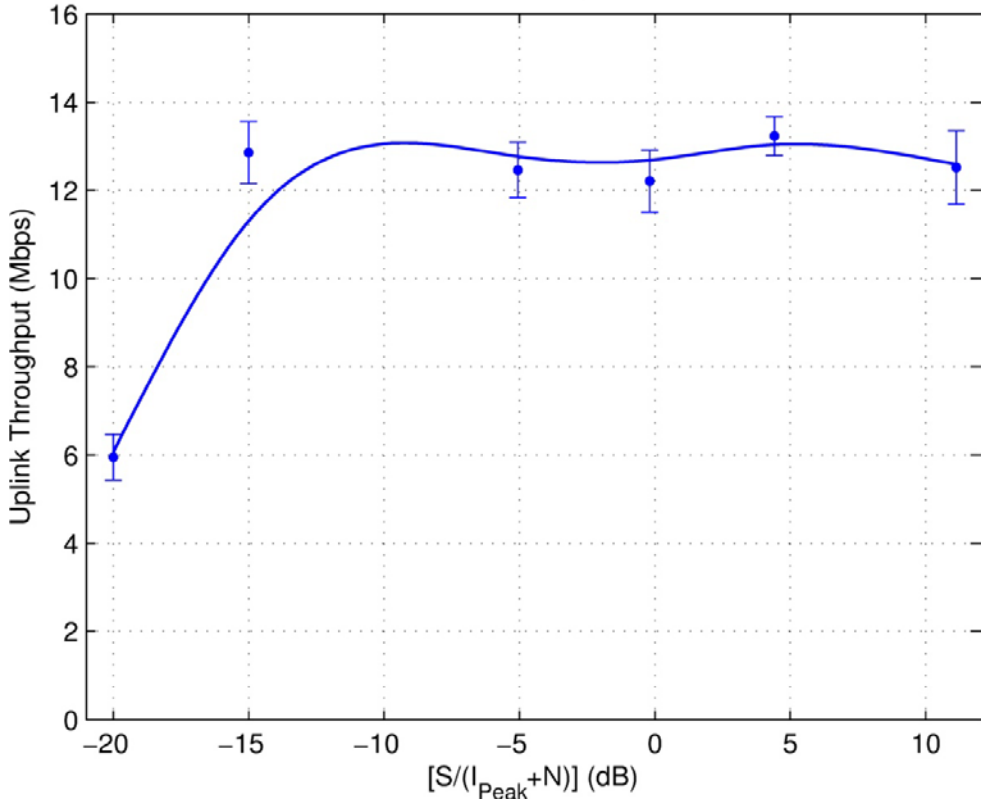

Figure B–44. Throughput, UE Tx power, BLER, and RBs for LTE (FDD) network for Q3N-9 interference.

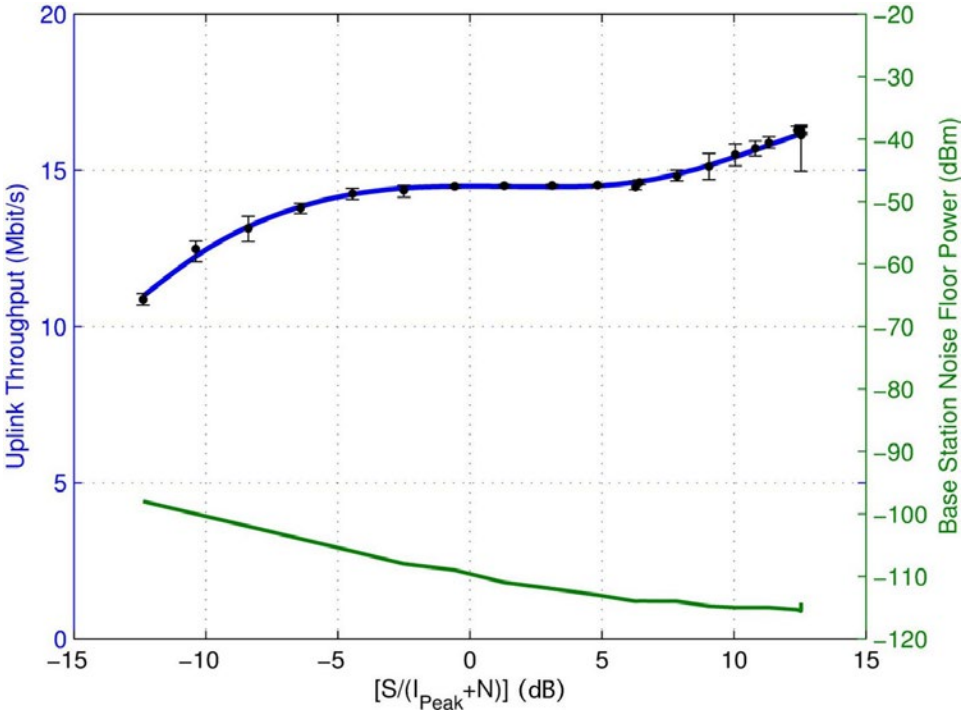

Figure B–45. Throughput and eNB Noise Floor for LTE (TDD) network for Q3N-12 interference.

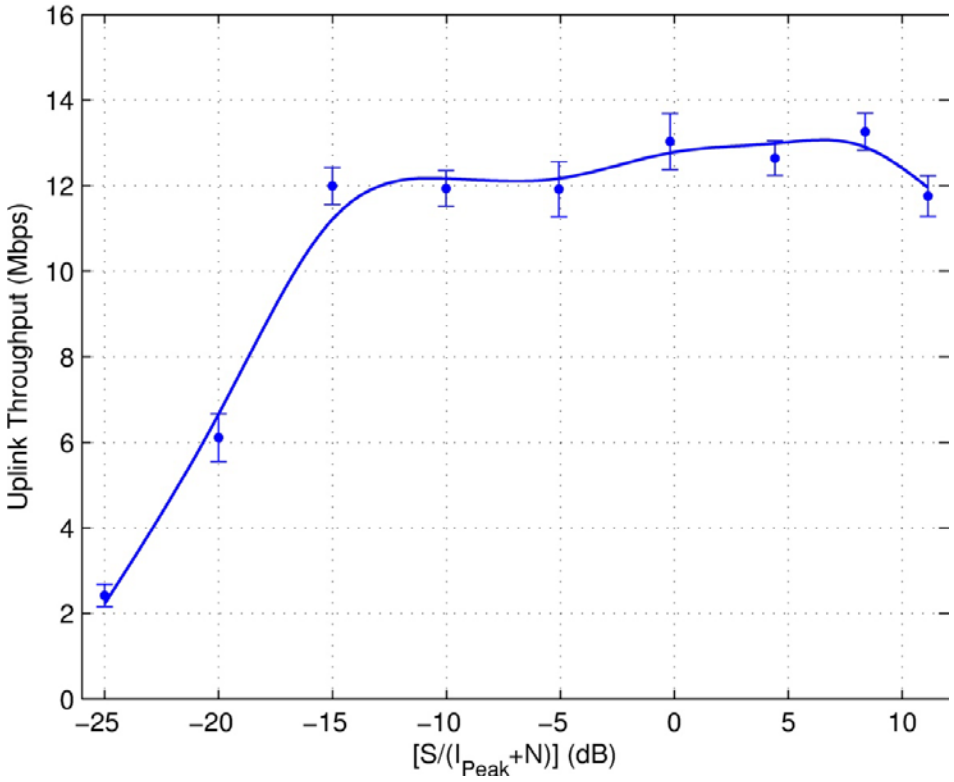

Figure B–46. Throughput, UE Tx power, BLER, and RBs for LTE (FDD) network for Q3N-10 interference (Q3N-10 waveform parameters are the same as Q3N-12 in previous study).

FORM **NTIA-29** (4-80)

U.S. DEPARTMENT OF COMMERCE
NAT'L. TELECOMMUNICATIONS AND INFORMATION ADMINISTRATION

BIBLIOGRAPHIC DATA SHEET

1. PUBLICATION NO.	2. Government Accession No.	3. Recipient's Accession No.
TR-14-506		

4. TITLE AND SUBTITLE	5. Publication Date
Effects of Radar Interference on LTE (FDD) eNodeB and UE Receiver Performance in the 3.5 GHz Band	July 2014
	6. Performing Organization Code NTIA ITS.T/NTIA OSM

7. AUTHOR(S)	9. Project/Task/Work Unit No.
Geoffrey A. Sanders, John E. Carroll, Frank H. Sanders, Robert L. Sole	6469000-200
8. PERFORMING ORGANIZATION NAME AND ADDRESS Institute for Telecommunication Sciences National Telecommunications & Information Administration U.S. Department of Commerce 325 Broadway Boulder, CO 80305	10. Contract/Grant Number.

11. Sponsoring Organization Name and Address	12. Type of Report and Period Covered
National Telecommunications & Information Administration Herbert C. Hoover Building 14th & Constitution Ave., NW Washington, DC 20230	

14. SUPPLEMENTARY NOTES

15. ABSTRACT (A 200-word or less factual summary of most significant information. If document includes a significant bibliography or literature survey, mention it here.)

In response to proposals to introduce new radio systems into the 3550 – 3650 MHz radio spectrum in the United States, the authors have performed measurements and analysis on effects of interference, from a variety of radar waveforms, to the performance of a prototype 3.5 GHz Long Term Evolution (LTE) network, consisting of one base station (known as an eNodeB) and one client (referred to as user equipment or UE) utilizing frequency-division duplexing (FDD). This work has been prompted by the possibility that LTE receivers may eventually share spectrum with radar operations in this spectrum range. Radar pulse parameters used in this testing spanned the range of both existing and anticipated future radar systems in the 3100 – 3650 MHz spectrum range. Effects of radar interference on the LTE uplink and downlink throughput, BLER, and modulation coding scheme (MCS) were measured. Additionally, for the uplink tests, resource block (RB) usage and UE transmit power were recorded. Effects on LTE performance are presented as a function of radar pulse parameters and the incident power level of radar pulses into the LTE receivers. The authors do not determine the interference protection criterion for nominal LTE network performance. Rather, the data presented can be used by spectrum managers and engineers as a building block in the construction of frequency-and-distance separation requirements for radar transmitters and LTE receivers, supporting possible future spectrum sharing at 3.5 GHz.

16. Key Words (Alphabetical order, separated by semicolons)

Block error rate (BLER); chirped pulses; Long Term Evolution (LTE); P0N pulses; radar; spectrum sharing; frequency-division duplexing (FDD); evolved-Node B (eNB); Q3N pulses

17. AVAILABILITY STATEMENT	18. Security Class. (This report)	20. Number of pages
☒ UNLIMITED.	Unclassified	141
☐ FOR OFFICIAL DISTRIBUTION.	19. Security Class. (This page) Unclassified	21. Price: n/a

NTIA FORMAL PUBLICATION SERIES

NTIA MONOGRAPH (MG)

A scholarly, professionally oriented publication dealing with state-of-the-art research or an authoritative treatment of a broad area. Expected to have long-lasting value.

NTIA SPECIAL PUBLICATION (SP)

Conference proceedings, bibliographies, selected speeches, course and instructional materials, directories, and major studies mandated by Congress.

NTIA REPORT (TR)

Important contributions to existing knowledge of less breadth than a monograph, such as results of completed projects and major activities. Subsets of this series include:

JOINT NTIA/OTHER-AGENCY REPORT (JR)

This report receives both local NTIA and other agency review. Both agencies' logos and report series numbering appear on the cover.

NTIA SOFTWARE & DATA PRODUCTS (SD)

Software such as programs, test data, and sound/video files. This series can be used to transfer technology to U.S. industry.

NTIA HANDBOOK (HB)

Information pertaining to technical procedures, reference and data guides, and formal user's manuals that are expected to be pertinent for a long time.

NTIA TECHNICAL MEMORANDUM (TM)

Technical information typically of less breadth than an NTIA Report. The series includes data, preliminary project results, and information for a specific, limited audience.

For information about NTIA publications, contact the NTIA/ITS Technical Publications Office at 325 Broadway, Boulder, CO, 80305 Tel. (303) 497-3572 or e-mail info@its.bldrdoc.gov.